Capability of glacial surface ecosystems as refuges for life on the Cryogenian Snowball Earth

by Jasmin L Millar

Thesis – Doctor of Philosophy, School of Earth and Environmental Sciences, Cardiff University

January 2022

Abstract

The Cryogenian Period in Earth's history extended from approximately 720 to 635 million years ago and was characterized by extensive global glaciations, known as 'Snowball Earth'. During this time life not only survived but appears to have diversified, staging the conditions for the development of animals in the subsequent Ediacaran period. The mechanisms and habitats that enabled microorganisms to survive and diversify through this time are not known. Cryoconite holes, diverse and robust habitats on glacier surfaces, have been proposed as a candidate refuge habitat as the communities within support both photoautotrophy and heterotrophy, and can survive complete freezing. DNA sequencing, lipid analysis and laboratory incubation of cryoconite communities from both poles identified key eukaryotic crown taxa and provided evidence for how microorganisms could have survived during Snowball Earth. The application of 16S rRNA and 18S rRNA gene high throughput sequencing and intact polar lipid analysis enabled evaluation of the richness, relative abundance and biogeographic distribution of microbial communities across both poles to higher resolution than ever before. The Arctic and Antarctic cryoconite holes harboured distinct microbial communities, but the various biotic niches (grazer, predator, photoautotroph, chemotroph) are filled in every location. Eukaryotic keystone taxa that had emerged prior to the Cryogenian were identified across both polar regions. Laboratory experiments were used to incubate sediments from cryoconite holes under "Snowball Earth" physical conditions. The community responses were measured using oxygen sensors, comparative intact polar lipid analysis and quantification of ^{3}H-Leucine incorporation. Community growth remained the same between Snowball Earth and modern polar conditions, indicating community resilience despite extreme cold and limited access to external resources. For cryoconite communities to have survived during Snowball Earth, the habitats that seed and distribute cryoconite must also have endured, particularly during glaciation and deglaciation. Signy Island of the maritime Antarctic South Orkney Islands was used as a model for these transitional habitats. Communities recovered from ponds, streams, ice margins and cryoconite on Signy Island did not thrive under Snowball Earth temperatures. However, DNA sequencing and intact polar lipid analyses revealed biodiverse and habitat-specific communities. The island presents a useful model for the networks of interconnected meltwater habitats during early glaciations and deglaciations of the Cryogenian. Through this combination of community DNA analysis and laboratory incubations, I present modern analogues for Cryogenian ecosystems, in which glacial surface ecosystems provide "diversity hotspots" that allowed the survival and proliferation of biodiversity during Snowball Earth.

Acknowledgements

The author would like to thank the following people and organisations for their contribution to this project:

The tuition, research, training and stipend funding for this project was kindly provided by the Natural Environmental Research Council Doctoral Training Partnership (GW4+ group). Illumina sequencing was carried out at the Natural History Museum London Molecular Labs sequencing facility. Cryoconite samples were kindly provided as follows: Utsteinen Nunatak samples were provided courtesy of Liane G. Benning, Jenine McCutcheon, and Lori Ziolkowski; Sweden samples were collected by Alexandre Anesio, and some Greenland margin samples were collected by James Bradley; Sweden, Greenland and Svalbard samples were provided by Ewa Poniecka; Taylor Glacier, Canada Glacier, and Commonwealth Glacier samples were provided by Elizabeth Bagshaw; the remaining McMurdo Dry Valleys samples were provided by Anne Jungblut. Additional Svalbard samples were collected by the author with assistance from the British Antarctic Survey and the UK Arctic Research Station. Signy Island sample collection was carried out by the author as part of the Collaborative Antarctic Science Scheme project: "Processes that influence Life in the southern high-latitudes" lead by Stephen Roberts, Anne Jungblut and David Naafs and facilitated by the British Antarctic Survey. The intact polar lipid analysis was kindly facilitated by Roger Summons and Thomas Evans at the Department of Earth, Atmospheric and Planetary Sciences, MIT, US and by Thomas Evans at MARUM - Zentrum für Marine Umweltwissenschaften der Universität Bremen, Bremen, Germany.

The author would also like to thank the following people for their support throughout the project:

Liz Bagshaw, Anne Jungblut, Arwyn Edwards and Ewa Poniecka for their support, guidance, kindness, and for encouraging me to take so many opportunities. Thank you to Thomas Evans, Roger Summons and everyone else at MIT who made me feel welcome. Becky Peel, the Signy Island staff and UK Arctic Research Centre staff for all your help during fieldwork. Rosslyn Watret, Dani Stewart and all my Hebridean Sky friends who turned long travels into adventures. Mabel Millar for giving me a home and good company during my months in London. Frances Bolley and Elle Barker for making sure I was always organised, supported and fed. My parents, for always being willing to proof read any applications and for supporting my education. Emanuela Piga, WGMEF ICE PACK, and my other friends and family for their encouragement throughout.

Table of Contents

List of Tables

List of Figures

Introduction

i. The Cryogenian Snowball Earth

Through Earth's history the planet has experienced many periods of warming and cooling, initiated predominantly by orbital forcing (Figure 1) and changes in greenhouse gas concentration in the atmosphere (Allmon *et al*., 2010). The first global glaciation, which followed the Great Oxygenation event, caused ice to cover the Earth from the poles to the equator over 2.29-2.25 Ga (Tang and Chen, 2013). In contrast, the most recent glacial period, from 2.6 Mya to the present day, has produced comparatively minor glaciation reaching only to the Southern Ocean, North America and middle Europe (Ehlers and Gibbard, 2008; Clark *et al*., 2009). Each of these glaciations has posed a challenge to the survival of life on earth due to cold stress, limited access to light in the frozen oceans, and limited access to nutrients and meltwater on the ice covered surface (Sutcliffe *et al*., 2000; Wolynski, 2012). The Cryogenian glacial period, from 720-635 Mya, took place during a particularly crucial point in evolutionary history (Figure 2). With the possible exception of early demosponges (as indicated by sterol signatures (Love *et al*., 2009)) life in the preceding Tonian is widely accepted to have been unicellular, while the following Ediacaran was populated by several forms of simple macroscopic metazoa (Droser and Gehling, 2015; Sergeev *et al*., 2017). Therefore life not only survived the Cryogenian but retained sufficient biodiversity for diversification into some of the first multicellular animals during or proceeding the Cryogenian. This thesis aims to address how microbial life survived the Cryogenian glaciations through examining potential biodiversity-oasis habitats.

The two Cryogenian Snowball Earth global glaciations or 'cryochrons' are known as the Sturtian (717-659 Mya) and Marinoan (~645-635 Mya) (Hoffman *et al*., 2017) (Figure 2). These cryochrons are widely regarded as some of history's most extensive glacial periods, due to the fact that geological deposits of glaciogenic

origin have been found from the tropical and equatorial regions of this time period (Sumner *et al*., 1987; Hoffman *et al*., 1998). However, the range of the glaciation has been a matter of debate in the years since these discoveries. The 'Snowball Earth' theory or 'hard Snowball Earth' refers to scenarios in which the planet was completely or near-completely covered in ice from the poles to the equator (Sumner *et al*., 1987; Kirschvink, 1992; Hoffman *et al*., 1998). According to this hypothesis, ice covered the oceans during the cryochrons, possibly limiting oceanic photosynthesis (Warren *et al*., 2002). The ice cover of the oceans would also separate the wind from ocean current processes and reduce oxygen exchange between the atmosphere and ocean resulting in ocean anoxia (Kirschvink, 1992). This would explain both the wide dispersal of glaciogenic deposits and associated banded iron formations which may reflect a dramatic change in ocean oxygenation (Kirschvink, 1992; Hoffman and Schrag, 2002; Young, 2002).

Annual average temperatures would be below 0°C, predicted to be -5°C at the highest CO_2 level in the late Cryogenian and -30°C at the low CO_2 early Cryogenian (Abbot *et al*., 2013). The low temperature caused the planet to be very dry, similar to the Antarctic dry valleys today (Hoffman *et al*., 2017).The biggest challenge to the 'hard' Snowball Earth scenario is its capacity to support life. Despite the wide scale glaciation of the Cryogenian, a variety of organisms persisted (Porter and Knoll, 2000; Peterson and Butterfield, 2005; Parfrey *et al*., 2011). By this point, the crown phyla of bacteria had already withstood many dramatic changes in environment including the 2.29-2.25 Ga global glaciation (Tang and Chen, 2013). Therefore what is more surprising is that microfossils and molecular clocks reveal crown groups of eukaryotes including Rhodophyta, Chlorophyta, Amoebozoa, Choanoflagellata and several members of SAR groups emerged in the interglacial age preceding the Cryogenian and persisted through the Cryogenian (Porter *et al*., 2003; Peterson and Butterfield, 2005; Parfrey *et al*., 2011; Sánchez-Baracaldo *et al*., 2017). This enabled

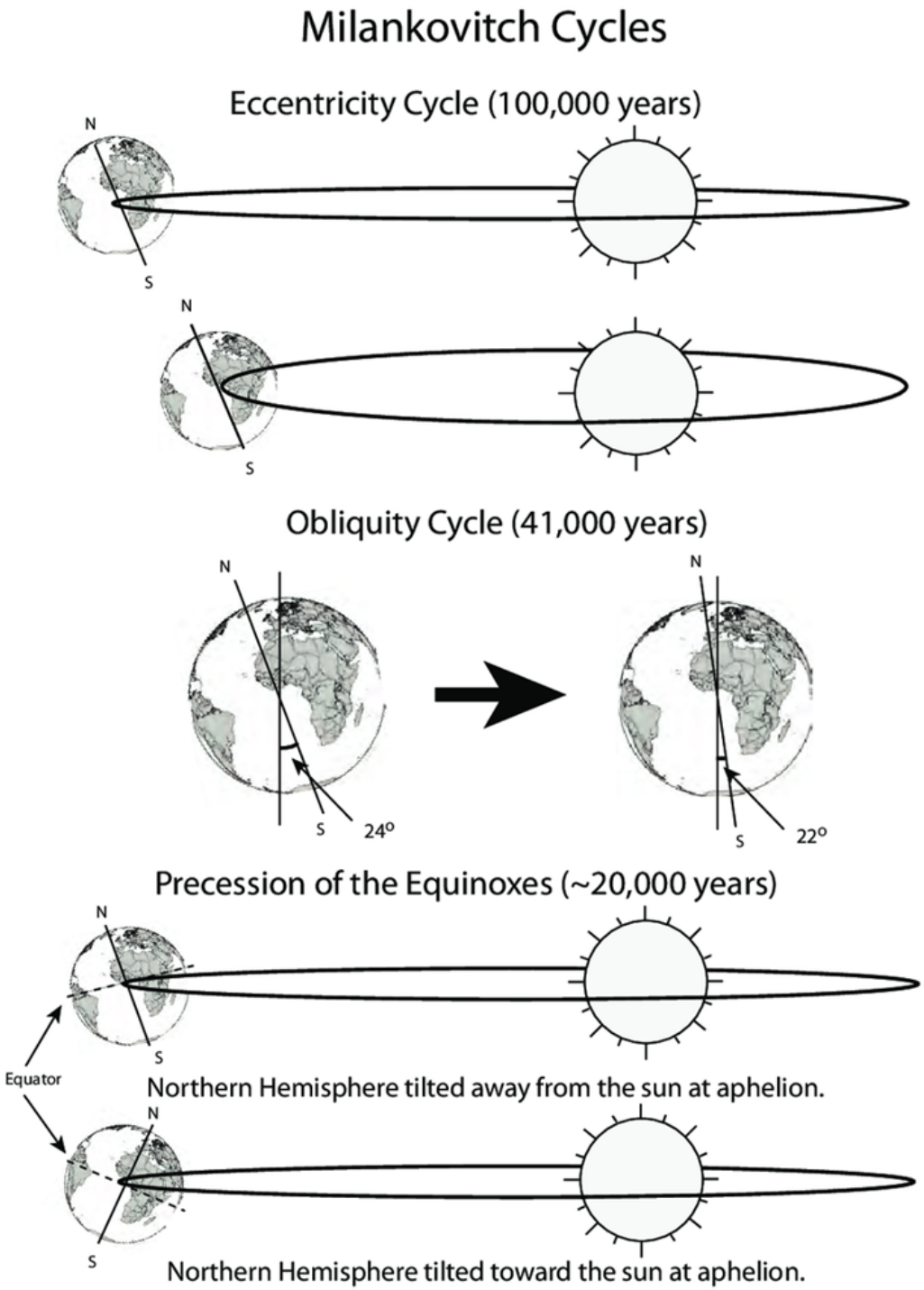

Figure 1 "Milankovitch Cycles. The Earth's orbital variation around the Sun experiences cyclic changes in shape. Eccentricity changes the shape of the orbit on a 100,000-year cycle from a circular to a more elliptical shape. Obliquity is the change of the angle of Earth's axis, which ranges from 22° to 24° from normal, and occurs on a 40,000-year cycle. Precession, commonly called the "wobble" of Earth's axis, affects the positions in Earth's orbit at which the Northern and Southern Hemispheres experience summer and winter. This changes on an approximately 20,000-year cycle." (Allmon et al., 2010)

the rise of metazoa and the early ancestry of land plants following global deglaciation (Heckman *et al*., 2001; Wheeler *et al*., 2009; Epp *et al*., 2015; Erwin, 2015).

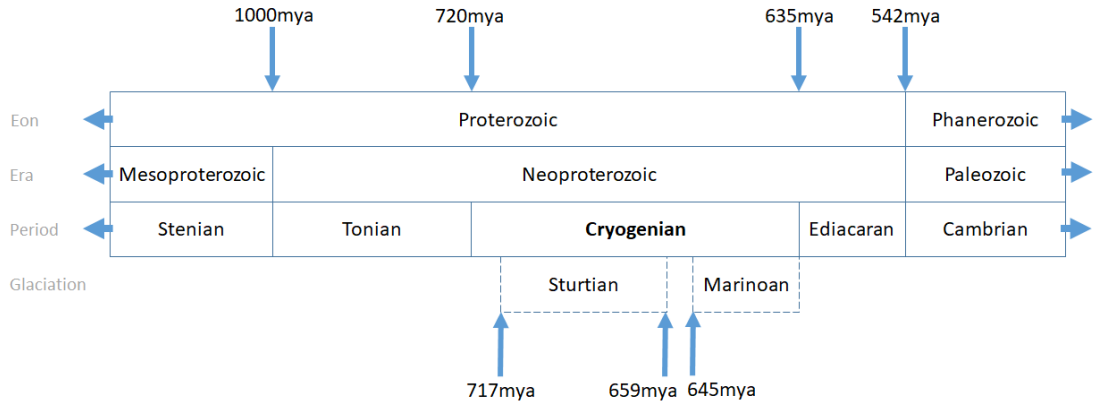

Figure 2 Geological timeline featuring the Cryogenian. Dates of the beginnings/ends of significant periods marked by number of millions of years ago.

Some researchers have raised concerns that a totally or near completely ice covered ocean is inconsistent with this fossil record (Moczydłowska, 2008). There appears to be a continuous record of marine organisms including autotrophs and protists reliant on sexual reproduction that survived the Cryogenian, which in the modern day rely on light and oxygenated oceans (Tappan, 1980; Vidal and Ford, 1985; Colbath and Grenfell, 1995; Vidal and Moczydłowska-Vidal, 1997; Moczydłowska *et al*., 2021). One response has been the proposal of a 'Waterbelt' or 'Slushball Earth' scenario, in which a significant area of open ocean is retained around the equator (Hyde *et al*., 2000; Runnegar, 2000). In this scenarios temperatures at the equator and subtropics could be as high as 10°C (Hyde *et al*., 2000). The hydrological cycle would be active; precipitation would be low over the ice sheet accumulation zones (less than 0.06 mm d^{-1}) but up to 10 mm d^{-1} over the open ocean areas (Hyde *et al*., 2000). This addresses some of the issues of biotic survival and several models have now produced stable Waterbelt solutions (Hyde *et al*., 2000; Yang *et al*., 2012; Rose, 2015). However, evidence for areas of open ocean

is lacking from the sedimentary record and the models have been criticised for lacking sea ice dynamics (Lewis *et al*., 2003, 2007; Braun *et al*., 2022). Proponents of a hard Snowball Earth scenario have therefore presented a different explanation, in which the ocean is periodically replenished with O_2 at cracks and moulins and alternative electron acceptors sulphate and Fe(III) are flushed into the ocean from glacier surface sediments (Le Hir *et al*., 2008a; Goodman and Strom, 2013; Hoffman, 2016). The thin ice in these warmer 'cracking' areas may also allow transmission of light to the water below (Goodman and Strom, 2013; Hoffman *et al*., 2017). It is still debatable whether this would have been sufficient to support continuous survival of marine autotrophs and other organisms with particular requirements including spore forming eukaryotes (Hoffman *et al*., 2017).

In both scenarios, whether there is complete ice cover or an equatorial Waterbelt, large parts of the continental terrestrial surface and oceans would be covered in ice (Hyde *et al*., 2000; Warren *et al*., 2002; Lewis *et al*., 2003; Abbot *et al*., 2013). Ice surface ecosystems are hypothesised to have been significant contributors to global ecology and biogeochemical cycling (Hoffman, 2016; Hawes *et al*., 2018). The 'harder' Snowball Earth scenarios are well supported by a range of geological, sedimentary, climate model evidence but their credibility is dependent on the possibility of substantial glacier surface microbial habitats maintaining refuges for eukaryotic life and providing sources of electron acceptors and organic matter to the oceans (Hoffman and Schrag, 2002; Lewis *et al*., 2007; Hoffman *et al*., 2017; Braun *et al*., 2022). Despite this, the capacity of microorganisms to survive under the conditions of global glaciation has not been investigated. This thesis aims to investigate this possibility, by identifying modern analogues to a range of Cryogenian potential habitats and testing their resilience to Snowball Earth conditions.

ii. Modern Cryogenian analogues

To understand how life may have survived this seemingly hostile period in Earth's history, many have turned to how life survives in ice and other cold climates in the present (Prave *et al*., 2016; Hawes *et al*., 2018). Around 10% of the Earth's surface is taken up by the modern terrestrial cryosphere (Lutz *et al*., 2017). Cold climate habitats are present across the globe, sustaining an abundance of life despite low temperatures (Anesio *et al*., 2017).

In ice-covered areas of modern Earth's ocean, the sea ice, seawater and benthos host a range of organisms from microbial chemotrophs to large macrofauna (Gibson and Atkinson, 2003; Runcie and Riddle, 2006; Fisher *et al*., 2007; Petersen *et al*., 2011; Arrigo *et al*., 2012). Algal blooms cling to the subsurface of the sea ice and some bacteria and algae have been found in small meltwater channels within ice (Riebesell *et al*., 1991; Michel *et al*., 1996). Many of these organisms remain metabolically active in the sea ice (Leventer, 1998; Junge *et al*., 2002; Junge Karen *et al*., 2004). Beneath land ice, the high solute concentrations in subglacial hydrological systems provide a habitat for chemolithotrophic communities (Sharp *et al*., 1999; Tranter *et al*., 2002; Statham *et al*., 2008; Wadham *et al*., 2010). On the ice surface, microorganisms accumulate on snow, ice and sediment deposited on the ice by wind and streams. Snow algae blooms such as *Chlamydomonas* 'watermelon snow' and ice surface blooms caused by glacier algae (e.g. *Ancylonema nordenskiöldii*) cover large areas of glacier surfaces (Ehrenberg, 1832; Berggren, 1871; Nordenskiöld, 1872). However, in contrast to the glacier and snow algae blooms which are dominated by a handful of species, particular hotspots of biodiversity occur when sediment, living cells and the organic matter accumulate (Yoshimura *et al*., 1997; Cameron *et al*., 2012b; Lutz *et al*., 2015, 2018; Millar *et al*., 2021). Cryoconite holes, aggregates of organic and inorganic matter housed in meltwater pockets, contain a wide range of bacteria and eukarya including Cyanobacteria, Proteobacteria, Actinobacteria, Archaeplastida, Amoebozoa, Rhizaria and Streptophyta (Edwards *et al*., 2011; Cameron *et al*., 2012b; Sommers *et al*., 2018; Lutz *et al*., 2019). The cryoconite holes are connected by streams on

and through the ice which may host their own unique communities (Irvine-Fynn *et al*., 2011; Bagshaw *et al*., 2013; SanClements *et al*., 2017). When cryoconite matter is swept towards ice cliffs by strong katabatic winds, it accumulates into larger "cryolakes" (Parish and Cassano, 2003; Laybourn-Parry and Wadham, 2014; Bagshaw *et al*., 2016a). Lakes also form at the edges and termini of glaciers, hosting higher biodiversity than the adjacent ice surfaces (Mindl *et al*., 2007; Liu *et al*., 2011).

Whilst the modern cryosphere supports active microbial communities, what is not known is how many of these habitats could have been maintained during Snowball Earth. The ice over the oceans may have been thick enough to prevent photoautotrophy, rendering algal blooms under the ice and photoautotrophic primary production in the water impossible or severely limited depending on the model used (Kirschvink, 1992; Hyde *et al*., 2000; Abbot *et al*., 2013; Hoffman *et al*., 2017). While chemotrophy is the main source of primary production on the benthos, these under-ice habitats are not completely isolated and are still supported by organic detritus falling from the photosynthetically active layer above (Jørgensen and Boetius, 2007). Ice free land and meltwater would also have been limited during Snowball Earth, reducing the frequency of periglacial, proglacial and supraglacial lakes, particular in a 'hard' Snowball Earth scenario. In addition, habitats under sea ice, under glaciers and in frozen lakes may have persisted through Snowball Earth but could not have supported the range of microorganisms known to have lived during this period, including photoautotrophs and crown group heterotrophic and mixotrophic eukarya (Peterson and Butterfield, 2005; Parfrey *et al.*, 2011; Javaux and Knoll, 2017; Loron *et al.*, 2019). This leads us to considering life at the Snowball Earth ice surface, where exposure to light could be assured regardless of the extent of ocean ice cover. Modern glacial surface ecosystems are home to bacteria, archaea and eukaryotes (Anesio & Bellas 2017). They sustain photosynthesis and support both single-cell and multicellular life (Takeuchi *et al*., 2001a; Liu *et al*., 2011; Cameron *et al*., 2012b, 2016; Lutz *et al*., 2017). Cryoconite (Figure 3) is a habitat of particular relevance to Snowball Earth because it supports a diverse range of heterotrophic and autotrophic organisms including

photoautotrophs that can be active at low temperatures (Cameron *et al*., 2012b; Edwards *et al*., 2013b; Sommers *et al*., 2018; Lutz *et al*., 2019; Millar *et al*., 2021). In addition, cryoconite ecosystems persist even when surface temperatures fall well below zero and the meltwater within the cryoconite holes freezes completely (Fountain *et al*., 2008; Stanish *et al*., 2013; Webster-Brown *et al*., 2015; Poniecka *et al*., 2020).

iii. Cryoconite holes

The term "cryoconite" refers to the microbe-mineral aggregates that form on supraglacial habitats; particularly the ablation zones of glaciers (Nordenskjold, 1875; Cook *et al*., 2015b). The sediment that seeds these aggregates can originate from both local and distal ground, ice margin and dust sources, transported by supraglacial streams and aeolian transport (Sharp, 1949; McIntyre, 1984). Many microbes produce extracellular polymeric substances that allow them to form biofilms and increase the habitability of their surrounding environment (Donlan, 2002). On the ice, these polymeric substances cause other materials to adhere to the cells (Langford *et al*., 2010). The low albedo and therefore high solar radiation absorption of the cryoconite causes the sediment to melt vertically into the glacier surface, forming near cylindrical pockets of liquid water several centimetres deep (Musilova *et al.*, 2016) (Figure 4). These cryoconite holes are found globally on the ablation surfaces of glaciers. (Nordenskjold, 1875; Wharton *et al*., 1985; Takeuchi *et al*., 2000).

The varied temperatures and physical environments across the cryosphere promote varied cryoconite hole structures and communities. In cold, dry climates such as the Dry Valleys of Antarctica, the water above the cryoconite sediment re-freezes leaving the cryoconite holes lidded with ice through most or all of the year (Tranter *et al*., 2004). In the McMurdo Dry Valleys, ice lids of up to 30cm have been observed on the majority of cryoconite holes year-round (Fountain *et al*., 2004). Some of these thick lids may only melt during particularly warm periods years apart

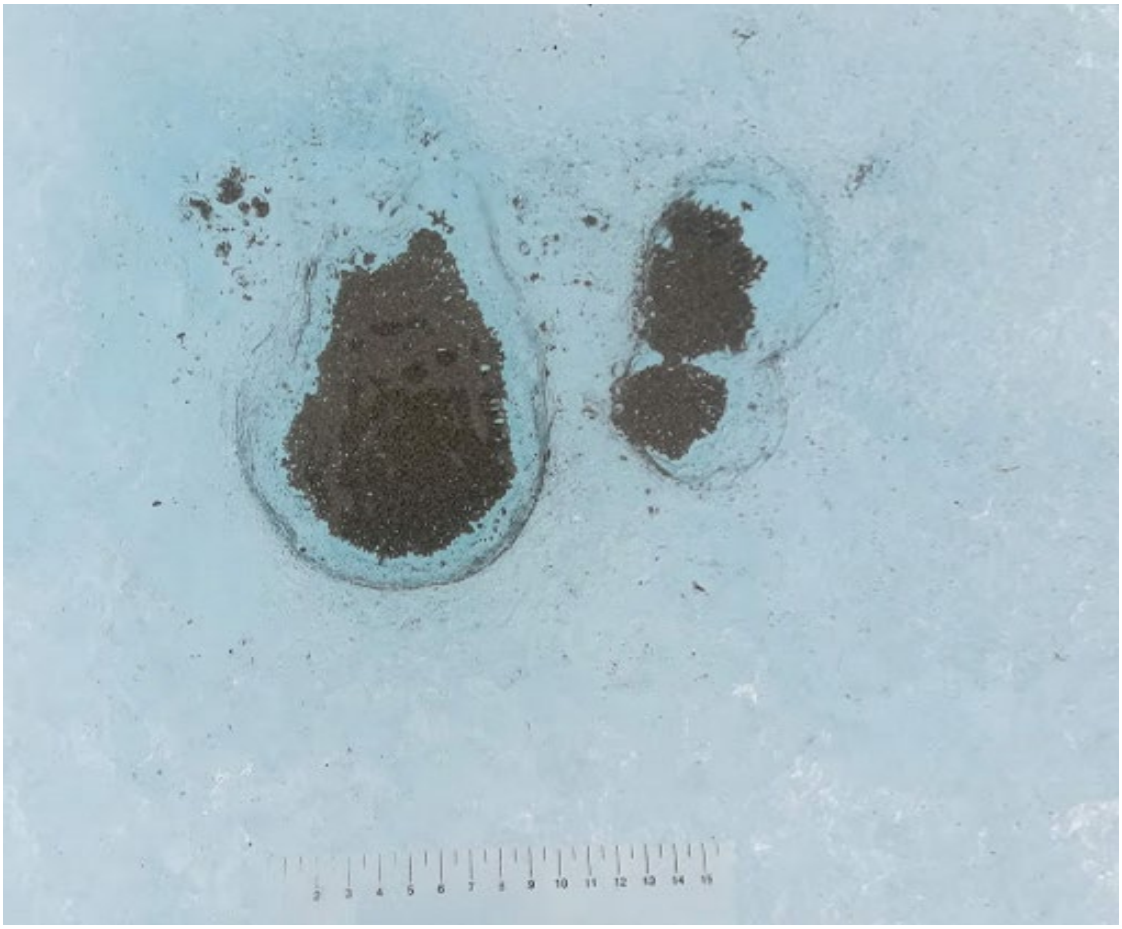

Figure 3: An open cryoconite hole on Midtre Lovénbreen glacier Svalbard

(Doran *et al*., 2002). Many Antarctic cryoconite holes are frozen completely and melted again on a seasonal or sub-seasonal timescale (Bagshaw *et al*., 2007). Around 50% of lidded holes are connected under the ice surface; the other 50% are completely isolated (Fountain *et al*., 2004). When closed holes are connected to one another this tends to occur through a network of small channels just below the glacial surface (MacDonell and Fitzsimons, 2008; Bagshaw *et al*., 2012; Macdonell *et al*., 2016). These are therefore hydrologically connected but still closed from the atmosphere above. In warmer regions including many Arctic and low latitude glaciers, cryoconite holes remain 'open' or unlidded and can also be connected at the surface by meltwater (Hodson *et al*., 2008). Eventually the cryoconite is flushed to the glacier terminus or supraglacial streams as it moves down the ablation zone (Hodson *et al*., 2010). This connects it to the wider network of streams, ponds, ice margins and seas. However, a recent study found microbial accumulation on the Greenland ice sheet outweighed export (Irvine-Fynn *et al*., 2021). This also means there is evidence that even in regions with cryoconite mobility, many of the habitats can persist.

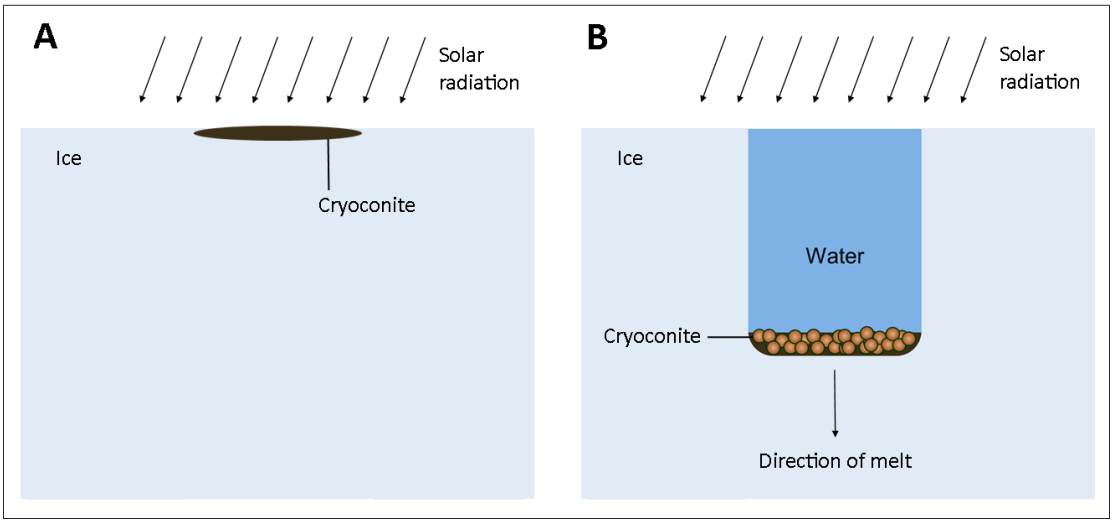

Figure 4: Cryoconite hole formation. The cryoconite absorbs solar radiation and melts vertically into the ice surface. **A** Shows cryoconite when just deposited onto the ice surface, before cryoconite hole has formed. **B** Shows the resulting cryoconite hole after a period of melting.

Cryoconite provides a habitat on the ice for a plethora of organisms. DNA sequencing of cryoconite communities has revealed a dominance of Proteobacteria, Bacteroidetes, Cyanobacteria and microalgae (Cameron *et al*., 2012b; Edwards *et al*., 2013b; Sommers *et al*., 2018). They also harbour fungi, protists and micro-animals (meiofauna) (Zawierucha *et al*., 2015). Virus production has been found to be just as prolific in cryoconite as other sediments (Bellas *et al*., 2013). The taxonomic group that distinguishes modern cryoconite from the kind of communities we might expect in Snowball Earth ~650 million years ago are the micro-animals. Micro-invertebrates such as tardigrades and rotifers feed on algae and bacteria (Van Rompu, 1994; Vincent *et al*., 2000). This means cryoconite sediment appears to have higher species richness than the surrounding glacier surfaces, although dedicated biodiversity studies of bare ice and snow and glacier algae blooms are limited (Liu *et al*., 2011; Lutz *et al*., 2015, 2017; Williamson *et al*., 2019; Anesio and Laybourn-Parry, 2021). Like cryoconite hole structure, the relative abundance of these organisms varies with biogeography (Liu *et al*., 2017; Darcy *et al*., 2018). It has also been shown that communities are more similar within glaciers than between glaciers (Liu *et al*., 2017; Darcy *et al*., 2018; Sommers *et al*., 2018; Millar *et al*., 2021).

Modern cryoconite sediment acts as a large store of carbon, nitrogen and phosphorus (C, N and P) than the surrounding ice, but also can contain a larger proportion of bioavailable C, N, and P than that of the cryoconite source terrestrial soils and sediments because of biogeochemical cycling (Bagshaw *et al*., 2013). However P may still be a limiting biological factor, particularly areas such as the McMurdo Dry Valleys with few allochthonous sources of P (Foreman *et al*., 2007; Bagshaw *et al*., 2013). Nitrogen fixation has been observed in cryoconite in the Arctic (Telling *et al*., 2011) and may also take place in Antarctic cryoconite (Bagshaw *et al*., 2007; Cameron *et al*., 2012a; Telling *et al*., 2014). Modern cryoconite can therefore function as a self-sustaining ecosystem, since biogeochemical cycling can extract the required nutrients from the sediment grains and via internal ecosystem processes.

This diversity of cryoconite communities, along with their resilience to extreme conditions, has led Snowball Earth researchers to consider them a habitat with particular potential for Cryogenian life. When cryoconite holes freeze completely, the organisms within are able to survive and can regain activity once thawed (Bagshaw *et al*., 2007; Fountain *et al*., 2008; Webster-Brown *et al*., 2015; Poniecka *et al*., 2020). Antarctic cryoconite communities are tolerant of low light conditions due to their adaptation to the ice lids, which limit light transmission to the sediment (Bagshaw *et al*., 2016b). Arctic cryoconite communities from open cryoconite holes, which must withstand long summer exposure to high light levels, are resilient to high UV (Bagshaw *et al*., 2016b; Perkins *et al*., 2017).

The first step in discerning whether cryoconite could have provided refuge for life on Snowball Earth is to determine whether cryoconite could have formed under Snowball Earth conditions. It is expected that dust and sediment would be present on the Snowball Earth ice surfaces, accumulated from continental boundaries with ice shelves and volcanic ash (Hoffman, 2016). Although at first the climate may be too cold for modern levels of dust accumulation, with rising CO_2 and climbing temperatures, thick deposits could be retained in the equatorial zone by the end-Sturtian (Hoffman, 2016). It has therefore been proposed that this would provide ideal conditions to seed large areas of cryoconite habitats (Hoffman, 2016; Hoffman *et al*., 2017). High atmospheric pressure and absorption of solar radiation by cryoconite is predicted to facilitate sufficient liquid surface water to form cryoconite holes (Hoffman and Schrag, 2002). The proceeding question is whether Cryogenian life could have survived in cryoconite at Snowball Earth temperatures and other environmental conditions. Although several studies have examined taxa that inhabit cryoconite, a pole-to-pole survey using techniques sufficient to resolve family-level composition had not been carried out prior to this study. Therefore it has been difficult to determine whether cryoconite holes universally support key Cryogenian taxa. Once analogous communities have been identified, it is necessary to determine whether modern cryoconite could survive Snowball Earth conditions. In contrast to modern polar cryoconite, Snowball Earth cryoconite would be concentrated at low latitudes in the warmer tropics. Hoffman *et al*. (2016) predict

the cryoconite would be largely sourced from volcanic origins and distributed in a belt encircling the planet. However, it is more likely that to provide sufficient organic matter and living cells to seed a sustainable community much of the material would be sourced from ice free terrestrial zones (Dong *et al*., 2016a, 2016b; Franzetti *et al*., 2017). It may receive numerous, perhaps daily, freeze thaw cycles and light dark cycles through the year that could inflict stress on the cryoconite microorganisms. Nutrient input would be limited as many nutrient sources would be ice covered, and air temperatures would rarely exceed 0°C during the cryochrons. These harsh conditions are consistent with the widespread extinction of a range of organisms over the Cryogenian (Vidal and Knoll, 1982; William Schopf and Klein, 1992; Vidal and Moczydłowska-Vidal, 1997; Knoll *et al*., 2006a). The surviving microorganisms could be similar to what we observe in cryoconite today: a mixture of psychrophiles, ubiquitous and widely tolerant crown groups such as Cyanobacteria, and other organisms that can exist in protective dormant states over winter (Cameron *et al*., 2012b; Quesada and Vincent, 2012; Edwards *et al*., 2013b). At least some of the interconnected cold climate habitats that seed and distribute cryoconite such as streams, lakes, and ice margins would also need to persist through these conditions to connect these 'oases' to the larger ecosystems (Cameron *et al*., 2020; Irvine-Fynn *et al*., 2021). Thus far, the resilience of cryoconite to these conditions has not been tested. This thesis addresses these gaps in the evidence for cryoconite on Snowball Earth, summarised in the hypotheses on the following page.

iv. Hypotheses and objectives

1. Hypothesis: Modern polar cryoconite hole communities are analogous to the biodiversity and eukaryotic key taxa of the Cryogenian
   1.1. Objective: Assess cryoconite hole microbial diversity and community composition
   1.2. Objective: Compare cryoconite taxonomy to Cryogenian keystone taxa
2. Hypothesis: Modern polar cryoconite is resilient to 'Snowball Earth' conditions
   2.1. Objective: Measure the response of cryoconite to 'low latitude Snowball Earth' light and temperature conditions
   2.2. Objective: Form cryoconite holes on ice in laboratory conditions, for closer replication of Snowball Earth conditions
3. Hypothesis: Supraglacial and periglacial habitats contain distinct but interconnected ecosystems analogous to Snowball Earth meltwater habitats
   3.1. Objective: Investigate geographical and ecological connections between interconnected glacial and near-glacial microbial ecosystems on Signy Island
   3.2. Objective: Determine the community response of Signy Island sediments to isolated "oasis" incubation conditions

Literature Review

i. The Snowball Earth theory

Evidence from the geological and sedimentary record

The Snowball Earth hypothesis first arose when deposits of rock and sediment from that period, that appeared to be glacial in origin, were found at low-latitude sites. These signature deposits were found first in South Australia and then later in Africa (Sumner *et al*., 1987; Hoffmann *et al*., 2004) and are described below. Diamictites were found, which are lithified sedimentary rocks consisting of poorly sorted and widely sized terrigenous sediments suspended in sand or mud stone (Figure 5) (Flint *et al*., 1960; Hoffman, 2011). The term diamictite does not exclusively refer to glaciogenic depositions, and may be marine, volcanic, tectonic, meteoric or even man made in origin (Aalto, 1986; Eyles and Lazorek, 2014; Letsch and Kiefer, 2017). However, their proximity to other characteristic glaciogenic facies can identify them as having glacial origin (Sumner *et al*., 1987; Eyles and Januszczak, 2004; Hoffmann *et al*., 2004). Varves, lamina created by annual cycles of sedimentation (DeGeer, 1912; Zolitschka, 2014), can be diagnostic of glacial environments; thicker coarse sediment deposited by freshwater streams followed by thin and fine winter layers suggest freeze thaw cycles of periglacial lakes (Peach and Perrie, 1975; Williams *et al*., 2016). As the glaciers flow, they carve multiple, straight parallel striations into the rock below, which provide yet another characteristic marker (Kirschvink, 1992). One of the most significant findings, however, was the presence of drop stones. Drop stones are rocks carried on a glacier as it flows and deposited as it melts, so appear in facies as large boulders captured in fine or mixed sediment (Preiss, 1987). The natural remnant magnetisation (NRM) of the drop stones confirmed that they were formed at equatorial and low-latitude locations (Sumner *et al*., 1987). A later review compiled age and locality constraints upon a range of rocks with the same results (Evans, 2000). This was presented as evidence that glaciers must once have

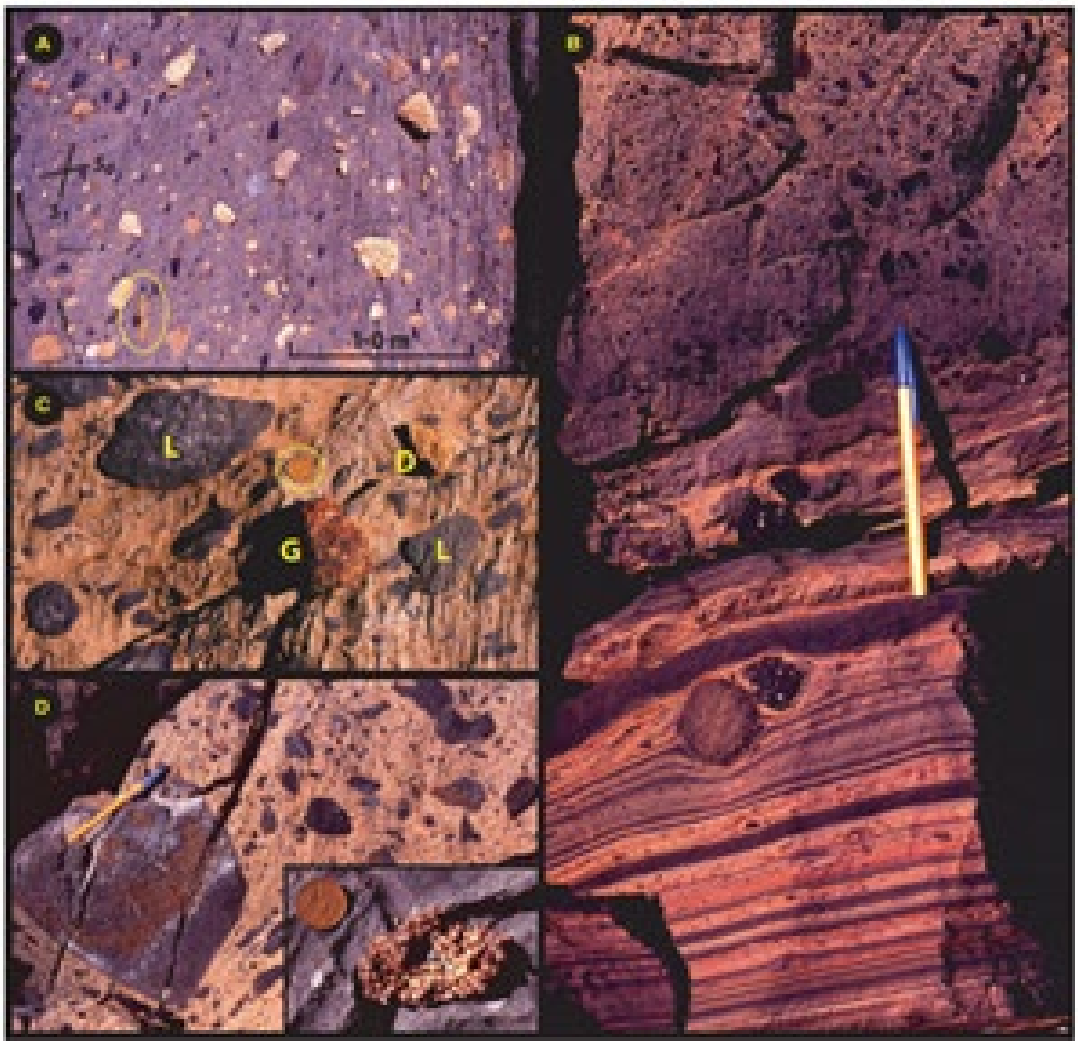

Figure 5 "Massive to weakly stratified diamictites of the Ghaub Formation. (A) Polymictic diamictite containing dolostone (light grey) and limestone (dark grey) clasts – note preferential flattening of limestone clasts in the cleavage plane. (B) Gradational contact between massive limestone diamictite and well-bedded turbidites (grey) and laminated dololutite (tan) with outsize clasts (IRD). Pen for scale is 15cm long. (C) Massive diamictite with clasts of limestone 'L', dolostone 'D' and basement-derived granitoid 'G'. The diameter of the coin is 2cm. (D) Limestone-dominated diamictite containing clasts of ooid grainstone derived from Franni-aus Member." (Hoffman 2011)

reached much closer to the equator than they do now (Kirschvink, 1992). The investigations into the sediment layers surrounding the drop stones and in other formations from the Cryogenian seem to support the theory. Banded iron formations which occur during a transition between anoxic and oxygenated oceans were observed at the drop stone sites (Sumner *et al*., 1987; Kirschvink, 1992; Young, 2002). Anoxic oceans are expected on Snowball Earth as the oceans are isolated from the atmosphere by ice (Kirschvink, 1992; Young, 2002). Cap

carbonates were also present, which are distinctive sedimentary layers of carbonate rocks which usually lie above Neoproterozoic glacial deposits (Grotzinger and Knoll, 1995; Hoffman *et al*., 1998). Over the cryochrons, the Snowball Earth hypothesis states silicate weathering would have been greatly reduced by ice and snow cover across the Earth and the halting of the hydrological cycle (Hoffman *et al*., 2017). This resulted in rising atmospheric CO_2 out of equilibrium with the oceans. Eventually, this high pCO_2 became a factor terminating the cryochron, transitioning the planet from ice house to greenhouse conditions (Prave *et al*., 2016). At this point the previously anoxic oceans were exposed to exchange with the atmosphere, rapidly gaining alkalinity resulting in the cap carbonate deposits coinciding with other markers of deglaciation (Kennedy, 1996).

Carbon isotope ratios in the carbon deposits also lend evidence to the climate changes of the Neoproterozoic. Particularly high proportions of $\delta^{13}C$ have been found in Neoproterozoic, which has been interpreted as high fractions of buried organic matter (as organic matter is depleted in $\delta^{13}C$ and so the remaining carbon pool becomes $\delta^{13}C$ enriched) (Hayes *et al*., 1999). The major contributor to this is predicted to be ocean anoxia, which enables greater phosphate recycling and therefore increases the carbon to phosphorus ratio in deposited ocean sediments (Van Cappellen and Ingall, 1996; Ingall and Jahnke, 1997). However more recently other researchers have challenged the time at which these isotopes were deposited (Jiang *et al*., 2010), the confidence with which we can attribute them to oxygen dissolved organic carbon (Bristow and Kennedy, 2008), and whether there is global coverage of ocean anoxia signatures (Sansjofre *et al*., 2011). It has also since been shown that $\delta^{13}C$ records can be altered post-deposition, limiting the confidence with which we can use them to interpret past climate (Oehlert and Swart, 2014). Another marker is oxygen isotopes in Neoproterozoic barite formations. A negative spike in ^{17}O isotopes at the end Marinoan has been interpreted to align with high pCO_2 and/or massive methane release which are predicted to take place at the transition from icehouse to greenhouse conditions (Jiang *et al*., 2003; Bao *et al*., 2008). Methane would have built up through the cryochrons during the organic carbon burial processes (Schrag *et al*., 2002; Jiang *et al*., 2003).The distinct

combination of sediment and glacial rock deposits that might indicate ice covered oceans have now been found worldwide, giving further credence to a Snowball Earth type event. Although the interpretation of geological and chemical evidence has encountered opposition (Eyles and Januszczak, 2004), the occurrence of wild scale glaciation covering much of the Earth is now widely accepted since it has been supported by geochronological and climate model evidence.

Geochronology

The Cryogenian period saw two global glaciations, the Sturtian (717-659 Mya) and Marinoan (~645-635 Mya), separated by an interglacial period (Figure 2) (Pierrehumbert *et al*., 2011; Rooney *et al*., 2015; Hoffman *et al*., 2017). The global glaciations (and sometimes deglaciation or "immediate aftermath") are referred to collectively as "cryochrons" (Hoffman *et al*., 1998). The geochronology of Snowball Earth has been verified by a combination of rhenium-osmium (dating deposition of organic-rich shales) and uranium-lead (dating zircon $ZrSiO_4$ from volcanic rock) radiometric dating, and geochemical data across several paleo-continents (Selby and Creaser, 2003; Mattinson, 2011; Hoffman *et al*., 2017). U-Pb zircon ages have tightly constrained the onset of the first (Sturtian) cryochron to between 717.5 and 716.3 Mya (Macdonald *et al*., 2010). Re-Os dating of multiple cap limestones which proceed glacial-type deposits in combination with U-Pb zircon dating of volcanic ash associated with an Australian glacio-marine deposit, constrain the end Sturtian to 659.3-658.5 Mya (Hoffman *et al*., 2011, 2017). These end-Sturtian cap limestones, absent within the cryochron, also set apart the terminal Sturtian deglaciation from more minor retreat and advance cycles (evidenced from ice-rafted debris) of the ice sheets within the cryochron (Kellerhals and Matter, 2003; Le Heron *et al*., 2013; Yonkee *et al*., 2014; Lan *et al*., 2015; Le Heron, 2015). The nonglacial interlude is characterised by terrigenous and carbonate strata that lack glacial deposits and feature peritidal cycles (Eisbacher, 1981; Hambrey, 1987; Day *et al*., 2004; Hoffman and Halverson, 2008; Rieu and Allen, 2008; Feng *et al*., 2010). During deglaciation ice would have retreated from the oceans and back to the accumulation zones on land. Streams from land terminating glaciers would have distributed ions and subglacial microorganisms across the terrestrial surface and into the sea (Boyd *et*

al., 2014; Lechte *et al*., 2019). The Marinoan glacial onset is loosely constrained between 649.9 and 639.0 Mya by Re-Os dating of South Australian organic rich shale, and U-Pb dating of volcanic zircon with glacio-marine diamictite (Kendall *et al*., 2006; Prave *et al*., 2016). Cap dolostone, continuous deposits of pale grainy dolostone created by post-glacial flooding, are characteristic of the end Marinoan and have been used to constrain its geochronology to between 636.0 and 634.7 Mya though U-Pb dating (Kennedy, 1996; Shields, 2005; Hoffman *et al*., 2007; Hoffman, 2011).

The primary theory for the mechanism of global glaciation is that after significant global cooling due to orbital forcing and low carbon dioxide, the ice-covered polar areas became large enough to initiate a runaway albedo effect (Hoffman *et al*., 1998). As global air temperature lowered, ice of the polar regions encroached north and south towards the equator. These areas, lighter in colour, reflect more light away from the surface, cooling the surface again. In addition, the lower temperature resulted in the precipitation of salt within sea ice brine inclusions, which further increases albedo (Carns *et al*., 2015). The overall cooling could theoretically continue exponentially. This would be made possible by the unusual situation of continental land mass at middle and low latitudes, lowering the albedo of the sub-tropics (Kirschvink, 1992). It has now been established that this process would not be irreversible, and a global glaciation could self-terminate (Walker *et al*., 1981). The disruption of normal precipitation, seafloor weathering and silicate weathering by a dry ice covered Earth surface and cold ocean would cause all CO_2 released by volcanic activity to accumulate in the atmosphere (Turbet *et al*., 2017). Sublimation of CO_2 at the poles enabled by strong solar radiation is estimated to be sufficient to prevent irreversible CO_2 deposition (Turbet *et al*., 2017). As the resulting CO_2 greenhouse effect increased, and dust covered increasingly large amounts of the Earth, deglaciation was able to occur (Walker *et al*., 1981; Pierrehumbert *et al*., 2011; Yang *et al*., 2017).

ii. Conditions on Snowball Earth

Paleogeography

Most land during the Cryogenian was positioned at low latitudes, as part of the supercontinent Rodinia (Figure 6). This absence of land at the poles may have further raised the planetary albedo, although diminished evaporative cooling at the tropics would countered some of the resultant global cooling (Kirschvink, 1992). Over the Cryogenian Rodinia broke up, though the uncertainty in configuration of Rodinia over the period poses challenges for interpreting more specific paleogeography (Evans, 2000; Hoffman *et al*., 2017).

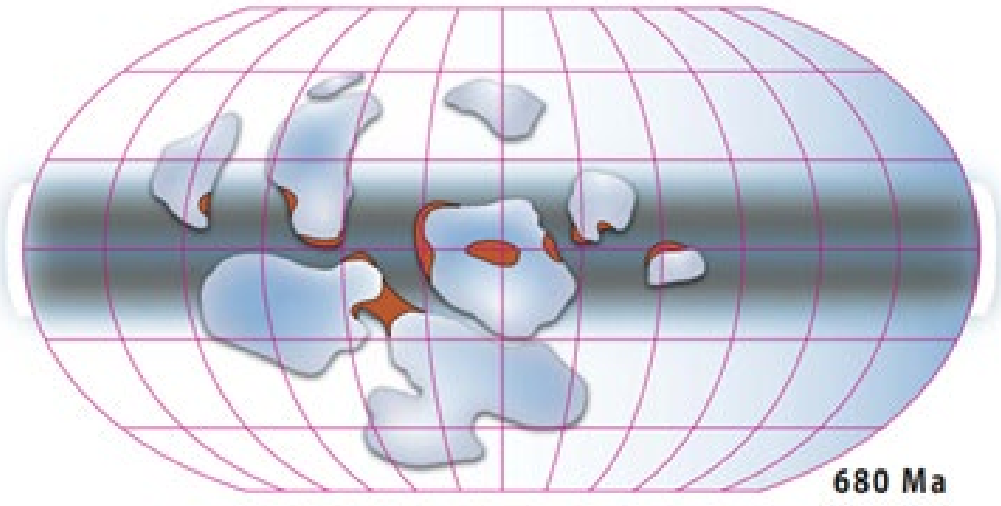

Figure 6 "Global paleogeography during the Sturtian cryochron at 680 Ma. Brown continental areas schematically indicate dry-valley dust sources. Gray areas in the low-latitude sublimation zone of the sea glacier [frozen ocean] are schematic cryoconite ponds." (Hoffman et al. 2017)

CO_2 and surface temperature

CO_2 levels rose throughout the Cryogenian period. Climate models suggest that the onset of Snowball Earth occurred at low CO_2 (0.1-1 mbar) (Benn *et al*., 2015). Eventually, through a combination of the reduction of photosynthesis in the ice covered oceans and continental weathering, the consumption of CO_2 crashed and the atmospheric levels soared to 0.1-100 mbar, initiating global deglaciation (Vidal

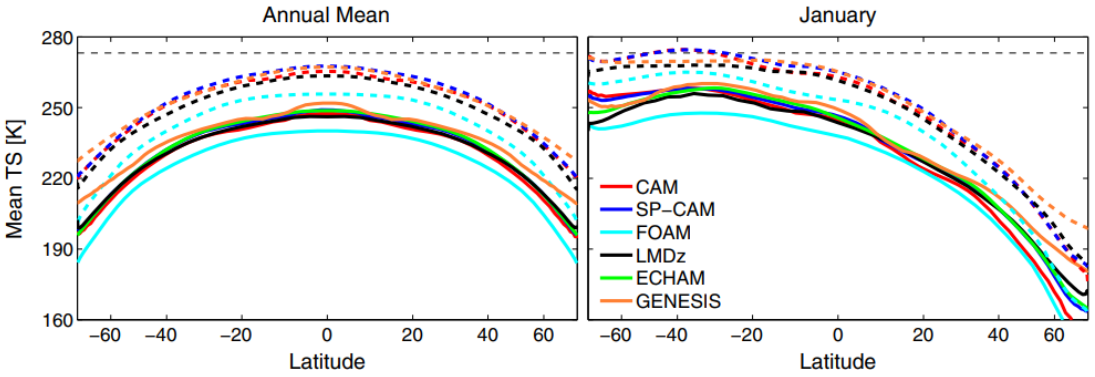

Figure 7 "(left) Annual and (right) January zonal mean surface temperature for the GCMs run with $CO_2 = 10^{-4}$ (thick solid lines) and $CO_2 = 0.1$ (thick dashed lines). The thin dashed black line denotes the melting temperature of pure ice. The surface albedo is set to 0.6 in these simulations, so we neglect the effect of snow and dust on the surface albedo." (Abbot et al. 2013)

and Moczydłowska-Vidal, 1997; Le Hir *et al*., 2008b; Benn *et al*., 2015). Abbot *et al* (2013) compiled several models for Cryogenian surface temperature at the early Snowball Earth low CO_2 and end Snowball Earth high CO_2 levels (Figure 7). At the low CO_2 value, all models predict temperatures firmly below -20°C at all latitudes. At high CO_2, some models predict summer temperature could rise above freezing in some regions while others place the entire temperature range below 0°C (Abbot *et al*., 2013).

Water availability

The presence or absence of liquid surface oceans is another factor that drastically affects global temperature. Heat is absorbed by the ocean during periods of warmth and released at periods of cold, warm water is transported across the Earth and to the poles, cold water is displaced by warmer water at the surface which is released into the atmosphere (Faizal and Ahmed, 2011). As this would not be possible on an entirely or predominantly ice-covered planet, Hoffman and Schrag predict temperature oscillations on a diurnal and annual scale on Snowball Earth would be amplified (Hoffman and Schrag, 2002). At afternoon temperatures, meltwater would evaporate to produce low levels of atmospheric water vapour (Hoffman and Schrag, 2002). While overall Snowball Earth had a cold, dry atmosphere more akin to Mars than our current planetary conditions, a higher

atmospheric pressure than that of Mars coupled with the amplified temperature oscillations could facilitate liquid surface water (Hoffman and Schrag, 2002). Water vapour would be also be able to accumulate at the equatorial sea ice through sublimation of ice (Hoffman *et al*., 2017). However, surface water would be limited and close to 0°C in temperature (Hoffman and Schrag, 2002; Hoffman *et al*., 2017). Sea water would be covered with ice, with little light availability (Warren *et al*., 2002; Goodman and Pierrehumbert, 2003).

Ice covered oceans are predicted to have contained low levels of dissolved oxygen, as gas exchange between air and water was limited (Kirschvink, 1992). Iron formations found in end-Cryogenian deposits are thought to represent the transition between anoxia and oxygenation during deglaciation (Kirschvink, 1992; Klein and Beukes, 1993). Redox conditions impact the behaviour of molybdenum in seawater, and molybdenum isotope studies (δ^{98}Mo) from Cryogenian shales also reflect anoxia across the Cryogenian oceans (Cheng *et al*., 2018). The authors assert this is evidence against areas of open ocean during the cryochrons (Cheng *et al*., 2018). Hoffman *et al*. predict that in the anoxic oceans, sulphate and Fe (III) will replace oxygen as terminal electron acceptors for microorganisms (Hoffman *et al*., 2017). The sulphate and Fe (III) would be replenished from glacier beds and meltwater from the surface, in the same way it occurs in the modern day (Hawkings *et al*., 2020). Curiously, there is evidence that the ocean of the interglacial period remained anoxic (Ye *et al*., 2018). This calls into question the relationship between ocean anoxia and ice free oceans. Regardless, open and oxygenated water would be limited compared to unglaciated climate conditions.

Ice sheet dynamics and thickness

The glacier signatures in the geological and sedimentary record (see section i) show that glaciers and ice sheets were dynamic throughout the cryochrons (Sumner *et al*., 1987; Hoffmann *et al*., 2004; Le Heron and Busfield, 2014). It has been suggested that the sea ice may also have been dynamic with several kilometre thick sea ice masses (sometimes referred to as ‘sea glaciers’) flowing through basal sliding, initiated by deformation and pressure at the base of the ice caused by the

ice weight (Thomas and MacAyeal, 1982; Hoffman *et al*., 1998, 1999; Christie-Blick *et al*., 1999; Goodman and Pierrehumbert, 2003). In a contrasting model (McKay, 2000), the sea ice is static and all geological evidence of dynamic ice would have been caused by land bound glaciers and ice sheets. However this model relies on lower sea ice thicknesses which has been called into question given predicted Snowball Earth temperatures (Warren *et al*., 2002). In Kirschvink's original proposal of the conditions of Snowball Earth, he imagined areas of open water at the regions of highest solar irradiance (Kirschvink, 1992). Some mathematical models based on predicted temperature suggest that during Snowball Earth there would have been some regions of ice that were under 10 m in thickness, allowing for light to pass through to the extent that photosynthesis would be possible (McKay, 2000). A study by Warren *et al*. (2002) used further models that also took into account absorption of solar radiation that produced two possible scenarios. In the first the high albedo of Snowball Earth would enable thick ice to form across the entire globe, rendering under-ice photosynthesis unlikely; in the second the ice freezes slower, allowing for more light to pass through and creating a lower albedo until ice is <1m thick in some regions (Warren *et al*., 2002). It was suggested that even in a scenario with sections on thin ice, the thick sea glaciers from higher latitudes would flow down and disrupt these areas (Warren *et al*., 2002; Goodman and Pierrehumbert, 2003).

As a "hard" Snowball Earth with thick ice covering much of the planet's surface fits best with geological data, models have been proposed where the Earth is predominantly covered in thick ice sheets, but lakes of thin ice <10m in thickness are protected from thick ice shelves by continental masses at the equatorial zone. One such model was devised by coupling an energy-balance climate model to an ice-shelf flow model (Pollard and Kasting, 2005). However, the value ranges used for the albedo of cold glacier ice, the depth of transition from snow to ice, and the thermal conductivity of ice in this model have been called into question (Warren and Brandt, 2006). It is still debated today whether Snowball Earth lacked large ice-free or thin ice areas but sub-ice photosynthesis cannot currently be relied on as the primary mode of survival of life (Pollard and Kasting, 2005; Hoffman, 2016).

iii. Life of the Cryogenian

Significance in the evolutionary timeline

The Cryogenian period falls between the Tonian (1000-720 Mya), at which time life was still generally unicellular, and the Ediacaran (635-542 Mya) (Ogg, 2004; Knoll *et al*., 2006b) (Figure 2). It is from the Ediacaran that we have recovered fossils of macroscopic organisms that appear to have recognisably metazoan body plans (Droser and Gehling, 2015). The end of this short period is marked by the Cambrian explosion 541 million years ago, the time when a large spike in evolution lead to the emergence of the phyla that encompass modern metazoans, such as arthropods and molluscs (Conway-Morris, 2003). Not only must life have survived Snowball Earth, it appears to have been a turning point in our evolutionary history.

Because of this, many have now argued Snowball Earth may have been a fundamental step in the sequence of events leading to the Cambrian explosion. Following the initiation of Snowball Earth, some expect a mass extinction to have occurred and a reduction in the emergence of new species: an 'evolutionary bottleneck' (Runnegar, 2000). Mass extinctions are often followed by a rapid increase in biodiversity as new species fill the available ecological niches (Courtillot and Gaudemer, 1996). It is difficult to reconcile these hypotheses with fossil data as the record is sparse for the Cryogenian (Cohen and Macdonald, 2015). Not only are there relatively few sites uncovered, identifying the organisms present can be very challenging. From microfossils it is only possible to gain a general sense of cell morphology, which will often inform us of a broad grouping in which the cell belongs but give little indication of its relation to extant species. For example, acritarch is a term used to denote a range of organic microfossils that are known to be eukaryotic but have few further markers for identification. Some are thought to be ancestors of algae or dinoflagellates and are re-classified but many remain a mystery (Evitt, 1963; Gaucher and Sprechmann, 2009). However, despite these

difficulties, some Cryogenian fossils are being studied to uncover what forms of life may have been present during the Snowball Earth period.

Fossil record

In his 2016 paper, Hoffman asserts that the fossil evidence of eukaryotic crown groups that emerged before the Cryogenian and survived into the Ediacaran challenges the theory of a eukaryotic evolutionary bottleneck (Hoffman, 2016). A study by Sergeev *et al* 2009 on the Mesoproterozoic Ust'-Il'ya Formation in Siberia shows that although Cyanobacteria could be said to be dominant at this time, a diverse array of eukaryotic microfossils were present (Sergeev *et al*., 2017). Diagnostic cell division patterns, morphology and other structural features identified what appears to be red and green algae from well before the first major glaciation of the Cryogenian (Butterfield *et al*., 1988; Butterfield, 2000; Graham *et al*., 2013). Vase-shaped microfossils found in the Grand Canyon and, more recently, Yukon Canada have been interpreted to be Neoproterozoic analogue of modern testate amoebae (Porter and Knoll, 2000; Porter *et al*., 2003; Strauss *et al*., 2014). One other example is a collection of microbial mats from Death Valley, California. These mats that contain what are proposed to be eukaryotic and bacterial autotrophs including Cyanobacteria, as well as eukaryotic heterotrophs (Corsetti *et al*., 2003). The heterotrophs also include similar vase-shaped fossils (Corsetti *et al*., 2003). In the Zambian Kakontwe Formation and the Mongolian Taishir Formation, microfossils have actually been discovered in the Cryogenian cap carbonate deposits that were formed following the Sturtian glaciation (Moore *et al*., 2017). These included fossils that, much like the other vase-shaped microfossils mentioned, resemble test-forming eukaryotes, such as testate amoeba (Moore *et al*., 2017).

Biomarker record

Complete preserved organisms are no longer the only remnants of past organisms it is possible to collect. Certain hydrocarbons have become fossilised, and remain intact for many millennia (Brocks and Summons, 2003). These are referred to as

biomarkers, as the type of organism they originate from can be traced from their molecular structure (Brocks and Pearson, 2005). In 2005, a report was published on biomarker evidence for photosynthetic activity from both bacteria and eukaryotes during the Cryogenian (Olcott *et al*., 2005). This was interpreted as evidence for a Waterbelt or thin-ice Snowball Earth. However, algal blooms colonising thinner ice "cracking" areas and the flushing of autotrophs into the ocean from the surface are permissible in current hard Snowball Earth scenarios (Hoffman *et al*., 2017); whether this would be sufficient to explain marine deposits of photoautotrophs is still uncertain. It is now possible to estimate the proportion of eukaryotic vs bacterial and archaeal organic matter contributing to Cryogenian sediment (Gold *et al*., 2017; Brocks, 2018). The results show a "rise of algae" in the interglacial gap between the Sturtian and Marinoan glaciations (Figure 2); the contribution of eukaryotic hydrocarbons greatly increased (Brocks *et al*., 2017; Brocks, 2018). Brocks (2018) proposed two possible mechanisms for this. The first is that there was in fact a mass extinction and evolutionary bottleneck, but that it only spanned the Sturtian glaciation and specifically affected those marine organisms not suited to the hyposaline water resulting from deglaciation (Brocks, 2018). The second is that before Snowball Earth, the oceans had low levels of nutrients and oxygen which favoured smaller cells and so favoured bacteria and archaea. The transport of nutrient rich debris upset this, and allowed the larger algal cells to thrive (Brocks, 2018). Zumberge *et al*. (2020) asserted that lipid biomarkers associated with red algae indicate that this group had proliferated and become a dominant group as early as the late Tonian, (Zumberge *et al*., 2020). Therefore the observations of changes over the Cryogenian interglacial gap may reflect a rise of green algae rather than a transition from prokaryotic to eukaryotic dominance.

Biomarkers can reveal not only taxa present but something of their functionality and activity. Methanogenesis and tolerance of high salinity have been found among bacteria and archaea of the Tonian (Schinteie and Brocks, 2017). The authors suggest that since the composition of biomarkers in these formations closely resemble lipid compositions from modern hypersaline Cyanobacterial mats, these communities may be evolutionarily conserved since the Neoproterozoic (Schinteie

and Brocks, 2017). If this is the case, halophiles must have persisted through the Cryogenian. In 2009 a continuous 100 million year sterane fossil record associated with demosponges was found underlying Marinoan cap carbonates, indicating that animal life had developed in the oceans by at the latest the late Cryogenian (Love *et al.*, 2009; Sperling *et al.*, 2010; Zumberge *et al.*, 2018). This important discovery pushes back the emergence of metazoans from the warmer Ediacaran, potentially to the cold Cryogenian. However, some doubt has been cast on whether these steranes are exclusively diagnostic for demosponges. A recent study found that one sterane in question, C_{30} 24-isopropylcholestane, can also be produced by the methylation of C_{29} sterols (produced by Chlorophyta) (Bobrovskiy *et al*., 2021). Another two proposed demosponge biomarkers, 26-methylcholestane and 26-methylstigmastane, have also been shown to have a potential abiogenic source, as they can be formed by pyrolysis under laboratory conditions (van Maldegem *et al*., 2021). This ongoing debate further illustrates the importance of understanding Cryogenian life, and how many forms of life could have survived through Snowball Earth.

Molecular clock record

This fossil record is being studied in conjunction with molecular data. Molecular clocks use the rate that DNA mutates and changes to trace back the divergence of organisms in evolutionary time. The appearance of different organisms in the fossil record is compared to the dates the molecular clock predicts that they emerged. The incorporation of dated fossils provides us with a time-calibrated molecular clock. The dates produced by the molecular clock tend to predict earlier divergences than have been proposed by examining the fossil record alone (Douzery *et al*., 2004). It is not always clear whether this is an accurate representation or due to limitations of the molecular dating technique.

The main application of these molecular clocks when studying the Cryogenian is to study the emergence of new eukaryotic species, known as the radiation of the eukaryotes. Molecular clocks suggest bacterial and archaeal single celled life was already well established by the time Snowball Earth occurred and the period

preceding it has been referred to as the “boring billion” as life progressed without developing complex multicellularity (Lyons *et al*., 2012). However, the Cryogenian takes place in a time of drastic change for eukaryotes; sitting between the ages of the single cell and complex multicellular life. A study (Sánchez-Baracaldo *et al*., 2017) focused on the origin and diversification of photosynthetic eukaryotes. It utilised a relaxed molecular clock, one that allows the rate of DNA alteration to vary between branches of the phylogenetic tree (Sánchez-Baracaldo *et al*., 2017). The relaxed clock is useful as it allows several independent calibrations and prior knowledge of divergence times to be integrated in the model. 18 fossil calibrations were integrated into maximum likelihood and Bayesian phylogenetic trees. The results placed the emergence of Rhodophyta and Chlorophyta in the Mesoproterozoic Stenian period (1200-1000 Mya); and the emergence of Palmophyllophyceae and Prasinophyceae in the late Tonian (1000-720 Mya) or early Cryogenian period (Sánchez-Baracaldo *et al*. 2017). A multigene molecular clock devised by Parfrey *et al*. 2011 correlates to some extent with these findings. The Rhodophyta were similarly placed at the end of the Stenian, but the Chlorophyta slightly more recently, in the early Tonian (Parfrey *et al*., 2011). An earlier relaxed molecular clock predicts dates even later, placing the emergence of the Rhodophyta and Chlorophyta and the early Tonian and late Tonian respectively (Douzery *et al*., 2004). Whatever the comparative accuracy of each clock, it seems to be the consensus that the Chlorophyta and Rhodophyta were established before the start of the Cryogenian and so must have persisted through this time (Table 1).

Interestingly, it has been predicted that some other unicellular eukaryotes emerged during the glaciations of the Cryogenian (Table 1). The model by Parfrey *et al* placed the emergence of protists belonging to the Excavata and SAR supergroups including members of the alveolates through the Cryogenian (Parfrey *et al*., 2011). The earlier clock by Douzery *et al* still places the first alveolates within this time frame (Douzery *et al*., 2004). If these groups continued to persist and diversify, this might be considered evidence against a mass eukaryotic extinction in the Cryogenian.

The timing of the metazoan radiation is an important debate. The two foci of the Douzery clock were the emergence of metazoans from choanoflagellates which was placed in the Tonian, and the divergence of protostomes and deuterostomes which was placed in the Cryogenian (Douzery *et al*. 2004). This closely correlates with results from the Parfrey clock and the expectations from the fossil record (Douzery *et al*., 2004; Parfrey *et al*., 2011). Two clocks that focused on the radiation of metazoans using microRNAs instead place the protostome-deuterostome divergence as the start of the Ediacaran 635 Mya (Peterson and Butterfield, 2005; Wheeler *et al*., 2009). Both predict that the earlier Porifera/Eumetazoa division (the divergence of other metazoans from the sponges) took place before the Cryogenian (Table 1).

Table 1 Dates in million years ago of the evolutionary emergence of significant taxa according to various authors. Data was collated from papers (listed left hand column) that used molecular clocks to estimate emergence dates.

	Rhodophyta	Chlorophyta	Metazoans	Eumetazoa/ Porifera	Protostomes/ Deuterostomes	Alveolates
Sánchez-Baracaldo et al 2017	1100	1200	/	/	/	/
Parfrey et al 2011	1250	900	900	750	700	1300
Wheeler et al 2009	/	/	/	760	635	/
Peterson & Butterfield 2005	/	/	/	875	635	/
Douzery et al 2004	928	729	849	/	695	750

Table 1 summarises the estimated dates described. Clearly, significant developments took place in the periods before and after the Cryogenian. It also appears that they continued to take place during this period, countering theories

that life was stunted through the Cryogenian. However, a limitation of using molecular clocks to explore changes in ecology over time is that only extant species can be used to trace back lineage. The result will be a collection of common ancestors of living species, while extinct lines won't be represented. It is therefore difficult to compare metrics such as diversity over time. In that case, apparent diversity found in collections of microfossils may be more useful. What the fossil record and molecular clocks together do tell us is that complex life including photosynthetic eukaryotes, protists and early animals must have survived the Cryogenian and Snowball Earth.

iv. Microbial ecosystems of the modern cryosphere

To understand how the microorganisms of the Cryogenian survived ice house conditions, I have evaluated likely analogues in the modern cryosphere.

Cold ocean habitats

The ocean holds >6 Gt of carbon in biomass, approximately two thirds of which is made up of unicellular organisms (Bar-On and Milo, 2019). Particular attention has been given to the benthic life under Antarctic sea ice due to the unique qualities of the ecosystem (large slow moving animals adapted to the cold waters) and its sensitivity to climate change (vulnerability of species to increased ice scouring and predation by colonisers from warmer waters) (Gibson and Atkinson, 2003; Thatje *et al*., 2005; Aronson *et al*., 2007; Barnes and Conlan, 2007). In the deep sea, life has survived under ice and open water where light cannot reach. Sources of significant heat in the polar seas are limited to hydrothermal vents and thermohaline currents (Wyrtki, 1961; Williams *et al*., 1974). Hydrothermal vents, support particular diversity of deep sea organisms in these regions. The vents are made of mineral chimneys containing metals such as copper and iron that form around a plume of hydrothermal fluid that has been heated by magma or rocks below (Fisher *et al*., 2007). The heat and chemical expulsions from hydrothermal vents sustain hotspots of biodiversity despite low temperature and low light under the ice.

Chemolithoautotrophs are the primary producers of these ecosystems, deriving all the energy they require from the chemical kinetics of the vents (Ruby *et al*., 1981). Metagenomic sequencing, in conjunction with immunohistochemistry and mass spectrometry, has revealed that a wide range of species from heterotrophic bacteria to metazoans form symbiotic relationships with chemolithotrophs on the vents (Petersen *et al*., 2011). Organisms as complex as tube worms, barnacles and mussels have been found alongside the bacteria and methanogenic archaea we might expect in the deep sea (Fisher *et al*., 2007). Upon discovery of hydrothermal vents, it was suggested the organisms found there could be a relic from early evolution; a deep sea origin of complex life (Newman, 1985). Molecular clocks give little support to this idea and suggest that the ecosystems of the vents have changed no less than any other (Little and Vrijenhoek, 2003). Some members of these deep sea ecosystems may have the ability to survive a global glaciation, as they survive solely on the exploitation of redox reactions by chemolithoautotrophs around the vents. However, the frozen oceans of Snowball Earth would still have had a significant impact. Much of the life of the deep sea is supported by organic detritus from the photosynthetically active layer above (Jørgensen and Boetius, 2007). It may well be that the ecosystems forming around these vents were far more isolated, so unrecognisable to those present today.

In shallow Antarctic seas <10m in depth, the sea bed also supports photosynthetic macroalgae despite thin ice above and extended periods of darkness during winter, their activity verified using fluorometry (Runcie and Riddle, 2006). However, the majority of photosynthetic life subsists at or near the surface. In the Arctic, vast phytoplankton blooms have been observed underneath sea ice, dominated by diatoms (Arrigo *et al*., 2012). Some blooms have been discovered associated with the bottom of the ice until they are suddenly released during seasonal sea ice melt (Michel *et al*., 1996). This forms the basis for a wider ecosystem, from single celled heterotrophs to crustacean families such as Gammaridae, Calliopiidae and Euphausiidae (krill) which graze on the bottom-ice algae (Michel *et al*., 1996; Werner, 1997). The possibility of widespread photosynthesis under Antarctic ice is now also starting to be explored (Horvat *et al*., 2021).

Lakes

Periglacial, proglacial and moraine lakes contain a range of bacterial and eukaryotic microorganisms. Mindl *et al*. measured aquatic bacterial abundance and productivity on a transect from the glacier surface to proglacial lakes on Midtre Lovénbreen glacier Svalbard and maximum values for both abundance and productivity were found at the proglacial lakes (Mindl *et al*., 2007). Both Cyanobacterial and algal mats have been recovered from such lakes, as have major groups of heterotrophs including Proteobacteria, Actinobacteria, Firmicutes and Bacteroidetes using DNA fingerprinting and community metabarcoding (Pearce, 2005; Liu *et al*., 2011; Anesio and Laybourn-Parry, 2012; Sohm *et al*., 2020). Many periglacial, proglacial and moraine lakes are ice covered for all or much of the year (Greco *et al*., 2020; Sohm *et al*., 2020). During this time, little to no meltwater is available and temperatures are low so many organisms are inactive, or their metabolism is severely reduced. The Cyanobacteria of the Antarctic McMurdo Dry Valleys mats become more metabolically active in the austral summer for a period of around eight weeks (Sohm *et al*., 2020). During the Cryogenian ice-free areas would be limited. Therefore perennially ice covered lakes such as Lake Untersee may represent the most relevant lake analogues. Greco *et al*. report that despite low light transmission through the ice, the benthos of Lake Untersee is covered by complex microbial mats capable of supporting bacterial, archaeal and eukaryotic life and dominated by Cyanobacteria, Proteobacteria, Verrucomicrobia, Planctomycetes, Actinobacteria, Ciliophora, Chlorophyta, Fungi, Cercozoa, and Discicristata (Greco *et al*., 2020).

Supraglacial lakes on glacier and ice sheet surfaces are formed by collected surface meltwater and precipitation. This meltwater is typically low in microbial richness and diversity (Leppäranta *et al*., 2013). The supraglacial lakes are often highly ephemeral and prone to rapid draining events, making them too unstable for complex ecosystems to develop (Laybourn-Parry and Wadham, 2014). However, the microorganisms and microbe-mineral aggregates in supraglacial lakes are increased when supraglacial lakes collect cryoconite matter, adjoining to cryoconite holes. For example, supraglacial lakes on Canada Glacier (Taylor Valley, McMurdo

Dry Valleys) are connected to numerous cryoconite holes through the drainage system (Bagshaw *et al*., 2010). The term 'cryolake' tends to refer in particular supraglacial bodies of water containing cryoconite-like sediment and microorganisms swept together by katabatic winds at ice cliff shelves (although it is sometimes used interchangeably with 'supraglacial lake') (Laybourn-Parry and Wadham, 2014; Anesio and Laybourn-Parry, 2021). Many of these lakes, like cryoconite holes, are covered by ice for all or most of the year (Bagshaw *et al*., 2010). When the supraglacial lakes containing microorganisms drain, this may connect the microbial ecosystems of the surface to the subglacial ecosystems (Anesio and Laybourn-Parry, 2021).

Subglacial ecosystems

Where the glacier ice and underlying ground meet, the pressure creates a lower melting threshold for water (Röthlisberger, 1972). As a result, water may accumulate beneath the ice (Lliboutry, 1968; Le Brocq *et al.*, 2013; Palmer *et al.*, 2013). In this environment water and bedrock come into contact with each other, exposing minerals in small particles and providing opportunity for chemolithotrophy (Sharp *et al*., 1999; Tranter *et al*., 2002; Statham *et al*., 2008; Wadham *et al*., 2010). Cell counts revealed subglacial bacterial populations are considerably larger than those found on and in the ice (Sharp *et al*., 1999). The chemolithotrophy then further contributes to mineral weathering (Sharp *et al*., 1999; Montross *et al*., 2013). Montross *et al*. found biotic weathering of glaciated sediments to be up to eight times more rapid than abiotic weathering (Montross *et al*., 2013). Cold adapted Thiobacillus anaerobes were found which oxidise sulphate, and may also fix carbon and respire both aerobically and anaerobically (Harrold *et al*., 2015). Strict anaerobes and facultative anaerobes have both been recovered from subglacial environments (Harrold *et al*., 2015; Zdanowski *et al*., 2017). Aerobes are also present and are thought to have persisted in subglacial environments through Snowball Earth (Skidmore *et al*., 2000; Lechte *et al*., 2019). Despite the generally low abundance of archaea in the polar regions, archaeal methanogens have been recovered from the Arctic, sub-Arctic and Antarctic (Boyd *et al*., 2010; Stibal *et al*., 2012c)

Ice surface and snow habitats

'Snow algae' and algal blooms on ice surfaces have been studied in many cold climates around the globe (Kawecka and Drake, 1978; Fujii *et al*., 2010; Lutz *et al*., 2014, 2015). "Red" and "green" snow algae appear in striking blooms during the summer, thanks to the colourful pigments employed by the abundant Chlorophyta to protect them from solar radiation (Lutz *et al*., 2015). Species such as *Ancylonema nordenskiöldii* and a *Mesotaenium* species were found to be able to directly colonise ice surfaces (Lutz *et al*., 2018). Blooms on the ice surface are known as 'glacier algae'. It has been suggested the algae survive the harsh conditions by staying dormant for most of the year (Remias, 2012). Their role as carbon fixers and primary producers identifies them as important components of the glacial surface ecosystem, which is also home to bacteria, archaea, fungi and viruses (Anesio *et al*., 2017). DNA amplicon sequencing has revealed bacterial taxa also reside in the algal layers; Betaproteobacteria, Cyanobacteria and Proteobacteria were particularly abundant. However, these habitats are generally less biodiverse than the cryoconite holes which snow and glacier algae are frequently swept into (Takeuchi *et al*., 2001a; Lutz *et al*., 2014).

Cryoconite

Cryoconite has been noted on glaciers since the 19th century described as "a sandy trachytic mineral" and "grey-coloured powder with some remains of vegetable fragments" on the surfaces of glaciers by Adolf Eric Nordenskjöld during a Greenland expedition, in the earliest formal written account of cryoconite (Nordenskjold, 1875). It was in this record that the term cryoconite (originally 'Kryoconite') was coined, a combination of the Greek terms 'cryo' and 'conite' meaning ice and dust respectively. Drygalski and Kühl determined the source of cryoconite inorganic matter is terrestrial but often distal, as there was evidence of organic matter and detritus deposited by animals in the cryoconite (von Drygalski and Kühl, 1897). Heterotrophic bacteria, microalgae, diatoms, fungi, protists and microinvertebrates were identified in cryoconite firstly using simple chemical assays and microscopy (Steinbock, 1936; Gerdel and Drouet, 1960; Charlesworth, 1966),

and then later using DNA terminal restriction fragment-length polymorphism (T-RFLP) (Cameron *et al*., 2012b; Edwards *et al*., 2013a), metabarcoding (Webster-Brown *et al*., 2015; Liu *et al*., 2017; Lutz *et al*., 2019) and metagenomics (Edwards *et al*., 2013b; Bellas *et al*., 2020). Filamentous Cyanobacteria were identified to be the component of the community that aggregates the component organic and inorganic matter (Gerdel and Drouet, 1960). Cryoconite is key part of glacier biogeochemistry and is a significant contributor to carbon and nitrogen cycling on the glacier surface (Porazinska *et al*., 2004; Bagshaw *et al*., 2007, 2013; Edwards *et al*., 2013b; Bagshaw *et al*., 2016a). Cryoconite communities are also known for their resilience to environmental stress. Cryoconite holes, the habitats formed when cryoconite melts into the glacier surface, freeze completely in colder glaciated areas (Figure 9). Frozen or ice lidded cryoconite must also endure low levels of light under the ice. Open lidded cryoconite holes are exposed to high light during the summer and low light over winter. Cryoconite holes, particularly entombed (ice lidded) and isolated (not hydrologically connected to other cryoconite holes or streams) reach extreme levels of pH and low levels of nutrients (Tranter *et al*., 2004; Webster-Brown *et al*., 2015; Poniecka *et al*., 2020). Due to this resilience coupled with cryoconite biodiversity (Nicholes *et al*., 2019), cryoconite habitats are important features of modern glaciers and therefore certainly glaciers of the past. Cryoconite holes have also been presented as model experimental mesocosms for the study of ecosystem development (Sommers *et al*., 2019). As cryoconite is given particular attention in this thesis, a more detailed review is presented below.

v. Cryoconite in the cryosphere

Development and structure of cryoconite holes

The melting and freezing of cryoconite holes was first described by Drygalski (von Drygalski and Kühl, 1897). The dark colour of the cryoconite absorbs solar radiation, often forming near cylindrical holes containing meltwater in ice surfaces known as cryoconite holes (Steinbock, 1936). The sediment becomes redistributed as the hole

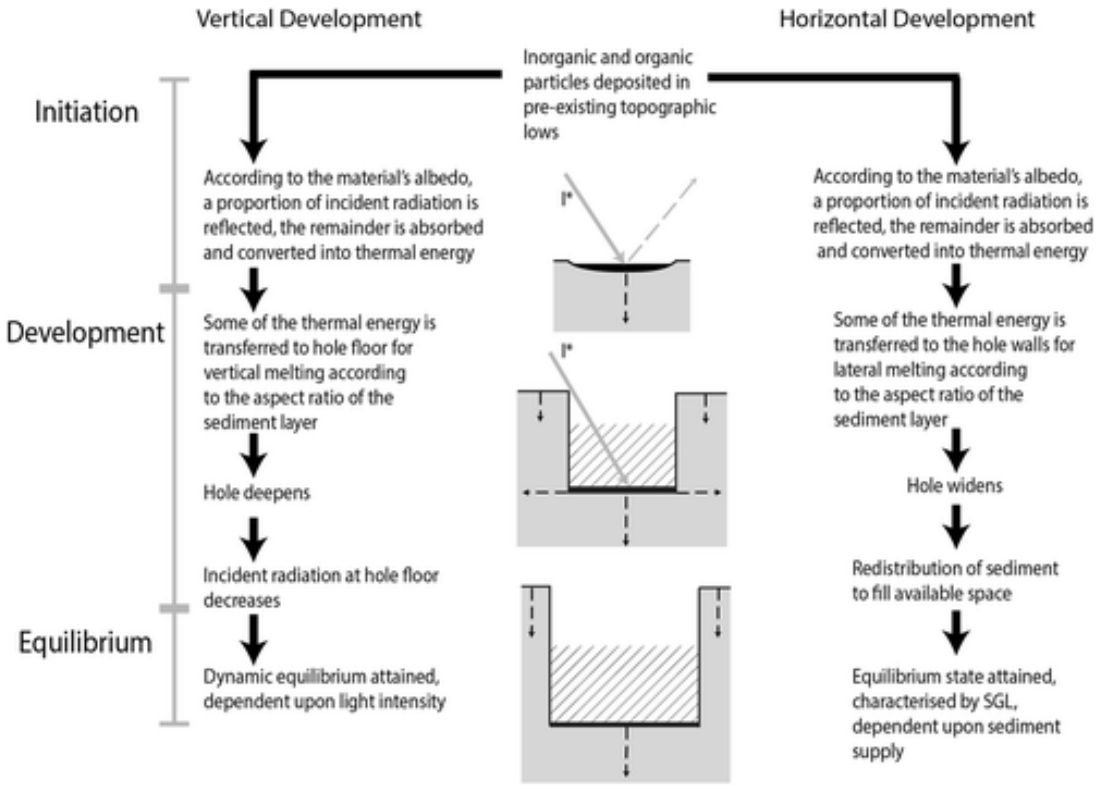

Figure 8 "Flow diagram depicting the vertical and horizontal development of cryoconite holes. The term 'I*' refers to solar radiation and 'SGL' stands for single grain layer. Ice is depicted using light grey shading and water is depicted using diagonal hatching." (Cook et al. 2015)

grows in diameter and depth (Figure 8). Eventually equilibrium is reached where the radiation is not sufficient to expand the hole any further (McIntyre, 1984; Zamora, 2018). The equilibrium depth is determined by cryoconite albedo, the penetration of solar radiation through ice, and environmental conditions such as glacier sub surface heat flux (McIntyre, 1984; Zamora, 2018). A hole evolution study compared near identical holes in the ice with and without cryoconite (cryoconite had been removed from developed cryoconite holes to produce "blank" holes) (Hodson *et al*., 2010). Holes containing cryoconite were confirmed to deepen at a far higher rate than blank holes. Hydraulic processes and microbial activities may contribute to hole development to some extent, but the primary factor is solar radiation (McIntyre, 1984). In colder regions, water above the cryoconite will then refreeze on a seasonal or sub-seasonal time scale forming 'ice lids' (von Drygalski and Kühl, 1897; Fountain *et al*., 2004).

The structure of the cryoconite holes varies greatly, driven by the local environmental conditions and described in the following sections (Figure 9). In cold, dry climates such as the McMurdo Dry Valleys of Antarctica, cryoconite holes are often lidded with ice through most or all of the year (Tranter *et al.*, 2004). Ice lids of up to 30cm have been observed on the majority of cryoconite holes year-round (Fountain *et al*., 2004). Some of these thick lids may only melt during particularly warm periods years apart (Doran *et al*., 2002). Many Antarctic cryoconite holes are frozen completely and melted again on a seasonal or sub-seasonal timescale (Bagshaw *et al*., 2007). In the McMurdo Dry Valleys,

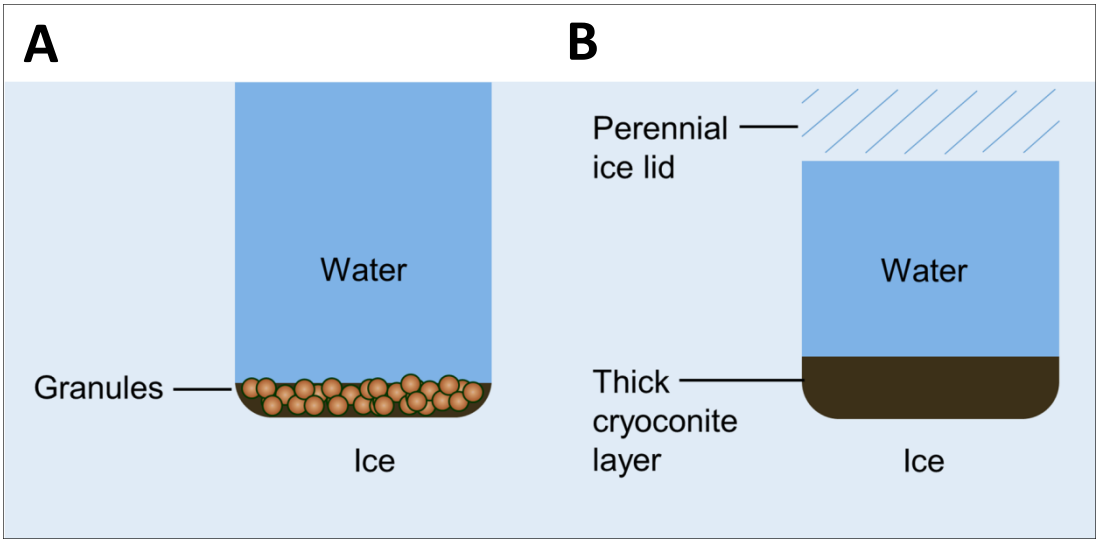

Figure 9 Two cryoconite structures. Structure **A** is typical for warmer Arctic and alpine cryoconite holes; the cryoconite hole is open to the atmosphere and contains a layer of granulated sediment. It may be connected to other cryoconite holes at the surface and possibly within the ice. Structure **B** is typical for cryoconite holes in colder region such as mainland Antarctica and is covered by a thick ice lid. The cryoconite within is a thick layer several centimetres in depth. Some ice lidded cryoconite holes also have a pocket of air between the water and ice lid. These cryoconite holes may be hydrologically connected underneath the ice.

temperatures are significantly below zero, but water in cryoconite holes is kept above freezing in the summer months,, absorbing solar radiation through the ice lid. In these closed lidded environments there is little interaction with the wider environment for the organisms within while they are entombed. Around 50% of lidded holes are connected under the ice surface; the other 50% are completely isolated (Fountain *et al*., 2004). The dissolved carbon, nitrogen, CO_2 and oxygen

that accumulate due to this isolation makes these lidded holes a unique environment with extreme levels of pH (Tranter *et al*., 2004). The weak pH buffering and microbial processes contribute to this phenomenon, in some cases raising the hole to as high as pH 11 (Webster-Brown *et al*., 2015). When closed holes are connected to one another this tends to occur through a network of small channels just below the glacial surface (Bagshaw *et al*., 2012). These are therefore hydrologically connected but still closed from the atmosphere above. In regions where seasonal melting occurs, connectivity between holes will increase with temperature to the point redistribution of cryoconite can occur. Holes may even connect as cryoconite accumulates in basins to form large pans known as "cryolakes" (Bagshaw *et al*., 2012).

These closed holes are a contrasting environment to the "open" cryoconite holes found elsewhere. Open holes can access the atmosphere, allowing for gas exchange. These holes occur at glacial ablation zones that exhibit seasonal melting (Bagshaw *et al*., 2012). This means they are common on polythermal glaciers and those in more temperate regions (Hodson *et al*., 2008). Melting causes these holes to be flushed regularly, distributing cryoconite across the glacier surface. This could provide an input of new material to support its ecosystem and buffer the pH, however, it also causes sudden changes in liquid water and nutrient availability (Bagshaw *et al*., 2012). The organisms present will be retained in a local community, but must tolerate some mixing and relocation of cryoconite granules within nearby cryoconite holes. The tracking of cryoconite granules in polar glaciers suggests seasonal flow of meltwater but also some redistribution through the whole year (Hodson *et al*., 2010; Irvine-Fynn *et al*., 2010). Eventually much of the cryoconite will be flushed to the glacier terminus or supraglacial streams (Hodson *et al*., 2010). Some cryoconite holes, rather than sitting at the surface, open into supraglacial stream or lake allowing even more connectivity and mixing of cryoconite (Hodson *et al*., 2008). Cryoconite is not only relevant as a self-contained ecosystem; rather, it contributes to processes across whole glaciers and ice lakes (Bagshaw *et al*., 2007). In an open hole system, the meltwater flushing means that the coverage of

cryoconite can change rapidly, with knock on effects for hydrology, albedo and carbon cycling in the surrounding environment.

Cryoconite composition

The composition of cryoconite, including the mineral content, biomass present and species present, also varies greatly between locations. The inorganic components of cryoconite originate from local and distal sources. Some comes from exposed ground at ice-margins and matter released from glaciers during ablation (Atkins and Dunbar, 2009; Stibal *et al*., 2012a). Fine dust can travel further by aeolian transport (Stibal *et al*., 2012a). The method of deposition and source of material will therefore depend on the geographical location, leading to varying compositions of inorganic material by site (Cook *et al*., 2015b). In addition to the variation between sites on a glacier, the wider surroundings and underlying geology will impact the makeup of the cryoconite. Through viewing thin sections of cryoconite with polarised light microscopy, it was revealed that Svalbard cryoconite was rich in rock of metamorphic origin: quartz, mica and feldspar (Langford *et al*., 2010; Edwards *et al*., 2011). XRD and FTIR revealed that some of the remaining weight was made up of clays, calcite and trace minerals (Langford *et al*., 2010). The composition of the inorganic matter impacts the biological community in a cryoconite hole. Bioavailable carbon, nitrogen and phosphorus is found in higher proportions in cryoconite than the source polar terrestrial soils due to the high biogeochemical cycling of cryoconite (Bagshaw *et al*., 2013). However, phosphorus is often found to be a limiting factor in biological growth, so phosphates from rock debris may determine ecological viability (Cook *et al*., 2015b). This is due to limited sources of phosphorus within transport range (Foreman *et al*., 2007; Stibal *et al*., 2008; Bagshaw *et al*., 2013). Biologically fixed nitrogen has been found in cryoconite in the Arctic (Telling *et al*., 2011) and nitrogen fixation in cryoconite may also take place in Antarctic cryoconite (Bagshaw *et al*., 2007; Cameron *et al*., 2012a; Telling *et al*., 2014). The major ions found in cryoconite holes vary between regions. For example in the McMurdo Dry Valleys, Canada Glacier cryoconite holes were enriched in SO_4^{2-}, Ca^{2+}, but depleted in Mg^{2+}, whereas the Taylor Glacier were enriched in SO_4^{2-}, Ca^{2+} and Mg^{2+} (Bagshaw *et al*., 2013). Amery Ice shelf cryoconite

holes were enriched in Na^+, K^+, Mg^{2+},Ca^{2+} and SO_4^{2-} (Samui *et al*., 2018). However this also changes throughout the year. Freeze and thaw cycles in the spring have been shown to produce "ionic pulses" of drastic and rapid changes in ionic enrichment (Telling *et al*., 2014). Regardless, the geochemical data show that cryoconite holes are enriched in major ions throughout the melt season when compared to compared to bare ice (Bagshaw *et al*. 2007).

Cryoconite layers vary in thickness and structure. This is often determined by the organic components. The organic matter has been found to make up between 1% and 20% of cryoconite across different samples (Cook *et al*., 2015b). This includes living and dead cells, in addition to the biogenic matter produced by these organisms (Hodson *et al*., 2008). In cryoconite holes with high proportions of humic substances and filamentous structures such as Cyanobacteria, the cryoconite matter tends to form granular structures as filaments and extracellular polymeric substances (EPS) coagulate the particles into aggregates though bridging structures and altered surface charge Cyanobacteria (Schmidt and Ahring, 1994; Langford *et al*., 2010; Takeuchi *et al*., 2010). Granules of cryoconite have been well documented in cryoconite across the northern hemisphere including sites in Svalbard, Greenland and China (Langford *et al*., 2010, 2014; Takeuchi *et al*., 2010; Uetake *et al*., 2016).The percentage organic matter content has been found to correlate to granule size; in a survey of five sites across Svalbard and Greenland, the cryoconite with the highest proportion of organic matter had the largest granule size, and the cryoconite with the lowest proportion of organic matter had the smallest granule size. (Langford *et al*., 2010; Stibal *et al*., 2010). While this is a small sample size where the statistical significance of this relationship was not explored, it mirrors findings in soil which show that inoculation of soils with live Cyanobacteria (and to a lesser extent Cyanobacterial EPS) result in the formation of larger aggregates of particles (de Caire *et al*., 1997). The size and shape of the cryoconite granules has again been found to vary within glacial sites and between glaciers across the world (Zarsky *et al*., 2013). The granule itself can be distinctly structured, with photoautotrophs populating the light-exposed surface, and heterotrophic organisms in the mineral-rich interior (Langford *et al*., 2010). In some cases the

centre of the granule is an anoxic as well as dark environment that contains anaerobic bacteria (Takeuchi *et al*., 2001a; Langford *et al*., 2010).

Modern day cryoconite supports a diverse array of organisms. Several molecular methods have been used to investigate these communities, in addition to observation by microscopy. Automated Ribosomal Intergenic Spacer Analysis (ARISA) and DNA amplicon sequencing allow taxa to be identified from environmental DNA extracted from cryoconite (Christner *et al*., 2003). Metagenomic analyses are also used to study species diversity, but in addition they allow an insight into functionality and community structure (Handelsman, 2004). Metagenomics is also capable of identifying viruses, which lack consistent genetic markers to be used in metabarcoding such as 16S or 18S rRNA genes (Kerepesi and Grolmusz, 2017). It is worth noting that the majority of these studies were carried out by examining environmental DNA so may not reflect the active communities of cryoconite. One study found that examining rRNA rather than rDNA in an area of Greenland revealed a less complex community, mostly dominated by Cyanobacteria, Alphaproteobacteria and Betaproteobacteria (Stibal *et al*., 2015). However, the number of studies using methods other than DNA surveys are limited. Here I present a brief review of the predictions of cryoconite community composition so far.

Heterotrophic bacteria are frequently abundant in cryoconite. The results of metagenomics show that the Proteobacteria, Bacteroidetes and Actinobacteria yield the most reads of the heterotrophic bacteria, and often the most common in ecosystem as a whole (Edwards *et al*., 2013b). This is the case in the Arctic and Antarctic (Edwards *et al*., 2013b; Sommers *et al*., 2018). Within the phyla of Proteobacteria, Bacteroidetes and Firmicutes, several anaerobic genera were identified in cryoconite. They were uncovered through 16S rRNA gene sequencing following enrichment of the culture to favour anaerobes (Zdanowski *et al.*, 2017). These included *Psychrosinus*, *Clostridium*, *Paludibacter*, *Acetobacterium*, *Pseudomonas*, *Carnobacterium*, and *Desulfosporosinus*. These heterotrophic cells subsist on the nutrients provided by the combination of biogenic primary production and matter released by the surrounding melting snow (Lutz *et al*., 2017).

The same can be said for the heterotrophic eukaryotes and archaea that also populate the cryoconite holes. Numerous genera of protists have been recorded in glacial environments around the world, although they make up a relatively small proportion of the organisms in found each cryoconite hole community (Kaczmarek *et al*., 2016). The fungi are known for their proficiency in recycling sources of carbon and this seems to hold true in cryoconite, although the exact processes taking place are unclear (Vincent *et al*., 2000; Anesio *et al*., 2017). Archaea, which first caught the world's attention for their ability to inhabit the most extreme and hostile climates, have been recorded in cryoconite (Cameron *et al*., 2012b; Kaczmarek *et al*., 2016), but cryoconite archaea are recovered in low abundance and are relatively poorly understood to date. Most of these recordings come from Antarctica, but interestingly a large proportion of the ammonia-oxidising organisms in Svalbard cryoconite were found to be archaea (Zarsky *et al*., 2013). This is the first finding of its kind from the Arctic and is an important insight into potential roles for archaea in cryoconite nutrient cycling.

Cyanobacteria are often the main primary producers of cryoconite holes, in some studies contributing up to 95% of the carbon present (Stibal and Tranter, 2007). As mentioned above, it is also often the Cyanobacteria produce extracellular polymeric substances that bind together the cryoconite in a filamentous structure. The Cyanobacteria can therefore be found at the bottom of the cryoconite hole forming biofilm and granular structures (Anesio *et al*., 2017). In systems with fewer Cyanobacteria, Eukaryotic algae are the primary photoautotrophs (Edwards *et al*., 2014; Uetake *et al*., 2016). These include *Chlamydomonus* snow algae, which are a member of the Chlorophyta. The cryoconite photoautotrophs must protect themselves from the high exposure to sunlight on the surface of glaciers and display behavioural and physiological photochemical downregulation (Perkins *et al.*, 2017).

Virus production has been found to be just as prolific in cryoconite as other sediments. It has been suggested that the death and subsequent lysis of cells due to viruses is a significant part of the carbon recycling in the cryoconite holes (Bellas *et al*., 2013).

Methodology

i. Sampling methodology

Modern cryoconite holes are particularly promising analogues for Snowball Earth habitats (Hoffman, 2016). Therefore the ecological composition of cryoconite was explored, and the ecosystem's response to "Snowball Earth like conditions" was investigated. All analysis and experimentation on polar cryoconite samples was carried out by the author. The original samples were collected by collaborators and provided to the author (see Acknowledgements, page ii). Polar cryoconite samples were collected from 85 individual cryoconite holes across 15 sites (see Results Chapter 1 for map). Ten locations were in the Antarctic and five were in the Arctic, and all were collected during the regional summer melt season. The Antarctic samples were collected in the McMurdo Dry Valleys, with the exception of the Utsteinen samples, which were collected in Queen Maud Land near the Utsteinen Nunatak (Lutz *et al*., 2019). Collection technique was determined by presence and thickness of ice lid or ice layers above. Three sample types were collected from the southwest of Greenland. Those labelled "Greenland Margin" were collected within 2km of the ice edge in 2014. Samples labelled "Greenland Core" were frozen cryoconite layers collected from shallow subsurface layers of 1m ice cores on inland ice in the 'Dark Zone', at Camp Black and Bloom (Poniecka *et al*., 2019; Williamson *et al*., 2020). Typically the layers are located around 10-30cm depth of the core and are believed to be retained from the previous year's cryoconite holes following burial under frozen snowpack (Nicholes *et al*., 2019). Greenland core samples were drilled in 2015 using a hand auger and the sediments separated from the meltwater (Poniecka, 2020). Greenland surface samples were also collected at Camp Black and Bloom 2016. Two samplesets were collected from elsewhere in the Arctic at Storglaciären in Sweden (2017), and Midtre Lovénbreen in Svalbard (2016). Additional Midtre Lovénbreen Svalbard cryoconite to be used for intact polar lipid (IPL) extraction was collected using the same method in 2018. Exposed cryoconite

was sampled using a syringe or spoon and stored in clean, sterile Whirlpak bags or tubes and frozen until analysis (Poniecka *et al*., 2019; Poniecka, 2020). Antarctic Dry Valley samples from Canada, Taylor and Commonwealth glaciers were collected from the base of frozen cores (20-50cm deep) drilled from cryoconite holes between 2005 and 2009 (Bagshaw *et al*., 2012). The cores were melted at room temperature, the meltwater removed, and the sediment transferred to Nalgene bottles previously rinsed six times with deionised water, then refrozen at -20°C. The cryoconite from Koettlitz, Wright and Darwin Glaciers were collected using a sterile spatula as described in Webster-Brown *et al*. (2015). Utsteinen Nunatak samples were accessed in 2017 using a Kovacs drill, and the sediment removed using a sterilised scoop (Lutz *et al*., 2019). Greenland margin and 'Kangerlussuaq' samples were collected from melted cryoconite holes in summer 2012 and 2014, where clean nitrile gloves were used to scoop sediment into Ziploc bags previously rinsed with deionised water. The fact that these samples were collected with different methods and at different times means there is some limitation to the certainty with which they can be used to represent *in situ* cryoconite communities, and with which they can be compared to one another. The effects of long term cold storage may have damaged certain organisms. Additionally, it is also very challenging to collect and transport polar sediment samples in completely sterile conditions. However, cryoconite organisms *in situ* survive a broad range of temperatures and long term freezing (Hodson *et al*., 2010; Webster-Brown *et al*., 2010; Poniecka *et al*., 2020). This, in addition to the measures employed to keep the community free of contamination, should establish suitably representative communities for the studies described.

Signy island pond, stream, cryoconite, ice margin and seal wallow samples were collected from a range of locations across Signy Island over March 2020. Temperature and pH of the water surrounding the samples was taken using a Hanna Instruments 98129 pH Meter (Hanna Instruments, US) approximately 0.5cm from the sediment collected. A sterile scoop was used to lift sediment and microbial mats and the samples were stored in sealed sterile bags and bottles. Samples were

frozen within a few hours of collection. All samples were transported frozen to home laboratories and remained frozen at -20 °C until analysis.

ii. Incubation growth experiments in serum vials

Although modern cryoconite has many qualities relevant for survival on Snowball Earth, such as its biodiversity and its ability to survive freezing, thus far no study has tested whether these communities can survive Snowball Earth conditions and how they might respond to them. Therefore I carried out incubations of cryoconite communities under "Snowball Earth type" conditions. Two proxies for community growth were chosen to measure this, oxygen measurements in the water column and radio-labelled leucine incorporation, which are described in sections iv and v. Sediment was thawed at 0°C and placed in 60ml autoclaved vials to 1-1.5cm sediment thickness. 45g of water was added to each vessel. An air gap was left, simulating the closed lidded cryoconite holes from which the cryoconite used was collected. The vials were sealed with autoclaved rubber stoppers and aluminium crimp caps using a manual crimping tool. See Results Chapter 3 for images of these vials. The rubber seal was pierced for oxygen measurements, and so as measurements were taken there was more opportunity for oxygen bleed into the vessels. See section v for mitigation of this in later calculations. These were then incubated in Weiss VT low temperature environmental climate chambers under the conditions described below. Synchronisation between light and temperature was ensured through monitoring of independent light and temperature monitors on a Campbell data logging system. Throughout these experiments, light was provided from LED lights emitting photosynthetically active radiation (PAR) at 145 µmol m^{-2} s^{-1} which enabled photosynthesis under non light limited conditions.

Table 2 Samples used in Results Chapter 1 McMurdo Dry Valleys cryoconite growth experiments

Experiment name	Source location	Mean weight of cryoconite in vials	Standard Deviation on mean weight
Light-Dark cycle (Objective 2.1.1 page 121)	Canada Glacier	23.9g	2.6g
Freeze-Thaw cycle (Objective 2.1.2 page 130)	Canada Glacier	22.7g	3.0g
Antarctic ice-cryoconite holes (Objective 2.2 page 131)	Canada Glacier	10.0g	0.4g
Arctic ice-cryoconite holes (Objective 2.2 page 131)	Longyearbreen	9.8g	0.4g

Table 3 Sampled used in Results Chapter 3 Signy Island sediments growth experiment

Sample ID	Source type	Source location	Weight used (average)
CCO1	Cryoconite	Snow Hills Nunatak	12.3g
NSST1	Narrow supraglacial meltwater channel	Khyber Pass	11.8g
SST1	Supraglacial stream	Erratics Valley	17.7g
IM3	Ice margin	Khyber Pass	20.6g
P1	Pond	Khyber Pass	18.9g

Cryoconite under day-night conditions

As cryoconite on Snowball Earth is predicted to have been concentrated around the warmer equatorial regions and sub tropics (Hoffman, 2016; Hoffman *et al*., 2017), I measured the response of cryoconite to an equatorial-like day night cycle. This was compared to full time light to represent a polar growth season. Dark bottles were also added to each incubation to determine the impact of autotrophy and so calculate net respiration. Vials of cryoconite (Table 2) were divided into incubations under three conditions: 24 hours per day light (climate chamber 1), 24 hours per day no light (a set for each climate chamber), bottles darkened using aluminium foil covering), and 12 hours of light followed by 12 hours of darkness (climate chamber 2). All vials were incubated at 0.5°C. This incubation ran for 27 days; this was chosen to allow time for the community to "reorganise" after sediment was added to the new container, and enter growth and stationary phase (Poniecka, 2020), while working within the constraints of available laboratory time. As no stationary phase was reached in this experiment, the following freeze-thaw experiment was run for an additional 8 days. Each incubation contained triplicates to be removed at each time point, abiotic controls, and blank vials containing only water. Abiotic controls were produced by adding glutaraldehyde to samples. Oxygen measurements were taken on days 0, 1, 2 and then once every 3-4 days. Every 7 days, one triplicate set of vials was removed to extract sediment for IPL analysis and ^{3}H-leucine incubation.

Cryoconite under freeze-thaw conditions

In a Cryogenian equatorial environment the communities may freeze and thaw with diurnal cycles. This could be a potential stress for microorganisms in the Cryogenian. Therefore community activity was tested under freeze-thaw cycle conditions. Triplicate vials of cryoconite (Table 2) were incubated in each condition in constant light: 'control' (climate chamber 1, 24 hours per day at 0.5°C) and 'freeze' (climate chamber 2, -5°C for 7 hours and then thawed at 1°C for 7 hours each day with a 5 hour transition period each side reducing or increasing temperature by 1°C each hour). -5°C chosen as it was sufficient to freeze the water

in the vessel completely, and this would melt at 1°C. An additional group of 'dark' triplicate vials (in aluminium covering) were added to each chamber for calculation of primary production and net productivity. Oxygen measurements were taken at days 0, 3, 7, 10 and 35.

Signy Island sediment

Signy Island was used as an analogue for a deglaciating and/or Slushball Earth scenario as the local climate is relatively warm for a glaciated area and its maritime location means that its ice cap is isolated from other glacial environments (Holdgate and Smith, 1967; Smith, 1990). Sediments were collected from a range of interconnected glacial and periglacial meltwater habitats to investigate these scenarios in which habitats become connected to one another by meltwater. One limitation of using Signy Island as a Snowball Earth analogue is that it is populated by animal wildlife including birds and seals, which may add chemical and microbial input into the system that would not have been present during the Cryogenian. A seal wallow area was sampled in addition to the other habitats to identify the signature of an area that has been heavily influenced by megafauna activity. Signy Island sediments were incubated under the polar growth season conditions used in the previous incubations: full time light, 0.5°C. Due to limited sediment availability, duplicate samples of each type (pond, supraglacial stream, ice margin, and cryoconite) were used (Table 3). These were incubated for 27 days and oxygen measurements were taken at days 0, 1, 2 and then once every 3-4 days.

iii. Development and measurement of ice cryoconite holes

Cryoconite community activity has typically been studied in glass vials or a similar enclosed vessel (Hodson *et al*., 2010; Telling *et al*., 2010; Bagshaw *et al*., 2016b, 2016a; Poniecka *et al*., 2020). In contrast, many cryoconite holes are dynamic; they are melting or freezing as the microbial community is active, rather than a system with a fixed amount of water and water-air exchange (Takeuchi *et al*., 2001a; Fountain *et al*., 2004, 2008; Cook *et al*., 2015b). This also means that the water and

sediment temperature may vary within the cryoconite hole, both over time and at different positions in the microcosm. The surface of ice also differs to that of glass, which may alter community organisation. Surface material has been shown to impact initial adherence, surface sensing and biofilm formation (Ammar *et al*., 2015; Zheng *et al*., 2021). Due to these differences, it cannot be assumed that systems such as glass vials are reliable analogues for a cryoconite hole. Cryoconite hole activity has been measured *in situ* in the field (Anesio *et al*., 2009; Telling *et al*., 2010; Bagshaw *et al*., 2011; Poniecka *et al*., 2018), but it is difficult to tell if variation between laboratory and field measurements resulted from differences in environmental conditions or the impact of replacing the cryoconite in an incubation vessel. Therefore, to study the development of cryoconite holes and monitor cryoconite under more representative glacier conditions, cryoconite holes were formed on ice blocks in the laboratory and oxygen measurements were carried out. Ice was prepared by boiling Milli-Q® purified water and placing in a plastic sterile container in a Weiss VT low temperature environmental climate chamber at -30°C until completely frozen. Boiling the water resulted in transparent ice with fewer bubbles, more akin to glacier ice. The container comprised of an outer container (335mm x 395mm x 170mm) and an inner container (310mm x 375mm x 90mm) which was separated into 6 compartments. The space between the outer and inner containers and all compartments were filled with ice to maximise the ice surrounding each cryoconite hole and therefore best represent a glacier. Cryoconite was thawed at 0°C and 10g of cryoconite sediment was placed in 3 of these 6 compartments as triplicate replicates (Figure 10). While similar sediment quantity to the previous experiments (22-24g) would have been preferable, this quantity of cryoconite resulted in unstable cryoconite holes which collapsed the cryoconite holes within 3 days. A larger incubation chamber would be required to form stable cryoconite holes with larger quantities of sediment. The container was covered with sterile clear polyethylene film and placed in the Weiss VT low temperature environmental climate chamber at 0.5°C and a distance of approximately 12cm from the light source. The film was lifted briefly and small (<3mm) holes were pierced in any ice lids to take oxygen measurements as described below in Methodology Section v (page 52). The incubation program was run until all

cryoconite holes had either collapsed (melted to the bottom of the inner container) or frozen to a thickness that could not be pierced (>10mm) which took place between days 15-17.

iv. ^{3}H-leucine incorporation

Community growth was measured though incorporation of ^{3}H radiolabelled leucine to subsamples of 0.05g of cryoconite. The consumption of radiolabelled leucine has been used previously to quantify protein production in microbial communities and therefore estimate overall biomass accumulation (e.g. (Smith and Azam, 1992; Kirchman, 2001; Gillies *et al*., 2006; Bradley *et al*., 2016). As this method is based on consumption, it is a measure of gross biomass accumulation. A drawback of this method is that is must assume a constant fraction of protein in biomass which is unlikely to precisely represent reality, especially in a community of a variety of eukaryotic and bacterial phyla. However, in this study, I am primarily interested in a comparison between test conditions rather than a quantification of biomass. Incubations of ^{3}H-leucine with subsamples of cryoconite taken from each condition of the day-night experiment were carried out according to the centrifuge method outlined by (Kirchman, 2001). (Bradley *et al*., 2016) determined an optimum incubation time and leucine concentration for near-glacial soils and sediments through saturation experiments, which were used in this study. This was deemed similar enough to the cryoconite used to be suitable. Cold leucine and hot (^{3}H) leucine were combined at a ratio of 4:1. Four replicates and one killed control (inactivated with 100% TCA) were prepared for each sample type. 50mg sediment, 1.7ml H_2O and 15µl leucine mix were added to each reaction mix. These were incubated for 3 hours, at which point the cells were inactivated with 100% TCA. The following steps were then taken to remove the external leucine. The reaction tubes were centrifuged at 15000rpm for 20 minutes. The supernatant was then aspirated, 1ml 5% TCA was

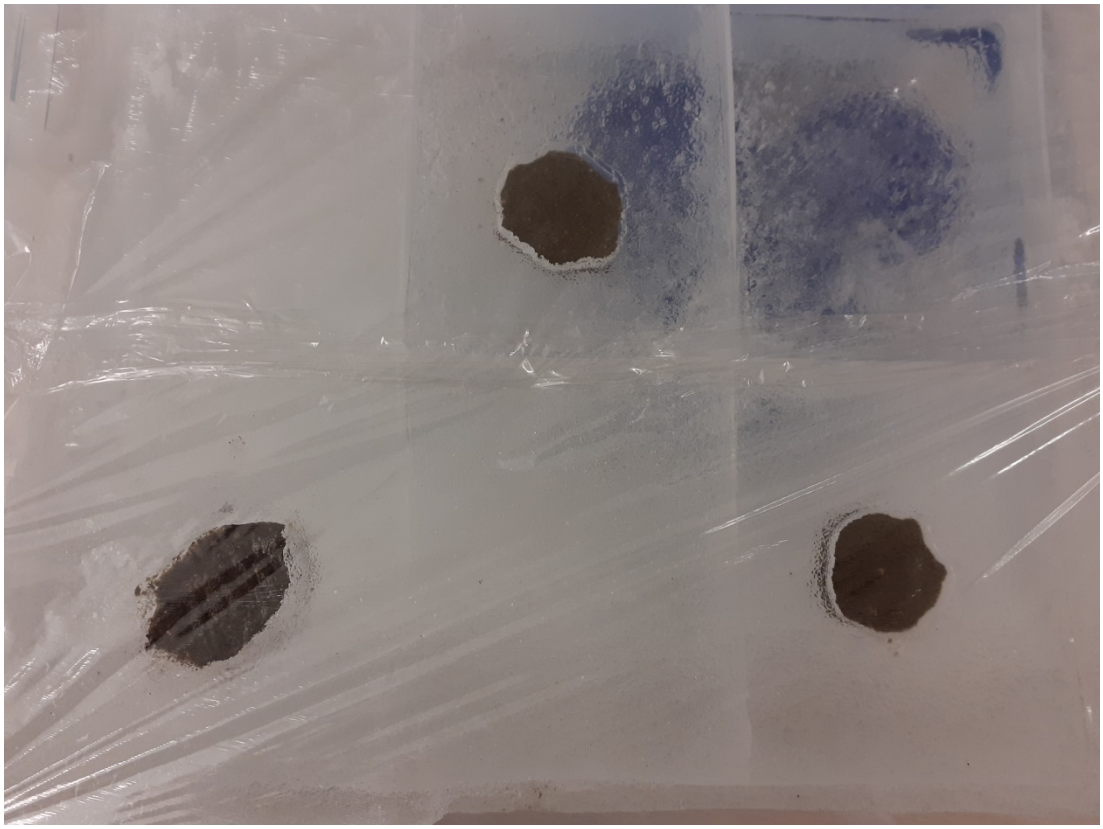

Figure 10 Ice cryoconite holes set-up. Pictured after 2 days in the climate-control chamber. Cryoconite was placed on the ice surface in triplicate and allowed to melt vertically into the ice.

added to each tube, and the centrifugation was repeated. This was followed by a further aspiration step and the addition of 1ml 80% ethanol, and then a final centrifugation and aspiration step. The pellet was allowed to dry completely and then 1ml of scintillation cocktail (Ultima Gold F cocktail) was added to each replicate. Scintillation counting was carried out using a TriCarb2900 scintillation counter. Disintegrations per minute were then converted to rate of microbial carbon production in μg/g/h as described by (Kirchman, 2001) after subtracting blank values. Average rate of carbon production of the triplicates and associated standard error values were plotted graphically using ggplot2 (Wickham, 2016).

v. Dissolved oxygen measurements and net productivity calculation

The dissolved oxygen method has been used in many cryoconite studies to assess photosynthesis, respiration and net community production (Telling *et al*., 2010; Bagshaw *et al*., 2011; Poniecka *et al*., 2018). Respired oxygen is used as a proxy for carbon accumulation in this method. Using two methods (^{3}H-leucine and dissolved oxygen) with different approaches lent greater confidence to the first experimental results. In the following experiments, it was not practical to continue both methods, especially given they appeared to produce the same trends. The dissolved oxygen method was continued to be used in the following experiments as it was more economical and has an established record of use for calculating cryoconite community growth, so can be compared to prior and future findings that use(d) this method.

Dissolved oxygen content was measured as % oxygen saturation in the water column of all serum vial and ice cryoconite hole sediment incubations using a Unisense Oxygen MicroOptode (Unisense, Denmark) and recorded on a Unisense Sensortrace datalogger. Primary production and respiration in micrograms of carbon per gram of sediment per day were calculated from dissolved oxygen figures ascertained from paired light sediment incubation, and dark sediment incubation

and blank bottles using the methodology and equations carried described in (Telling *et al*., 2010; Bagshaw *et al*., 2011). Oxygen values representing (R) respiration only (no photosynthetic activity) were calculated as the difference between the average dark vial values and water blank vial values. The values representing (P) photosynthetic activity only (no respiration) were the average test vial values with dark vial values subtracted. These two sets of values were then converted from % air saturation to µg C per gram by multiplying them by the oxygen content of pure water at the control temperature used (14 mg/l), the mass of water used and the atomic weight of carbon, and dividing by the molecular weight of oxygen times the mass of sediment used. This assumes a constant ratio of oxygen respiration to carbon accumulation. The sum of these 'P' and 'R' carbon concentrations can then be interpreted the as total C per gram in the system. This is described by Bagshaw *et al*., (2011): "P and R as µg C/g/day were calculated by Equations (1) and (2) (Telling *et al*., 2010), where O2 P is the recorded saturation of oxygen in the light sample (%), O2 R is the recorded saturation of oxygen in the dark sample (%), O2 Blk is the oxygen saturation of the blank, O2 0 °C is the oxygen content of water at 0 °C (14 mg/l), 32 is the molecular weight of oxygen, 12 is the atomic weight of carbon and Hours is the duration of each incubation step in hours. The equations assume a quotient of unity."

$$P = \frac{(O_2^P - O_2^R)O_2^{0\,^\circ\mathrm{C}} \cdot Mass_{water} \cdot 12}{32 \cdot Mass_{sediment} \cdot 100 \cdot \left(\frac{Hours}{24}\right)} \qquad (1)$$

$$R = \frac{(O_2^{Blk} - O_2^R)O_2^{^\circ\mathrm{C}} \cdot Mass_{water} \cdot 12}{32 \cdot Mass_{sediment} \cdot 100 \cdot \left(\frac{Hours}{24}\right)} \qquad (2)$$

The average oxygen values and standard error on these values, and the values for rate of carbon accumulation, were visualised graphically using ggplot2 (Wickham, 2016).

This method is a proxy for carbon accumulation rather than a direct measurement, and therefore is a calculated approximation. Not only does it rely on the

assumption of a constant ratio between oxygen in the water column of the cryoconite and carbon in the sediment, it assumes a closed system. The impact of oxygen input due to leakage once the vial stopped has been pierced for measurement is somewhat mitigated by the subtraction of blank values that have also been subject to this effect.

vi. Intact Polar Lipid assessment

Membrane lipids are important microbial community biomarkers in environmental samples, and provide considerable chemotaxonomic information (Rütters *et al*., 2002; Sturt *et al*., 2004). Intact polar lipids are a major component of those membranes. For this reason intact polar lipids (IPLs) were used to compare the composition of sediment samples from different locations. IPL analysis has been carried out for the investigation of microbial communities in a variety of different environments (Lipp *et al*., 2008; Jungblut *et al*., 2009; Schubotz *et al*., 2013). Unlike DNA they degrade quickly after cell death so are more representative markers of the active microbial community (Sturt *et al*., 2004). IPLs are formed of a hydrophobic hydrocarbon tail, a glycerol backbone and a polar head (Figure 11) and can be identified by mass spectrometry (Renkonen, 1967; Sturt *et al*., 2004). During analysis, I screened for IPLs that had previously been reported in microbial communities (e.g. (Lipp and Hinrichs, 2009; Wörmer *et al*., 2013; Evans *et al*., 2017). All of those identified are included in this study. These lipids have been identified previously in polar habitats but also in soils and ocean habitats (Evans *et al*., 2017, 2022; Schubotz *et al*., 2018; Ding *et al*., 2020). Ornithine lipids and PE-DAGs are widespread in bacteria (Geiger et al., 2010), whereas PC-DAGs and betaine lipids are typically found in eukaryotic algae, fungi, and protista (Kato *et al*., 1996; Sohlenkamp *et al*., 2003), although betaine lipids have been reported in Cyanobacteria as well (Rezanka *et al*., 2003). Glycolipids are the IPLs that are primarily produced by Cyanobacteria, followed by PG-DAGs DPG-DAGs and SQ-DAGs (Wada and Murata, 2006). However, a limitation on the use of these methods for taxonomy is that none of these lipids are exclusively produced by these groups

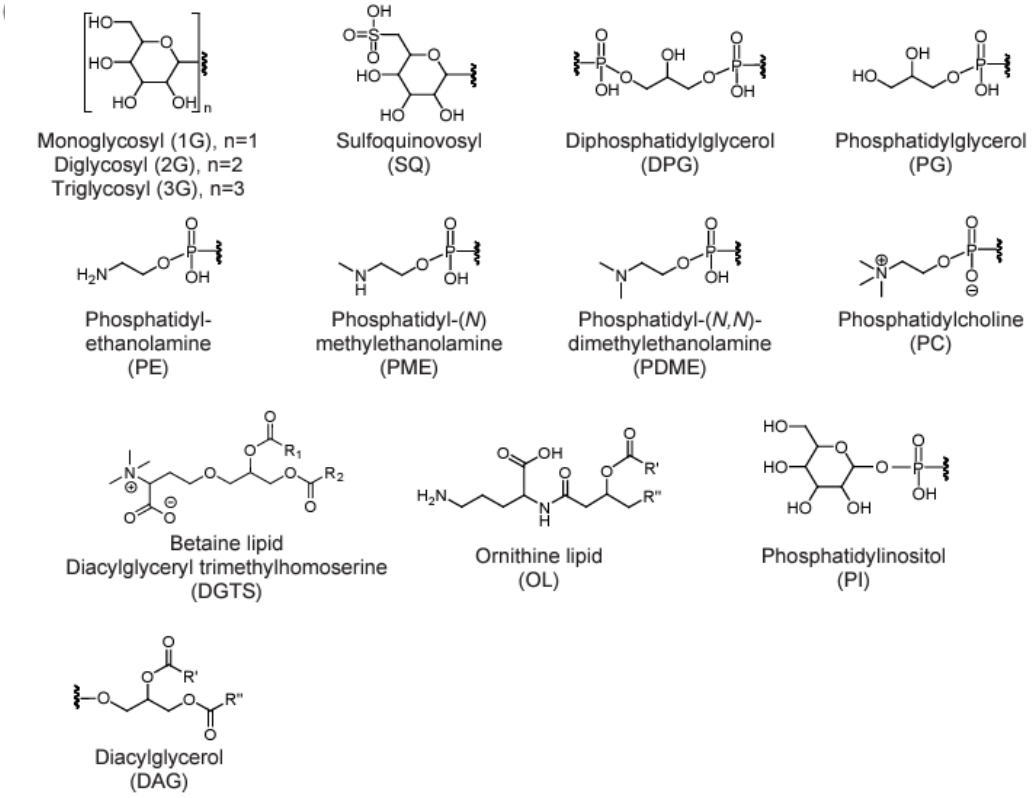

Figure 11 Structure of Intact Polar Lipid head groups identified in this study. Structure diagrams here were first published in supplementary material of Schubotz. et al 2018.

(Kato *et al*., 1996; Wada and Murata, 2006). Therefore here it is presented in conjunction with DNA data. In addition to their chemotaxonomic use, membrane lipids are at the interface of organisms and their environments, and can reflect adaptations to the environment such as cold and light tolerance. When available phosphorus is low, the aminolipid (BL, OL, OL-OH) to phospholipid (DPG-DAG, PG-DAG, PC-DAG, PE-DAG, PME-DAG and PI-DAG) ratio in microbial communities may be raised. The percentage of carbon unsaturations were recorded as they have been found to reflect stress adaptation through altering membrane flexibility.

IPL analysis (extraction, identification, quantification and calculations) of the sediments used in day-night growth experiments was carried out by the author at MIT, USA. Analysis of original Arctic and Antarctic cryoconite sediments and Signy island sediments was carried out by Thomas Evans at MIT (Arctic and Antarctic cryoconite) and Universität Bremen, Germany. Extraction and quantification was carried out according to methodology described by (Evans *et al*., 2022).

Extraction

Sediments and microbial mat pieces were freeze dried at -40°C for transport and lipid analysis. IPLs were extracted following a modified Bligh and Dyer protocol (Bligh and Dyer, 1959; Sturt *et al*., 2004) as reported by (Evans *et al*., 2022) with methanol (MeOH), dichloromethane (DCM) and an aqueous solution (aqueous buffer prepared from monopotassium phosphate (8.7g/l; pH 7.4) or trichloroacetic acid (TCA)). These solutions separated the lipid fraction from the remainder of the sediment. Approximately 6g of freeze dried sediment and 25ml of a DCM, MeOH, and phosphate buffer was added at a volume ratio of 8:20:10. This mix was sonicated in an ultrasonic bath for 20 minutes, centrifuged for 10 minutes at 2000rpm and supernatant phases were separated in a separation funnel. These steps were repeated a further time with the same mix and a further two times with TCA in place of phosphate buffer. A final extraction step was undertaken with a 9:1 volume DCM:MeOH for enhanced extraction of lower polarity lipids. 25ml deionized H_2O was added to the funnel to separate the solution. The organic phase was drawn out, the aqueous layer was further extracted three times with DCM, and

then it was washed with deionized H_2O. The washed organic phase was gradually dried under a nitrogen flux dryer to extract remaining water. Samples which could not be processed right away at this point were stored at -20°C.

Identification and quantification

Table 4 Acronyms used to describe intact polar lipids (IPLs) throughout

Abbreviation used	Intact Polar Lipid
1G-DAG	Monogalactosyl diacylglycerol
2G-DAG	Digalactosyl diacylglcyerol
BL	Betaine lipids
DPG-DAG	Diphosphatidylglycerol diacylglycerol
OL	Ornithine lipids
PC-DAG	Phosphatidylcholine diacylglcyerol
PDME-DAG	Phosphodimethylethanolamine diacylglycerol
PE-DAG	Phosphoethanolamine diacylglycerol
PG	Phosphatidylglycerol
PI-DAG	Phosphoinositol diacylglycerol
PME-DAG	Phosphomethylethanolamine diacylglycerol
SQDAG	Sulfoquinovosyl diacylglycerol

IPLs were detected and quantified using a 6520 accurate mass quadrupole time of flight mass spectrometer (Agilent Technologies, US) with an electrospray ionization source, coupled to a 1200 series high performance liquid chromatograph (HPLC;

Agilent Technologies, US). Methodology was carried out as described in Evans *et al*., 2017. IPLs were separated using a Waters Acquity amide column, as described by (Wörmer *et al*., 2013). Eluents consisted of acetonitrile, DCM, formic acid, and ammonium hydroxide (volume ratio 75:25:0.01:0.01); HPLC-grade water, MeOH, formic acid, and ammonium hydroxide (volume ratio 50:50:0.4:04). The eluent flowed at 0.4 mL min^{-1} at a temperature of 40˚C throughout the analysis. The mass spectrometer was operated in positive ionization mode, scanning from 200 to 2000 Da. IPL identification was carried out by discerning exact mass and characteristic fragmentation patterns (Sturt *et al*., 2004; Bauersachs *et al*., 2009; Wörmer *et al*., 2012; Bale *et al*., 2018)

Quantification of IPLs was achieved by comparison to a known quantity of injection standard (phosphocholine archaeol, 10ng injected). Comparative masses of IPLs were determined from commercially available standard masses of each IPL. No standard was available for betaine lipids (BL), ornithine lipids (OL), sulfoquinovosyl diacylglycerol (SQ-DAG) and phosphoinositol diacylglycerol (PI-DAG), so a relative response factor was chosen for these compounds from which their mass could be estimated. The reported relative abundances of IPLs are therefore semi-quantitative. Both the DNA and IPL profiles are semi quantitative and are reported as estimated relative abundance. Acronyms will be used for IPLs throughout, described in Table 4.

To evaluate the membrane environmental response properties, the double bond index and the average chain length of the IPLs was calculated as described by Evans *et al*. (2017). The area of the compound was multiplied by the number of unsaturations and divided by the total area of all compounds to provide the double bond index. Average chain length was calculated by multiplying the number of carbons in the side chain with the area of the compound divided by the total summed area of compounds. To account for varying chain lengths within IPL species, the number of unsaturations was normalized according to their average chain length.

vii. Illlumina sequencing

Environmental DNA sequencing is a powerful tool that has been used to assess microbial communities from a wide range of habitats, including cryoconite holes (Cameron *et al*., 2012b; Hell *et al*., 2013). The advent of DNA sequencing allowed the identification of taxa that could not be distinguished by other analyses such as microscopy (Vaneechoutte, 1996). DNA is stable for a long period of time, especially when kept at low temperatures (Marmur, 1963), and so is practical to work with on polar samples which are difficult to acquire and so may be in transport and storage for some time before opportunistic use. However the drawback of this stability is that legacy DNA and the DNA of dormant microorganisms may be present, and it is uncertain whether the results represent microorganisms that are active in the surveyed habitat (Stibal *et al*., 2015). Despite its limitations in assessing active communities, DNA sequencing continues to be used to predict community composition of microbial ecosystems due to its efficacy in taxonomic identification. Sequencing of the highly conserved 16S and 18S ribosomal RNA genes enabled metabarcoding that covered bacteria, archaea and eukarya. Illumina Miseq allows efficient and high throughput DNA sequencing and has been established as a useful platform for DNA metabarcoding (Caporaso *et al*., 2012).

DNA extraction, polymerase chain reaction (PCR), purification, quantification and Illumina Miseq sequencing

1ml subsamples of each cryoconite sample were thawed at 4°C for 20 minutes. Genomic DNA was extracted using the DNeasy PowerSoil Kit (QIAGEN, Germany) according to manufacturer's instructions. The prokaryotic 16S (V4 region) and eukaryotic 18S (V9 region) rRNA genes were amplified by polymerase chain reaction (PCR). These targets were selected as they are hypervariable regions within a highly conserved gene so are suitable for the discernment of bacterial and archaeal (16S) and eukaryotic (18S) taxa (Amaral-Zettler *et al*., 2009). PCR cycles were run with three DNA volumes, 0.5 µl, 1.0µl and 1.5µl, to maximise chances of

successful polymerisation and the resulting amplified DNA was pooled. In cases where the DNA concentration was too low to yield detectable quantities of PCR product, volumes of 1.5µl, 2.0µl and 2.5µl were used. The extracted DNA was added to 19µl of GoTaq Polymerase reaction mix. The final PCR master mix contained 4 µl 5x GoTaq Flexi buffer, 2µl MgCl2 to enable DNA binding (25µM, Promega, Madison US), 0.8 µl Bovine Serum Albumin for the stabilisation of enzymatic reactions (BSA, 20 mg/ml BSA, NEB, UK), 0.16 µl of 200 µM dnTPs (Bioline, UK), 9.84µl H_2O, 0.2 µl Taq polymerase (5 U/µl, Promega, Madison US) and 1µl of each forward and reverse primer (10µM). The forward primer 515F (GTGCCAGCMGCCGCGGTAA) and reverse primer 806R (GGACTACHVGGGTWTCTAAT) containing the MiSeq sequencing adapters and 12-nucleotide Golay barcodes were used to amplify the V4 hyper-variable region of the bacteria and archaea 16S rRNA gene (260 bp, (Caporaso *et al*., 2011)). The primers 1391F and EukBr containing MiSeq sequencing adapters and a 12-nucleotide Golay barcode on the reverse primer were used to amplify the V9 hypervariable region of the eukaryote 18S rRNA genes (130 bp, (Amaral-Zettler *et al*., 2009; Caporaso *et al*., 2011, 2012)). The 16S rRNA gene was amplified in a thermocycler using the following program: initial denaturation at 94°C for 2 minutes followed by 30 cycles of denaturation at 94°C for 45 seconds; annealing at 50°C for 60 seconds and elongation at 72°C for 90 seconds; then, a final extension of 72°C for 10 minutes. The 18S rRNA gene was amplified using the following program: initial denaturation at 94°C for 3 minutes followed by 35 cycles of denaturation at 94°C for 45 seconds; annealing at 57°C for 60 seconds and elongation at 72°C for 90 seconds; then, a final extension of 72°C for 10 minutes. The PCR products along with a negative control were verified by gel electrophoresis using 1.5% agarose for 18S rRNA gene and 1% agarose gel for 16S rRNA gene PCR-products. Following purification according to AxyPrep Mag PCR clean-up protocol (Axygen, US), the triplicate PCR-products per sample were combined and concentrations determined using a Qubit 2.0 Fluorometer (ThermoFisher Scientific, US) and the manufacturer's protocol. The 16S and 18S rRNA gene amplicons of each sample were separated in preparation for sequencing. Final DNA concentrations for sequencing were 75ng/µl. The PCR

products were sequenced at the Natural History Museum sequencing facility using an Illumina MiSeq platform (Illumina, US).

16S and 18S rRNA gene sequence analysis

The raw sequence data was processed using QIIME2 v2018.8 (Caporaso *et al.*, 2012; Bolyen *et al.*, 2019). Sequences were demultiplexed based on Golay barcodes as a pre-processing step on the Illumina Miseq platform. Reads were quality-filtered, joined, chimeras were removed and amplicon sequence variants (ASVs) were generated using DADA2 (Callahan *et al.*, 2016). Alignment was performed with MAFFT (Katoh and Standley, 2013), and low complexity and repeating sequences were removed using the mask function in QIIME2. Phylogenetic trees were constructed with Fasttree (Price *et al*., 2009). Taxonomy was assigned with sklearn-based taxonomy classifier using the SILVA 138 database (Quast *et al.*, 2013). Representative sequences for each ASV were assigned to the highest confidence and identity match on the SILVA 138 database. ASVs assigned to the same taxon were grouped for relative abundance analyses. Chloroplast and mitochondrial DNA were excluded from the 16S rRNA gene dataset. ASVs with a frequency <3 were removed and the dataset was rarefied to 13044 16S rRNA gene sequences and 6261 18S rRNA gene sequences. Relative taxa abundance and ASV counts were then generated using QIIME2. 0.04% of the 16S rRNA gene assignment output, and 12.62% of 18S rRNA gene assignment output were unassigned to a domain or any lower classification. These were removed as they are unlikely to be relevant and correct sequences. The highest Genbank BLASTn match was also obtained for top most abundant 20 16S rRNA gene features and 20 18S rRNA gene features for verification.

viii. Nanopore sequencing

The 16S and 18S rRNA gene Illumina sequencing described above was selected for the first set of DNA analysis due to its broad coverage of bacterial, archaeal and eukaryotic species and high throughput. However, this scale was outside of the

scope of the Signy Island analyses. Therefore the analysis was kept to 16S rRNA gene sequencing, i.e. the bacterial and archaeal communities, which had been shown to be the stronger indicators of community structure in Results Chapter 1. Additionally, Oxford Nanopore sequencing was employed as a faster and more economical alternative. Nanopore has become widespread in its use as a fast and effective DNA metabarcoding tool with alignment accuracy often rivalling that of Illlumina sequencing (Benítez-Páez *et al*., 2016; Sevim *et al*., 2019), as has been shown in a comparison of techniques on a well characterised glacier microbiome (Edwards *et al*., 2019).

Oxford Nanopore Technologies (ONT) MinION-MinIT sequencing techniques are still under scrutiny, as 'third generation sequencing' has been a developing area over the last decade. Higher error rates than other sequencing methods have been a cause for concern, particularly for microbial community analyses (Venkatesan and Bashir, 2011; Deamer *et al*., 2016; Kerkhof, 2021). However, error rates in base calling have been continually reduced with the Guppy base-calling algorithm, the first release providing a median read accuracy of 89–94% from four microbial genomes and subsequent versions improving upon this score (Wick *et al*., 2019). While used here in a semi-quantitative capacity, the capability of ONT sequencing for sequence quantification has also improved in the last few years (Benítez-Páez *et al*., 2016; Sevim *et al*., 2019). Nanopore methods are now routinely used for a range of community analyses (Kerkhof, 2021). This includes their use on glacial surface ecosystems, where nanopore metagenome sequencing was shown to yield strong correlation to prior 16S rRNA gene profiles and captured the diversity of a well characterised glacier microbiome (Edwards *et al*., 2019). This sequencing method was therefore deemed suitable for the Signy Island analyses, but as the supraglacial and periglacial habitats of Signy Island are relatively understudied there is unfortunately no available sequence data for comparison to the genus level community composition.

DNA extraction, polymerase chain reaction (PCR), purification, quantification and Nanopore sequencing

Subsamples of each sediment sample were thawed at 4°C. Genomic DNA was extracted using the DNeasy PowerSoil Kit (QIAGEN) according to manufacturer's instructions. Forward primers used were 48 Oxford Nanopore Technologies standard barcodes fused to 27F (Hongoh *et al.*, 2003). Reverse primers were 1389R (Osborn *et al*., 2000; Hongoh *et al*., 2003). The primers were at 10µM and 100µM stock concentration respectively. Each reaction contained 15µl 2x Green Taq mix (OneTaq), 10.2µl nuclease free water, 1.5µl forward primer, 0.1µl reverse primer mix, 0.2µl BSA to stabilise enzymatic reactions, and 5µl DNA extract. Reactions were run for 35 cycles of: 45s at 94°C, 50s at 54°C, 90s at 68°C with a 5 minute pre-denature step at 94°C and 10 minute post-anneal step at 68°C. The PCR products along with a negative control were verified by gel electrophoresis using 1.5% for 16S rRNA gene PCR-products. Concentrations were determined using a Qubit 2.0 Fluorometer (ThermoFisher, US) and the manufacturer's protocol. Pooled PCR products were cleaned and concentrated using a QIAGEN gel extraction kit before libraries were made using the SQK-LSK109 kit (Oxford Nanopore Technologies, UK) according to the manufacturer's default protocol and the recommended NEB enzyme companion kit. 2µg PCR product was Formalin-Fixed Paraffin-Embedded (FFPE) treated for preservation and end repaired prior to ligation of AMX adaptors. SPRI bead clean-up (New England Biolabs) was carried out at a bead ratio of 0.8x and using short-fragment buffers for both washes before elution in a final volume of 15µl EB. This elution was loaded on a R9.4.1 flow cell and run to exhaustion using a MinIT (Oxford Nanopore Technologies), with real-time base-calling enabled by Oxford Nanopore Technologies Guppy 1.8.5 (Wick *et al*., 2019).

16S rRNA gene sequence analysis

Base-called sequences were concatenated to a single FastQ file which was then demultiplexed using porechop (https://github.com/rrwick/Porechop) with default settings for adaptor trimming and barcode demultiplexing. Reads successfully demultiplexed to their unique barcodes were then analysed using an in-house

custom pipeline (Andre Soares, Arwyn Edwards, Melanie Hay, Samuel Nicholls, Nicholas Loman, Sara Rassner, Andrew Mitchell, manuscript in preparation; "16SNAME offers nanopore acceleration of microbial ecology") which uses reads strictly quality filtered using filtlong (https://github.com/rrwick/Filtlong) for length and quality before alignment against a selected taxonomic database with minimap2 (Li, 2018) and processing of alignment outputs to form OTU-like tables reporting the raw abundance of reads matching named taxa for each sample. The database selected was the most recent release of SILVA at the time of utilisation (SILVA Ref NR 99 138.1).

ix. Statistical analyses

Unless stated otherwise all analysis described in this section was carried out using R software (R Core Team, 2021). Alpha diversity of the DNA-based community composition results was calculated using both Shannon's diversity (Shannon, 1948), and the Simpson index (Simpson, 1949) using the R package vegan (Oksanen *et al*., 2019). The Shannon index assesses both richness and evenness while the Simpson index indicates dominant groups in the sample by reporting proportions within the community. A simple species richness correlation between 16S rRNA gene and 18S rRNA gene results was calculated using Pearson's test for correlation (Pearson, 1931).

Beta diversity was tested using R packages vegan and phyloseq, and ggplot2 was used to visualise the results (McMurdie and Holmes, 2013; Wickham, 2016; Oksanen *et al.*, 2019). Non-metric dimensional scaling (NMDS) of ASV relative abundance and IPL compositions was performed using Bray-Curtis distances. NMDS allowed ordination of relative abundance data by similarity to identify clusters of similar communities. Bray-Curtis is a well-established method of identifying (dis)similarity between data (Bray and Curtis, 1957). The dataset of the 18S rRNA gene results was too small for reliable Bray-Curtis NMDS ordination, as indicated by very low stress values. Weighted Unifrac ordination was employed instead which

also took into account relative abundance and phylogenetic distance to ordinate beta diversity (Chang *et al*., 2011).

Occupancy of ASVs in each sample from the Illumina DNA sequence results was plotted based on mean relative abundance of each ASV per sample against presence of ASV in samples using ggplot2 (Wickham, 2016). Analysis of similarity (ANOSIM) and similarity percentage (SIMPER) analysis was also carried out using the R package vegan (Oksanen *et al*., 2019). ANOSIM was employed to determine whether taxa were significantly dissimilar between glaciers and polar regions according to the Bray-Curtis method (Clarke, 1993). SIMPER was employed to discern the average percentage contribution of taxa to the dissimilarity between polar regions (Clarke, 1993).

Co-occurrence was studied with the aim to identify whether certain organisms from Signy Island supraglacial and periglacial habitats tended to appear together in characteristic groupings in the differing habitats across the island. Co-occurrence of lowest-rank taxa determined from the Signy Island DNA sequencing results was calculated using a probabilistic co-occurrence model through the R package cooccur (Veech, 2013). The network of statistically significant co-occurrences was visualised using the software Cytoscape (Shannon *et al*., 2003).

Results Chapter 1: The microbiome of Arctic and Antarctic cryoconite and its parallels with Snowball Earth

Summary

High-throughput 16S and 18S rRNA gene sequencing and intact polar lipid quantification was used to investigate the communities of a wide range of cryoconite holes from 15 locations across the Arctic and Antarctic. I was able to determine the groups contributing to this difference at the family and genus level. The various biotic niches (grazer, predator, photoautotroph, chemotroph), are filled in every location. However, there is a clear difference between the bacterial and microalgal communities of the Arctic and that of the Antarctic. Therefore cryoconite holes may be a global feature of glacier landscapes, but they are inhabited by regionally distinct microbial communities. This enabled identification of Cryogenian analogue communities according to similarities in taxonomic composition and local environment. Together, these results provide an in-depth analysis of microbial cryoconite communities at a global scale, allowing for comparison between these distinct modern polar cryoconite communities and Snowball Earth life. The results of 16S and 18S rRNA gene sequencing have been reported in Millar *et al* 2021, published as a result of this project in *Frontiers in Microbiology: Extreme Microbiology*.

Introduction

Hypothesis 1: Modern polar cryoconite hole communities are analogous to the biodiversity and eukaryotic key taxa of the Cryogenian.

There are notable similarities between the constituent microorganisms of cryoconite and the taxa known to have survived Snowball Earth, in particular the presence of both bacterial and eukaryotic phototrophs along with a wide range of heterotrophic eukaryotic phyla (Hoffman, 2016). However, the structure of cryoconite holes is not consistent worldwide, rather it varies according to the prevailing physical conditions. In cold, dry climates such as continental Antarctica, cryoconite holes are usually covered by an ice lid through most or all of the year (Tranter *et al*., 2004; Webster-Brown *et al*., 2015). In the McMurdo Dry Valleys, ice lids of up to 30cm have been observed on the majority of cryoconite holes year-round (Fountain *et al*., 2004; Tranter *et al*., 2004). Some of these thick lids may melt during particularly warm periods, years apart (Foreman *et al*., 2007). Around 50% of lidded holes are hydrologically connected under the ice surface, the other 50% are completely isolated (Fountain *et al*., 2004). The holes may melt under the ice lid, connecting to one another on a seasonal or sub-seasonal timescale (Bagshaw *et al*., 2007). These closed holes are a contrasting environment to the seasonally "open" cryoconite holes found elsewhere, particularly in many Arctic and mountainous regions (Cook *et al*., 2015b). Open holes do not have a permanent ice lid and can hence exchange gas with the atmosphere. They primarily occur on glacial ablation zones that exhibit seasonal melting (Bagshaw *et al*., 2012), experiencing regular flushing by stream flow which distributes cryoconite across the glacier surface (Irvine-Fynn *et al*., 2010).

Varying cryoconite environments induce variation in cryoconite microbial ecosystems (Edwards *et al*., 2011). DNA sequences extracted from cryoconite communities tend to be dominated by Proteobacteria, Bacteroidetes, Cyanobacteria and microalgae (Cameron *et al*., 2012b; Edwards *et al*., 2013b; Sommers *et al*., 2018). They also harbour fungi, protists and micro-animals (meiofauna) (Zawierucha *et al*., 2015). The relative abundance of these organisms

Table 5 GPS locations and site names for cryoconite samples from the Arctic and Antarctic.

Sample site	Location	No. of Samples	Width (cm)	Ice Lid
Canada Glacier, Antarctica	77.6°S, 163.0°E	9	23-57	Present
Commonwealth Glacier, Antarctica	77.6°S, 163.3°E	9	28-64	Present
Taylor Glacier, Antarctica	77.7°S, 162.0°E	9	41-52	Present
Upper Wright Glacier, Antarctica	77.5°S, 162.9°E	7	37-57	Present
Lower Wright Glacier, Antarctica	77.5°S, 160.7°E	6	27-43	Present
Diamond Glacier, Antarctica	79.8°S, 159.0°E	4	41-52	Present
Miers Glacier, Antarctica	78.8°S, 163.7°E	5	14-39	Present
Upper Koettlitz Glacier, Antarctica	78.3°S, 163.63°E	9	28-97	Present
Lower Koettlitz Glacier, Antarctica	78.1°S, 164.2°E	5	35-55	Present
Utsteinen Scoop, Antarctica	72.0°S, 23.3°E	2	5-10	Present
Kangerlussuaq, Greenland	67.1°N, 50.7°E	3	15-40	Absent
Ice Margin, Greenland	67.2°N, 50.0°E	4	5-20	Absent
Ice Core, Greenland	67.1°N, 50.7°E	3	1-15	Present (layers of ice above)
Storglaciären, Sweden	67.1°N, 18.6°E	3	Unknown	Absent
Midtre Lovénbreen, Svalbard	78.8°N, 12.1°E	5	1-15	Absent

varies with biogeography (Liu *et al*., 2017; Darcy *et al*., 2018). Research to date has revealed that communities are more similar within glaciers than between glaciers, but lack sufficient detail to determine whether trends are local, regional or global. In a study using community fingerprinting and clone library analysis, it was discovered that there is a divide between the bacterial communities of the Arctic and Antarctic (Cameron *et al*., 2012b). These results raised important questions about the potentially distinct biomes of the poles and the variability of cryoconite. However, the methods used could only yield limited detail in comparison to insights arising from the rapid evolution of high throughput DNA sequencing technologies in the ensuing decade. It has not yet been established which taxa are contributing to this difference in community composition. Therefore, this chapter addresses the following objective.

Objective 1.1: Assess cryoconite hole microbial diversity and community composition.

Cryoconite community composition was assessed using 16S and 18S rRNA gene high throughput sequencing, covering Archaea and Bacteria, as well as Eukarya. The breadth of geographic coverage in our sample s*et al*lowed comparison not only between the polar regions, but between different environments within each polar region (Table 5, Figure 12). I compare surface cryoconite, cryoconite collected from an ice core and ice margin sediment, and compare samples from ice sheet interiors with marginal locations.

In addition, the composition of intact polar lipids (IPLs) was examined to provide an additional metric with which to investigate differences between cryoconite across glaciers and between the polar regions. Previously the IPL composition of cryoconite holes had not been characterised. Unlike DNA gene sequence analysis which cannot distinguish between living organisms and legacy DNA, the polar head group of IPLs is rapidly hydrolysed upon cell death (White *et al*., 1979; Harvey *et al*., 1986) and so the IPL results here can be considered to be representative of living

cells. IPL composition in the Arctic and Antarctic cryoconites was compared to the to 16S and 18S rRNA gene composition.

The community composition as revealed by 16S and 18S rRNA gene sequencing and IPL composition analysis was then compared to predicted Cryogenian taxa. Taxa such as Amoebozoa have been confirmed to have emerged by the Cryogenian through microfossil evidence from the Neoproterozoic (Porter and Knoll, 2000). Through the implementation of molecular clocks, further crown groups have been predicted to have survived through the Cryogenian (Peterson and Butterfield, 2005; Parfrey *et al*., 2011; Sánchez-Baracaldo *et al*., 2017). The main application of these molecular clocks when studying the Cryogenian has been to study the emergence of new eukaryotic species, known as the radiation of the eukaryotes (Peterson and Butterfield, 2005). Groups such as Excavata, Alveolates and Choanoflagellates are predicted to have emerged prior to the Cryogenian by consensus of multiple molecular clocks (Douzery *et al*., 2004; Peterson and Butterfield, 2005; Parfrey *et al*., 2011). By comparing the organisms present in a range of modern cryoconite to key Cryogenian taxa, it was possible to identify particularly suitable analogue ecosystems.

The environmental conditions in which the cryoconite holes were found were also compared to those of the Cryogenian. The Cryogenian saw a wide range of climates over its 85 million years and over different areas of the planet. Some areas were ice free during glaciations while others are predicted to have been covered by vast ice sheets (Hoffman *et al*., 2017). Warmer temperatures (above 0°C) occurred during the interglacial and end-Marinoan phases, but also within the Sturtian glaciation there may have been multiple ice sheet advances and retreats (Le Heron, 2015). Temperature, local geography and latitude varied between sample sites, and between the Arctic and Antarctic cryoconite. The sites were assessed on their suitability as analogues to various potential Cryogenian conditions. These results are reported under the following aim and objective:

Objective 1.2: Compare cryoconite taxonomy to Cryogenian keystone taxa.

Results

Objective 1.1: Assess cryoconite hole microbial diversity and community composition

Bacteria and Archaea community composition

Following filtering and rarefaction, 13044 16S rRNA gene sequences per sample were obtained and 24 bacterial and one archaeal phyla were identified. 4497 distinct 16S rRNA gene amplicon sequence variants (ASVs) were identified, 313 of which were shared between the Arctic and Antarctic. Only nine archaeal sequences were found, appearing in seven samples in the McMurdo Dry Valleys. Cyanobacteria, Proteobacteria, Bacteroidetes, and Actinobacteria were the most abundant bacterial phyla, accounting for 65% of the total 16S rRNA gene ASVs (Figure 13). These phyla were present across all samples. All other phyla contributed to <6% of the total 16S rRNA gene ASVs. The most abundant of these minor lineages was the Deinococcota (0.8% of total 16S rRNA gene ASVs), which are broadly tolerant polyextremophiles (Rew, 2003).

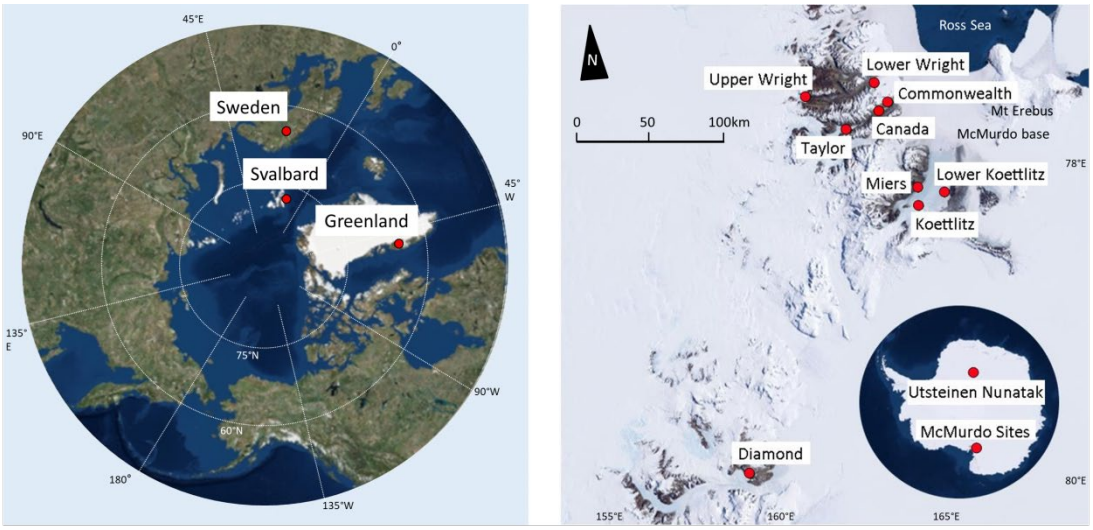

Figure 12 Sampling locations. (A) Arctic map, highlighting regions sampled. Points marked indicate sample site locations and names. (B) Map of Antarctic sampling locations. Antarctic continental map highlighting the Utsteinen Scoop and the McMurdo Dry Valleys. Underlying is a McMurdo Valleys map, which shows a detailed view of those sites. Base maps were created using ArcGIS® software by Esri. ArcGIS® and ArcMap™ are the intellectual property of Esri and are used herein under license. Source: ArcWorld Supplement.

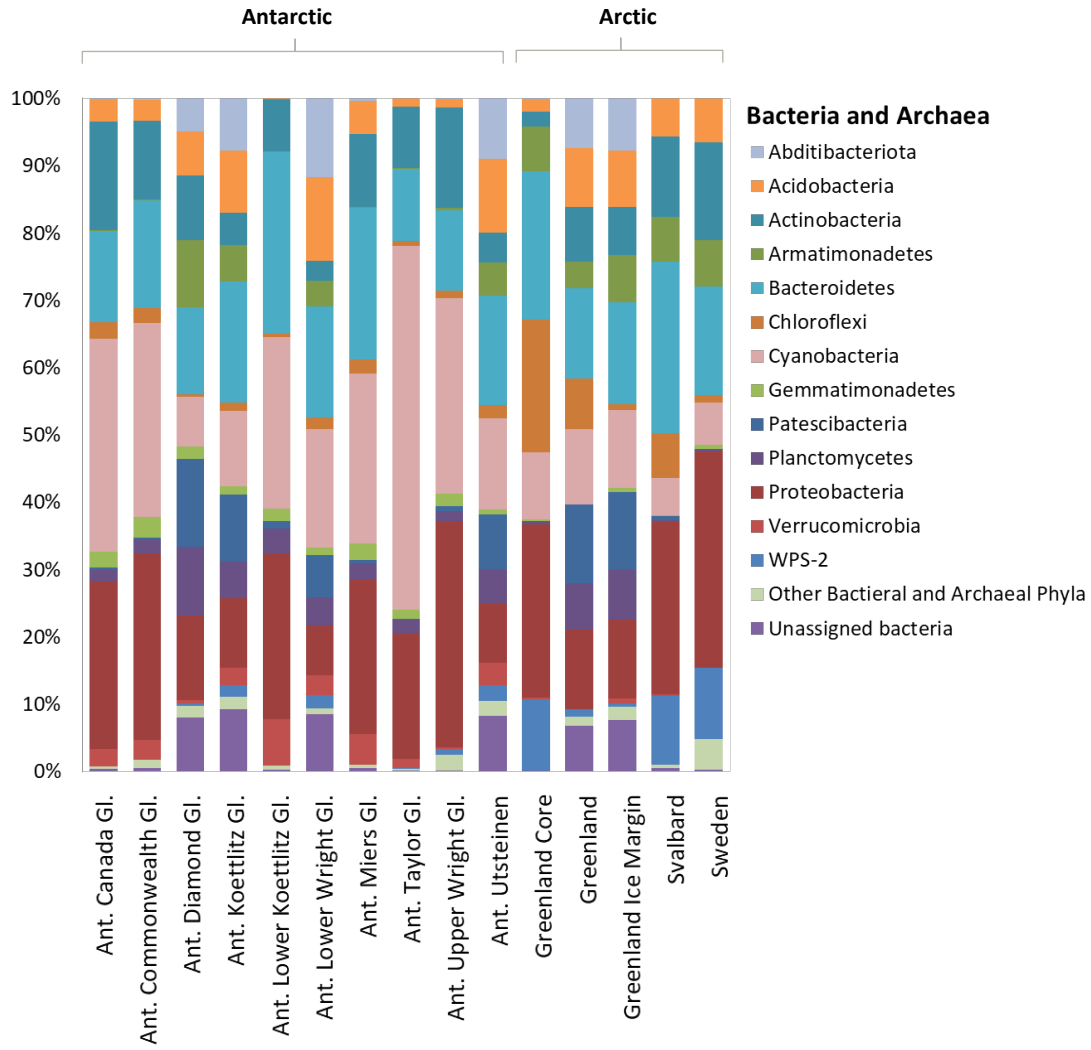

Figure 13A Relative abundance of bacteria in Arctic and Antarctic cryoconite, averaged by glacier. **A** Bacterial phyla. Phyla contributing to <1% of the total abundance are grouped as "Other." **B-H** Relative abundance of genera within the top four most abundant phyla. Proteobacteria have been divided into alpha-, beta-, delta-, and Gammaproteobacteria. Genera contributing to <1% of the total abundance are grouped as "Other." Where a genus was unknown, lowest rank known is shown. Taxa were assigned according to the SILVA database. "Ant. Gl." denotes Antarctic Glaciers.

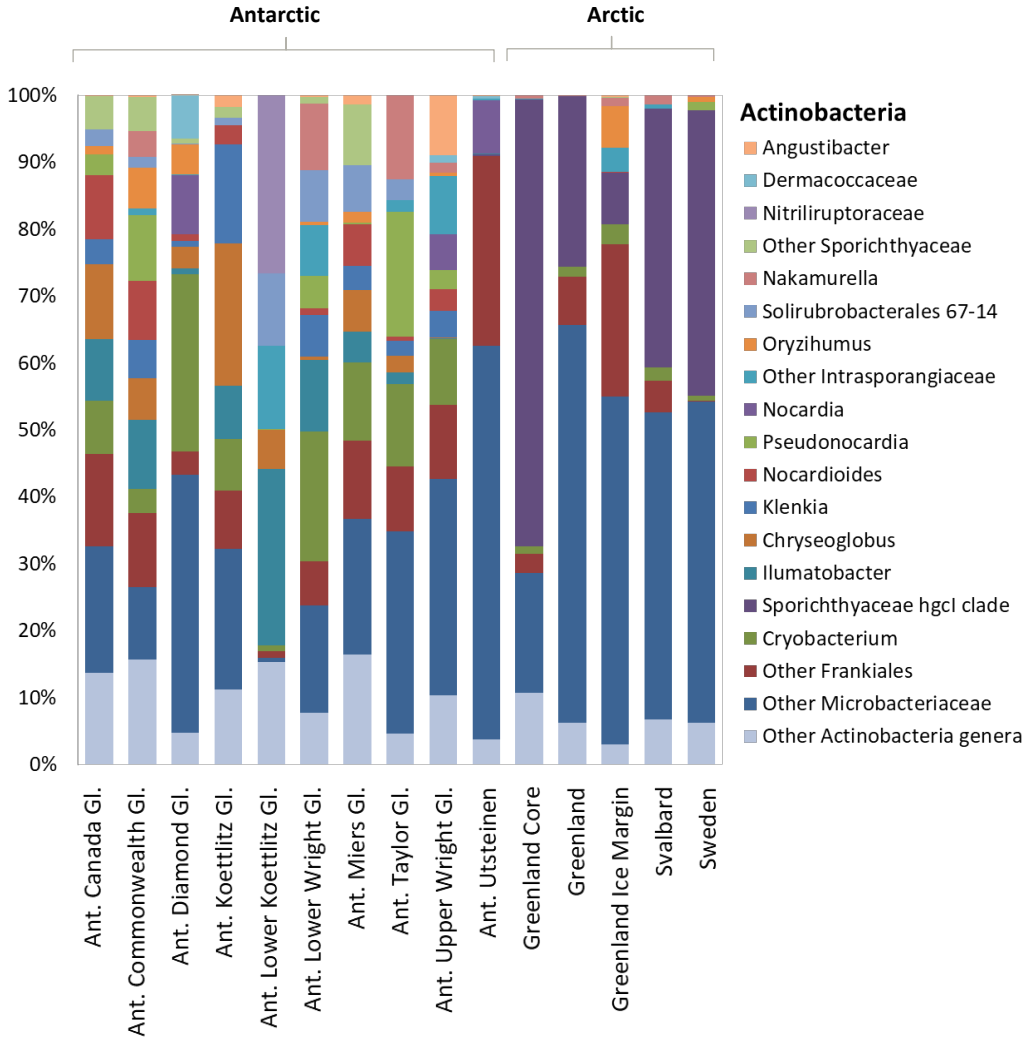

Figure 13B Relative abundance of bacteria in Arctic and Antarctic cryoconite, averaged by glacier. **A** Bacterial phyla. Phyla contributing to <1% of the total abundance are grouped as "Other." **B-H** Relative abundance of genera within the top four most abundant phyla. Proteobacteria have been divided into alpha-, beta-, delta-, and Gammaproteobacteria. Genera contributing to <1% of the total abundance are grouped as "Other." Where a genus was unknown, lowest rank known is shown. Taxa were assigned according to the SILVA database. "Ant. Gl." denotes Antarctic Glaciers.

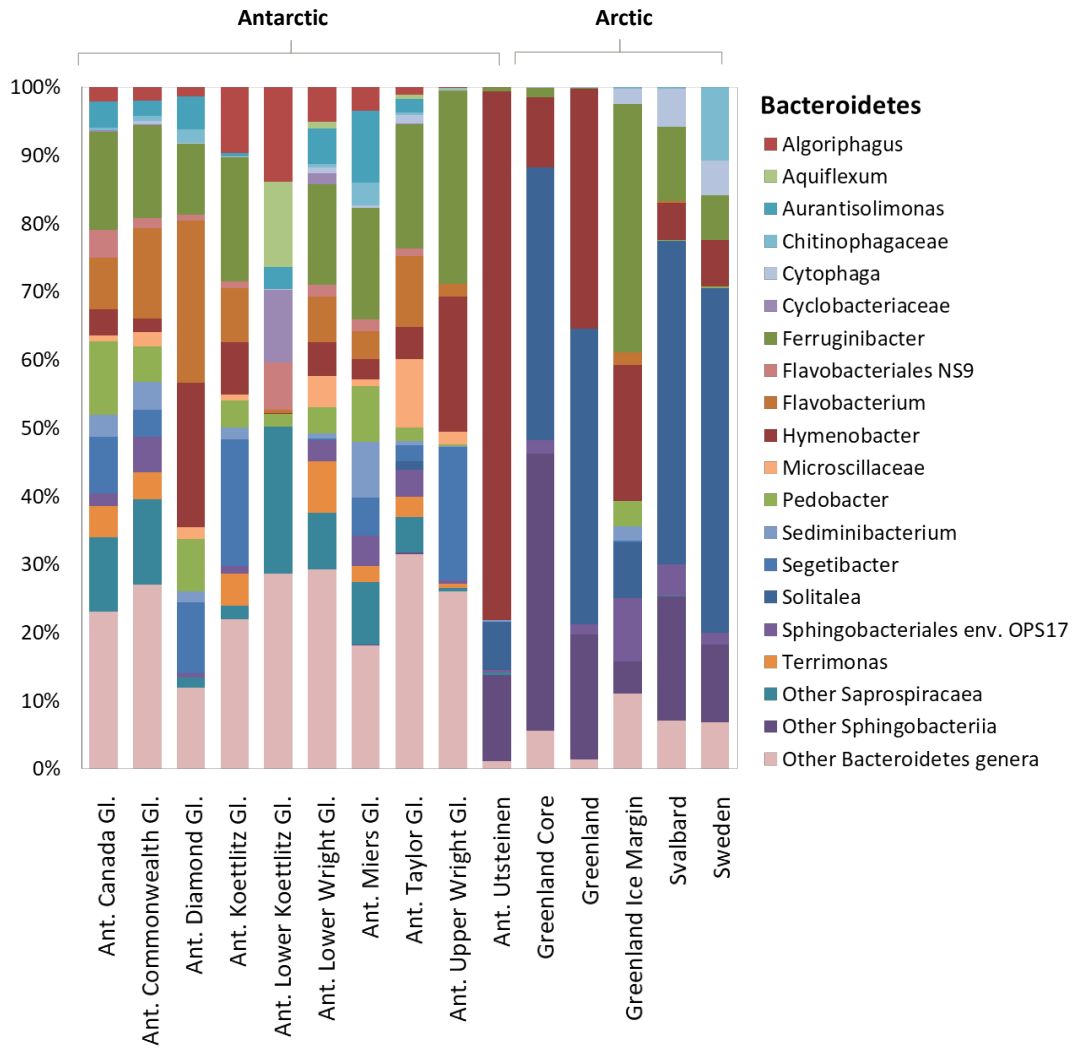

Figure 13C Relative abundance of bacteria in Arctic and Antarctic cryoconite, averaged by glacier. **A** Bacterial phyla. Phyla contributing to <1% of the total abundance are grouped as "Other." **B-H** Relative abundance of genera within the top four most abundant phyla. Proteobacteria have been divided into alpha-, beta-, delta-, and Gammaproteobacteria. Genera contributing to <1% of the total abundance are grouped as "Other." Where a genus was unknown, lowest rank known is shown. Taxa were assigned according to the SILVA database. "Ant. Gl." denotes Antarctic Glaciers.

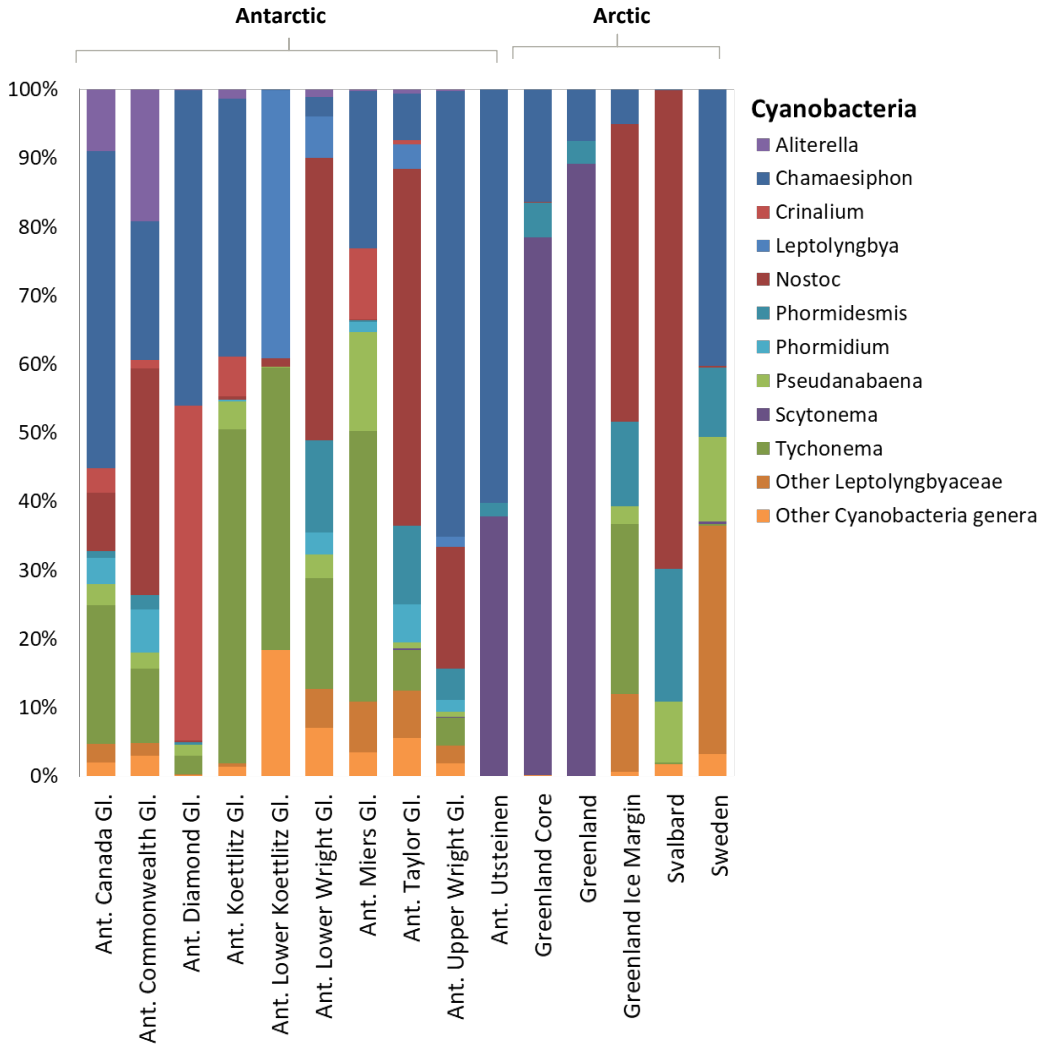

Figure 13D Relative abundance of bacteria in Arctic and Antarctic cryoconite, averaged by glacier. **A** Bacterial phyla. Phyla contributing to <1% of the total abundance are grouped as "Other." **B-H** Relative abundance of genera within the top four most abundant phyla. Proteobacteria have been divided into alpha-, beta-, delta-, and Gammaproteobacteria. Genera contributing to <1% of the total abundance are grouped as "Other." Where a genus was unknown, lowest rank known is shown. Taxa were assigned according to the SILVA database. "Ant. Gl." denotes Antarctic Glaciers.

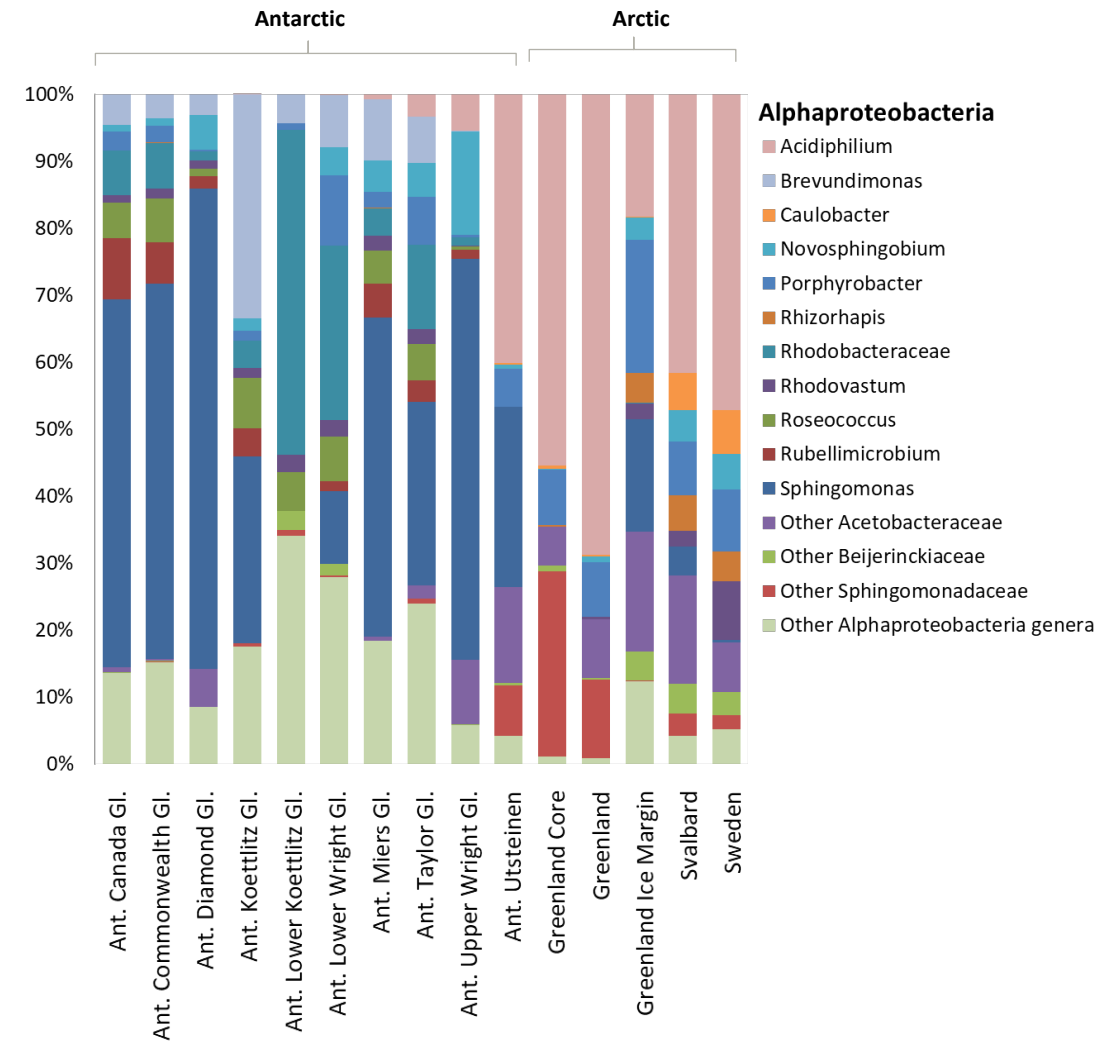

Figure 13E Relative abundance of bacteria in Arctic and Antarctic cryoconite, averaged by glacier. **A** Bacterial phyla. Phyla contributing to <1% of the total abundance are grouped as "Other." **B-H** Relative abundance of genera within the top four most abundant phyla. Proteobacteria have been divided into alpha-, beta-, delta-, and Gammaproteobacteria. Genera contributing to <1% of the total abundance are grouped as "Other." Where a genus was unknown, lowest rank known is shown. Taxa were assigned according to the SILVA database. "Ant. Gl." denotes Antarctic Glaciers.

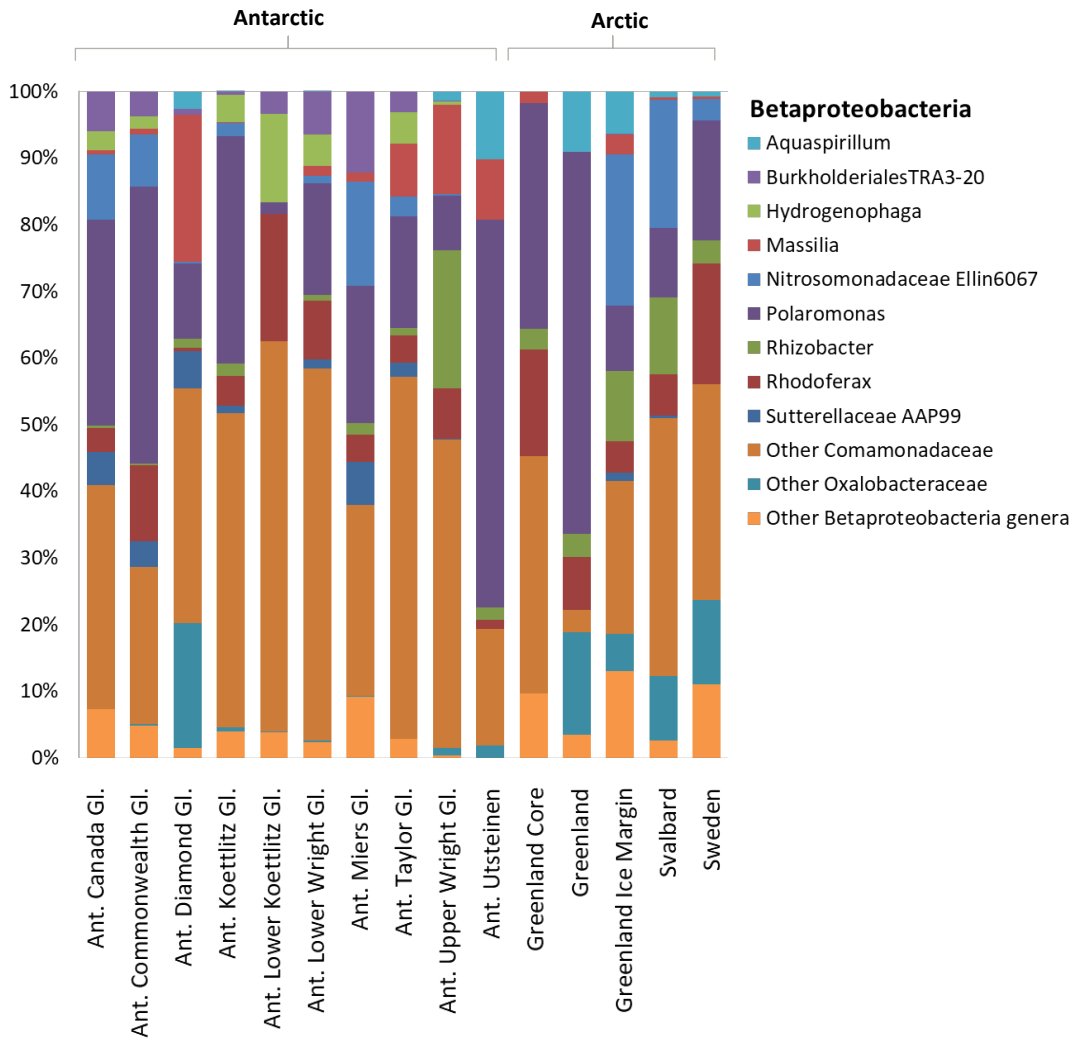

Figure 13F Relative abundance of bacteria in Arctic and Antarctic cryoconite, averaged by glacier. **A** Bacterial phyla. Phyla contributing to <1% of the total abundance are grouped as "Other." **B-H** Relative abundance of genera within the top four most abundant phyla. Proteobacteria have been divided into alpha-, beta-, delta-, and Gammaproteobacteria. Genera contributing to <1% of the total abundance are grouped as "Other." Where a genus was unknown, lowest rank known is shown. Taxa were assigned according to the SILVA database. "Ant. Gl." denotes Antarctic Glaciers.

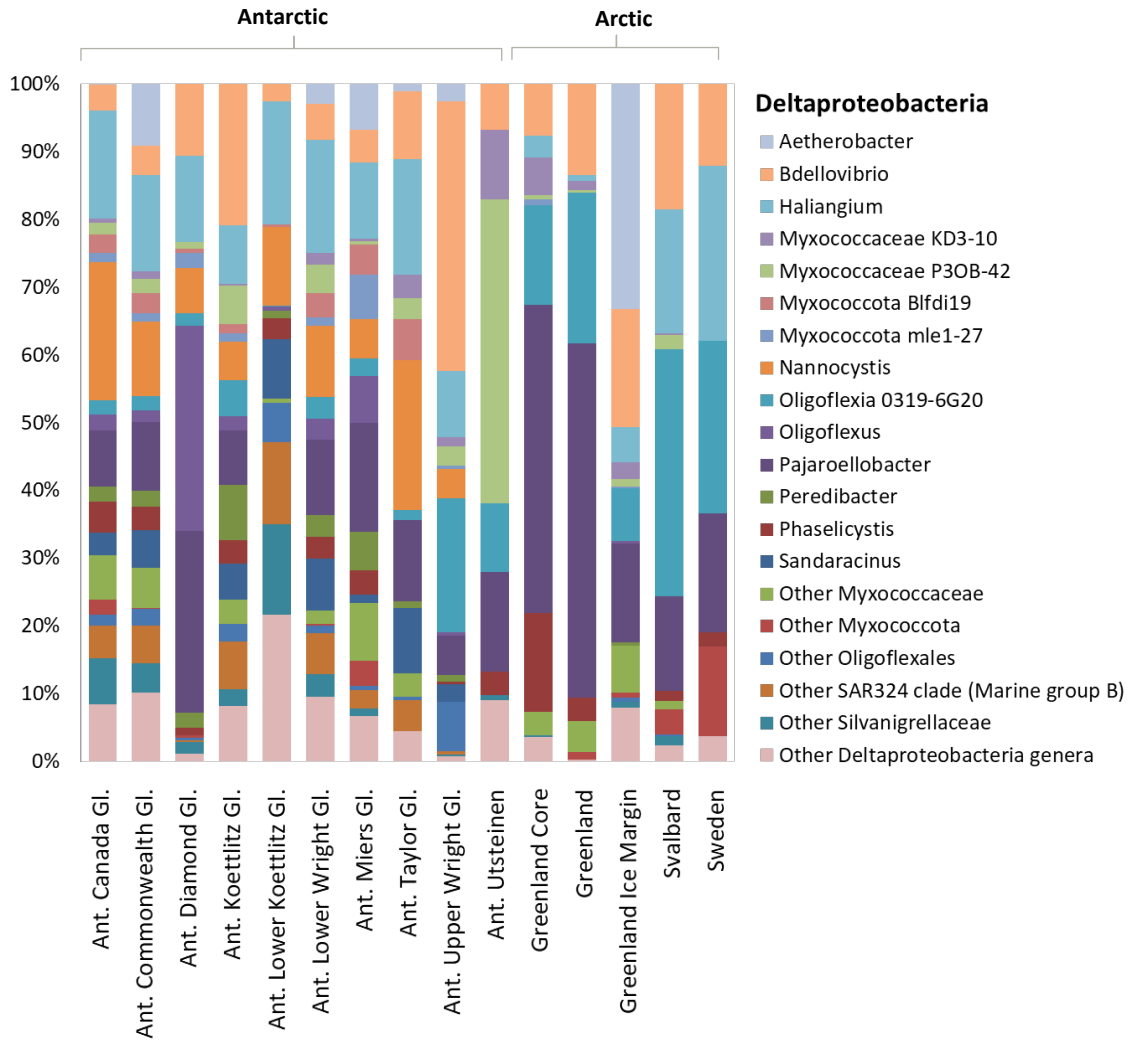

Figure 13G Relative abundance of bacteria in Arctic and Antarctic cryoconite, averaged by glacier. **A** Bacterial phyla. Phyla contributing to <1% of the total abundance are grouped as "Other." **B-H** Relative abundance of genera within the top four most abundant phyla. Proteobacteria have been divided into alpha-, beta-, delta-, and Gammaproteobacteria. Genera contributing to <1% of the total abundance are grouped as "Other." Where a genus was unknown, lowest rank known is shown. Taxa were assigned according to the SILVA database. "Ant. Gl." denotes Antarctic Glaciers.

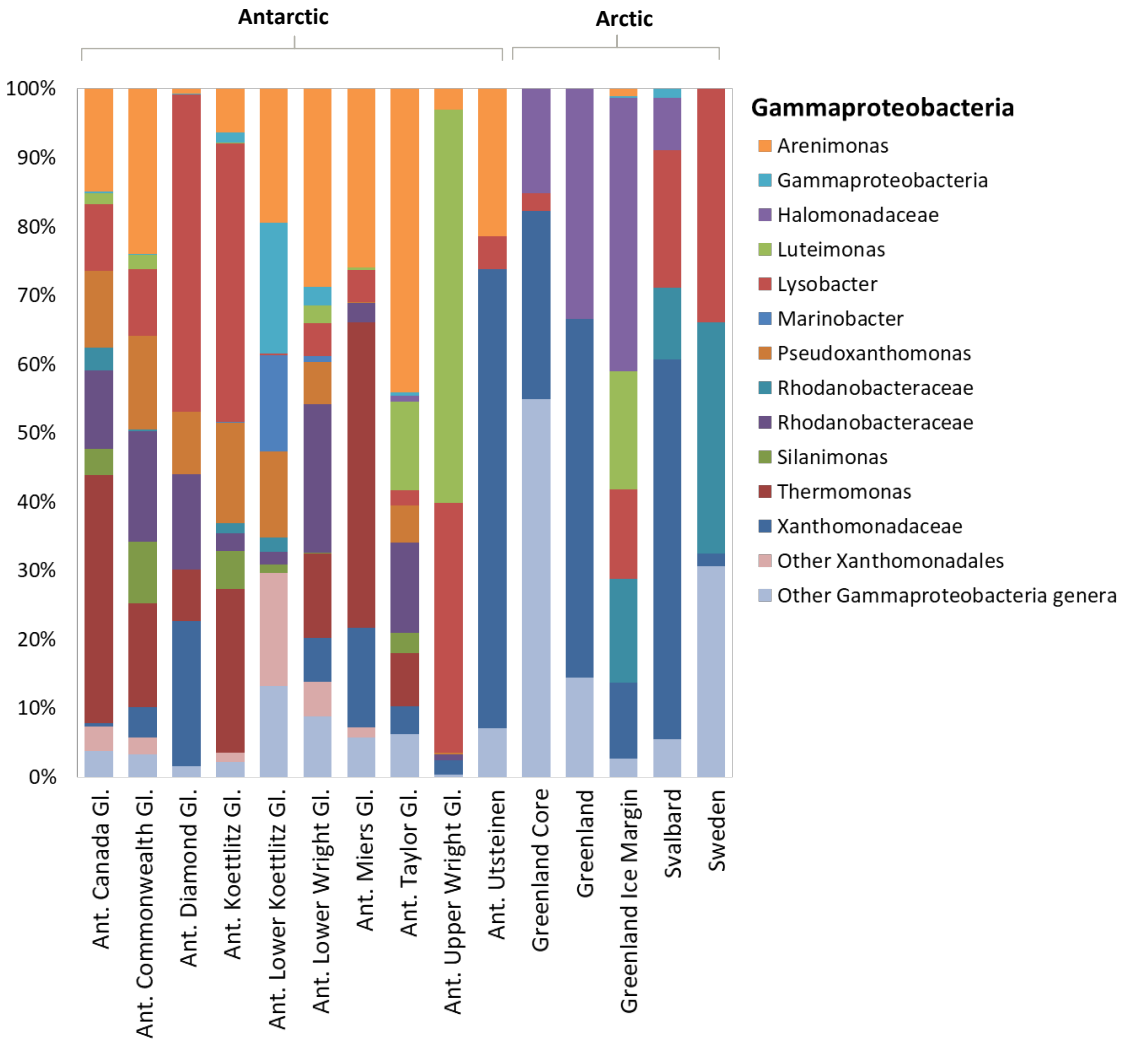

Figure 13H Relative abundance of bacteria in Arctic and Antarctic cryoconite, averaged by glacier. **A** Bacterial phyla. Phyla contributing to <1% of the total abundance are grouped as "Other." **B-H** Relative abundance of genera within the top four most abundant phyla. Proteobacteria have been divided into alpha-, beta-, delta-, and Gammaproteobacteria. Genera contributing to <1% of the total abundance are grouped as "Other." Where a genus was unknown, lowest rank known is shown. Taxa were assigned according to the SILVA database. "Ant. Gl." denotes Antarctic Glaciers.

Although all locations were found to have the same highest relative abundance phyla, there are noticeable differences between the Arctic and Antarctic 16S rRNA gene cryoconite composition. Arctic cryoconite communities had a higher relative abundance of Chloroflexi and Armatimonadetes, and a lower relative abundance of Cyanobacteria. Cyanobacteria accounted for 9% of ASVs across Arctic locations compared to 24% in cryoconite from Antarctica. The variation between Arctic and Antarctic taxonomic diversity within the datasets was explored by analysis of beta diversity. I found a compositional divide between Arctic and Antarctic cryoconite ecosystems based on the relative abundance of taxa. An ANOSIM test of the dissimilarity between poles using the Bray-Curtis method produced an R value of 0.723 at p=0.0001 (pairwise community dissimilarity), suggesting a significant level of dissimilarity (Table 6). Non-metric multi-dimensional scaling (NMDS) of Bray-Curtis distances ordinates this separation between Arctic and Antarctic cryoconite communities (Figure 14). The Greenland margin and ice core samples cluster closest with the other Greenland samples, and then other Arctic sites.

Table 6 ANOSIM analysis of 16S and 18S ASVs in between polar regions and individual glaciers across the Arctic and Antarctic. Shown over all taxa and most abundant phyla individually. Significance levels of <0.05 are marked with "*".

	Polar Region		Location	
Group	R Value	Significance	R Value	Significance
All 16S	0.723	1.00E-04*	0.7175	1.00E-04*
Cyanobacteria	0.4583	1.00E-04*	0.6017	1.00E-04*
Actinobacteria	0.5552	1.00E-04*	0.7378	1.00E-04*
Proteobacteria	0.6611	1.00E-04*	0.7530	1.00E-04*
Bacteroidetes	0.2418	1.00E-04*	0.2461	1.00E-04*
All 18S	0.02559	0.0859	0.1171	1.00E-04*
SAR Group	0	1	0	1
Archaeplastida	0	1	0	1
Opisthokonta	0.1603	0.0134*	0.5454	1.00E-04*

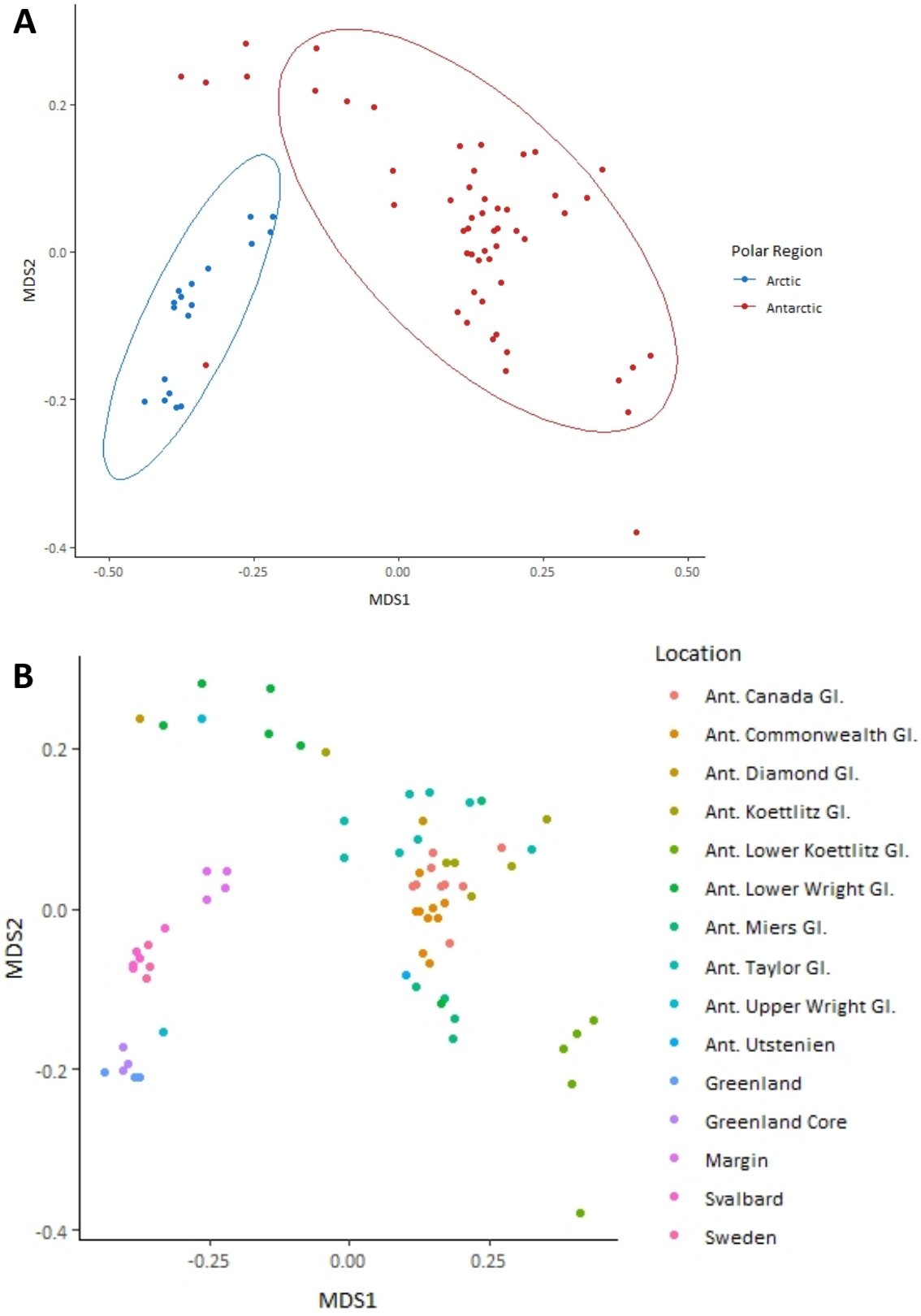

Figure 14 Bray-Curtis dissimilarity of 16S rRNA gene amplicon sequence variants (ASVs) found in each cryoconite and visualised by non-metric multidimensional scaling (NMDS) ordination. Cryoconite holes are grouped by **A** polar region and **B** glacier. Ellipses represent 95% confidence intervals.

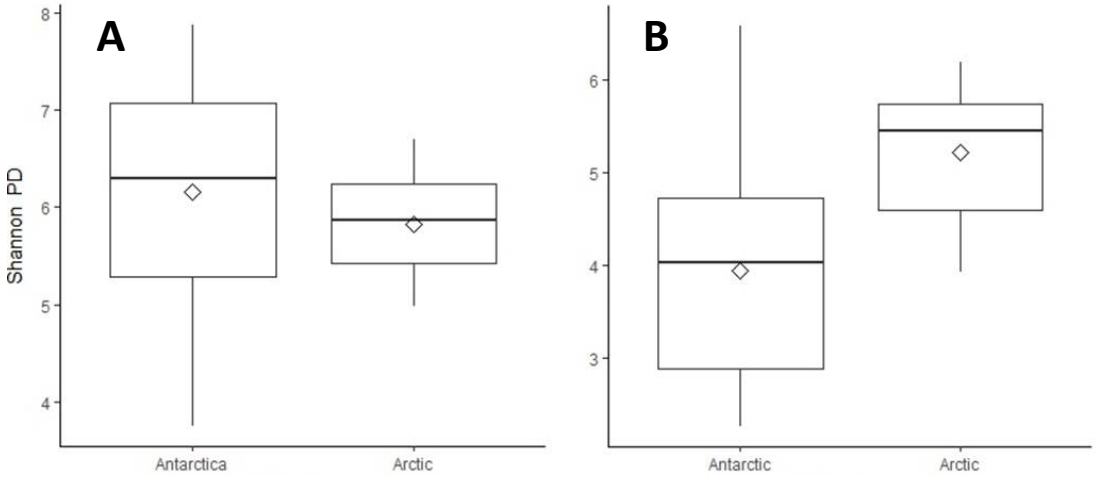

Figure 15 Shannon's phylogenetic diversity of **A** 16S rRNA gene ASVs and **B** 18S rRNA gene ASVs in cryoconite samples, grouped by polar region. Diamonds indicate mean values.

While there was more variation between the types of Greenland samples (margin, ice core and ice sheet surface) than within groups, none were outliers within a 95% confidence interval of the Arctic samples. Therefore Greenland margin and Greenland ice core samples have been grouped with the other Arctic samples during polar region comparisons. The range and mean number of distinct ASVs was considerably lower in the Arctic than Antarctic (Table 7). Alpha diversity and evenness of bacteria and archaea in the samples was investigated further using the Shannon diversity indices (Figure 15). The lowest richness was identified in cryoconite samples from the Antarctic Upper Wright (4.76) and Lower Wright (4.85) glaciers. The highest values were also from the Antarctic: the Commonwealth (7.15) and Canada (6.66) glaciers. The mean values were 6.22 for the Antarctic and 5.62 for the Arctic.

The four most abundant bacterial phyla were investigated further to elucidate the composition of their genera and contribution to the dissimilarity between the poles (Figure 13). In the Actinobacteria, there is a striking difference between Arctic and Antarctic samples. While the Antarctic samples, with the exception of the Upper Wright glacier, contain a diverse array of Actinobacteria, the Arctic samples are dominated by Sporichthyaceae hgcl clade and Microbacteriaceae which make up 77% of Arctic Actinobacteria sequences. In the Antarctic samples, the Sporichthyaceae hgcl clade contributes 0.04% and the Microbacteriaceae 27%.

Table 7 Alpha diversity microorganisms in cryoconite holes as measured by average number of 16S and 18S ASVs, and the Shannon and Simpson indices. Metazoa were removed from the 18S sample set.

16s				18s			
Location	Average ASVs	Shannon	Simpson	Location	Average ASVs	Shannon	Simpson
Ant.Canada Gl.	488.444	6.659	0.956	Ant.Canada Gl.	116.556	4.197	0.792
Ant. Commonwealth Gl.	615.111	7.152	0.967	Ant. Commonwealth Gl.	123.333	3.755	0.734
Ant. Diamond Gl.	226.500	5.557	0.950	Ant. Diamond Gl.	87.000	5.320	0.959
Ant. Koettlitz Gl.	271.833	5.624	0.932	Ant. Koettlitz Gl.	75.125	3.382	0.757
Ant. Lower Koettlitz Gl.	349.600	6.164	0.952	Ant. Lower Koettlitz Gl.	112.000	5.097	0.928
Ant. Wright Gl.	169.500	4.850	0.896	Ant. Wright Gl.	26.600	2.603	0.739
Ant. Miers Gl.	475.200	6.558	0.953	Ant. Miers Gl.	132.000	4.625	0.854
Ant. Taylor Gl.	325.250	6.057	0.946	Ant. Taylor Gl.	45.000	3.886	0.856
Ant. Upper Wright Gl.	114.000	4.762	0.914	Ant. Upper Wright Gl.	93.000	3.324	0.677
Ant. Usteinen Scoop	530.000	6.302	0.929	Ant. Usteinen Scoop	104.000	4.805	0.900
Greenland Core	136.667	5.112	0.944	Greenland Core	54.000	3.998	0.877
Greenland	141.333	5.349	0.958	Greenland	118.000	5.055	0.937
Greenland Ice Margin	333.500	6.295	0.963	Greenland Ice Margin	158.750	5.672	0.957
Svalbard	273.600	5.966	0.962	Svalbard	111.429	5.891	0.969
Sweden	230.333	6.141	0.972	Sweden	91.667	4.685	0.926

The psychrophile *Cryobacterium* contributes to 9% of total Actinobacteria sequences and 12% of Antarctic Actinobacteria sequences. In the Bacteroidetes, the Arctic cryoconite holes vary from the Antarctic cryoconite holes in their high relative abundance of *Solitalea* (39% of Bacteroidetes sequences in the Arctic compared to 1% in the Antarctic). The Bacteroidetes ASVs cover 155 genera. 139 of these were present in the Antarctic and only 51 in Arctic cryoconite communities. Of these 51 present in Arctic samples, 11 were only present in the Greenland margin site. These included the *Segetibacter* and *Spirosoma*. The most abundant Cyanobacterial genera were *Tychonema*, *Chamaesiphon*, *Nostoc*, *Scytonema and Tychonema*. Together these contributed to 71% of the total Cyanobacterial ASVs. All other groups each contributed <6%. 28 genera were found in total, all of which were present in the Antarctic cryoconite communities, but only 11 of these were found in the Arctic samples. The largest difference in percentage proportion between the Arctic and Antarctic was *Scytonema* (42% of Arctic and 3% of Antarctic samples). This genus is absent from the Greenland margin sediment but dominated the other Greenland samples. It was also absent in cryoconite from Svalbard.

The Alphaproteobacteria made up 38% of Proteobacteria 16S rRNA gene sequences in the Antarctic and 66% of Proteobacteria sequences in Arctic cryoconite, the Betaproteobacteria comprised 33% of Antarctic and 18% of Arctic Proteobacteria sequences, and the Gammaproteobacteria comprised 22% of Antarctic and 6% of Arctic Proteobacteria sequences. Other 16S rRNA gene sequences belonged to Deltaproteobacteria (7% and 10% of Proteobacteria 16S rRNA gene sequences in Antarctic and Arctic cryoconite respectively) and unassigned Proteobacteria (0.02% and 0.05% of Proteobacteria 16S rRNA gene sequences in the Antarctic and Arctic cryoconite respectively). The composition of Betaproteobacteria genera was similar between the Arctic and Antarctic, but there were more differences between the polar regions in the Alphaproteobacteria, Deltaproteobacteria and Gammaproteobacteria. In the Alphaproteobacteria, *Sphingomonas* had a high relative abundance in the Antarctic (41% of Alphaproteobacteria compared to 3% in the Arctic) whereas *Acidiphilium* had higher relative abundant in the Arctic (50% of Alphaproteobacteria compared to 7% in the Antarctic). The genus *Nannocystis*,

which contributed 10% to the Antarctic Deltaproteobacteria, was absent from the Arctic samples. Oligoflexia 0319-6G20 contributed to 4% of Antarctic Deltaproteobacteria sequences and 4% of Arctic Deltaproteobacteria. Of the 31 genera that contributed to >1% of Deltaproteobacteria 16S rRNA gene sequences, 28 were present in the Antarctic samples and 9 in the Arctic samples. A large proportion of the 16S rRNA gene sequences assigned as Gammaproteobacteria in the Arctic was assigned to the Halomonadaceae (21%), a group of halophiles, and Xanthomonadaceae (24%). Interestingly, the Gammaproteobacteria 16S rRNA gene composition in samples from the Greenland margin samples bore a greater similarity to the Svalbard samples than the other Greenland samples, largely consisting of *Lysobacter* and unassigned Rhodanobacteraceae in addition to Halomonadaceae and Xanthomonadaceae. 49 of the 51 Gammaproteobacteria genera were found in the Antarctic, 17 were present in the Arctic, 15 were present in both polar regions.

Separate non-metric multidimensional scaling analysis of the four most abundant phyla Cyanobacteria, Bacteroidetes, Proteobacteria and Actinobacteria 16S rRNA gene sequences suggested that the presence of distinct communities in the Arctic and Antarctica (Figure 16). ANOSIM analyses produce R values of 0.5 or above for Actinobacteria and Proteobacteria at a significance level of p=0.0001. However, the R values are greater when testing for differences in phyla composition between locations (0.24-0.66 between poles p=000.1, 0.24-0.75 between locations p=000.1) (Table 6). The contribution of each bacterial and archaeal phylum to the dissimilarity between poles was investigated using SIMPER analysis (Table 8). The phyla with a significant contribution to the dissimilarity between the poles were less abundant groups including Chloroflexi and the WPS-2 group. To further investigate the distribution of ASVs and its differences between the poles, occupancy of each ASV across the cryoconite holes was plotted against mean relative abundance of that ASV for each polar region (Figure 17). Both polar regions contain a “core group” of ASVs that are present in the majority of cryoconite holes and each contribute >1% of total abundance.

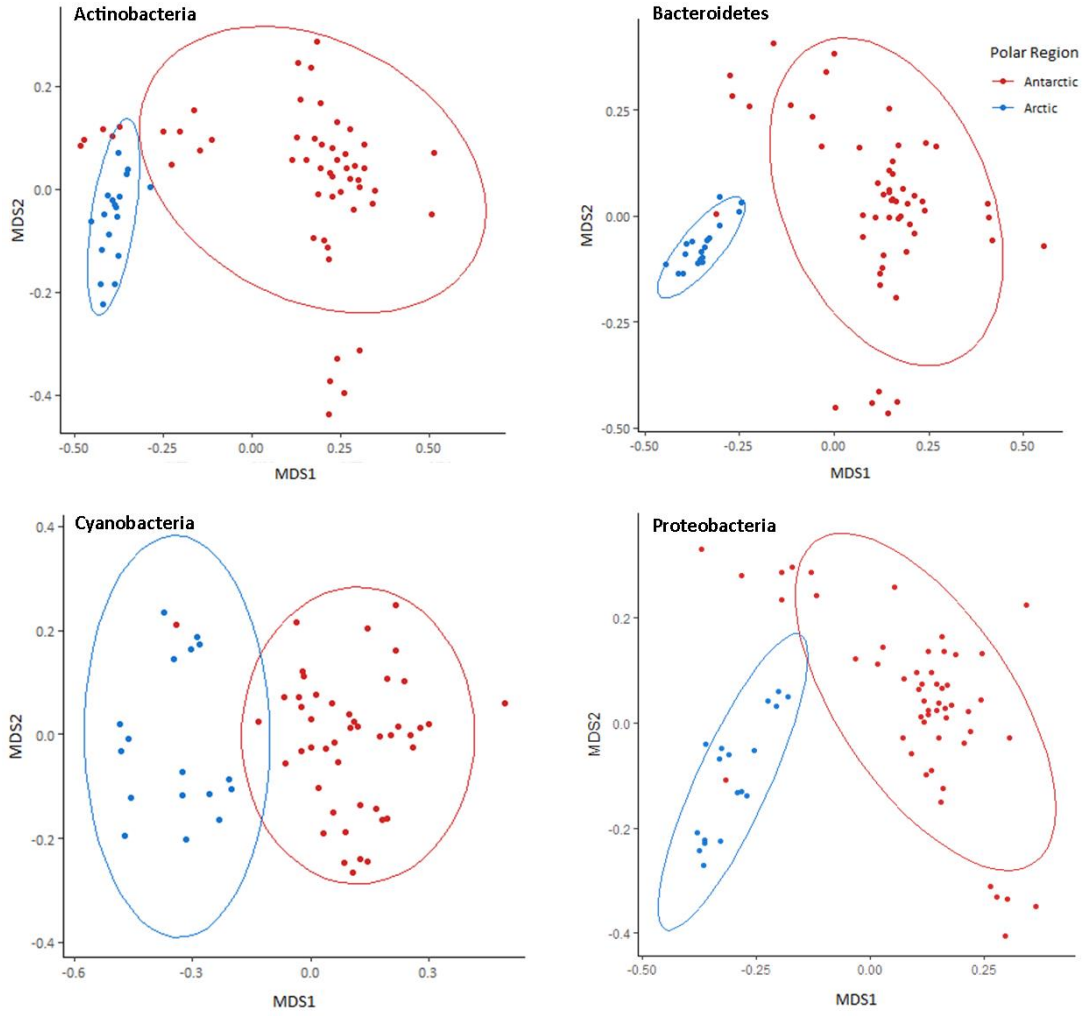

Figure 16 Bray-Curtis dissimilarity of Arctic and Antarctic 16S rRNA gene ASVs in the most abundant four bacterial phyla. Visualised by NMDS ordination. Cryoconite holes are grouped by polar region. Ellipses represent 95% confidence intervals.

Table 8 Similarity percentages (SIMPER) of phyla contributions to Arctic and Antarctic communities. Significance codes: 0 '***' 0.001 '**' 0.01 '*' 0.05 '.' 0.1 ' '.

	Average	SD	Ratio	Average (Antarctic)	Average (Arctic)	Cum. Sum	p-value	
Bacteria and Archaea								
Cyanobacteria	8.08E-02	6.19E-02	1.3047	3.21E+03	1.16E+03	0.201	0.198	
Proteobacteria	4.76E-02	3.57E-02	1.3356	2.51E+03	2.79E+03	0.319	0.733	
Chloroflexi	3.09E-02	3.24E-02	0.9546	1.88E+02	9.32E+02	0.396	0.020	*
WPS-2	3.07E-02	2.22E-02	1.381	9.93E+01	8.63E+02	0.472	0.010	**
Bacteroidetes	2.77E-02	2.05E-02	1.351	2.18E+03	2.41E+03	0.541	0.663	
Patescibacteria	2.69E-02	2.44E-02	1.1054	5.33E+02	6.24E+02	0.608	0.416	
Actinobacteria	2.41E-02	1.69E-02	1.4266	1.20E+03	1.15E+03	0.668	0.723	
Armatimonadetes	2.24E-02	1.15E-02	1.9455	3.26E+02	8.11E+02	0.723	0.059	.
Acidobacteria	2.15E-02	1.31E-02	1.6494	7.08E+02	8.10E+02	0.777	0.921	
Abditibacteriota	2.13E-02	1.99E-02	1.0715	4.66E+02	3.99E+02	0.830	0.891	
Unassigned Bacteria	1.97E-02	1.82E-02	1.0853	4.79E+02	4.02E+02	0.879	1	
Planctomycetes	1.80E-02	1.07E-02	1.6801	5.00E+02	4.02E+02	0.924	0.139	
Verrucomicrobia	1.28E-02	9.14E-03	1.4027	3.66E+02	3.29E+01	0.955	0.050	*
Gemmatimonadetes	7.23E-03	3.48E-03	2.0766	2.31E+02	4.19E+01	0.973	0.010	**
Firmicutes	5.02E-03	8.27E-03	0.6064	2.02E+01	1.29E+02	0.986	0.168	
Deinococcota	4.21E-03	3.43E-03	1.2283	1.19E+02	6.04E+01	0.996	0.733	
Fibrobacterota	6.87E-04	6.64E-04	1.0339	1.11E+01	1.13E+01	0.998	0.099	.
Caldisericota	5.52E-04	8.21E-04	0.6719	9.10E-01	1.42E+01	0.999	0.1089	
Sumerlaeota	1.67E-04	2.96E-04	0.5656	4.39E+00	1.67E-02	0.999	0.5050	
Elusimicrobiota	5.65E-05	1.13E-04	0.499	1.50E+00	0.00E+00	0.999	0.3069	
Nitrospirota	4.80E-05	1.29E-04	0.3706	1.25E+00	1.67E-02	1	0.7921	
Dependentiae	6.70E-06	1.30E-05	0.5146	1.68E-01	1.67E-02	1	0.8911	
Archaea	3.62E-06	7.70E-06	0.4694	9.44E-02	0.00E+00	1	0.9109	
Hydrogenedentes	8.52E-07	2.58E-06	0.33	2.22E-02	0.00E+00	1	1	

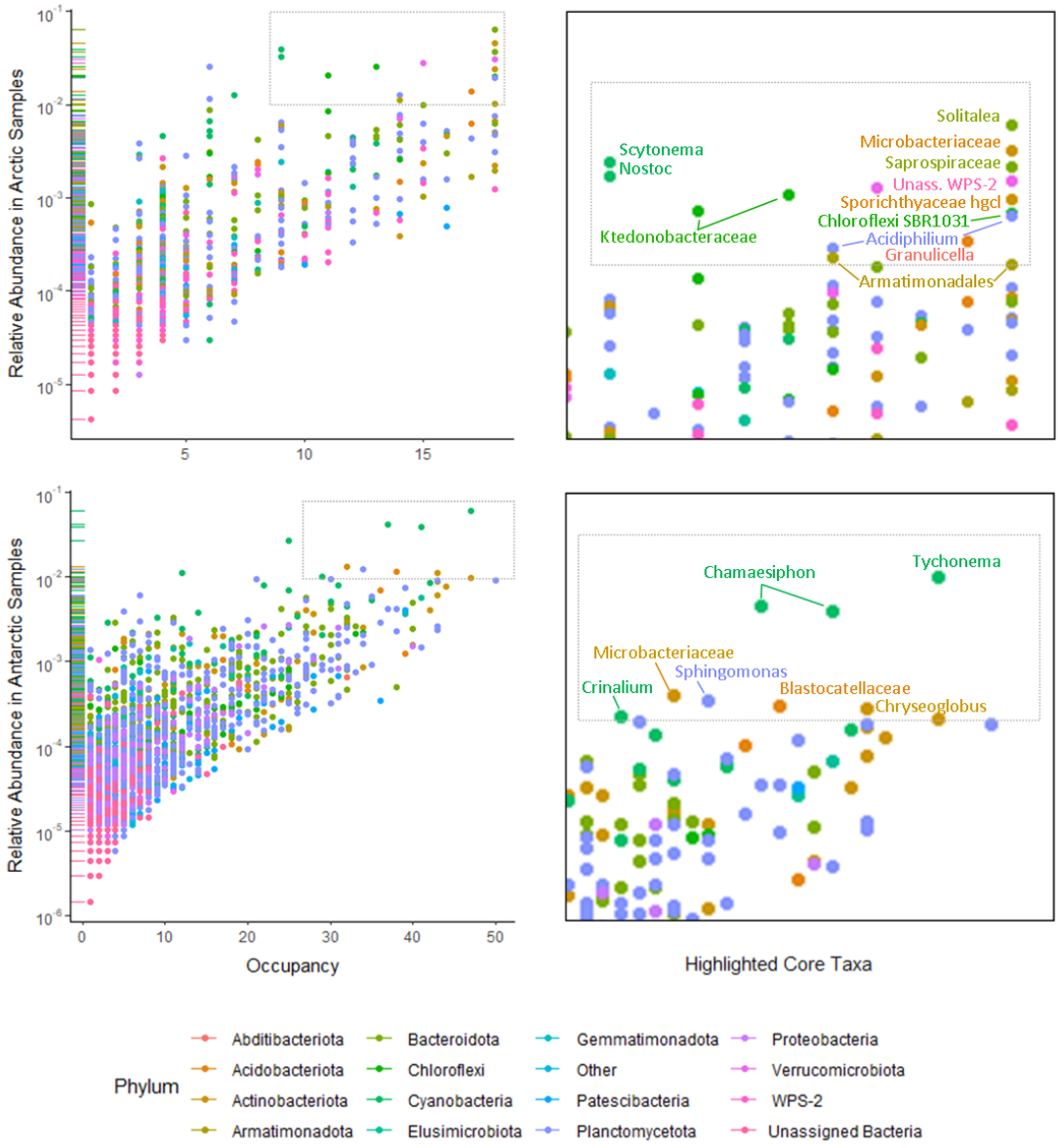

Figure 17 Occupancy of 16S rRNA ASVs in Arctic (upper left) and Antarctic (lower left) cryoconite holes by phyla. Phyla contributing to <1% of the total 16S rRNA gene sequences were grouped as "Other." Taxa present in ≥75% of samples from that polar region that contributed to ≥1% of relative abundance are highlighted as core taxa (upper and lower right).

However, the genera in these groups differ between the Arctic and Antarctic. Whilst both groups contain Microbacteriaceae, the remaining members are specific to the core group of each polar region. All core taxa contained in the Arctic and Antarctic groups are present in some proportion on both poles with the exception of Blastocatellaceae.

Eukaryote community composition

Following filtering, 6261 18S rRNA gene sequences were analysed from each Arctic and Antarctic cryoconite sample, which were assigned to a total of 11 eukaryotic phyla. 6865 distinct 18S rRNA gene ASVs were found, 82 of which were shared between the Arctic and Antarctic (Figure 17). Metazoa accounted for 31% of 18S rRNA gene ASVs. Parachela tardigrades were the most abundant metazoans in the Arctic (64% of Arctic metazoan ASVs and 39% of Antarctic metazoan ASVs) and Adinetida rotifers were the most abundant metazoans in the Antarctic (36% of Arctic metazoan ASVs and 59% of Antarctic metazoan ASVs). The remaining metazoa recovered were Monogononta, Ploimida and the platyhelminth Rhabdocoela Neodalyellida, which were only present in Antarctic cryoconite holes (contributing to 0.23% and 1.34% of Antarctic metazoan ASVs respectively). Figure 13 shows microbial eukaryotes without metazoan 18S rRNA gene sequences. 94% ASVs assigned to microbial eukaryotic phyla were assigned to the SAR group, Opisthokonta and Archaeplastida.

The 18S rRNA gene eukaryote taxonomic community structure showed less a clear divide between the Arctic and Antarctic cryoconite samples. However, when examining weighted UniFrac distances and abundance of taxa I observed variation of microbial eukaryote composition with polar region (Figure 19). A much larger proportion of microbial Opisthokonta was found in the Arctic, 32% of assigned Arctic sequences belonged to the Opisthokonta compared to only 6% in the Antarctic. SIMPER analysis showed microbial Opisthokonta contributed significantly to the dissimilarity between poles (Table 8).

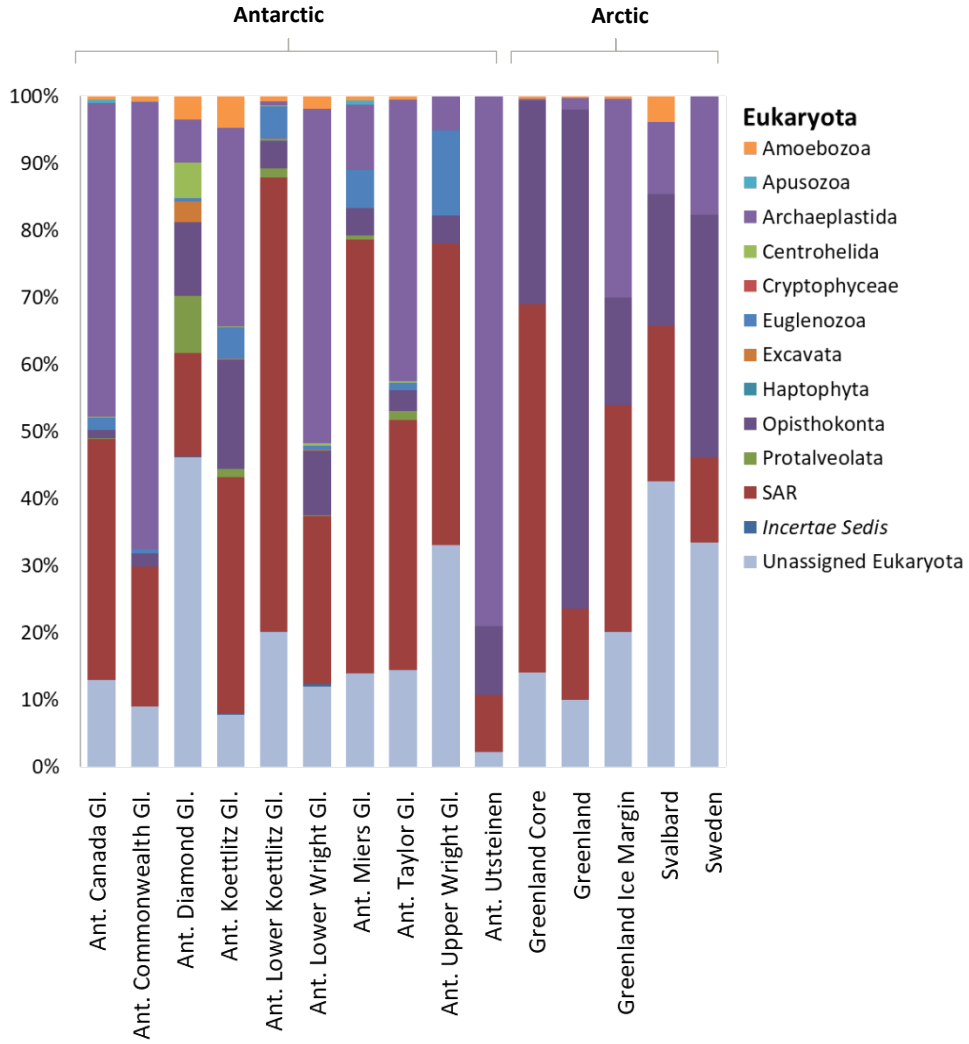

Figure 18A Relative abundance of microbial eukaryotes in Arctic and Antarctic cryoconite, averaged by glacier. Metazoa were excluded from these data. **A** Eukaryotic phyla. Phyla contributing to <1% of the total abundance are not included. **B-D** Relative abundance of genera within the top three most abundant phyla. Genera contributing to <1% of the total abundance are grouped as "Other." Where a genus was unknown, lowest rank known is shown. Taxa were assigned according to the SILVA database. "Ant. Gl." denotes Antarctic Glaciers.

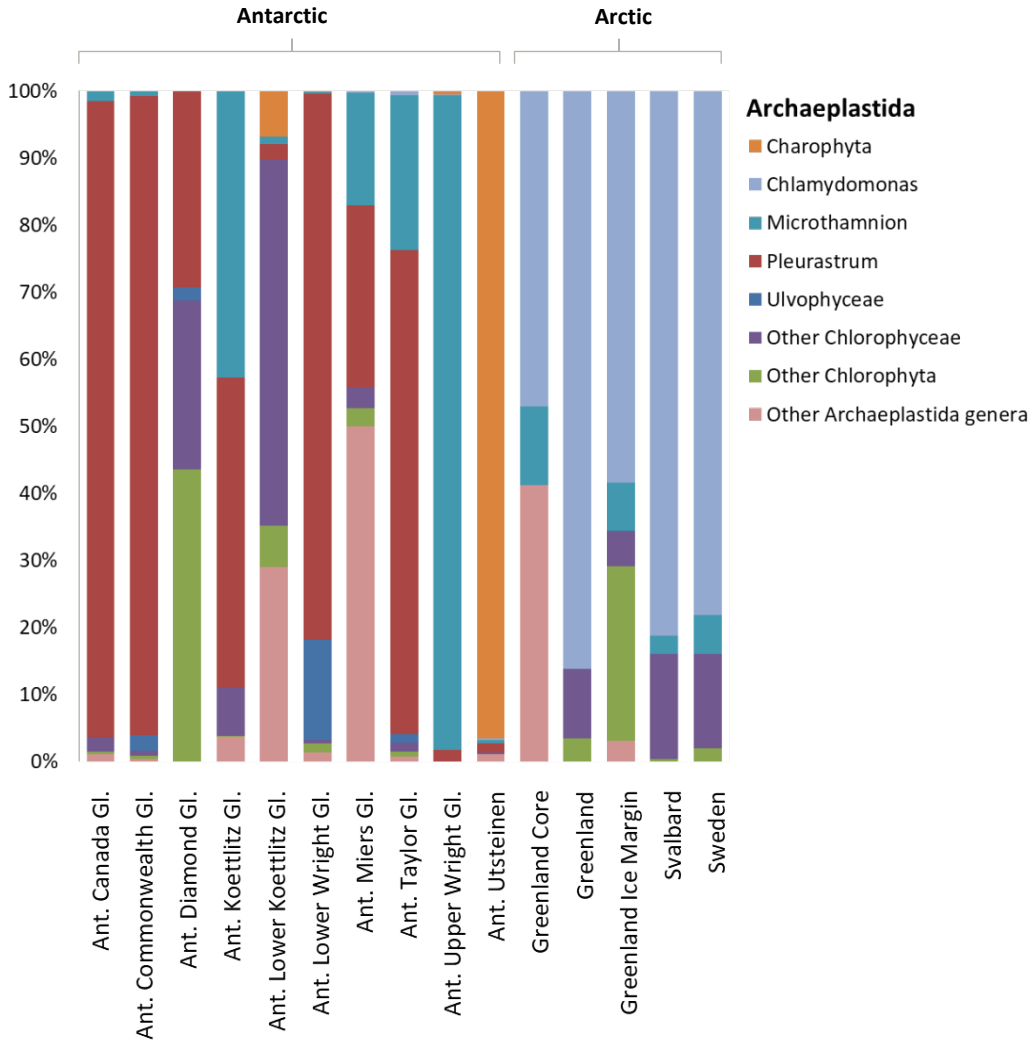

Figure 18B Relative abundance of microbial eukaryotes in Arctic and Antarctic cryoconite, averaged by glacier. Metazoa were excluded from these data. **A** Eukaryotic phyla. Phyla contributing to <1% of the total abundance are not included. **B-D** Relative abundance of genera within the top three most abundant phyla. Genera contributing to <1% of the total abundance are grouped as "Other." Where a genus was unknown, lowest rank known is shown. Taxa were assigned according to the SILVA database. "Ant. Gl." denotes Antarctic Glaciers.

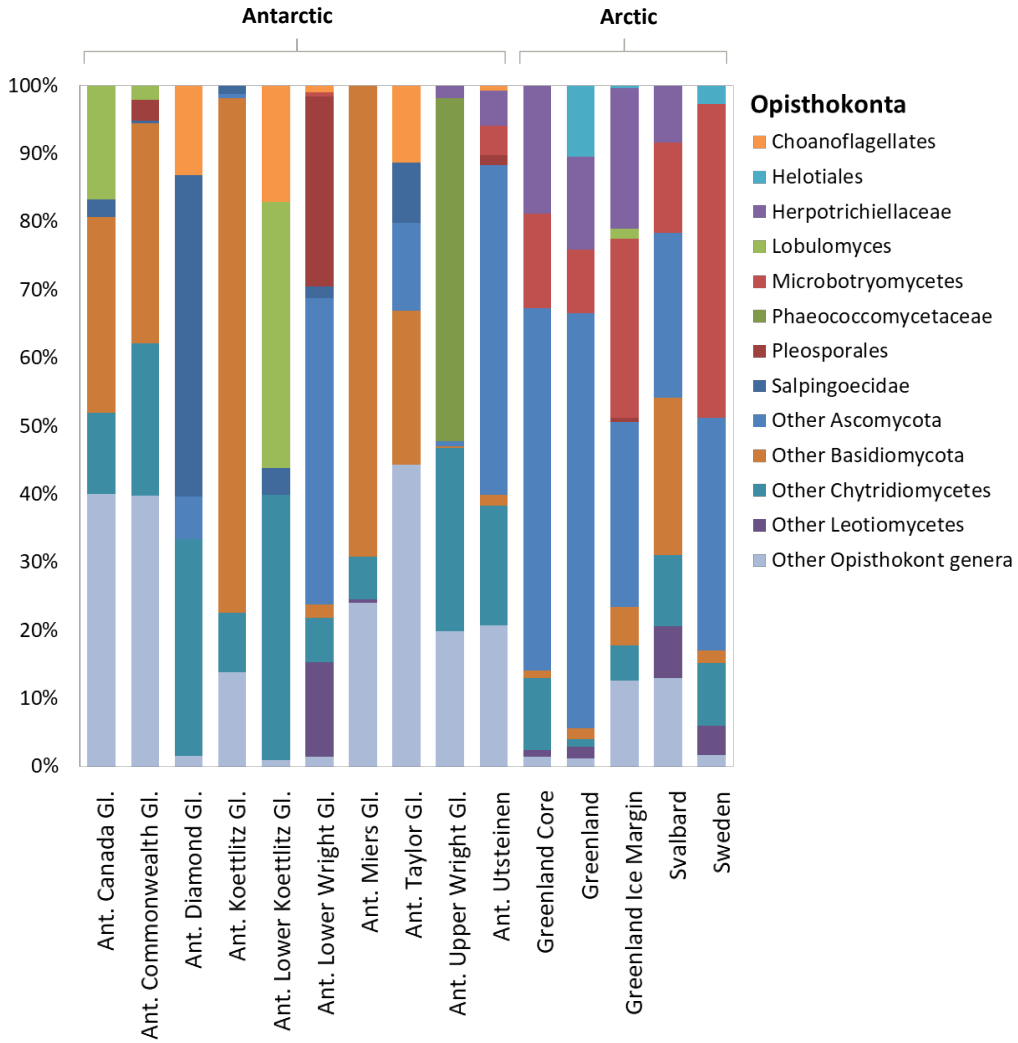

Figure 18C Relative abundance of microbial eukaryotes in Arctic and Antarctic cryoconite, averaged by glacier. Metazoa were excluded from these data. **A** Eukaryotic phyla. Phyla contributing to <1% of the total abundance are not included. **B-D** Relative abundance of genera within the top three most abundant phyla. Genera contributing to <1% of the total abundance are grouped as "Other." Where a genus was unknown, lowest rank known is shown. Taxa were assigned according to the SILVA database. "Ant. Gl." denotes Antarctic Glaciers.

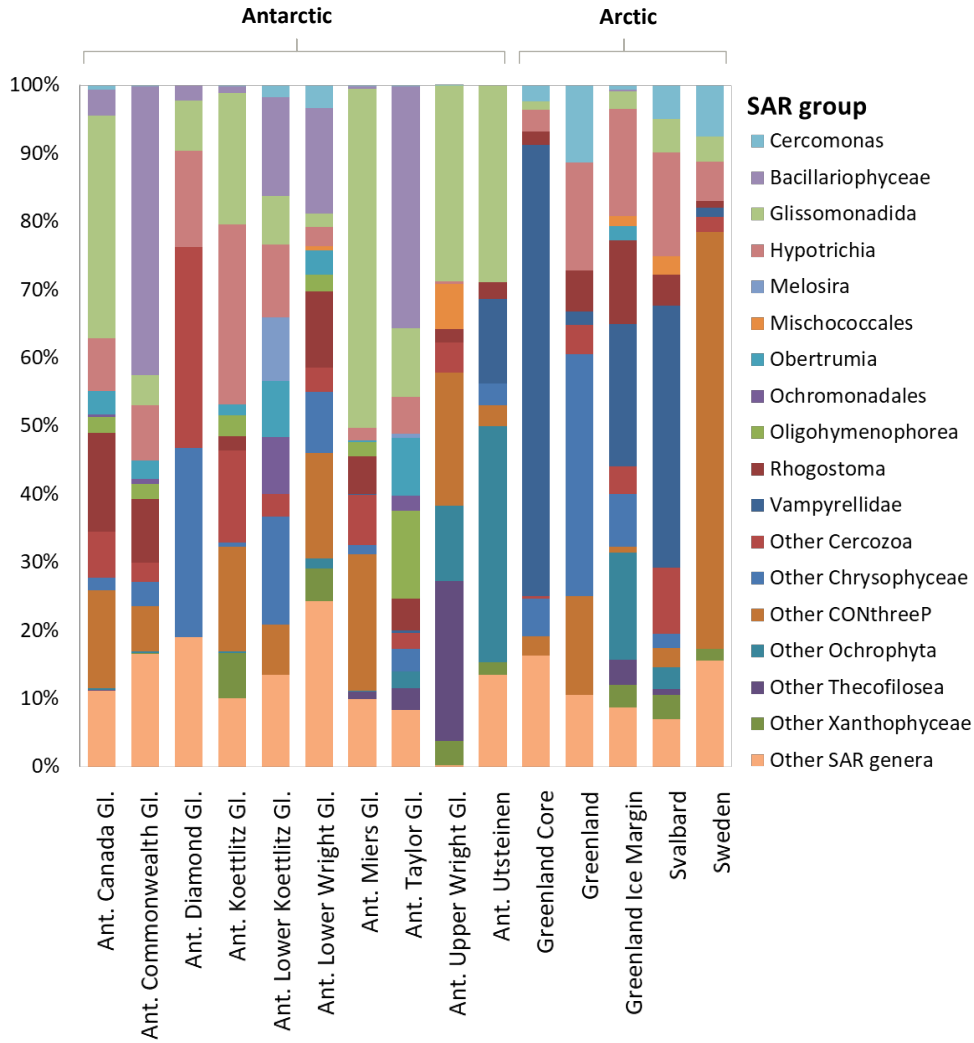

Figure 18D Relative abundance of microbial eukaryotes in Arctic and Antarctic cryoconite, averaged by glacier. Metazoa were excluded from these data. **A** Eukaryotic phyla. Phyla contributing to <1% of the total abundance are not included. **B-D** Relative abundance of genera within the top three most abundant phyla. Genera contributing to <1% of the total abundance are grouped as "Other." Where a genus was unknown, lowest rank known is shown. Taxa were assigned according to the SILVA database. "Ant. Gl." denotes Antarctic Glaciers.

Several eukaryotic phyla present in the Antarctic were absent in Arctic cryoconite samples, but all of these phyla contribute less than 0.1% to the total number of 18S rRNA gene sequences across both poles with exception for 18S rRNA gene sequences assigned to Euglenozoa which were present in all Antarctic locations but the Upper Wright glacier. The Euglenozoa made up 2.5% of the total ASVs.

The most abundant eukaryotic phyla were Opisthokonta, Archaeplastida and the SAR group, which were investigated in further detail. The most striking difference between the Arctic and Antarctic compositions of the SAR group is that the Vampyrellidae, a predatory family of cercozoans, made up 32% of the Arctic SAR 18S rRNA gene sequences but less than 1% of Antarctic 18S rRNA gene sequences in Greenland and Svalbard. The sites in Sweden had 61% of its SAR 18S rRNA genes sequences belonging to CONthreeP ciliates. Bacillariophyceae (diatoms) represented 12% of Antarctic SAR sequences but 0.1% of Arctic sequences (an average of 4.75 ASVs assigned to Bacillariophyceae present, found in the Greenland Margin samples).

89% of Archaeplastida were assigned to one of only four genera. 3% of the remaining sequences were unassigned Chlorophyta, 3% unassigned Chlorophyceae, 3% unassigned Ulvophyceae and the remaining 18S rRNA gene sequences each contributed to >1% of the community composition. In the Archaeplastida 18S rRNA gene sequence from the Arctic, 67% belonged to the snow algae genus *Chlamydomonas*, and 16% of 18S rRNA gene sequences were attributed to unassigned Chlorophyta. In contrast, the Antarctic cryoconite samples contained 0.1% *Chlamydomonas* 18S rRNA gene sequences. 52% belonged to *Pleurastrum*, 13% to *Microthamnion*, and 26% to an unassigned group of Charophyta. No Arctic 18S rRNA gene ASVs were assigned to *Pleurastrum* or Charophyta.

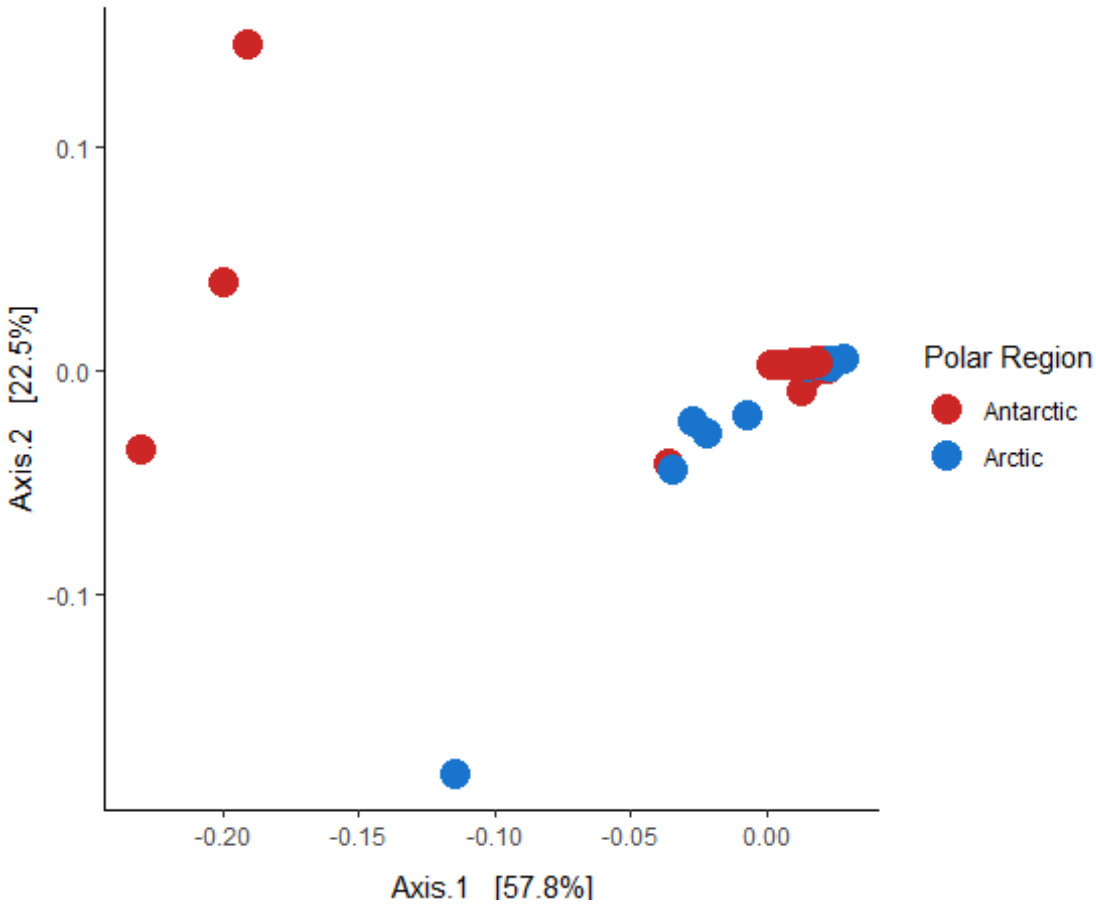

Figure 19 Weighted Unifrac distances of eukaryotic ASVs in Arctic and Antarctic cryoconite grouped by polar region. Metazoa were excluded.

Of the 52 genera assigned to the Opisthokonta, only 11 appear in both the Arctic and Antarctic samples. Overall, 66% of Opisthokonta sequences belonged to the metazoa. The other metazoa contributed less than 1% to the total number 18S rRNA gene sequences. To better distinguish the microbial community, metazoa were excluded from the Opisthokonta in Figure 13. Of the microbial Opisthokonts, all samples were dominated by a group of unassigned Ascomycota fungi (39% of total microbial Opisthokont sequences). Microbotryomycetes (19% of Arctic and 1% of Antarctic Opisthokonta) and Herpotrichiellaceae (12% of Arctic and 2% of Antarctic microbial Opisthokonta) were also significant contributors to the Arctic microbial Opisthokonta, whereas Chytridiomycetes were more abundant in the Antarctic (19% of Antarctic sequences and 5% of Arctic sequences). All other assigned groups contributed to >4% of total microbial Opisthokont ASVs.

The mean number of different ASVs was 102 in the Arctic samples and 125 in the Antarctic samples (Table 7). Alpha diversity and evenness of eukaryotes in the samples was further investigated using the Shannon diversity indices (Figure 15). Similar to 16S rRNA gene communities, the lowest richness was in cryoconite from the Antarctic Lower Wright (2.30) and Upper Wright (3.32) glaciers. However, the highest values were from the Arctic: Svalbard cryoconite (5.94) and the Greenland margin sediment samples (5.87). The average values were 4.00 for the Antarctic and 5.02 for the Arctic sites. Only five of the total assigned 18S rRNA gene ASVs were present in more than one sample. These belonged to (by lowest rank assigned) *Monomastix minuta*, Herpotrichiellaceae, Microbotryomycetes and Ascomycota.

Intact polar lipid distribution

All of the IPLs screened for were present at both poles and in all samples, with the exception of the OL-OH (Figure 20). These contribute to 10% of the Arctic IPLs but were absent in all Antarctic samples. The highest contributor to the Antarctic samples was the 1G-DAGs which make up 17% and 7% of Antarctic and Arctic IPLs

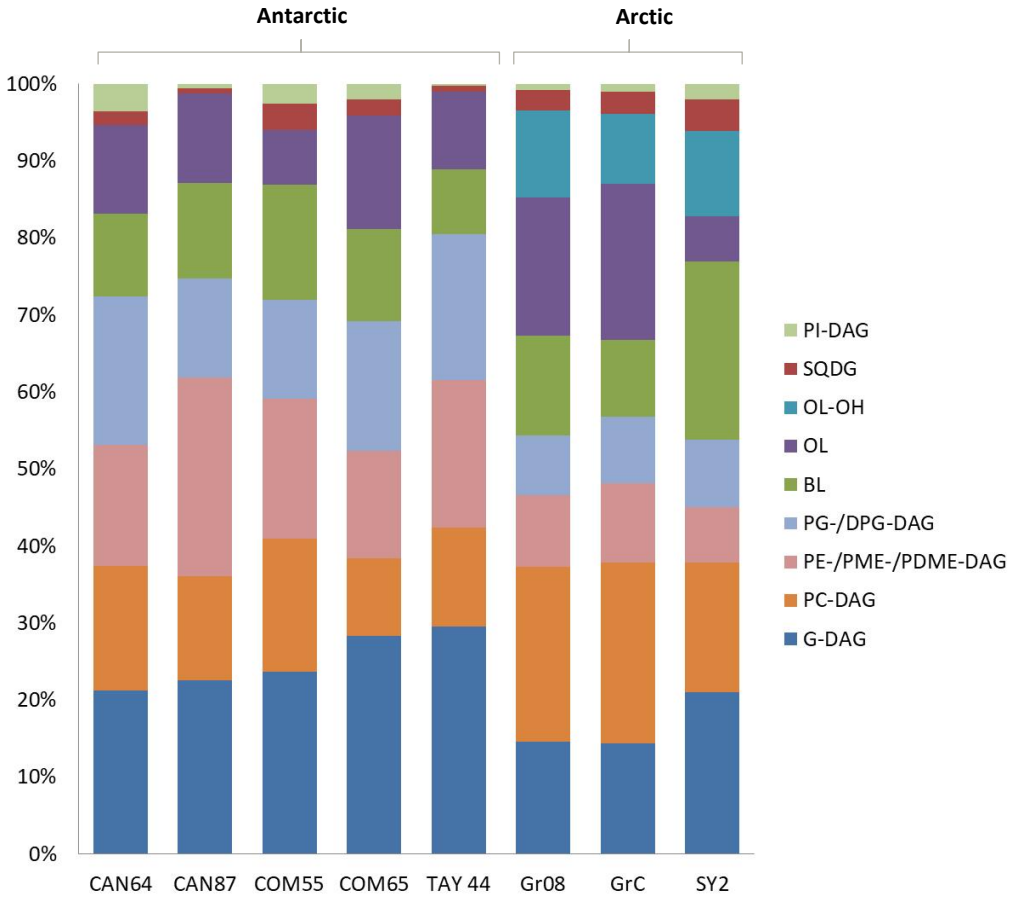

Figure 20: Relative abundance of intact polar Lipids in polar cryoconite. Sources of cryoconite are as follows CAN = Canada Glacier, COM = Commonwealth Glacier, TAY = Taylor Glacier, Gr = Greenland, SY = Sweden

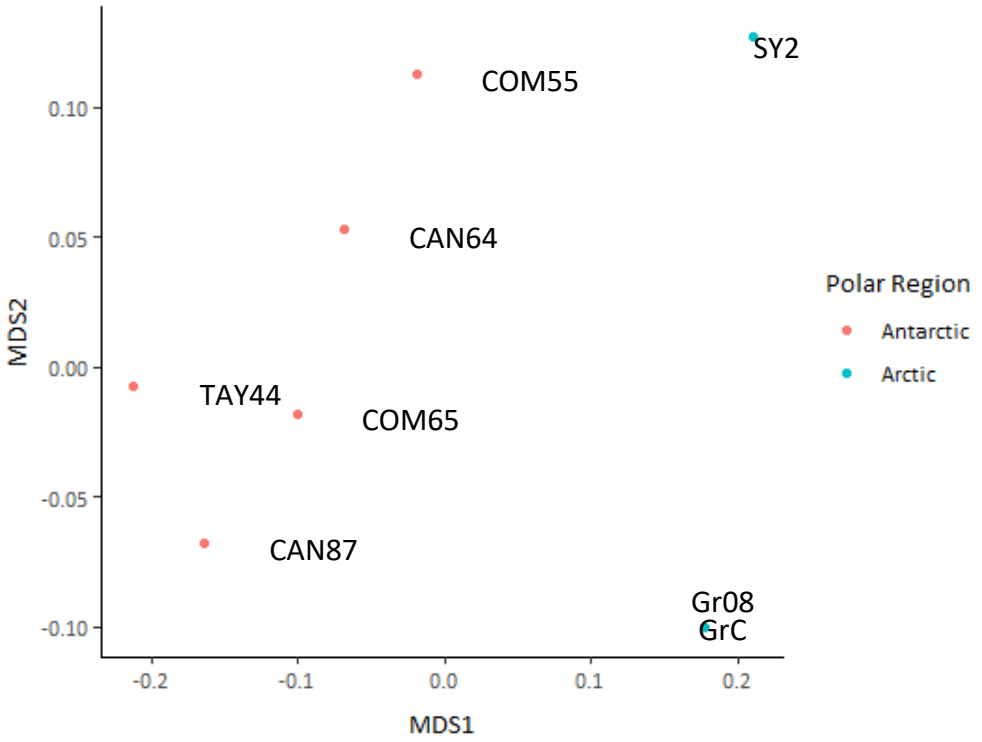

Figure 21: Bray-Curtis dissimilarity of IPL composition found in each cryoconite and visualised by non-metric multidimensional scaling (NMDS) ordination.

respectively. The highest contributor Arctic IPLs were the PC-DAGs. These contribute 21% to the Arctic total IPLs and 14% to the Antarctic total IPLs. The dissimilarity between polar regions and between locations was tested by ANOSIM using the Bray-Curtis method Figure 21. The highest dissimilarity was between the Arctic and the Antarctic, producing a value of R = 0.97 at significance level of p = 0.017. The dissimilarity between locations was R = 0.68 at p = 0.049. This dissimilarity was visualized using non-metric multidimensional scaling (Figure 20). The two Greenland samples were positioned at the same coordinates in this ordination due to their close similarity in IPL composition. The Canada, Commonwealth and Taylor Glacier samples did not cluster in this way.

Objective 1.2: Compare cryoconite taxonomy to Cryogenian keystone taxa.

Taxonomic composition

The 16S and 18S rRNA gene sequence results show that a range of organisms that are diverse in both function and taxonomy inhabit the cryoconite holes of the Arctic

and Antarctic. Some of these organisms are members of the eukaryotic crown groups predicted to have persisted through the Cryogenian period (Table 9). The Amoebozoa, Archaeplastida, Excavata and SAR group had all emerged by the Cryogenian according to fossil, molecular clock and biomarker predictors (Porter and Knoll, 2000; Peterson and Butterfield, 2005; Parfrey *et al*., 2011; Sánchez-Baracaldo *et al*., 2017; Lahr *et al*., 2019). These are also the four most abundant eukaryotic phyla in the cryoconite holes. Chlorophyta, Cercozoa and Alveolata were present in all sites. Fungi, which are now thought to have emerged over 1000 million years ago (Loron *et al*., 2019) were present at all sites. At least one organisms with testate morphology (which had also developed at least once by the Cryogenian (Figure 22) (Porter and Knoll, 2000; Strauss *et al*., 2014)) was present at each site, with Rhogostoma, appearing in the most sites. Choanoflagellates, a sister group to early metazoa and one of similar morphology to collared sponges, are present in the majority Antarctic cryoconite holes but absent in the Arctic. Excavata are also absent in the Arctic but present in the Antarctic.

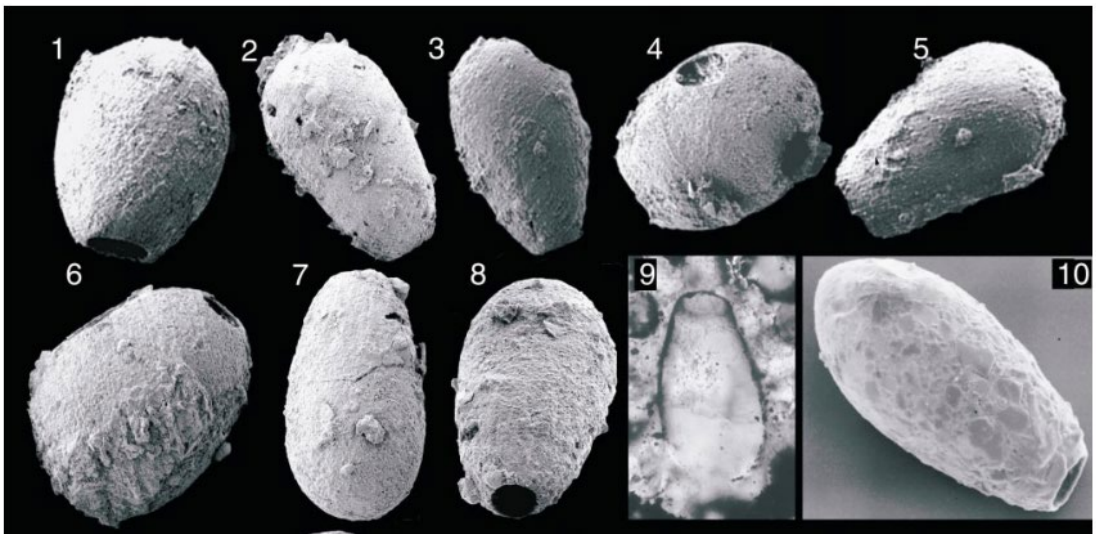

Figure 22 "The genus *Cycliocyrillium* and modern testate amoeban analogs. 1–9, *Cycliocyrillium simplex* taken from vase-shaped microfossil assemblages from early diagenetic carbonate nodules in >742 ± 6 Mya black shales of the Chuar Group, Grand Canyon]. 10, The modern lobose testate amoeba *Difflugia lanceolata*." (Porter 2003)

Abiotic conditions

Models of Cryogenian Snowball Earth temperature compiled by Abbot *et al* (2013) over a range of potential atmospheric CO_2 levels predict global annual average temperatures between -5°C and -30°C (Figure 7). Some models predicted summer solstice temperature could rise above freezing at the 40th parallel south, while others place the entire temperature range firmly below -20°C (Abbot *et al*. 2013). This temperature range places Snowball earth most closely to the coldest areas of Antarctica. In the McMurdo Dry Valleys the mean annual air temperatures range between −15°C and −30°C, with an absolute maximum of 8-12°C (Obryk *et al*., 2020). The temperatures in Queen Maud Land generally range between -36°C and -4°C, rarely rising above 0°C (Gorodetskaya *et al*., 2013). In contrast, on Midtre Lovénbreen, annual air temperatures are on average −6°C and positive air temperatures occur during winter as well as summer (Hanssen-Bauer, 1990; Wadham and Nuttall, 2002). On Kangerlussuaq air temperatures fall on a similar range, mean temperatures between 5°C and -15°C depending on time of year and altitude (van As *et al*., 2012). The highest temperatures were in the region of 10°C (Hanna *et al*., 2012).

Due to the low temperatures during the Cryogenian, the climate would have been dry. Dry valleys, comparable to the McMurdo Dry Valleys are predicted to have formed during the Cryogenian (Hoffman *et al*., 2017). Although cloud-resolving models for Snowball Earth climate exist, it is unlikely that there would have been significant quantities of rain (Abbot, 2014). Most water would have been provided by meltwater and water vapour (Hoffman *et al*., 2017). Strong katabatic winds such as those found in the McMurdo Dry Valleys are also predicted to have been present and responsible for warming of ice sheets and distribution of microorganisms (Parish and Cassano, 2003; Hoffman *et al*., 2017).

Table 9 Presence/absence of taxa known to have persisted through the Cryogenian, found in polar cryoconite. Presence is marked "x". Sources for each group's emergence date are listed in the bottom three rows, according to which source was used for emergence data estimation. Organisms are grouped by phyla with the exception of those grouped by testate morphology, which represent potential relations to testate microfossils.

Phylum	Amoebozoa	Excavata	SAR			Opisthokonta			Archaeplastida		Testate morphology			
	Any	Any	Any	Cercozoa	Alveolata	Any	Eumetazoa	Choanoflagellata	Any	Chlorophyta	Arcellinida	Rhogostoma	Sorodiplophrys	Diplophrys
Ant. Canada Gl.	x	x	x	x	x	x	x		x	x		x	x	x
Ant. Commonwealth Gl.	x	x	x	x	x	x	x	x	x	x		x		x
Ant. Diamond Gl.	x	x	x	x	x	x	x	x	x	x	x		x	x
Ant. Koettlitz Gl.	x	x	x	x	x	x	x	x	x	x		x	x	x
Ant. Koettlitz Gl. (Lower)	x	x	x	x	x	x	x	x	x	x				
Ant. Miers Gl.	x	x	x	x	x	x	x	x	x	x		x	x	x
Ant. Taylor Gl.	x	x	x	x	x	x	x		x	x		x		x
Ant. Utsteinen	x	x	x	x	x	x	x	x	x	x		x		x
Ant. Wright Gl. (Lower)	x	x	x	x	x	x	x		x	x		x		x
Ant. Wright Gl. (Upper)			x	x	x	x	x	x	x	x		x		
Greenland	x		x	x	x	x	x		x	x		x		
Greenland Core	x		x	x	x	x	x		x	x		x		
Greenland Margin	x		x	x	x	x	x		x	x		x		
Svalbard	x		x	x	x	x	x		x	x		x		x
Sweden	x		x	x	x	x			x	x		x		
Fossil	e.g. Porter & Knoll 2000										e.g. Lahr et al. 2019			
Molecular clock		e.g. Parfrey et al. 2011	e.g. Parfrey et al 2011			e.g. Peterson & Butterfield 2005			e.g. Sanchez-Baracaldo et al 2017					

Discussion

Objective 1.1: Assess cryoconite hole microbial diversity and community composition.

Composition of polar cryoconite communities

Cryoconite holes are proposed as a refuge for life on Snowball Earth in part due to their biodiversity and ability to support many types of microoganisms. Through 16S and 18S rRNA gene sequencing I recovered a total of 35 phyla and superphyla; a considerably higher taxonomic diversity compared to previous studies that did not use next generation sequencing (Mueller *et al*., 2001; Christner *et al*., 2003; Mueller and Pollard, 2004; Porazinska *et al*., 2004; Cameron *et al*., 2012b). While DNA analyses cannot prove the presence of an active community, the number of potentially active phyla present is notable when considering cryoconite as a refuge for biodiversity on Snowball Earth. The most abundant phyla (16S rRNA gene: Bacteroidetes, Actinobacteria, Cyanobacteria and Proteobacteria; 18S rRNA gene: SAR group, Archaeplastida and Opisthokonta) were present in all samples, although the relative abundance and genera present varied. The average species richness of the Arctic was lower than that of the Antarctic, however, species richness varied widely between glaciers within each polar region. The Antarctic cryoconite assemblages showed more variation, both when measured by ASVs and by the Shannon diversity index (Table 7). In contrast to the findings reported by Sommers *et al*. 2018, only a weak correlation was found between bacterial and eukaryotic diversity in cryoconite holes (r=4.1). The environmental conditions on individual glaciers, such as position within the valley, may contribute to variations in species richness (Stanish *et al*., 2013). The intact polar lipid distribution also indicated active bacterial microorganisms by the presence of PE-DAGs (Goldfine and Hagen, 1968) and ornithine lipids (Geiger *et al*., 2010) and eukaryotic microorganisms by the presence of PC-DAGs (Raetz, 1986) and betaine lipids (Kato *et al*., 1996) (Figure 20). These IPL group detected have been reported in Antarctic sediments but also in soils and oceans (Lipp and Hinrichs, 2009; Schubotz *et al*., 2018; Ding *et al*., 2020; Evans *et al*., 2022). A higher number of studies from a wide variety of habitats will

be required if we are to one day identify characteristic IPL signatures from different biomes.

Bacterial and eukaryotic photoautotrophs were found across all locations and several mixotrophs were recovered, including the *Chlamydomonas* which dominate the Arctic eukaryotic algal population (Lalibertè and de la Noüie, 1993). I also detected chemotrophic bacteria such as *Thiobaccillus*, which plays an important part in sulphur cycling in subglacial environments (Harrold *et al*., 2015), and may have a role in sulphate reduction in the anoxic zone of cryoconite holes (Bagshaw *et al*., 2007; Poniecka *et al*., 2018). IPLs that are primarily produced by Cyanobacteria (glycolipids, and to a lesser extent PG-DAG, DPG-DAG and SQ-DAG) and eukaryotic algae (betaine lipids) were present in all samples, suggesting an active phototroph community (Kato *et al*., 1996; Wada and Murata, 2006). However, none of these lipids are exclusively produced by these groups (Kato *et al*., 1996; Wada and Murata, 2006). There is also a range of organisms predating and grazing on the community. The Vampyrellidae are likely microbial predators in the Arctic cryoconite habitats. Other heterotrophic and predatory groups such as the Ciliophora were found across both poles. Tardigrades and rotifers were found on glaciers with the exception of Sweden. Sweden may be outside the range of Arctic metazoa, though the microbial community is otherwise remarkably similar to that of the Svalbard cryoconite. The tardigrades and rotifers are likely to have been alive and active in the community, as these metazoans are commonly present in cryoconite communities (Porazinska *et al*., 2004; Zawierucha *et al*., 2021), and are key constituents of adjacent soil communities (Treonis *et al*., 1999; Virginia and Wall, 1999). Together these data suggest a trophic web within cryoconite holes across both poles, with metazoans as the top level grazer, microbial predation and heterotrophy, chemotrophy, diverse bacterial photoautotrophy and microalgal assemblages but dominated by a small number of families.

Archaea were detected in very low relative abundances (<0.001% of 16S rRNA gene sequences) in the Arctic and Antarctic cryoconite holes. Other 16S rRNA gene sequencing surveys on cryoconite have found comparably low relative abundances of archaea (Lutz *et al*., 2015, 2017; Sommers *et al*., 2018) when using universal 16S

rRNA gene primers (Caporaso *et al*., 2012). This may be due to these primers being less well suited for the amplification of the archaeal 16S rRNA gene (Parada *et al*., 2016). Although other studies using the Earth Microbiome Project (EMP) primers on other habitats have uncovered a wider range of archaea they have been found to be biased against Crenarchaeota and Thaumarchaeota (Hugerth *et al*., 2014). Investigations on cryoconite that have used alternate specific primers designed for archaea detected more archaeal ASVs richness, though they are still predicted to be a minor component of the ecosystem in alpha diversity and possibly in biomass (Cameron *et al*., 2012b; Weisleitner *et al*., 2020)

Using DNA sequences means that there is no assurance that the active community was measured. There may be legacy DNA in the sample, and a study on Greenland cryoconite has found that there is significant difference between bulk and active communities (Stibal *et al*., 2015). Until global surveys of active cryoconite communities (such as transcriptomic analyses) are carried out, it is only possible to speculate.

Differences in community composition between Arctic and Antarctic cryoconite holes

The use of Illumina sequencing enabled the examination of community composition across more locations and to a greater depth than previous comparisons of Arctic-Antarctic cryoconite microbial communities (e.g. Mueller *et al*., 2001; Cameron *et al*., 2012). The comparison of 16S and 18S rRNA gene communities shows that variation between poles was greater than between glaciers or individual cryoconite holes. The bacterial and archaea assemblages in particular clustered according to polar region (Figure 14 and Figure 16). Additionally, of the “core group” of ASVs that were both more abundant (contributing to >1% of total abundance) and present in the majority of cryoconite holes in each pole, only two genera were shared between the Arctic and Antarctic (Figure 17). Over 99% of eukaryotic ASVs were only present in one sample, illustrating that unlike the biogeography of bacteria in cryoconite, highly localised variation between cryoconite communities are predominant over regional and hemispheric differences. However, within each

of the most abundant eukaryotic phyla (Archaeplastida, Opisthokonta, and the SAR group), there were genera contributing to a compositional divide between the cryoconite of the two polar regions. The results agree with findings by Cameron *et al*. (2012) that Arctic and Antarctic cryoconite holes harbour distinct bacterial and eukaryotic communities.

It is also possible to observe this difference through the lens of intact polar lipid composition (Figure 19 and Figure 20). One IPL group, the OL aminolipids, were absent in Antarctic samples but present in all Arctic samples. The highest contributor to the Antarctic IPLs was G-DAG, which is known to be the major constituent of Cyanobacterial lipids (Wada and Murata, 2006). In contrast, the highest contributor to Arctic IPLs was the PC-DAGs, which are commonly associated with eukaryotes, although they are also produced by a number of bacteria (Raetz, 1986; Geiger *et al*., 2013). Overall there was a clear compositional divide between the Arctic and Antarctic samples, illustrated by ANOSIM using the Bray-Curtis method ($R = 0.97$ $p = 0.017$).

One possible explanation for this is that the glacier surface environments of the two poles have different physical characteristics governed by differences in temperature, radiation and surrounding landscapes, and so may exhibit different selection pressures. For example, lower air and ice temperatures mean that many of the Antarctic cryoconite holes were closed (ice lidded), as is typical for the McMurdo Dry Valleys (Fountain *et al*., 2004). Most of these holes had a thick layer of sediment at the bottom (between 1cm and 10cm). By contrast, the Arctic cryoconite holes tend to be open and contain thinner, more aggregated sediment (<1cm thickness), which is often clustered into granules (Cook *et al*., 2016). Cyanobacteria (particularly filamentous Cyanobacteria) is associated with the formation of granules commonly observed in Arctic cryoconite and yet the Cyanobacteria appears to be a lower proportion of the Arctic cryoconite microbial community (de Caire *et al*., 1997; Langford *et al*., 2010; Stibal *et al*., 2010). The core groups of both the Arctic and Antarctic cryoconite contain filamentous Cyanobacteria (Scytonema, Nostoc and Tychonema) (Komárek and Johansen, 2015). However, the Arctic cryoconite is likely to have a higher proportion of cells

and organic matter in its thinner granular layer. An analysis of components of the cryoconite sediment, such as total organic carbon present, would complement this study. The ice lid also results in lower levels of light reaching the cryoconite. These differences in habitat may create preferential conditions for some species, altering the community composition and selecting for particular species. Indeed, abiotic variability between cryoconite holes (e.g. pCO2, mineral availability, temperature) has been shown to impact community structure (Edwards *et al.*, 2011) and Antarctic cryoconite communities are adapted to low light availability (Bagshaw *et al*., 2016b).

Limitations of transport and dispersal have also been shown to contribute to community differences (Telford *et al*., 2006). The Antarctic soil ecosystem, which is one important source of cryoconite matter, has limited connectivity to the airborne non-polar microbial pool demonstrating the Antarctic soil microorganisms are not transported far as the non-polar pool (Pearce *et al*., 2009; Bottos *et al*., 2014; Archer *et al*., 2019). Similar dispersal limitation has been found in the Arctic soils through studies on Actinobacteria community assemblage (Eisenlord *et al*., 2012). Therefore, differences in community composition may not be solely caused by differing environments, but selection due to transport. There are also strong local winds in Antarctica and transport of biological material has been documented in the McMurdo Dry Valleys (Michaud *et al*., 2012; Šabacká *et al*., 2012), which may overshadow lower levels of biological material from long-range transport. If limitations of aeolian transport leads to selection, it follows that there should be segregation between the Arctic and Antarctic microbial communities. Through biogeographical analyses it may be possible for future studies to determine the contribution of these abiotic factors to community dissimilarity, although this is beyond the scope of our analysis. Co-correlation mapping between taxa and environmental variables such as pCO2, mineral availability, temperature, and cryoconite hole physical parameters would be beneficial, as has been carried out previously in soil microorganisms (King *et al*., 2010). It would also be valuable to obtain transcriptomic data in addition to gene metabarcoding or genomic data to ascertain differences in active communities (Shakya *et al*., 2019). A comparison of

active and legacy genes in cryoconite holes may also lend insight into which organisms successfully disperse within regions.

It is most likely that both geographical separation and the environment within the poles contribute to the community differences I have found. Our 16S and 18S rRNA gene results show that a number of ASVs were present across all locations on one pole and absent on the other. The proportion of highly abundant groups such as Proteobacteria and Cyanobacteria vary between poles, but not to a statistically significant extent. The significant differences ($p < 0.05$) include low abundance phyla: Chloroflexi and the WPS-2 supergroup (Table 8). Surprisingly, the proportion of photosynthetic organisms was lower in the Arctic than the Antarctic samples (14% of Arctic 16S rRNA gene sequences, 32% of Antarctic 16S rRNA gene sequences, 20% of Arctic 18S rRNA gene sequences, 49% of Antarctic 18S rRNA gene sequences). This may have implications for the overall autotrophy of the system. It should be noted that the present study uses ribosomal RNA gene sequences which naturally cannot differentiate between living, dormant or legacy sources of ribosomal RNA gene fragments (Blazewicz *et al*., 2013; Edwards *et al*., 2020). Such legacy genes may be stored inside cryoconite granules, which show stratification between a photoautotroph-rich exterior and the storage of degraded organic matter within their interiors (Takeuchi *et al*., 2001b; Langford *et al*., 2010) and is potentially consistent with the enhanced accumulation of phylotypes within larger cryoconite granules (Uetake *et al*., 2016). By contrast, ribosomal RNA (rRNA) based analyses of communities in western Greenland return highly distinctive (potentially) active communities notable for the dominance of photoautotrophic bacterial lineages (Stibal *et al*., 2015; Gokul *et al*., 2019). It is therefore possible that in addition to the potential impact of biogeography, differences in the retention and flushing of legacy DNA between cryoconite habitats may contribute to some difference in gene community composition; however this is a factor that varies within the polar regions as well as between them.

Environmental differences and the limits of transport contribute to biogeographical clustering within glaciers (Edwards *et al*., 2011), and clustering such as this is demonstrated in our data. Cryoconite communities within individual glaciers also

tended to cluster, and so the differences between the glaciers could be viewed as the same contributing factors as the differences between poles on a smaller scale. In the Arctic and in Queen Maud Land in Antarctica, geographical clustering is stronger in the bacteria than eukaryotes (Cameron *et al*., 2012b; Lutz *et al*., 2019), but curiously this result was not previously found in the McMurdo Dry Valleys (Cameron *et al*., 2012b). Our results show clustering by glacier and by polar region to be stronger in the bacteria across all locations on both poles, including the McMurdo Dry Valley sites.

The major phyla present (Actinobacteria, Bacteroidetes, Cyanobacteria, Proteobacteria, Archaeplastida, Opisthokonta and the SAR group) are consistent with prior studies (Cameron *et al*., 2012b; Kaczmarek *et al*., 2016) but there were some notable differences. *Mrakia*, a psychrophilic genus were absent in the Antarctic cryoconite and one of the more abundant Opisthokont groups in the Arctic samples, despite having been discovered in the Antarctic (Xin and Zhou, 2007). In the eukaryotic microalgae, a higher proportion of *Chlamydomonas* and lower proportion of unknown Chloroccocales algae have been reported in Antarctic cryoconites (Christner *et al*., 2003; Sommers *et al*., 2018). Similarly, Bacillariophyceae (diatoms) were found in the Antarctic cryoconite as has been reported previously (Stanish *et al*., 2013) but, with the exception of one ASV recovered from the Greenland Margin, were absent in the Arctic cryoconite in contrast with previous findings from Greenland and Svalbard (Yallop *et al*., 2012; Vinšová *et al*., 2015). Although I found a clear split between the microalgae of the Arctic and Antarctic, it does not follow that those algae are only present on one pole. In light of previous studies, it is more likely that cryoconite holes became dominated by the residents of algal blooms flushed into those cryoconite holes in the season they were collected (Yallop *et al*., 2012; Williamson *et al*., 2020). Sampling at other times of year and in other locations may yield a different algal community. In addition, 6% of the Archaeplastida could not be assigned to a genus or family (Figure 18), so could potentially belong to groups mentioned above or others that have been found in polar cryoconite but not detected here such as Zygnematophyceae (Vonnahme *et al*., 2016).

The impact of local environment on cryoconite community composition

While cryoconite aggregate material can remain in a site for some years, the cryoconite holes may be flushed, buried and otherwise deformed (Hodson *et al*., 2008; Bagshaw *et al*., 2012). In the Arctic sites this may happen more regularly, on a seasonal or sub seasonal timescale, whereas McMurdo Dry Valley cryoconite holes may not be completely flushed for several years (Foreman *et al*., 2007). Cryoconite is also washed towards the glacial margins over time, in the direction of melt. Previous studies have found retention of a local foundational community on glacier sites over time, but also selection based on highly localised environments (Edwards *et al*., 2011; Gokul *et al*., 2016; Segawa *et al*., 2017). As well as comparing supraglacial habitats between poles, I was also able to compare the communities of ice margin open cryoconite holes, mid- ice sheet open cryoconite holes, and ice covered cryoconite holes formed the previous year in Greenland to broaden our representation of Arctic cryoconite and examine the impact of local habitat within glacier sites. In Svalbard, it has been established that the microbial communities of cryoconite holes were distinct from those of the ice marginal habitats, with only a minority of phylotypes appearing in both habitats (Edwards *et al*., 2013b). I have found that there is also a distinct difference between cryoconite communities found 60km onto the ice sheet and those within a few hundred metres of the ice margin in Greenland. There was significantly more variation between the types of Greenland samples (margin, ice core and ice sheet surface) than within groups. The communities from cryoconite core samples were similar to the communities obtained from the surface Greenland cryoconite. The samples from Greenland core cryoconite and surface cryoconite formed two distinct clusters, but were considerably more similar to each other than to the other Arctic and Antarctic cryoconite communities (Figure 14B). This suggests consistency over the subsequent year as well as location in the Greenland cryoconite, and reinforces its distinction from the community present at the Greenland margin, which is likely influenced by uprafted subglacial debris (Knight *et al*., 2002). Mixing with a distinctive subglacial microbial community results in a higher abundance of

methanogenic and sulphate reducing groups in margin samples when comparing to interior samples (Poniecka, 2020).

The Utsteinen region is situated in Queen Maud Land, an understudied region considerably far removed from the McMurdo Dry Valleys sites (Lutz *et al*., 2019). Despite the distance between the McMurdo Dry Valley and Utsteinen glaciers, the microbial community composition showed a high similarity. This suggests that there might be similar environmental drivers and sources for microbial communities in cryoconite holes across the Antarctic continent. Both regions are arid inland and glaciers will likely support closed-lidded cryoconite holes. They house recognisable hemisphere-specific cryoconite communities despite the limitations of aeolian transport across the Antarctic (Pearce *et al*., 2009). However, the Upper Wright Glacier samples bore a closer resemblance to the Arctic samples in several metrics and in some aspects, such the presence of Charophyta in several cryoconite holes, they were unique. There is no clear explanation for this. The Upper Wright sampling site was somewhat distinctive, as it is far from the sea and high altitude (950 m) compared to the other Dry Valley samples. However, there is no certainty in the contributing factors to the Upper Wright's distinct ecology.

Objective 1.2 Compare cryoconite taxonomy to Cryogenian keystone taxa

Since cryoconite holes support relatively high biodiversity within the cryosphere, it is possible that they could have provided refuge for complex and stable Cryogenian communities that may not have been successful in other habitats, such as under ice and in snow. The results of the comparison of modern cryoconite taxonomy and Cryogenian organisms support this assertion. Eukaryotes were the focus of this comparison for several reasons. Crown taxa of bacteria and archaea were well established by the Cryogenian, and had already survived several severe changes in climate including extreme cold since the Archaean. Because of the ages of the lineages and scant fossil data from bacteria and archaea, it is also difficult to identify specific taxa that may have been significant in the Cryogenian. However, it

should be noted that several known psychrophilic and psychrotolerant bacteria were recovered including *Cryobacterium* and Deinococcota, and analogue genes for stress tolerance and analogue cold protective proteins may have been a key part of survival through the extreme cold of the cryochrons. Archaea have also only been recovered in very low abundance. Although this may be in part due to primers used, it is unlikely that a high diversity of archaea will be found in cryoconite. Studies using used specific primers designed for archaea still found them to be a minor component of the cryoconite alpha diversity (Cameron *et al*., 2012b; Weisleitner *et al*., 2020). The majority of cold-adapted archaea have been isolated from lake and marine habitats (Cavicchioli, 2006). Therefore, it's possible that the oases of biodiversity for archaea in the Cryogenian may have been different to those of bacteria and eukarya. Snowball earth archaea are likely to have been concentrated in lakes and oceans as they are in today's cryosphere. Lastly, Cryogenian eukaryotes are of particular interest because of their position in the history of multicellular life. The first fossil evidence of animal body plans is found in the Ediacaran, and biomarkers suggest that the first demosponge-like organisms emerged before the Marinoan glaciation. No demosponges have been found in cryoconite, but Choanoflagelletes, one of the closest living sister groups to metazoa, were found in several Antarctic locations.

All key Cryogenian taxa that were searched for were found in at least one location. Cercozoans and Alveolates were found at all locations. The presence of test-forming amoebozoa such as Rhogostoma show not only similar phylogenetically taxa present but also similar morphologies are present in modern cryoconite holes. Therefore, cryoconite holes are capable of supporting the key eukaryotic taxa which inhabited Snowball Earth. However, the Antarctic cryoconite holes in particular represent a strong analogue to Cryogenian communities due to the number of significant organisms present. It is possible that their stability, as a more enclosed and consistent habitat in comparison to the more regularly flushed Arctic cryoconite holes favours eukaryotes such as the Excavata. However, in general the Arctic samples had a higher richness and alpha diversity of 18S ASVs. Therefore it

may be the geographical separation between the Arctic and Antarctic that is responsible for this difference between the polar regions.

The coldest of the sample sites used was the Utsteinen Nunatak, which rarely rises above an air temperature of 0°C (Gorodetskaya *et al*., 2013; Lutz *et al*., 2019). The Utsteinen site also presents an interesting analogue to extreme Snowball Earth life because of its isolation from the sea and the limited ice-free areas in the vicinity. On Snowball Earth, ice free areas of land and sea would have been very limited, especially on the large ice sheets (Hoffman *et al*., 2017). However, the amount of cryoconite collected in this region is limited. This provides a practical barrier to its use in further study, but also means that this region bears little resemblance to the description of areas of cryoconite holes, ponds and lakes in ablative zones providing an area of biodiversity (Hoffman, 2016; Hoffman *et al*., 2017). Rather, the cryoconite holes of Queen Maud Land are widely dispersed, low in biomass and few in number.

In the Arctic regions, it is common to find many interconnected cryoconite holes across ablation zones of glaciers. They also host considerable eukaryotic diversity (Figure 17) compared to ice surfaces (Mindl *et al*., 2007; Liu *et al*., 2011), but the conditions under which they are formed are considerably warmer than Snowball Earth temperatures (Abbot *et al*., 2013). Therefore, Arctic open lidded “warmer” cryoconite holes may be an apt analogue for the end Sturtian deglaciation into the interglacial gap, and Marinoan deglaciation into the Ediacaran. However, this depends on whether the types of organisms that currently live in the comparatively warmer open Arctic cryoconite holes could have survived through the cold, dry, conditions of the glaciations to persist to the proceeding deglaciations. As it is a short time in evolutionary terms, any organisms that lived during the deglaciations would have lived through the cryochron(s). Many of genera found in the Arctic cryoconite holes were also found in the colder McMurdo Dry Valleys cryoconite holes. However, species and strains can vary greatly within a genus so this does not guarantee the Arctic cryoconite organisms have the same adaptations as the Antarctic cryoconite organisms.

The McMurdo Dry Valleys are the closest modern environment to the mid-cryochron Snowball Earth. They contain ice lidded cryoconite in a dry habitat that is below freezing for much of the year. Cryoconite holes are found across many glaciers in the region and in considerable number. Many McMurdo Dry Valleys cryoconite holes also carry a relatively large quantity of cryoconite sediment (up to 10cm in thickness) compared to those collected from the Arctic and Utsteinen Nunatak.

Cryolakes form in the McMurdo Dry Valleys when sediment aggregates are blown towards ice cliffs (Bagshaw *et al*., 2016a; Dubnick *et al*., 2017). If the strong katabatic winds of Snowball Earth were to blow over a McMurdo Dry Valley –like environment, this process may form habitats such as the cryoconite pans proposed by Hoffman *et al* (2016) that allow larger ecosystems to form. Networks of Cryoconite holes may also allow connections between cryoconite communities. McMurdo Dry Valley cryoconite holes may not be completely flushed for several years (Foreman *et al*., 2007). Previous studies have also found that while community composition is influenced by highly localised environments, the local foundational community on glacier sites remains over time even when water flowed through (Edwards *et al*., 2011; Gokul *et al*., 2016; Segawa *et al*., 2017). Therefore dry valley cryoconite may provide a stable network of communities encompassing a large quantity of sediment across ablation zones and other warmer areas of ice.

In terms of both environmental conditions and taxonomic membership, the modern McMurdo Dry Valleys bear a strong resemblance to Snowball Earth habitats. However there remain some considerable differences between these two environments. The areas of the Cryogenian Snowball Earth warm enough to support life on the surface would have been situated at low latitudes, between the equator and subtropics (Abbot and Pierrehumbert, 2010; Hoffman *et al.*, 2017). A modern example of this is the Himalayas, which hold the largest ice mass outside the polar regions and has been found to sustain cryoconite holes (Takeuchi *et al*., 2001b; Wagnon *et al*., 2007; Singh *et al*., 2017; Sanyal *et al*., 2018). However, the Himalayas lack the cold dry valleys of Antarctica (Sanyal *et al*., 2018). The

cryoconite is warmer and only present at high altitude (King *et al*., 2010; Singh *et al*., 2020). They are also frequently contaminated by man-made pollutants so may be less suitable as Cryogenian analogues (Singh *et al*., 2017). Further insight on the development and microbiology of this understudied region may yield insight on how low latitude may have impacted Cryogenian cryoconite. Results chapter 2 takes a different approach to finding analogous habitat, by exploring the impact of low latitude Cryogenian conditions on the growth of cryoconite communities sourced from the McMurdo Dry Valleys.

Conclusion

The use of 16S and 18S rRNA gene high throughput sequencing enabled a more comprehensive examination of taxonomic diversity of bacteria, archaea and eukaryotes across Arctic and Antarctic cryoconite ecosystems than previous studies. I was able to resolve community composition to the family and often genus level, revealing a diverse community of microbes with the potential to contribute to a complex tropic web. Most significantly, it allowed for the direct comparison of microbial assemblages in cryoconite holes from both the Arctic and Antarctic. Intact polar lipid analysis revealed a diversity of IPL groups in all samples but a divide in composition between active communities of Arctic and Antarctic cryoconite. Our findings suggest that the Arctic and Antarctic cryoconite holes harbour distinct microbial communities, but the various biotic niches (grazer, predator, photoautotroph, chemotroph), are filled in every location. The “core taxa” which are numerous in both abundance and occupancy share little similarity between the poles. The characteristics of the local environment and neighbouring habitats play a distinct role in the community composition. Therefore while cryoconite holes may be a global feature of glacier landscapes, they are inhabited by regionally distinct microbial communities. Due to this distinction, the communities of the Antarctic are a particularly strong analogue for Snowball Earth life as they support many of the eukaryotic crown groups known to have persisted through the Cryogenian. The climate of the McMurdo Dry Valleys is also the closest analogue to the cold dry

conditions of the mid-cryochrons. Supraglacial life must have survived conditions such as these during the mid Sturtian and Marinoan glaciations.

Results Chapter 2: Resilience of modern cryoconite to Snowball Earth environments

Summary

Although it has been theorised that cryoconite was a key habitat on Snowball Earth, its ability to survive under such conditions has never been reported. In this chapter, cryoconite was incubated in serum vials under two potential Snowball Earth conditions. The first, 24 hour cycles of 12 hours of light followed by 12 hours of dark to simulate low latitude light conditions. The second, 24 hour cycles of 12 hours of freeze followed by 12 hours of thaw to simulate the freeze-thaw cycles at these latitudes. In both cases the carbon production patterns were unchanged between cryoconite communities under the control (24 hours of light and temperature of 0.5°C to simulate modern polar growth season conditions) and "Snowball Earth" conditions, as measured by oxygen saturation and ^{3}H-leucine incorporation. To verify the suitability of serum vials for simulations of cryoconite holes, cryoconite holes were formed and monitored in the laboratory. It was possible to create cryoconite holes on an ice surface that remained stable for several days in climate-controlled incubation chambers. This created a novel opportunity to measure and document the development of a cryoconite hole. Arctic and Antarctic cryoconite was found to vary in its development of cryoconite holes *ex situ*. The oxygen saturation of these cryoconite holes was similar to those in equivalent conditions in serum vials, confirming their suitability as cryoconite hole analogues.

Introduction

Hypothesis 2: Modern polar cryoconite is resilient to 'Snowball Earth' conditions.

Results Chapter 1 used 16S and 18S rRNA gene sequencing (Objective 1.1, page 14) to demonstrate that many of the key taxa known to have persisted through the Cryogenian Snowball Earth period inhabit cryoconite holes of the polar regions. These results also showed that across the Arctic and Antarctic, cryoconite holes host notably high biodiversity, in terms of both species richness and taxonomic diversity (Figure 13). These two findings concur with studies that have presented modern cryoconite holes as an analogue for diversity hotspots on Snowball Earth (Hoffman, 2016; Hawes *et al*., 2018). However, there are numerous differences between a modern polar environment and a Cryogenian glacial environment, which this chapter aims to explore through laboratory simulation.

The overall global temperatures were considerably lower on Snowball Earth. Models compiled by Abbot *et al* (2013) over a range of potential atmospheric CO_2 levels predict global annual average temperatures between -5°C and -30°C. Some models predicted summer solstice temperature could rise above freezing at the 40th parallel south, while others place the entire temperature range firmly below -20°C (Abbot *et al*. 2013) (Figure 7). All models predict a drop in temperature of ~90°C between the 40th parallel and 70th parallel. Therefore oases of life on Snowball Earth were most likely to have been located in low latitude tropical and subtropical regions. Modern cryoconite is formed by material deposited by local winds from ice free land and ocean microbiota. Again, equivalent ice free areas of land required to form cryoconite on Snowball Earth are likely to have been mostly located in the subtropics, tropics and equatorial regions where temperatures were warmest and land mass was congregated (Li *et al*., 2013). If the majority of viable cryoconite holes were present in low latitude regions, it follows that rather than a growth season over the light warm summer and dormancy and freezing over winter, the cryoconite would be influenced by day-night cycles throughout the year.

In previous studies, measurements of cryoconite productivity under ambient growth conditions have been carried out *in situ* and *ex situ* on both Arctic and Antarctic cryoconite (Anesio *et al*., 2009; Cook *et al*., 2010; Hodson *et al*., 2010; Bagshaw *et al*., 2011; Stibal *et al*., 2012b; Telling *et al*., 2012; Bagshaw *et al*., 2016a; Poniecka *et al*., 2018). In some cases, physiological capabilities of cryoconite have been tested by exposing it to extreme conditions. Bagshaw *et al* (2016) describe the stress response in cryoconite organisms under high light levels during *ex situ* incubation. *Ex situ* incubations by Poniecka *et al* (2020) showed a broad tolerance of cryoconite strains to salinity and extremes of pH. However, there was a mixed response to freeze-thaw cycles (at 6 h at -18°C and 3 h at 0.9°C), with some strains surviving and others becoming unviable after 25-100 cycles. No study to date has shown cryoconite response to a low latitude type light or temperature cycle. Therefore the first objective of this chapter is:

Objective 2.1: Measure the response of cryoconite to 'low latitude Snowball Earth' light and temperature conditions.

The dissolved oxygen method, used previously to determine community productivity in *ex situ* cryoconite (Hodson *et al*., 2010; Telling *et al*., 2010; Bagshaw *et al*., 2011; Telling *et al*., 2012; Bagshaw *et al*., 2016a, 2016b; Poniecka *et al*., 2018, 2020) is used here to assess cryoconite community response to the test conditions. By comparing "Snowball Earth test condition" and control bottles to dark bottles measured in the same climate incubation chamber, it was possible to calculate gross photosynthesis, respiration and net carbon production (NCP). For verification, in the first experiment NCP rate was also measured using the ^{3}H-leucine incorporation method, calculated using measurements for quantity of radio-labelled leucine consumed over a 3 hour incubation (Kirchman, 2001). This method has been used previously for glacial microbial communities in supraglacial and proglacial systems (Anesio *et al*., 2010; Edwards *et al*., 2013b; Bradley *et al*., 2016; Rassner *et al*., 2016). In addition, the composition of intact polar lipids at the incubation end point was compared between conditions and to the composition at the start point. This allowed examination of changes in community composition and

physiology (or lack thereof) in addition to overall community primary production and respiration (Rütters *et al*., 2002; Sturt *et al*., 2004).

The incubations described in this chapter so far have been carried out in enclosed glass serum vials, as is common in cryoconite incubations (Hodson *et al*., 2010; Telling *et al*., 2010; Bagshaw *et al*., 2016b, 2016a; Poniecka *et al*., 2020). To compare these results to those of a potentially more representative cryoconite, an additional aim of forming and measuring ice cryoconite holes in the lab was undertaken. I was able to form *ex situ* ice cryoconite holes of sediment on ice and compare oxygen measurements to those produced from cryoconite in serum vials, to fulfil the following objective:

Objective 2.2: Form cryoconite holes on ice in laboratory conditions, for closer replication of Snowball Earth conditions

Results

Objective 2.1: Measure the response of cryoconite to 'low latitude Snowball Earth' light and temperature conditions

2.1.1 Cryoconite community response to low latitude light cycle

Oxygen saturation

McMurdo Dry Valley cryoconite communities grown in "low latitude" day-night cycle conditions (12 hours light followed by 12 hours dark each day) were compared to McMurdo Dry Valley cryoconite communities grown in full time dark and full time light conditions. Oxygen concentration (% air saturation) in the water column was measured over 27 days (Figure 23A). Initial oxygen readings show the values for day-night and light conditions grouped closely together throughout the incubation, while the dark samples produced lower values through the majority of time points (Mann-Whitney scores at midpoint: p=0.4 for day-night and dark comparison, p=1 for day-night and dark comparison. Mann-Whitney scores at

endpoint: p=0.1 for day-night and dark comparison, p=1 for day-night and dark comparison). % air saturation in the 'blank' bottles (water only) increased from day 2 to day 27, steadily from 79.7% to 100.9% which is most likely due to oxygen ingress when the needle has pierced the lid of the serum vials. This is less of a dramatic increase than that observed in the dark bottles. Unfortunately this means that the ingress of oxygen may not have impacted all vials equally. The quantity (µg) of organic carbon produced per gram of sediment was calculated through subtraction of the non-photosynthesising dark community's organic carbon quantities from the light and day-night condition quantities. Blank values were subtracted from test vials to control for bleed of air into the serum vials during and after measurements were taken, however if the impact of oxygen ingress is different between vials this may not completely account for this issue. The quantity (µg) of organic carbon produced per gram of sediment also followed the same

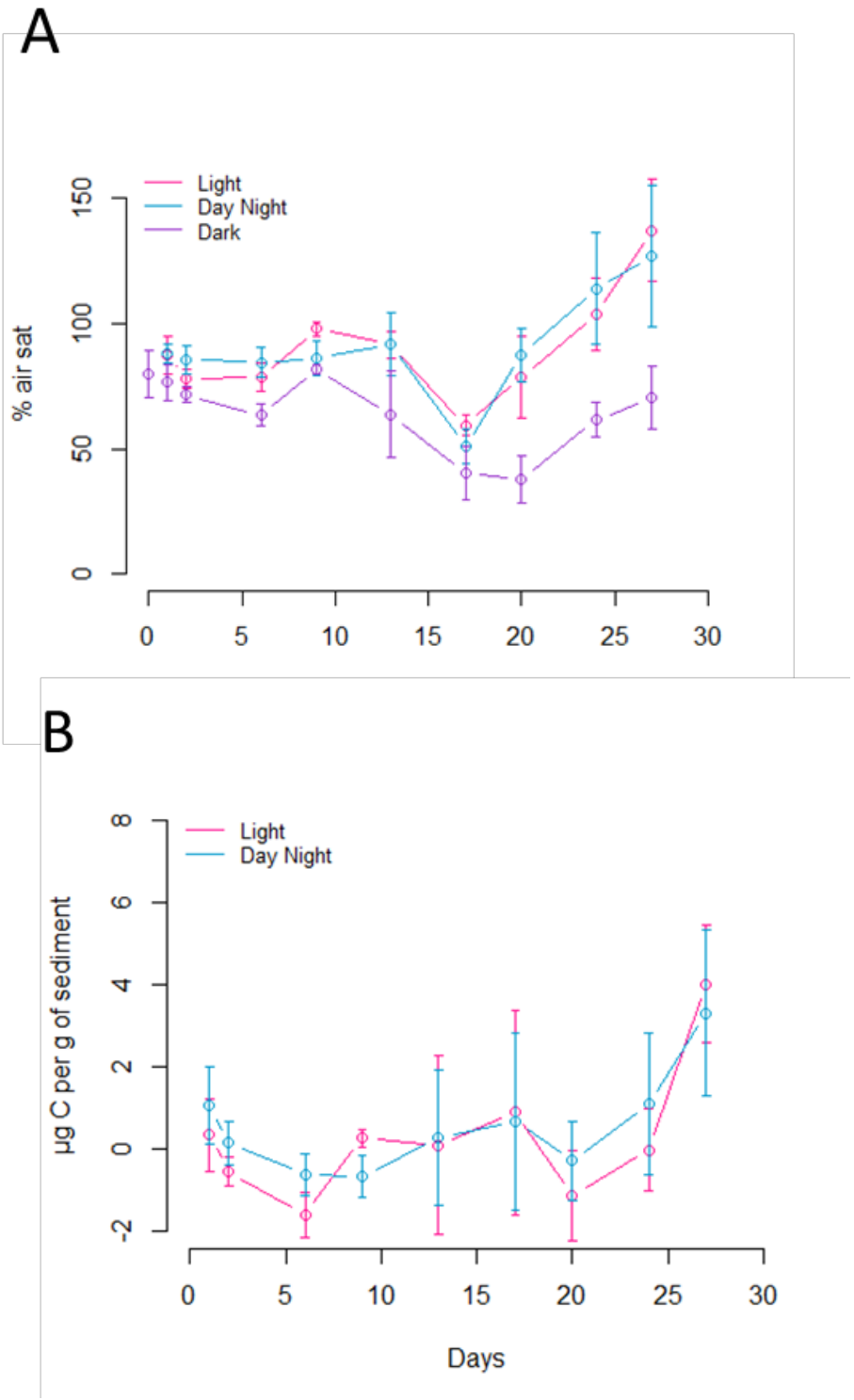

Figure 23 Cryoconite community response to 28 days of growth under one of three light conditions. "Light": 24 hour light representing a modern polar growth season, "Day Night": 12 hour day-night cycle representing a Snowball Earth growth season, "Dark": 24 hour darkness. Panel **A** shows dissolved oxygen content as % air saturation in the water, panel **B** shows µg of carbon per gram of sediment produced, as calculated from oxygen values. Panels **C** and **D** show two metrics of rate of carbon production. Panel C plots rate of carbon production per hour (panel **B**). Panel **D** shows rate of carbon production as calculated over a 3 hour incubation with radio-labelled leucine at each time point.

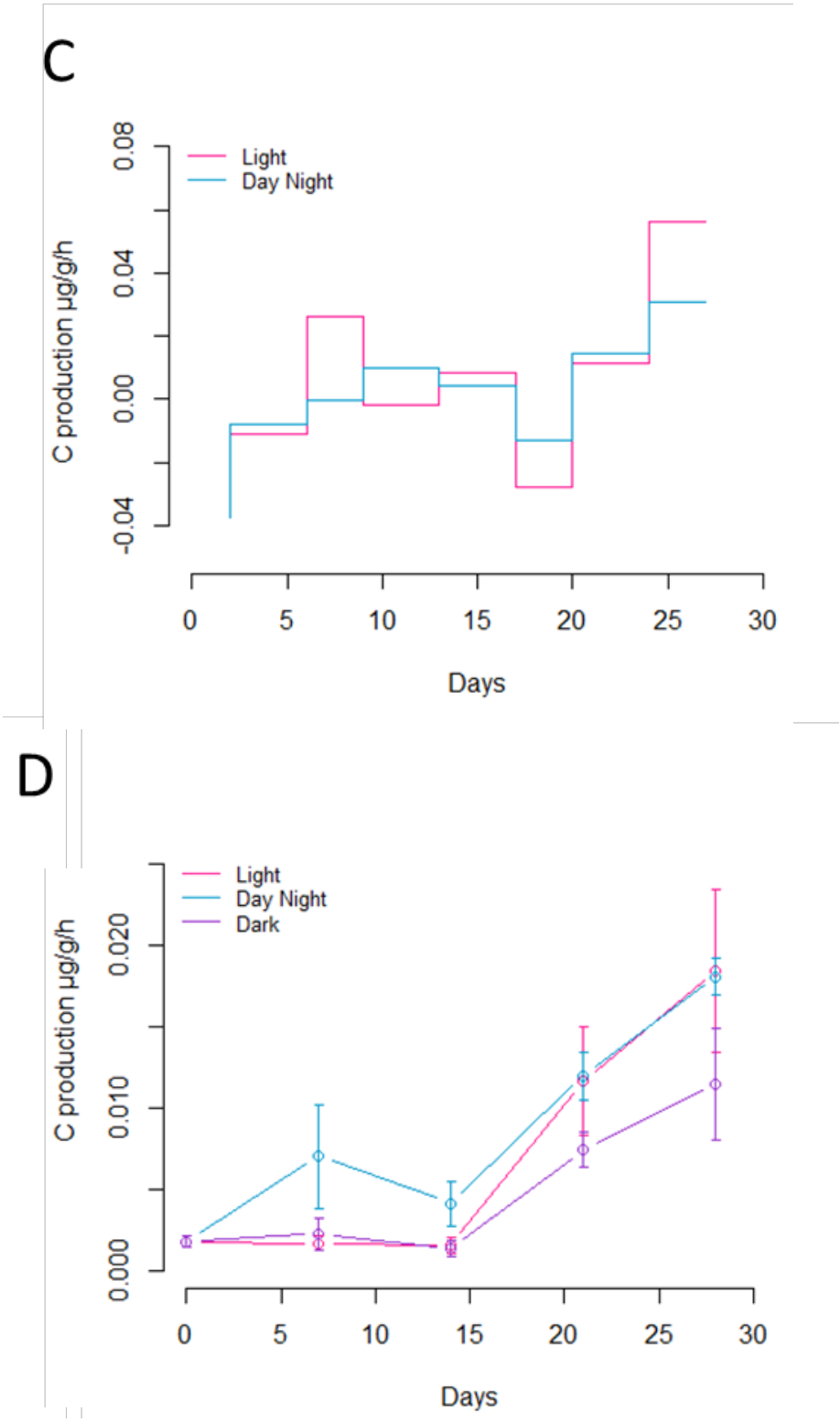

Figure 24 Cryoconite community response to 28 days of growth under one of three light conditions. "Light": 24 hour light representing a modern polar growth season, "Day Night": 12 hour day-night cycle representing a Snowball Earth growth season, "Dark": 24 hour darkness. Panel **A** shows dissolved oxygen content as % air saturation in the water, panel **B** shows µg of carbon per gram of sediment produced, as calculated from oxygen values. Panels **C** and **D** show two metrics of rate of carbon production. Panel C plots rate of carbon production per hour (panel **B**). Panel **D** shows rate of carbon production as calculated over a 3 hour incubation with radio-labelled leucine at each time point.

trend in both the light and day-night conditions (Figure 23B). It decreased for the first few days (from 0.349 μg/g at day 1 to -1.592 μg/g at day 6 under light conditions, and from 1.061 μg/g at day 1 to -0.612 μg/g at day 6 under day-night conditions), and increase after 6 days (at day 17, 0.911 μg/g under light conditions, and to 2.487 μg/g under day-night conditions). Following the 17 day measurement there was a sharp drop in organic carbon production (at day 20, -1.113 μg/g under light conditions, -0.271 μg/g under day-night conditions), and then an increase from 20 days to the highest point at 27 days (4.026 μg/g under light conditions and 3.329 μg/g under day/night conditions). The rate of organic carbon accumulation was somewhat lower in the light-dark cryoconites at the end of the final phase (0.0560 μg/g/h under day-night conditions compared to 0.0308 μg/g/h under light conditions), however the average rate from day 20 to day 27 was more similar (0.0338 μgC/g/h under day night conditions, 0.0226 μgC/g/h under light conditions) (Figure 23C).

Rate of radiolabelled leucine incorporation

The rate of overall organic carbon production was calculated based on incorporation of ^{3}H-leucine over an incubation of 3 hours on each sampling day (Figure 23D). In accord with the findings of the oxygen saturation method, the trend and end points were similar between the full time light and day-night cycle conditions. While the values deviated from those obtained from oxygen measurements (a range of 0.00142 to 0.0185 μg/g/h for the leucine method, -0.0378 to 0.0560 μg/g/h for the oxygen method), the trends in organic carbon production rate are similar. The first half of the 28 day period sees a small increase followed by a decrease in rate of organic carbon production (from 0.00185 μg/g/h at day 0 to 0.00174 μg/g/h on day 7 and 0.00163 μg/g/h at day 14 under light conditions, and 0.00708 μg/g/h on day 7 and 0.00419 μg/g/h at day 14 under day night conditions). The second half showed a steep increase in organic carbon production rate in both light and day night cycles (ending at 0.0185 μg/g/h under light conditions and 0.0181 μg/g/h under day night conditions). Through this method it was also possible to evaluate rate of organic carbon production in the dark condition. As was the case in the oxygen measurements, the rate of organic

carbon production is noticeably lower in the final phase under dark conditions, days 21 (0.00746 µg/g/h under dark conditions and 0.0120µg/g/h under day night conditions) and 28 (0.0115 µg/g/h under dark conditions and 0.0181 µg/g/h under day night conditions).

Intact polar lipid composition

All samples contained a diversity of IPLs (Figure 24) which would be expected for an active microbial community (Sturt *et al*., 2004; Evans *et al*., 2017, 2022). All IPLs detected were recovered in all samples. The most abundant three IPL groups were 1G-DAG (20% total IPLs), PC-DAGs (17%), and BLs (14%). 1G-DAG is one of the major constituents of thylakoid membranes and so may be indicative of microalgae. PC-DAGs are also primarily produced by eukaryotes. BLs have been primarily examined in algae but are produced by a wide range of organisms, particularly under phosphate limited conditions (Murakami *et al*., 2018). 21% of the total IPLs were aminolipids, 34% glycolipids and 45% phospholipids.

There was no significant difference in composition between the starting IPL composition from subsamples extracted on Day 0, and subsamples taken at the experiment end point under the three conditions (24 hours per day light, 24 hours

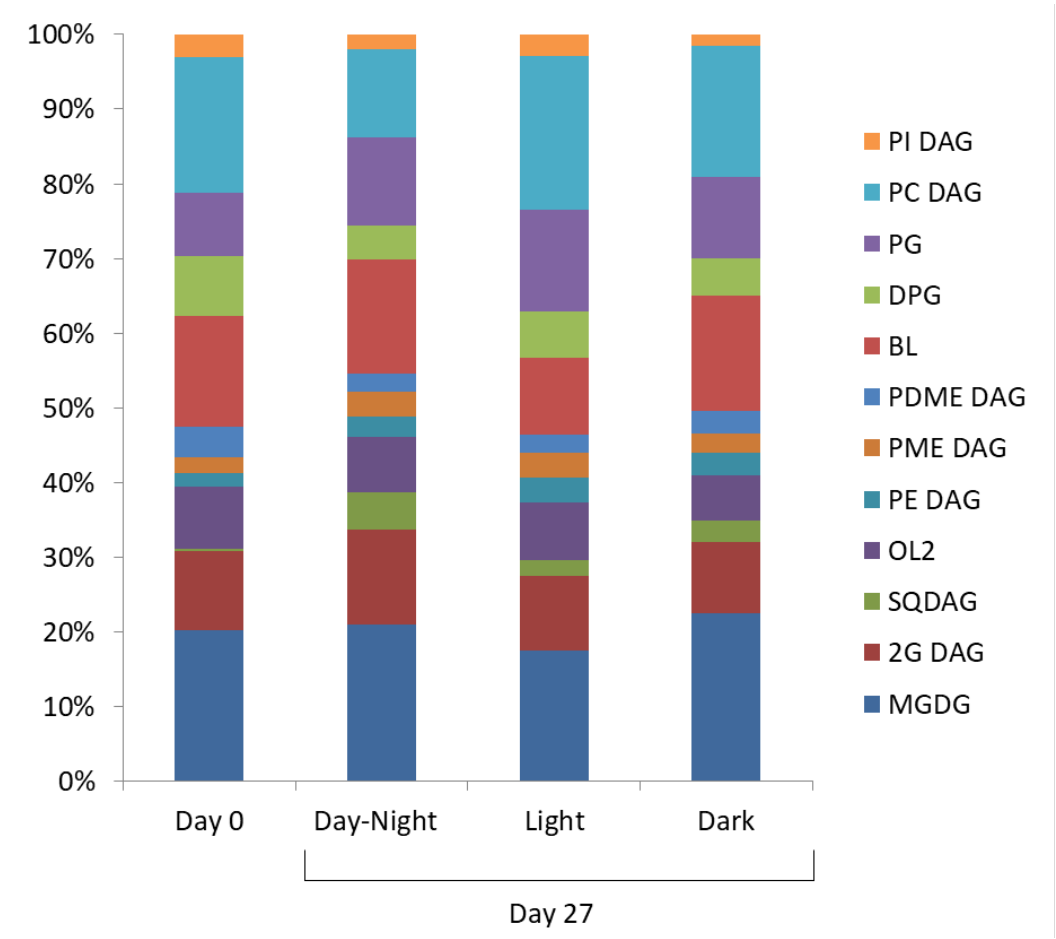

Figure 25 Intact Polar Lipid composition at start point and end points under each light growth condition

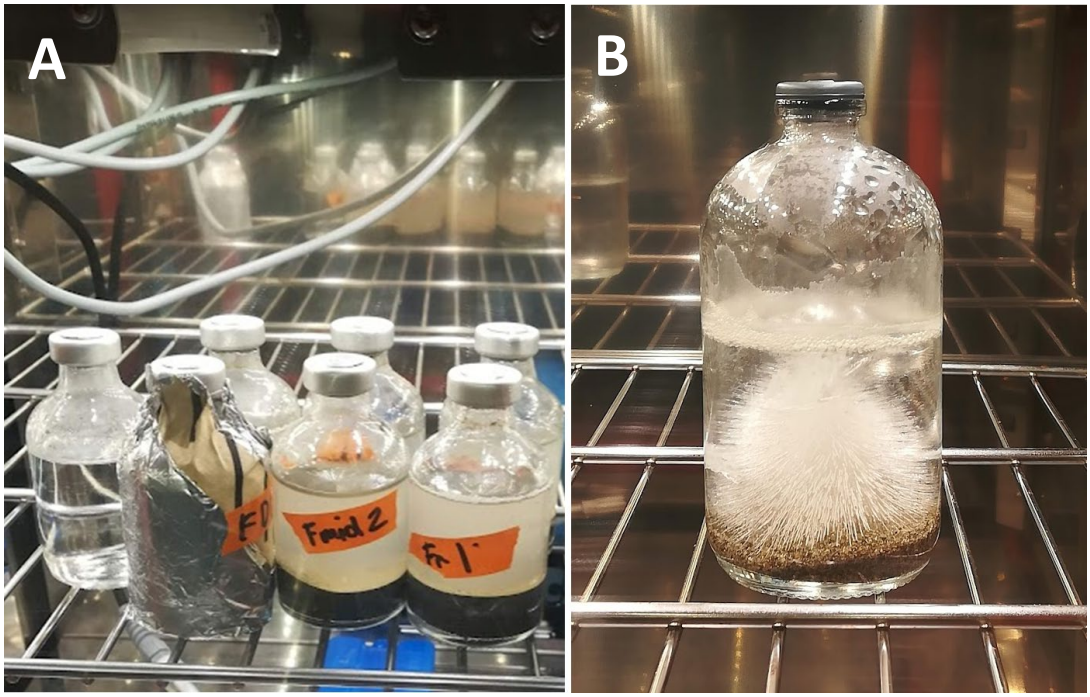

Figure 26 Serum vials during freeze-thaw cycle incubation. **A** Cryoconite samples, “dark” no-photosynthesis bottles and blank during a thaw phase (1°C) **B** A cryoconite sample.

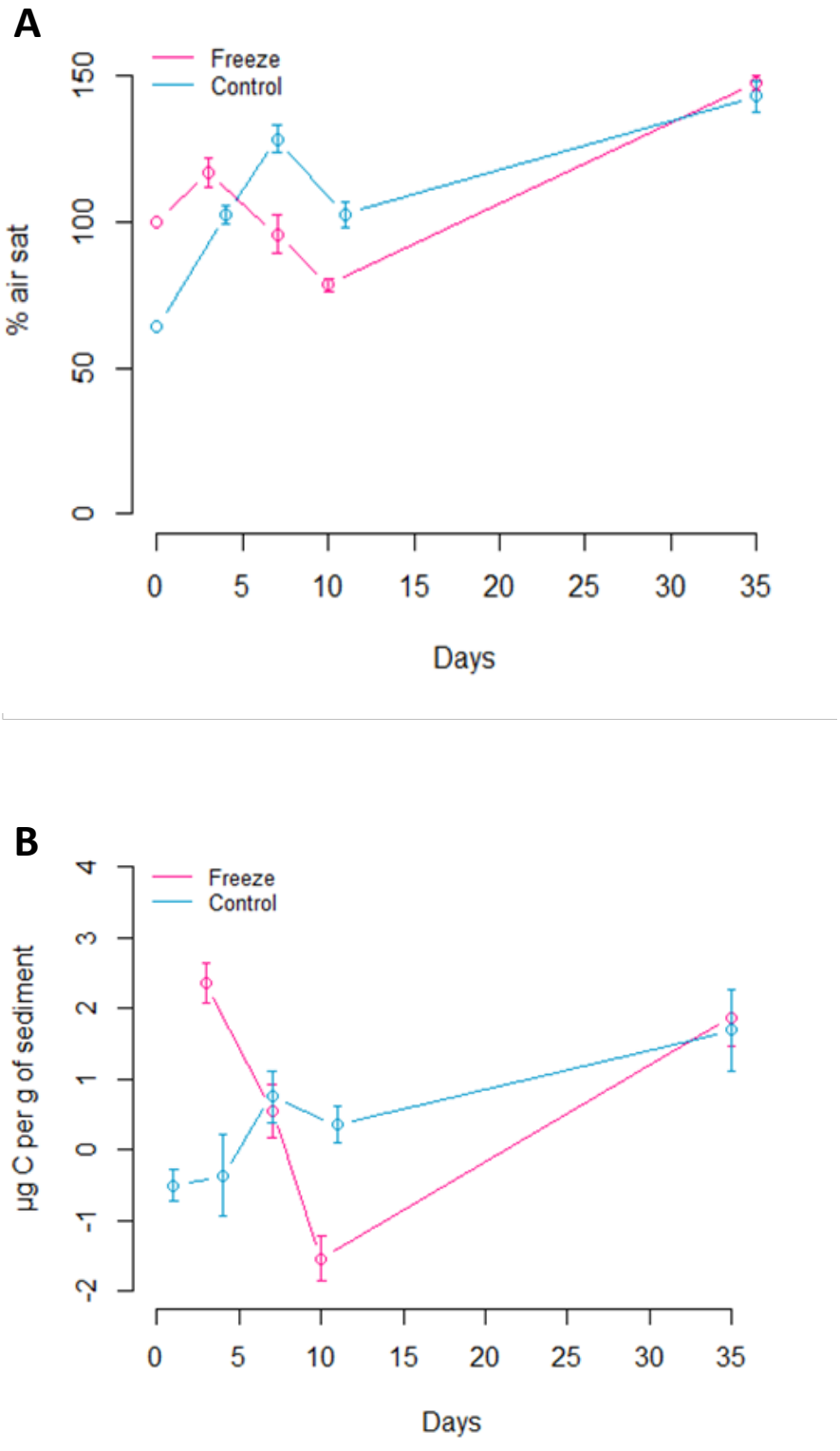

Figure 27 Cryoconite community response to 35 days of growth under one of two temperature conditions. "Freeze": 12 hours freezing at -5°C followed by 12 hours thaw at 1°C each day transition period. "Control": 24 hours at 0.5°C. Panel **A** shows dissolved oxygen content as % air saturation in water, panel **B** shows µg of carbon per gram of sediment produced calculated from dissolved oxygen content.

per day dark and 12 hour day-night cycle). PERMANOVA results are reported in Table 10. The end-point IPL composition under all conditions had a higher relative abundance of SQ-DAGs than Day 0 (0.32% of IPL composition at Day 0, 5.02% at Day 27 Day-night, 2.19% Day 27 Light, 2.97% Day 27 Dark). However this was not sufficient to produce an overall significant difference in composition.

Table 10 Pairwise PERMANOVA results of IPL composition comparison at incubation start point and end points under each light condition.

PERMANOVA Pairs	P value
Day 0 vs Day 28 Day-Night	0.1
Day 0 vs Day 28 Light	0.3
Day 0 vs Day 28 Dark	0.7
Day 28 Day-Night vs Day 28 Light	0.2
Day 28 Day-Night vs Day 28 Dark	0.6
Day 28 Light vs Day 28 Dark	0.4

2.1.2: Cryoconite community response to low latitude freeze-thaw cycle

Oxygen saturation

Freeze-thaw samples were frozen in the environmental chamber (Figure 25) at -5°C for 7 hours and then thawed at 1°C for 7 hours each day with a 5 hour transition period each side (reducing or increasing temperature by 1°C each hour) (Figure 26). Because the light-dark incubation (see Objective 2.1.1, page 121) appeared to

capture the start of an exponential growth phase, the freeze-thaw incubation was run for an additional seven days to investigate this trend further (35 days total). At the freeze temperature (-5°C), ice formed in all samples. At the thaw temperature (1°C), the majority of ice in the vials consistently melted but a small area sometimes remained frozen. The quantity of organic carbon produced per gram of sediment (calculated from dissolved oxygen content) declined for the first 10 days, whereas the carbon production in the control (no freezing, constant temperature of 0.5°C) cryoconite increased (from a mean of -0.503 to 0.757 µg C/g) over the first 10 days (Figure 23). The final measurements of carbon production values were 0.401 µg C/g for freeze-thaw conditions and 0.572 µg C/g for control conditions. Therefore, despite the earlier divergence between community response to freeze and control conditions (Mann-Whitney p=0.01) the end values converged (Mann-Whitney p=0.07) suggesting a return to normal modern Antarctic levels of growth, as represented by the control conditions.

Objective 2.2: Form cryoconite holes on ice in laboratory conditions, for closer replication of Snowball Earth conditions

Evolution of laboratory cryoconite holes

The evolution of laboratory ice cryoconite holes containing McMurdo Dry Valley sediment is shown in Figure 27. Cryoconite holes began to form immediately following placement of cryoconite sediment on the ice surface ~20cm from the climate chamber lights which delivered ~86.5 µmol/m^2/s photosynthetically available radiation. After 24-48 hours, sufficient meltwater had accumulated to measure oxygen saturation in the water. Following the initial melt into the underlying ice, the majority of melting continued in a circular or oval zone at the centre of the cryoconite where most of the sediment was located. The cryoconite continued to melt the underlying ice in this area, moving downwards. Slight variations in temperature, sediment quantity and sediment quality resulted in variation in how long this process continued but generally at day two the cryoconite

had sunk from 1-2cm and by day seven, 5-6.5cm. In some samples the sediment continued to move downwards until it reached the base of the ice container. In others, the freezing of the cryoconite hole was sufficient to hold the sediment in place. Re-freezing of the cryoconite hole meltwater occurred after 6-7 days. The column of the cryoconite hole narrowed above the area containing sediment as ice re-froze at the walls (Figure 27, days 7-9). A thin layer of ice also formed at the surface, encroaching from the edges to the centre. Through this time the sediment remained unfrozen. After 12-15 days this had become an ice lid, with only a small hole or thinner ice area in the centre. From 15 days onwards the lid was several centimetres thick over the whole cryoconite hole. In some samples, a small air bubble would form in the centre, trapped by ice freezing from the surface and ice freezing from the walls of the cryoconite hole.

The cryoconite hole evolution was repeated using Arctic cryoconite. Although the 'Arctic' cryoconite holes follow the same structural development as the 'Antarctic'

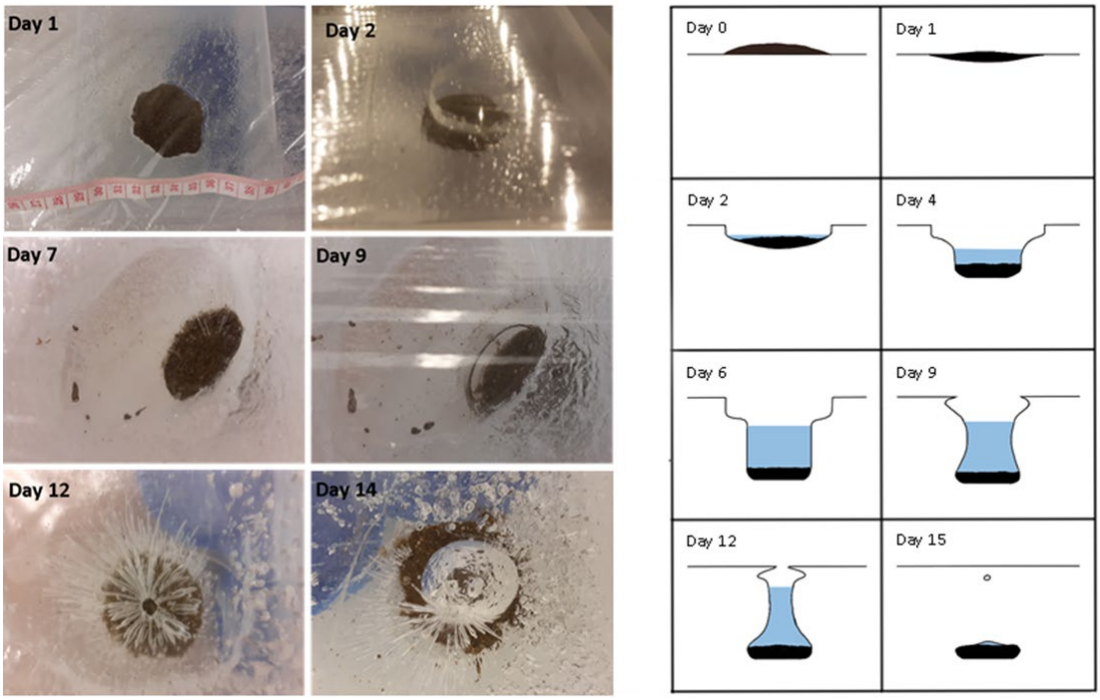

Figure 28 Development of laboratory grown cryoconite holes using McMurdo Dry Valleys cryoconite sediment. Cryoconite sediment was placed on ice in temperature controlled chambers at ambient light and temperature (0.5°C) and left to develop. Left panel: photographs of cryoconite hole development from above. Right panel: illustration of side view of laboratory cryoconite hole development. Blue denotes meltwater, black denotes cryoconite sediment. The cryoconite melts the underlying ice, and spreads laterally for the first two days. By days 4-6 the area of deepest sediment that has still retained relative warmth continues to melt into the ice. From day 7 the cooled sides of the cryoconite hole and surface water begin to freeze from the sides inwards. By day 15 a thick ice lid has formed with minimal meltwater covering the cryoconite sediment layer. An air bubble may form, trapped by the ice freezing from the surface and cryoconite holes sides.

cryoconite holes, the pace of development varied. It took two days longer for the cryoconite holes to begin to form (for vertical melting to occur); this occurred at days 3-4 rather than days 1-2. However, from this point the development was rapid, and the cryoconite holes reached a depth of 5-6.5cm by day 7 as the 'Antarctic' cryoconite holes had done. The holes formed by Arctic cryoconite were also more stable, in that the pace of vertical melting slowed at this point, allowing the holes to last 48 hours longer than the Antarctic counterparts.

Comparison of on-ice and glass vial cryoconite incubations

The oxygen saturation in on-ice cryoconite holes was compared to that of cryoconite incubated in serum vials under the same temperature and light conditions (24 hours light, 0.5°C) as previous tests (Figure 28). The cryoconite used in the light/day-night/dark test is referred to as LC1 (Light, constant temperature 1) and the cryoconite used in the freeze-thaw/constant temperature test is referred to as LC2. The values fall within a similar range and show the same characteristic initial rise, then fall in % air sat. The ice experiment could not run for the same time period as the vial experiment because the holes melted to the base of the ice container and eventually collapsed. However, the initial behaviour suggests that the same process should occur: rise in oxygen over the first 7 days, followed by a decline, and then what may be an exponential growth phase between days 15 and 35.

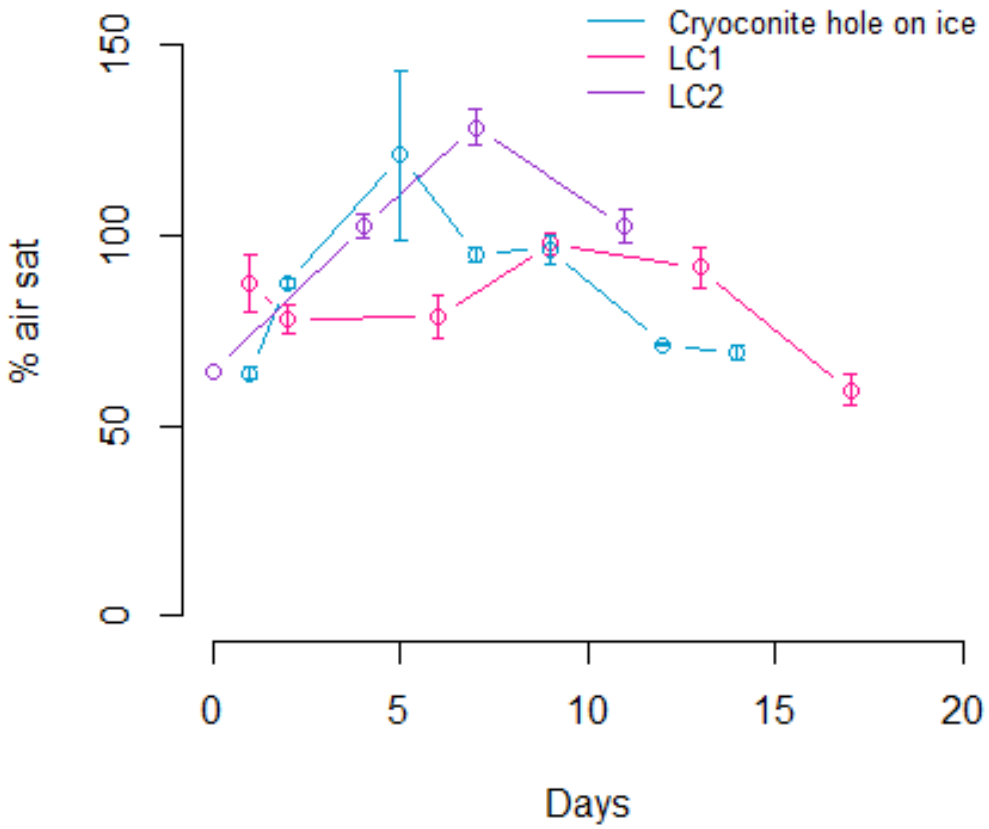

Figure 29 Comparison of dissolved oxygen content in a laboratory-formed ice cryoconite hole and cryoconite incubated in glass serum vials. LC1 and LC2 represent cryoconites incubated in glass vials under control ambient polar growth conditions from previous tests. LC1, LC2 and ice cryoconite holes were incubated at a constant water temperature of 0.5°C in 24 hours of light.

Discussion

Objective 2.1: Measure the response of cryoconite to 'low latitude Snowball Earth' light and temperature conditions

Cryoconite community response to day-night light cycle

To determine the suitability of modern cryoconite holes as analogues for Snowball Earth habitats, cryoconite was monitored under Snowball Earth type conditions that may influence microbial activity. Light has been shown to play an important part in cryoconite hole development and community survival (Bagshaw *et al*., 2016b; Perkins *et al*., 2017). Phototrophs are an important component of cryoconite ecosystems in general and Results Chapter 1 Objective 1.1 demonstrated that they are a significant contributor to the McMurdo Dry Valleys cryoconite ecosystems in particular (Takeuchi *et al*., 2001a; Fountain *et al*., 2004; Cameron *et al*., 2012b; Millar *et al*., 2021). Both algae and Cyanobacteria are supported by the cryoconite, as demonstrated by Results Chapter 1. The Canada Glacier cryoconite used contained DNA of the Cyanobacteria *Tychonema*, *Nostoc*, *Chamaesiphon* and *Aliterella*, and the microalgae Chlorococcales in addition to other minor autotrophic lineages (though it is not known which and what quantity of this DNA belonged to active cells). Both low light and high light present a potential stress to these organisms, and a reduction in autotrophic capability (Vass *et al*., 2007; Zhu *et al*., 2017).

During a polar growth season in the polar regions, cryoconite holes can receive up to 24 hours of light each day. The Antarctic solar low angle of incidence and depleted ozone layer produces high levels of light and UV radiation during the austral summer. The noon UV index generally varied between 2-5.5 but reached as high as 7.5 in the McMurdo Dry valleys over the years this study's cryoconite was collected (Bernhard *et al*., 2006). These values are now considerably higher across the Antarctic (Lakkala *et al*., 2020). Therefore some autotrophs across the polar regions, particularly those found in microbial mats on surfaces, in glacier algae blooms, and in ice free lakes and cryoconite holes have developed protective

pigments (Post and Larkum, 1993; Remias, 2012; Yallop *et al*., 2012; Bagshaw *et al*., 2016b; Perkins *et al*., 2017; Marizcurrena *et al*., 2019; Williamson *et al*., 2020). However, ice lids and sediment shading reduce the visible and UV light reaching the cryoconite-associated microbiota (Cook *et al*., 2010; Telling *et al*., 2012, 2014; Hodson *et al*., 2013; Bagshaw *et al*., 2016b). Indeed the Canada Glacier cryoconite holes featured both ice lids and thick sediment layers. Organisms including Tychonema, the genus contributing to the highest Cyanobacterial abundance in the Canada glacier, have also been recovered from lakes covered by ~3m of ice resulting in lower light conditions (Runcie and Riddle, 2006; Greco *et al*., 2020). In some cases these organisms are not only tolerant of the light condition they are in but are highly adapted to them, and are inhibited by changes in light (Bagshaw *et al*., 2016b; Perkins *et al*., 2017). Therefore it was uncertain whether organisms used to long periods of particularly high or low light (more likely in Canada glacier cryoconite) would be resilient to a Snowball Earth type light cycle.

The growth season in the modern polar regions can last from a couple of weeks to a few months depending on distance from the ablation terminus and snow coverage (Takeuchi *et al*., 2000; Fountain *et al*., 2004). However this would not be the case in the majority of regions on of Snowball Earth, especially in the tropics where life is likely to have accumulated in the warmer regions (Abbot *et al*., 2013; Hoffman, 2016). These equatorial, tropical and subtropical regions had a light/dark cycle throughout the year, with less dramatic differences between summer and winter. Hoffman and Schrag predict temperature oscillations on a diurnal scale on Snowball Earth would be amplified (Hoffman and Schrag, 2002). By comparing cryoconite incubated under full time light compared to cryoconite incubated under a day night cycle (12 hour of light followed by 12 hours of darkness) it was possible to discern whether low latitude -type light conditions disrupt the community growth of cryoconite communities.

Results demonstrate that cryoconite communities are resilient to this change in light, since the relative organic carbon production trend remains unchanged between the light and day-night conditions (Figure 23). This result was found both when organic carbon production was measured by oxygen content, and when it

was measured by ^{3}H-leucine incorporation: an initial increase over the first 7 days (under saturated at ~70% air saturation to saturated at ~80-100% air saturation), followed by a decline to initial values (~50-70% air saturation) in days 7-15, and then finally steep increase (to supersaturation ~120-140%). Surprisingly, the values of rate of carbon accumulation vary significantly between the oxygen method and ^{3}H-leucine method. It is difficult to ascertain why this may be and which method produces the more accurate value (e.g. the comparison between ^{14}C and the dissolved oxygen method carried out by Telling *et al*. 2010). There are several differences in these methods that could lead to this differences in results. The ^{3}H-leucine method yields the best results when used for communities where mass of protein per cell and cell mass is constant and known (Kirchman, 2001). Protein content tends to be ~60% of bacterial biomass (Simon and Azam, 1989) but the cryoconite communities may contain a range of eukaryotic and bacterial active organisms with differing fractions of protein. This weakens the estimation of biomass accumulation calculated from ^{3}H-leucine incorporation. Experimental steps that could introduce error into the value are the calibration steps in the oxygen sensor and scintillation analyser. In addition, the 'blank' water only vessels should produce the same values for % air saturation throughout the experiment. The increase observed between days 2 and 27 indicates that despite the rubber seal on the serum vials, some oxygen is entering during or following the needle piercing the seal. While the blank values are subtracted from the oxygen test measurements to control for this effect, this rests on the assumption that all vials have the same amount of air ingress which may not be the case. A more completely sealed system would yield more reliable results. However, although there is some difference between the calculated quantities of carbon per gram of sediment between the methods, there is consensus between the trends of increase and decrease and the rate of carbon production/consumption between the two methods. Therefore while this cannot be relied upon as a quantitative measurement of carbon quantity, it is however clear that the light condition and day-night condition results are distinct from those found produced under dark conditions, which accumulated less carbon per gram of sediment. Photoautotrophy was completely inhibited in the dark bottles, hence there was minimal carbon production via this route. These

results show that a cryoconite hole's community growth during a polar growth season is analogous to cryoconite communities growing under a day-night low latitude light cycle, despite the difference in light availability through the day.

The intact polar lipid composition of the samples supports the assertion that the cryoconite communities remain active under all conditions and are therefore resilient to the day-night cycles (Figure 24). The presence and diversity of IPLs indicates an active community of both bacteria and eukaryotes under all conditions. The composition does not vary significantly between day-night, dark and light condition end points. It also does not vary significantly between Day 0 and any of the end points. IPL composition reflects the active community (as IPLs degrade quickly after cell death). However, the measurement was semi quantitative and not sensitive to differences between dark and light conditions that were detected by oxygen and 3H measurements, so this method cannot be used to detect differences in activity between conditions but can indicate that the community relative abundance remained stable. Membrane lipids have been shown previously to respond to differences in light levels in microalgae (Widzgowski *et al*., 2020; Maltsev *et al*., 2021). If the incubation was continued for an extended period of time, we might expect to see the signatures of photoautotrophs such as G-DAGs lower in relative abundance as these groups experience falls in growth rate and increased inactivity relative to the heterotrophs in the community, and perhaps a response to the light levels themselves.

Previous studies have shown Antarctic organisms sourced from generally ice lidded cryoconite holes to be well adapted to low light and lack the ability of photoacclimation to high light (Bagshaw *et al*., 2016b). The McMurdo Dry Valley cryoconite organisms in this study were sourced from ice lidded cryoconite holes which may explain the similarity between net production during 24 hour light and 12 hour per day light conditions; it may be that these organisms are already adapted to low light of cryoconite holes and 12 hours light per day was sufficient to produce peak levels of photosynthesis at that temperature. Therefore in both the 24 hour light and day-night cycle conditions these organisms were at their maximum capacity for primary production in the incubation period given.

It is worth noting that the experimental incubation was carried out over 28 days; an entire year of these levels of growth may yield a different community structure to that of a modern cryoconite hole. For example, the year-long light may create more preferential conditions for photoautotrophs, leading to a dominance of algae and Cyanobacteria and net autotrophy in the system. Or heterotrophs that benefit from the energy created by the photoautotrophs may also proliferate. However, the warmest areas on Snowball Earth are likely to have been situated in what is today the upper tropics, subtropics and lower temperate zone, so would still experience seasonality (Abbot *et al*., 2013; Hoffman, 2016; Hoffman *et al*., 2017). Models compiled by Abbot *et al* predict summer subtropical (40° latitude) temperatures of ~0°C and winter subtropical temperatures of ~-50°C, at Marinoan CO_2 levels (10^5 ppm) (Abbot *et al*., 2013). These values are ~-20°C and ~-70°C at early Sturtian CO_2 levels (10^2 ppm). This indicates that while seasonality would not be as extreme in the tropical regions as at the polar regions, it may still create a yearly summer growth and winter dormancy cycle similar to the modern polar cryoconite (Fountain *et al*., 2008).

Both the modern McMurdo Dry Valleys and Snowball Earth cryoconite holes would be ice lidded due to the low temperatures and dry conditions, reducing light levels to the cryoconite particularly in winter when ice lids would be thickest. In the modern McMurdo Dry Valleys, regional cooling causes reductions in meltwater (e.g. streams) and thicker ice covering on lakes (Doran *et al*., 2002). Ice lids on cryoconite also thicken and melt on a daily and yearly cycle (Fountain *et al*., 2008; Sommers *et al*., 2019). In addition, Snowball Earth climate models with clouds have been successfully resolved, so ice surfaces may not have been exposed to direct light year-round (Abbot, 2014). Therefore Cryogenian cryoconite hole microorganisms would have been low light adapted, similar to the low light adapted modern McMurdo Dry Valley cryoconite organisms (Bagshaw *et al*., 2016b), but broadly tolerant to higher light to survive periods of melt as the Canada Glacier cryoconite organisms have been shown to be through Objective 2.1. It would be a beneficial avenue of future study to incubate cryoconite organisms under a day night cycle with light levels representative of those that reach the sediment in ice lidded

cryoconite holes. This would test the ability of cryoconite communities to survive over the coldest times and areas of the cryochrons (Abbot *et al*., 2013).

Cryoconite community response to freezing; low latitude freeze-thaw cycle

Previous studies have shown cryoconite organisms to be resilient to freezing (Porazinska *et al*., 2004; Stanish *et al*., 2013; Webster-Brown *et al*., 2015; Poniecka *et al*., 2020); cryoconite community activity has been measured following cryoconite holes becoming frozen (Bagshaw *et al*., 2011). However, repeated freezing and thawing can cause considerable stress to many organisms, including some of those found in cryoconite (Poniecka *et al*., 2020). During Snowball Earth it is possible that cryoconite would be subjected to nightly low temperatures. Without light radiation to be absorbed by and warm the dark cryoconite (Fountain *et al*., 2008), and surrounding ice (Liston *et al.*, 1999) temperatures could drop to those closer to the surrounding environment (summer subtropical temperatures of ~0°C and winter subtropical temperatures of ~-50°C, at Marinoan CO_2 levels (10^5 ppm), ~-20°C summer and ~-70°C winter at early Sturtian CO_2 levels (10^2 ppm) (Abbot *et al*., 2013; Carns *et al*., 2015)). The experimental results show that over 35 days of 12 hour freeze-thaw cycles, calculated carbon production follows a similar trend and range between freeze-thaw cycle conditions and the control polar growth season conditions (constant temperature 0.5°C) (Figure 23). The final values were remarkably similar (1.878 µg C/g sediment under freeze conditions, 1.694 µg C/g sediment under control conditions). This suggests that the cryoconite organisms in the sediment are resilient to regular freezing. This is perhaps unsurprising since many cryoconite organisms in the Antarctic survive freeze-thaw cycles at the beginning of the growth season (Fountain *et al*., 2004, 2008; Bagshaw *et al*., 2011). There have been several studies into microbial cold tolerance in cryoconite and other cold climate habitats that may explain this resilience. Antifreeze proteins that prevent the growth of ice crystals and therefore protect microbial membranes have been found in the bacteria of cryoconite holes (Singh *et al*., 2014a). Specialised enzymes that are active under cold temperatures are produced by bacteria and fungi to aid with organic macromolecule degradation at low temperatures (Singh and Singh, 2012; Singh *et al*., 2014b). Nucleic acid-binding

cold shock proteins have also been found, which improve transcription and translation at cold temperatures among other cellular processes (Singh *et al*., 2015; Chrismas *et al*., 2016; Maggiori *et al*., 2021; Murakami *et al*., 2022). While equivalent cold shock proteins are not part of the cold protection found in the cryoconite algae such as Chlamydomonas, a different group known as heat shock proteins seem to perform an equivalent role (Maikova *et al*., 2016). Unsaturated and branching fatty acids in membranes of bacteria, archaea and eukaryotes allow membrane flexibility at low temperatures and temperature sensing to activate other cold protection mechanisms (Shivaji *et al*., 2007; Valledor *et al*., 2013; Singh *et al*., 2014b).

It is not possible to tell from these measurements if the community composition remained the same throughout the experiment, and it is has been shown that some cryoconite species are likely to be more sensitive than others to freeze stress (Poniecka *et al.*, 2020). However, as there is no observable difference between control and freeze-thaw communities, it seems unlikely the communities are significantly different. There is no evidence of a population or growth bottleneck resulting from cell death or reduced function during the 35 day incubation, which might be marked by a cease or dramatic drop in carbon accumulation. Furthermore, Poniecka *et al*. demonstrated that some McMurdo Dry Valley cryoconite hole isolates were able to survive 100 cycles of freezing (at 6 h at -18°C and 3 h at 0.9°C) whereas Arctic cryoconite communities became unviable (Poniecka *et al*., 2020). It is possible that the taxa that are more sensitive to freeze stress had already died or become inactive during sample storage at -20°C and so freeze tolerant groups have been artificially selected before this and similar studies. Also, as mentioned previously (see discussion Objective 2.1) it remains possible that an entire year or a longer season of these levels of growth may yield a different community structure to that of a modern cryoconite hole.

Overall the conclusions of Objective 2.1 are that the Snowball Earth conditions tested (24 hour light-dark cycle and 24 hour freeze-thaw cycle) result in similar community growth to modern Antarctic growth season conditions over the time monitored. This agrees with suggestions that cryoconite organisms would be able

to survive expected Snowball Earth conditions (Hoffman, 2016). Both of these experiments took place in closed vials and as such the only source of organic matter and key minerals and ions was the cryoconite sediment. This shows the microbial communities can survive over this time frame with no nutrient input. This is unsurprising as cryoconite in the McMurdo Dry Valleys is known to be entombed and disconnected from other cryoconite holes for potentially up to 20 years (Bagshaw *et al*., 2007; Telling *et al*., 2014). This is presumably similar to a Cryogenian scenario, particularly in colder "hard" Snowball Earth conditions, where most cryoconite would likely be covered by ice and entombed for much of the year. However, it is difficult to say whether over several hundred million years there would be enough periodic genetic and nutrient input to sustain the network of communities. A sustainable network of cryoconite holes across the tropics, as described by Hoffman *et al*. (2016), would likely require connection between terrestrial sources of microbes and sediment, the cryoconite zones and larger bodies of water such as cryolakes. This should be considered when modelling Snowball Earth scenarios. Degassing was also highly limited in these enclosed serum vials with only a few cm^3 of air space. When the cryoconite is separated from the atmosphere, it is capable of sustaining oxygenated conditions for some time. Again, field studied show this is true over longer periods of time than the experiments carried out here, although over time it may result in extremes of pH and anoxic zones in the sediment. In a low oxygen atmosphere such as that of the Cryogenian, ice covered and entombed cryoconite holes may have been a preferable environment for aerobic microbes. However, whether this would have been sustainable over millennia is unclear.

Objective 2.2: Form cryoconite holes on ice in laboratory conditions, for closer replication of Snowball Earth conditions

Creation of cryoconite holes on ice under laboratory conditions

The results of objective 2.1 have indicated how cryoconite incubated in serum vials responds to Cryogenian type conditions. However, there are no data published to

date on the activity of cryoconite holes formed on ice under laboratory conditions, and whether activity measured in other vessels incubated under the same conditions differs. I was able to create model cryoconite holes that develop in the same manner as cryoconite holes on glacier surfaces and compare productivity measurements against cryoconite incubated in serum vials. As described from field studies of McMurdo Dry Valley cryoconite holes (Fountain *et al*., 2004; Zamora, 2018), the cryoconite holes developed in the following ways. Cryoconite was observed to melt the ice surface laterally to form a circular imprint in the underlying ice and then sink vertically into the ice surface. As is typical of cryoconite formed under cold Antarctic conditions, the shape was generally round and the sediment remained as a thick layer in contrast to the irregular shaped and "one granule thick" Arctic cryoconite holes (Cook *et al*., 2010). The irregularity of particles and the ice surface prevented the cryoconite holes from forming in a completely cylindrical form. An ice lid formed once the sediment was at a depth to allow the water column above to cool (Fountain *et al*., 2004; MacDonell and Fitzsimons, 2008; Zamora, 2018). The melting began quickly, and then slowed as the holes approached an equilibrium state (Fountain *et al*., 2008). Freezing of the cryoconite hole took place from the ice lid downwards and the sides of the cryoconite hole inwards (Fountain *et al*., 2004; MacDonell and Fitzsimons, 2008; Zamora, 2018). If melting occurs in an ice lidded hole, it melts from within in proximity to the sediment (Fountain *et al*., 2008).

Since the laboratory-formed cryoconite holes melted and froze in a similar topology to those observed on glaciers, they provided a varying amount of water and sediment distribution through the incubation. This may be a significant factor to create an accurate representation of cryoconite holes, as cryoconite hole morphology has been shown to impact biogeochemistry (Fountain *et al*., 2008; Cook *et al*., 2010, 2015a). Thicker sediment layers increase sediment shading and so reduces system autotrophy (Cook *et al*., 2010). Changes in meltwater quantity are also significant. The chemicals in initial meltwater will be highly concentrated and will then become more dilute as the hole deepens (Telling *et al*., 2014). The early conditions may facilitate initial autotrophy by providing nutrients required for

photosynthesis (Fountain *et al*., 2008). The surface texture and temperature of the ice was also representative of a cryoconite hole. Not only has surface texture been shown to influence microorganisms' initial adherence, surface sensing and biofilm formation (Ammar *et al*., 2015; Zheng *et al*., 2021), ice roughness contributes to surface energy balance which in turn impacts hole morphology, and therefore cryoconite biogeochemistry (Cook *et al*., 2010). It is interesting that the Arctic cryoconite forms cryoconite holes of the same structure (approximate depth, width and ice lid thickness) as those formed by Antarctic cryoconite, despite the fact the source cryoconite holes were quite different (Table 5). This may suggest that the conditions of the ice and temperature are more significant contributors to cryoconite hole structure than cryoconite composition.

The day-night and freeze-thaw condition experiments described in Objective 2.1 above were tested in sealed glass serum vials. These contained a 1cm layer of cryoconite, 45g of water and an air space to allow gas exchange, within the gas-tight sealed vial. Although this is an established method that has been used previously in conjunction with field incubations (Telling *et al*., 2010; Bagshaw *et al*., 2011; Poniecka *et al*., 2018), it has not been possible to discern causes of variation between field and laboratory cryoconite activity. The surface morphology, water content and temperature variation differ between a natural ice cryoconite hole and a glass vessel. Through replicating the control conditions for these experiments with cryoconite on ice, I was able to attain a closer representation of an in situ cryoconite hole (Figure 27).

Comparison of on-ice and glass vial cryoconite incubations

The laboratory grown ice cryoconite holes were highly sensitive to temperature. Those positioned 10cm closer to the door of the climate-controlled incubation chamber were slightly (<0.5°C) warmer and therefore melted faster. After 15 days most cryoconite hole replicates had a thick ice lid. However, several had also melted through to the bottom of the ice container and were no longer suspended by the ice. This meant comparison to the serum vial results over the entire incubation periods (28 days – 35 days) was not possible. Exploration of longer time

periods would require a larger incubation chamber capable of holding sufficiently deep ice for the cryoconite hole to reach an equilibrium state, where melting downwards vertically could cease (Gribbon, 1979; Wharton *et al*., 1985; Fountain *et al*., 2004).

Over the 14 day period in which it was possible to compare the ice cryoconite holes to the cryoconite incubated in serum vials, there was a strong similarity between the oxygen concentrations measured from ice cryoconite hole and serum vial oxygen levels (Figure 27). All oxygen concentrations fall within the range of values measured from cryoconite in serum vials. The trend is also similar, an increase of % air saturation on average over the first 7 days followed by a decrease in % air saturation, indicative of the first phase of cryoconite incubations, perhaps in which the organisms organise within the sediment and become active. The experiment therefore demonstrates that the glass serum vial habitat is not changing community activity in any way that is measurable by oxygen sensing. The cryoconite oxygen consumption and production was unchanged between an ice cryoconite hole and a sealed glass container. In conclusion, the use of closed glass incubation vials does not appear to alter cryoconite community activity from that which takes place in an ice cryoconite hole.

Altering one environmental parameter at a time allowed the possibility to pinpoint the cause of any changes in community activity between conditions. However, in actuality environmental stresses tend to have compound effects. For example, it is theoretically possible that autotrophs under low or high light stress conditions may have less resilience to freezing (Huner *et al*., 1998). During Snowball Earth not only would temperature and light be different, but the gas in the atmosphere. Oxygen levels may have been very low (Des Marais *et al*., 1992; Hoffman and Schrag, 2002). However, as has been demonstrated through these closed vial experiments, and has been demonstrated in field experiments (Tranter *et al*., 2004; Bagshaw *et al*., 2007; Telling *et al*., 2014), cryoconite can be self-sustaining for some time in entombed conditions largely or entirely independent of the atmosphere. The nutrients in the sediment may have been different to the those recovered from the McMurdo Dry Valleys in the modern day, for example they may have contained

more volcanic tephra (Hoffman, 2016). A cryoconite community could be "constructed" from target minerals and organisms, and tested under Cryogenian type atmospheric conditions in an incubation with gas content control. However, to artificially create a functioning and representative community would be a complex task in which community growth or limitation could be impacted by several local environmental factors at once. Therefore there is merit in continuing to test the impact of individual variables on an established cryoconite community first.

Conclusion

Antarctic cryoconite was resilient to two Snowball Earth low latitude conditions, daily day-night cycles and daily freeze-thaw cycles. Under both conditions the cryoconite communities were able reach growth phase, comparable to that of "control" conditions of constant light and temperature. Both the oxygen saturation method and the ^{3}H-leucine incorporation methods were able to produce this trend. However, as rate of carbon production values differed between these methods these can only be treated as estimates. Using laboratory-formed cryoconite holes on blocks of ice it was possible to repeat and verify the oxygen measurements for control conditions in a mesocosm that more closely resembled an *in situ* cryoconite hole. This also revealed the similarity in structure and development of *in situ* Antarctic cryoconite holes and laboratory cryoconite holes, and illustrated the potential of *ex situ* laboratory cryoconite holes for growth experiments.

Results Chapter 3: Signy Island as a model analogue for a Cryogenian meltwater habitat network

Summary

Signy Island, located in maritime Antarctica, contains a range of interconnected supraglacial and periglacial habitats over a small area. This presents a promising model area for investigating how ecosystems change during times of freeze and melt. The community composition of cryoconite, supraglacial streams, ice margins, meltwater ponds, moraine streams and seal wallows was investigated using 16S rRNA gene sequencing and intact polar lipid (IPL) profiling. 16S rRNA gene composition varied with distance from the island's ice cap, and the supraglacial habitats were most similar. The IPL profile highlighted stark differences between the moraine habitats, the moraine stream containing an active mat of Cyanobacteria and the meltwater pond supporting diverse heterotrophic assemblages. Under *ex situ* incubation conditions (also used in RC2) the majority of sediments were unable to initiate a growth phase. While certain microorganisms must have survived through a wide range of conditions and in a number of habitat formations to persist through the Cryogenian, not all cold climate communities are resilient to the stress of Snowball Earth temperatures and isolation in the ice. Highly local habitat differences impacted community composition. It is possible that therefore community composition determines resilience to habitat change.

Introduction

Hypothesis 3: Supraglacial and periglacial habitats contain distinct but interconnected ecosystems analogous to Snowball Earth meltwater habitats

While Cryoconite holes may have provided "biodiversity hotspots" on Snowball Earth, they cannot have been the sole habitat on the surface of the land and ice. Cryoconite is seeded from other habitats that already contain living cells associated with inorganic matter. During times of melt, the cryoconite holes may become more connected to streams and meltwater channels. Eventually, when the cryoconite hole melts completely at the ablation zone, the cryoconite will enter the ice margin, periglacial streams, ponds, moraine and sea. All of these habitats are also capable of supporting life (Boetius *et al*., 2015). It has been predicted that on Snowball Earth, when much of the planet was glaciated, this may take the form of areas of interconnected 'cryoconite pan' ponds connected by ice margins and meltwater streams (Hoffman, 2016). Modern cryoconite is part of an interconnected network of dynamic habitats. In order for the organisms that resided in cryoconite holes to have survived through the Cryogenian, they must also have been able to survive in adjoining habitats. In a mid-cryochron 'hard' Snowball Earth scenario, the low temperatures would mean meltwater would be very limited. Cryoconite holes or local cryoconite networks would be isolated for many years. The dynamic interconnected systems may only appear in the height of summer. However, in a Waterbelt mid cryochron scenario, and during the transitions in and out of glaciations, networks of streams, ponds and cryoconite holes would be present for most or all of the year.

Previous studies have found that different cold climate habitats produce different ecology (Liu *et al*., 2011; Cameron *et al*., 2012b; Edwards *et al*., 2013c; Lutz *et al*., 2019). Therefore different organisms may have been selected for and against when cryoconite holes merged with other habitats at times and places of melt on Snowball Earth. By examining the ecosystems connected to cryoconite, we can predict how community structure in the Cryogenian changed between habitats locally and how global ecology might have changed during times of deglaciation.

Most comparisons between habitats so far only extended to two or three habitats compared in each study (Mueller *et al*., 2001; Mindl *et al*., 2007; Liu *et al*., 2011; Edwards *et al*., 2013c). Cryoconite is linked to numerous habitats on and near the ice by water and aeolian transport. This chapter focuses on seven distinct glacial and periglacial habitats across Signy Island, Antarctica.

Signy Island is approximately 3km across. It is roughly triangular with a maximum length (north to south) of 8km and a maximum width (east to west) of 5km. The total area is roughly 20km^2 (Holdgate and Smith, 1967). Lower areas of coast are populated by rocky penguin rookeries and beaches inhabited by fur seals and elephant seals. Higher cliffs are covered moss banks. The island has a single ice cap at the centre, which flows into glaciers on the south, west and east sides (Figure 29). Roughly 50% of the island is covered by ice and snow year round (Holdgate and Smith, 1967). During winter this proportion is considerably higher. Several habitats are located over this relatively small area: cryoconite, streams, ponds, lakes and ice margins are all present across each side of the ice cap, connected to one another by meltwater. Signy Island has been described as a model site for studying Antarctic biological and environmental change as the current climatic warming is causing glacial recession, creating new terrestrial surfaces on which biota may become established (Smith, 1990). While the McMurdo Dry Valleys are an analogous habitat to the cold and dry cryochron ice sheets, Signy Island bears a stronger resemblance to areas of 'Slushball' or 'Mudball' scenarios and/or melt during warmer periods at the end-cryochrons (Abbot and Pierrehumbert, 2010). Whereas the first areas to melt around nunataks would have been isolated by colder ice sheets, Signy Island is isolated by the sea. This means that long range transport of sediment is limited and sediment-microbe aggregates are largely seeded by local sources as they would have been on an ice covered Snowball Earth.

The cryoconite of Signy Island supports many microbial Eukarya, including several of the key eukaryotic crown groups known to have survived the Cryogenian: Cercozoa, Alveolata, Stramenopiles, Haptophyceae, Archaeplastida, Centrohelida, Choanomonada and Fungi (Cameron *et al*., 2012b). A few studies on freshwater habitats of Signy Island have been carried out, which revealed the lakes and

cryoconite holes to have a diversity of bacteria and eukarya but these were not resolved to the family or genus level (Laybourn-Parry *et al*., 1996; Pearce, 2005; Cameron *et al*., 2012b). Most microbial ecological surveys on Signy Island have focused on the bacteria of soil. Different locations contained different microbial communities (Chong *et al*., 2009). The strongest similarities were found within habitat "types" e.g. areas populated by animals. Soil disturbance, conductivity and pH were found to contribute significantly to differences in community composition (Chong *et al*., 2009, 2010). Alpha diversity also varied between site types; higher alpha diversity was found at undisturbed shore, the moss banks, and areas populated by vertebrate animals (Chong *et al*., 2010). However lower genetic distance within the population was found at these sites. Higher genetic distance was found in "pristine and barren" locations such as the inland Jane Col and Knob Lake (Chong *et al*., 2010). Research on the lakes of Signy Island revealed differences in nutrient input correlated with differences in community composition (Pearce, 2005; Pearce *et al*., 2005). No equivalent study has been carried out on the sediments carried on the glacier surfaces. This chapter explores whether glacier surface and periglacial habitats are also subject to small-scale localised variation.

Objective 3.1: Investigate geographical and ecological connections between interconnected glacial and near-glacial microbial ecosystems on Signy Island

Bacterial community composition across the habitats identified was assessed using 16S rRNA gene sequencing. In addition, the composition of intact polar lipids (IPLs) was examined through Quadrupole Time of Flight Mass Spectrometry (Q-ToF). This provided a representation of the active community and an additional metric with which to investigate differences between habitats (White *et al*., 1979; Harvey *et al*., 1986). Intact polar lipids are becoming valuable chemotaxonomic markers in environmental microbiology (Sturt *et al*., 2004; Wörmer *et al*., 2013; Ding *et al*., 2020). Membrane lipids are also at the interface between a cell and its environment. The composition and structure of membrane lipids has been shown to alter in response to temperature, pH, P and N availability (Chintalapati *et al*., 2004; Řezanka *et al*., 2016; Siliakus *et al*., 2017; Warren, 2020).

The secondary aim was to assess similarities and differences in physiological capabilities between supraglacial and periglacial environments. In addition to exploring how habitats change in times of melt, this chapter examines what may have happened to the planet's ecology during times of cooling, in the transition into global glaciation. It has been suggested that biodiversity on Snowball Earth survived in supraglacial meltwater oases including cryoconite holes and cryoconite pans. In Results Chapter 2, I established that cryoconite ecosystems are able to survive in meltwater isolated from external sources of nutrients for some time, and under Cryogenian levels of light and temperature. The cryoconite used was collected from established cryoconite holes, in which the community structure and cold adaptation within the community produces a well-adapted microbial ecosystem (Poniecka *et al*., 2020). Other types of sediments besides cryoconite holes also exhibit many of these qualities. This may mean that during glaciation, these sediments from several sources could also seed supraglacial oases for biodiversity, such as the network of streams and cryoconite ponds described as 'Cryoconite pans' (Hoffman, 2016). However their microbiota's ability to survive when the sediment is isolated from adjoining habitats has not yet been tested. As areas cooled, the number of streams would have frozen and meltwater would have been reduced to more isolated pockets where sediment raised albedo. As glaciations began, some habitats would have remained viable while others became hostile due to lack of nutrients, light, water and increased abiotic stress conditions. Here, using oxygen sensing, I have measured the responses of a range of sediments from various Signy Island habitats to determine which were resilient to cold and isolated conditions according to the following aim and objective:

Objective 3.2: Determine the community response of Signy Island sediments to isolated "oasis" incubation conditions

Signy Island sediments were incubated and measured under the same conditions as the modern McMurdo Valley summer conditions in Results Chapter 2, Objective 2.1 (page 121). This allowed comparison not only between Signy Island habitats but between the warmer and maritime Signy Island cryoconite holes and the McMurdo Dry Valleys cryoconite holes.

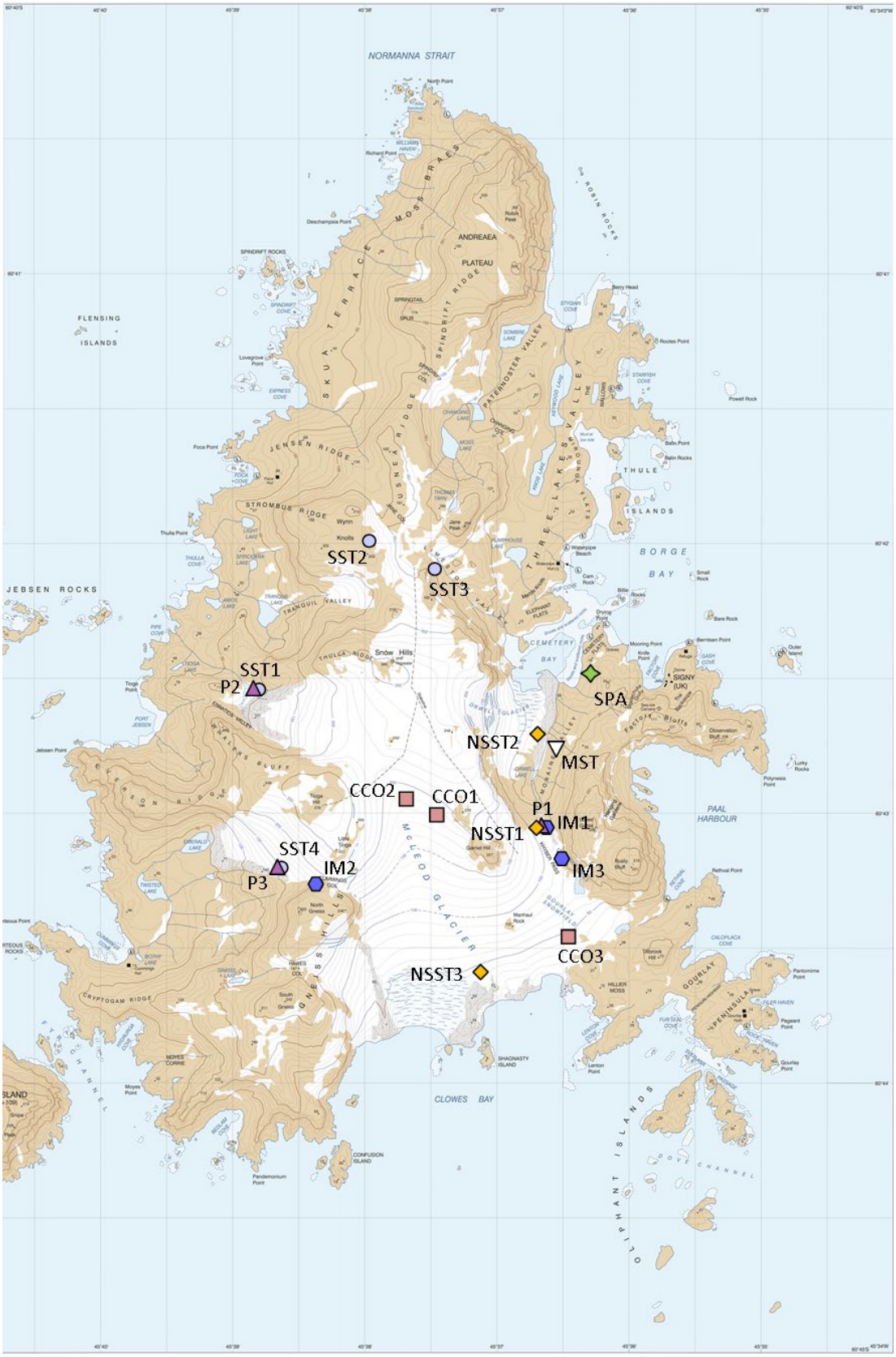

Figure 30 Map of sampling sites Signy Island. Sample types denoted by icon colour, shape and label. CCO: cryoconite holes. NSST: narrow supraglacial meltwater channel streams. SST: wider supraglacial streams. IM: ice margin. MST: moraine stream. SPA: seal populated area. Full descriptions of sites and samples can be found in table. Base map is the intellectual property of the British Antarctic Survey and is used herein under license.

Table 11 Signy Island sediment samples collected and used in subsequent experiments and analyses

Sample ID	Type	Location	Coordinates (°E, °N)	Size	Water pH	Water Temp. °C	Description
CCO1	Cryoconite hole	Snow Hills Nunatak	-45.6241, -60.7120	Width 80mm x 160mm Depth 70mm	4.88	0.4	Ice lidded cryoconite hole covered by snow. Contained liquid water and cryoconite sediment.
CCO2	Cryoconite hole	Snow Hills Nunatak	-45.6275, -60.7103	Width 60mm x 70mm Depth 140mm	6.88	1.7	Ice lidded cryoconite hole covered by snow. Contained liquid water and cryoconite sediment.
CCO3	Cryoconite hole	Gorlay Snowfield	-45.6101, -60.7239	Width 20-80mm Depth 40-60mm	4.37	1.2	Interconnected group of small open cryoconite holes.
NSST1	Narrow Supraglacial stream	Khyber Pass	-45.6096, -60.7191	Width 100mm x 200m Depth 30mm	7.24	0.8	One of several narrow parallel supraglacial meltwater channels spanning Khyber pass side of McLeod Glacier.
NSST2	Narrow Supraglacial stream	Orwell glacier	-45.6119, -60.7109	Width 40mm x 10m Depth 10mm	7.61	0.9	One of several very narrow supraglacial meltwater channels at various angles across 10m at the edge of Orwell glacier.
NSST3	Narrow Supraglacial stream	Gorlay Snowfield	-45.6206, -60.7266	Width 80mm x 10m Depth 20mm	5.45	0.1	Meltwater channel close (3m) from McLeod glacier edge on Gorlay Snowfield side. Running over ice and frozen sediment.
SST1	Supraglacial stream	Erratics Valley	-45.6450, -60.7105	Width 250mm x 20m Depth 100mm	5.78	0.1	Supraglacial stream running parallel to moraine ~2m onto glacier. Some portions covered by thin ice. Upstream little sediment but green and brown biofilms adhered to ice, downstream larger quantities of sediment (>10mm thickness).

Table 11 continued Signy Island sediment samples collected and used in subsequent experiments and analyses

SST2	Supraglacial stream	Jane Col	-45.6319, -60.6976	Width 200mm x 20m Depth 100mm	6.57	0.2	Slow flowing meltwater under thin ice (~2mm) and snow. Sediment distributed across bottom of the stream, some frozen to the underlying ice.
SST3	Supraglacial stream	Limestone Valley	-45.6260, -60.7002	Width 1.5m x 50m Depth 150mm	6.77	0.7	Water flowing under ice. Sediment, rocks and air bubbles under the ice covering.
SST4	Supraglacial stream	Cummings pass	-45.6433, -60.7210	Width 250mm x 8m Depth 300mm	6.43	0.1	Supraglacial stream 1-2m from glacier edge flowing parallel to moraine, terminating at pond. Covered by several centimeters of ice. Water column was cloudy with fine sediment, and thick sediment was found at the bottom of the stream.
IM1	Ice margin	Khyber Pass	-45.6117, -60.7172	3m x 20m area	-	-	Ice margin between McLeod Glacier and P1. Thin layer of sediment and possibly algae over this area of ice.
IM2	Ice margin	Cummings pass	-45.6397, -60.7216	8m x 1m area	-	-	Dark muddy sediment on ice margin 3-10m from moraine. Sediment was frozen into underlying ice.
IM3	Ice margin	Khyber Pass	-45.6095, -60.7191	200mm x 2.5m area	-	-	Ice margin between McLeod Glacier east side and streams at edge of the glacier. Sediment dark brown and fine, and less stony than the nearby moraine.
P1	Meltwater Pond	Khyber Pass	-45.6117, -60.7172	Width 10m x 40m	7.51	0.8	Sediment was taken at the edge of the pond, at a 50mm depth. Thin orange biofilm and fine sediment was present. A stream flowed out of the pond onto the moraine.

Table 11 continued Signy Island sediment samples collected and used in subsequent experiments and analyses

P2	Meltwater Pond/Lake	Erratics Valley	-45.6453, -60.7105	Width 20m x 40m	5.83	0.4	Sediment was taken at the edge of the pond, at a 50mm depth. SST1 flowed into this lake.
P3	Meltwater Pond/Lake	Cummings pass	-45.6434, -60.7210	Width 30m x 40m	6.52	0.4	Covered by several centimeters of ice; SST4 inflowing. Limited sediment available at lake edge, largely ice and rocks.
MST	Moraine stream	Moraine stream	-45.6100, -60.7117	Width 1m x 6m Depth 10mm	6.96	2.5	Sediment and thick, layered microbial mat in moraine stream. Middle of the mat was orange-red but patches of green biofilms cover the sediment at the stream edges.
SPA1&2	Unglaciated seal populated area	Cemetery Flats	-45.6028, -60.7065	Taken from 100mm square area of seal wallow	-	-	Seal wallow near end of moraine streams. Traces of animal (macrofauna) matter.

Results

Objective 3.1: Investigate geographical and ecological connections between interconnected glacial and near-glacial microbial ecosystems on Signy Island

Habitat structures, geography and connections

Figure 29 shows the location of all sampling sites, which are described in Table 11. At the furthest inland points of Signy Island, closed-lidded cryoconite holes could be found covered by snow and ice nearby to nunataks, which were the highest altitude points on the island (up to 288m above sea level). They contained liquid water and a thin (approximately 5mm) layer of cryoconite sediment. Nearby the ice lidded cryoconite holes were streams running underneath the surface layers of ice and snow. These streams were not, at the time of sampling, connected to the cryoconite holes. However, some carried sediment over the glacier. Figure 30 illustrates how the habitats were positioned in relation to one another, and potentially connected. Figure 31 shows photos of each sample used. The surface ice covering these streams and cryoconite holes was between 1-5cm in areas where the streams were visible. Downhill from the ice lidded cryoconite and under-ice streams, another distinct habitat was narrow meltwater channels carrying small amounts of sediment, observed beginning roughly two thirds of the way down the sides the ice cap. The exception was on Gorlay Snowfield following periods of rain, when meltwater channels were only observable close to the south terminal edge. At these times, north and uphill of this position there were several open lidded cryoconite holes 2-8cm in diameter (Figure 30). Snow algae were observable on many glacier surfaces, appearing no later than a day after each snowfall. However, these visible snow algae blooms were largely observed within 100m of terminal edges of the glaciers and snowbanks. The narrow meltwater channels ran into larger streams and ponds at the edges of the glaciers. The larger streams were usually positioned flowing over ice less than 10m from the moraine and ended at ponds or lakes (Figure 30). Rather than the dark scattered sediment of the narrow supraglacial meltwater streams, the larger streams had more variable aggregates. Some contained green biofilms, and the amount of sediment carried was highly

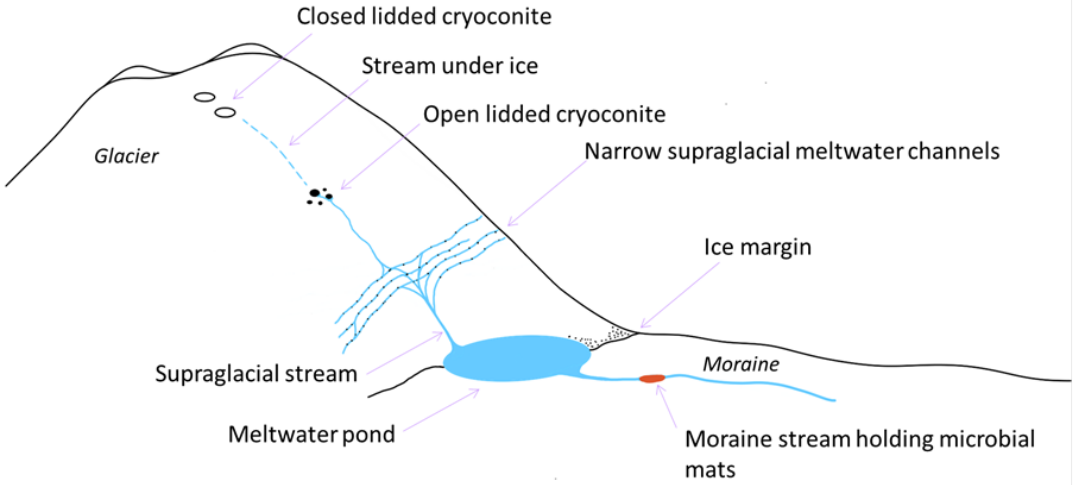

Figure 31 The interconnected habitats of Signy Island. This diagram illustrates the relational positions of the habitats included in the analyses. Water flows underneath the ice at the highest points of the island. Closer to the glacial edge, narrow meltwater channels run across the glaciers. These flow into larger supraglacial streams, which usually terminate in meltwater ponds. Streams frequently flow out of these ponds across the moraine.

variable (from 1mm to >10mm). At the ice edges, at the termini of glaciers and lateral sides, ice margins had higher accumulations of snow algae and deposited sediment from the streams than the ice sheet central region. The ponds were situated at the join of glacier edges and termini where the ice met the moraine. The bottom of these meltwater ponds were rocks, and sandy, sometimes silt-like sediment. Pond 1 contained thin orange biofilms approximately 10cm across. Some of these meltwater ponds had outgoing streams flowing down through the moraine. In one such stream, site MST, a thick orange microbial mat and thinner green biofilms were found. These streams often terminated at the sea. The unglaciated areas were populated with elephant seals, fur seals and birds including skewers, petrels and at the coast, penguins. Some seals were found on the glacier edge but most resided on or near the beach. Feathers and occasional bird droppings were found at the supraglacial and periglacial sites, mostly in the ice margin samples. Table 11 outlines the sample sites used.

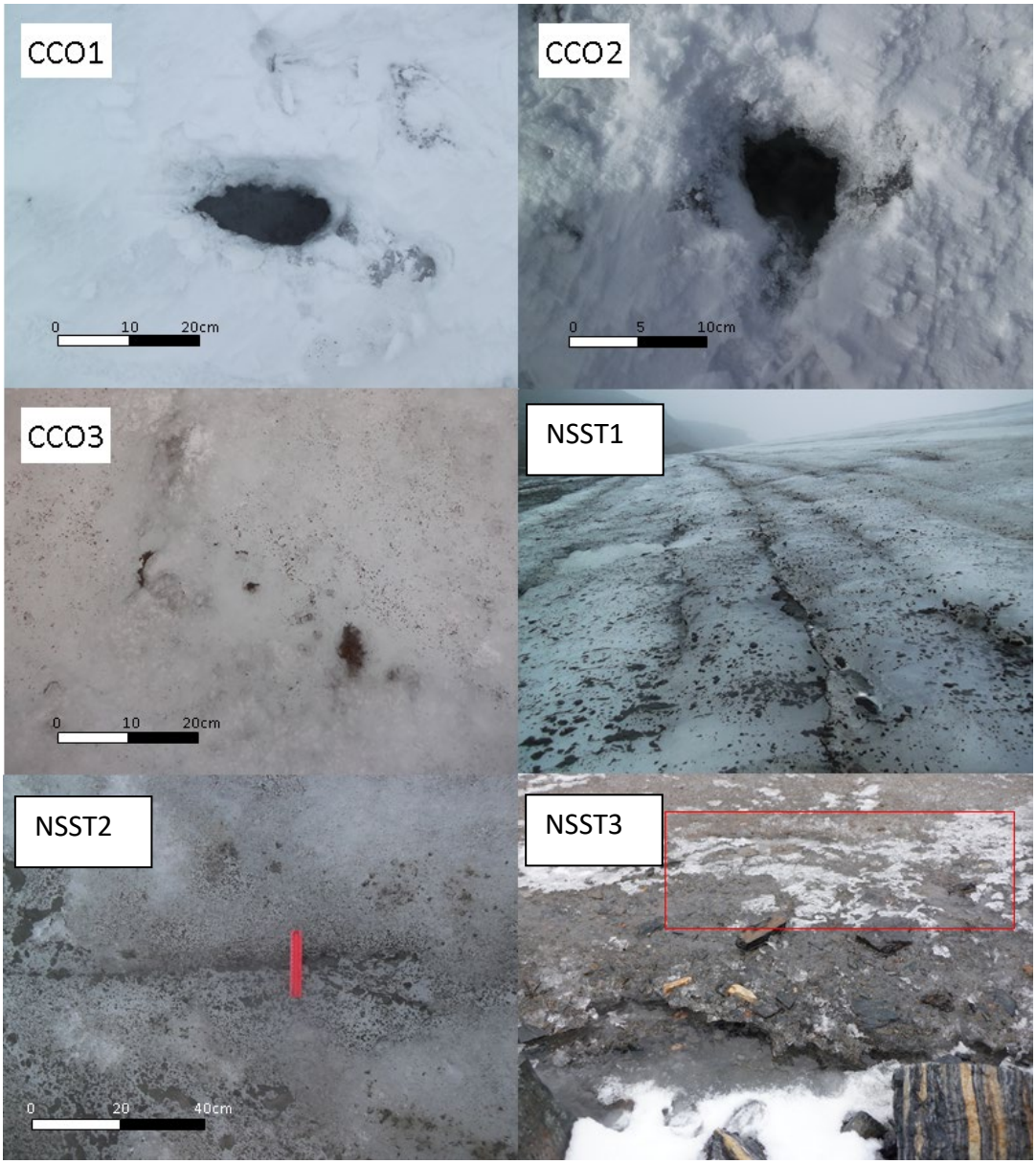

Figure 32 Photographs of Signy Island sample sites. CCO: cryoconite holes. NSST: narrow supraglacial meltwater channel streams. ST: wider supraglacial streams. IM: ice margin. MST: moraine stream. SPA: seal populated area. Full descriptions of sites and samples can be found in table 5.

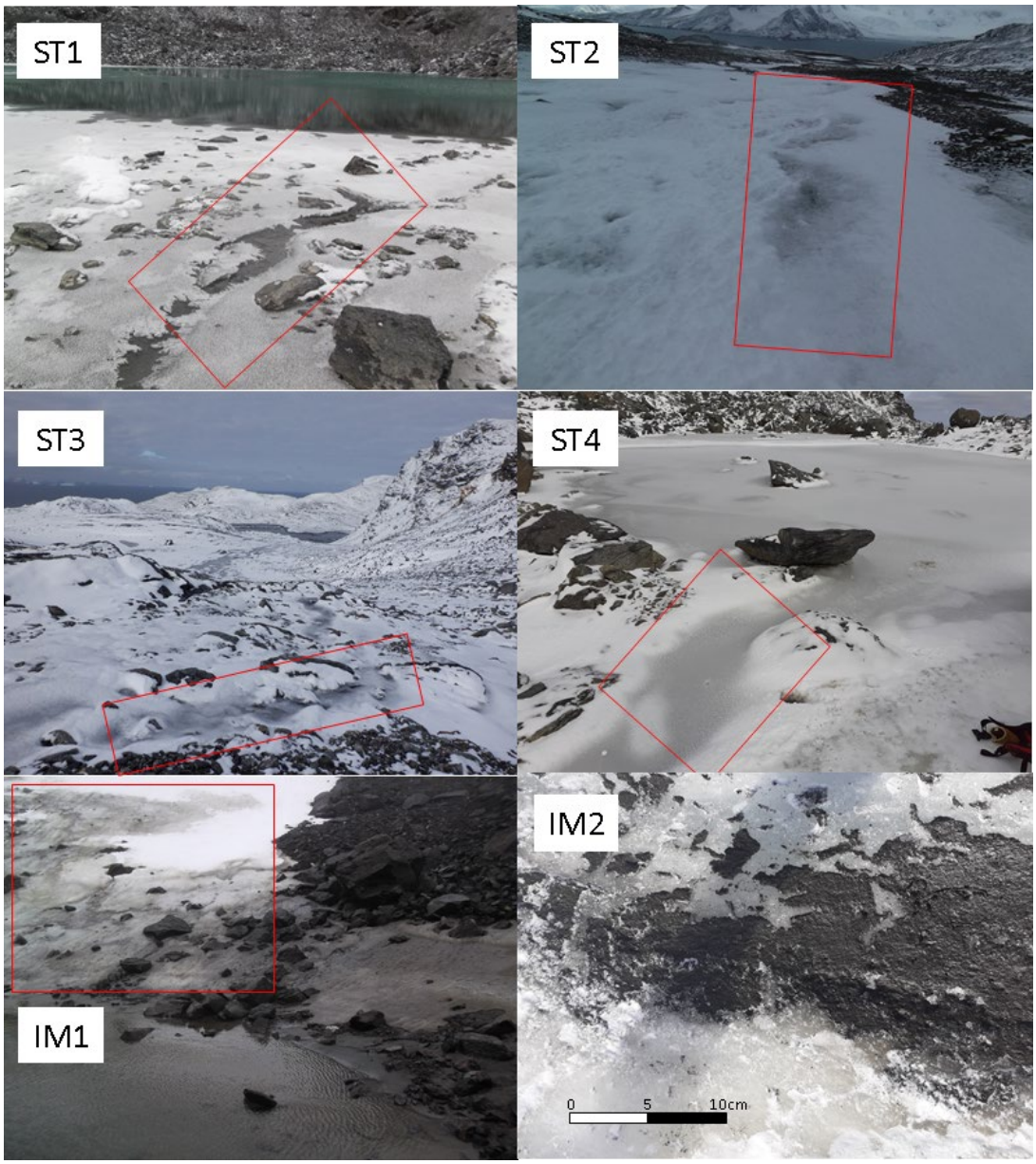

Figure 30 continued Photographs of Signy Island sample sites. CCO: cryoconite holes. NSST: narrow supraglacial meltwater channel streams. ST: wider supraglacial streams. IM: ice margin. MST: moraine stream. SPA: seal populated area. Full descriptions of sites and samples can be found in table 5.

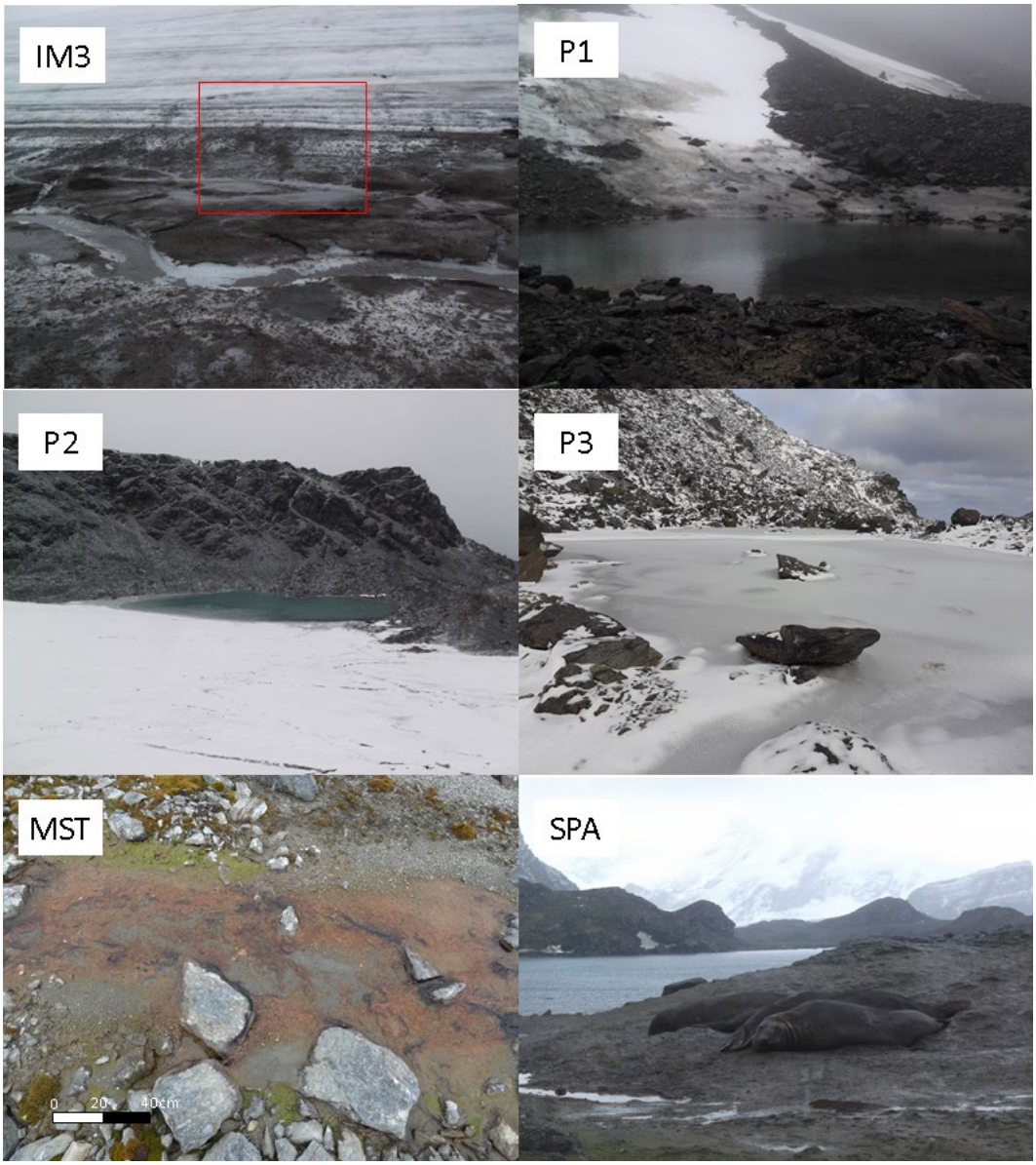

Figure 30 continued Photographs of Signy Island sample sites. CCO: cryoconite holes. NSST: narrow supraglacial meltwater channel streams. ST: wider supraglacial streams. IM: ice margin. MST: moraine stream. SPA: seal populated area. Full descriptions of sites and samples can be found in table 5.

Bacteria and Archaea community composition among supraglacial and periglacial habitats

Following Oxford Nanopore 16S rRNA gene sequencing, 30 bacterial phyla were identified across the Signy Island habitats (Figure 32). No archaea were detected. Unassigned sequences were removed prior to calculating bacterial relative abundance. An average of 0.53% of ASVs in each sample belonged to Chloroplast DNA (Figure 33). Chloroplast relative abundance was particularly high in the Khyber Pass narrow supraglacial stream (2.24% of ASVs from this site). Over the entire island Actinobacteria, Cyanobacteria, and Proteobacteria were the most abundant phyla accounting for 86% of assigned 16S rRNA gene ASVs. These phyla were present in all samples, as were Bacteroidetes, Chloroflexi, Deinococcus, Firmicutes, Gemmatimonadetes, Planctomycetes and WPS-2 group. All other phyla contributed <6%. Cyanobacteria alone accounted for 43% of the total assigned ASVs. The cryoconites, microbial mat, narrow supraglacial streams, and one larger stream were dominated by Cyanobacteria sequences. The ice margins contained a higher proportion of Proteobacteria and the remaining sites (ponds, streams and seal populated areas) contained high proportions of both Proteobacteria and Actinobacteria.

The variation between taxonomic diversity in different sample types was explored by analysis of beta diversity. Non-metric multi-dimensional scaling of Bray-Curtis dissimilarity between taxa abundances revealed that the cryoconite and narrow supraglacial stream sediments clustered closely together (Figure 34). The seal populated area samples were distinct from all other groups. The remaining habitat types were more widely dispersed in ordination. Although most sampling replicates (samples taken from the same site within 30cm) clustered closely, there is still heterogeneity in some samples such as the moraine stream microbial mat, stream 2 and narrow stream 1. An ANOSIM test of the dissimilarity between types using the Bray-Curtis method produced an R value of 0.6248 at p=0.0001 (pairwise community dissimilarity), suggesting a moderate level of dissimilarity between types. The mean number of distinct ASVs was lowest in the cryoconite and narrow

supraglacial stream samples, and highest in the seal populated area. This pattern was also found

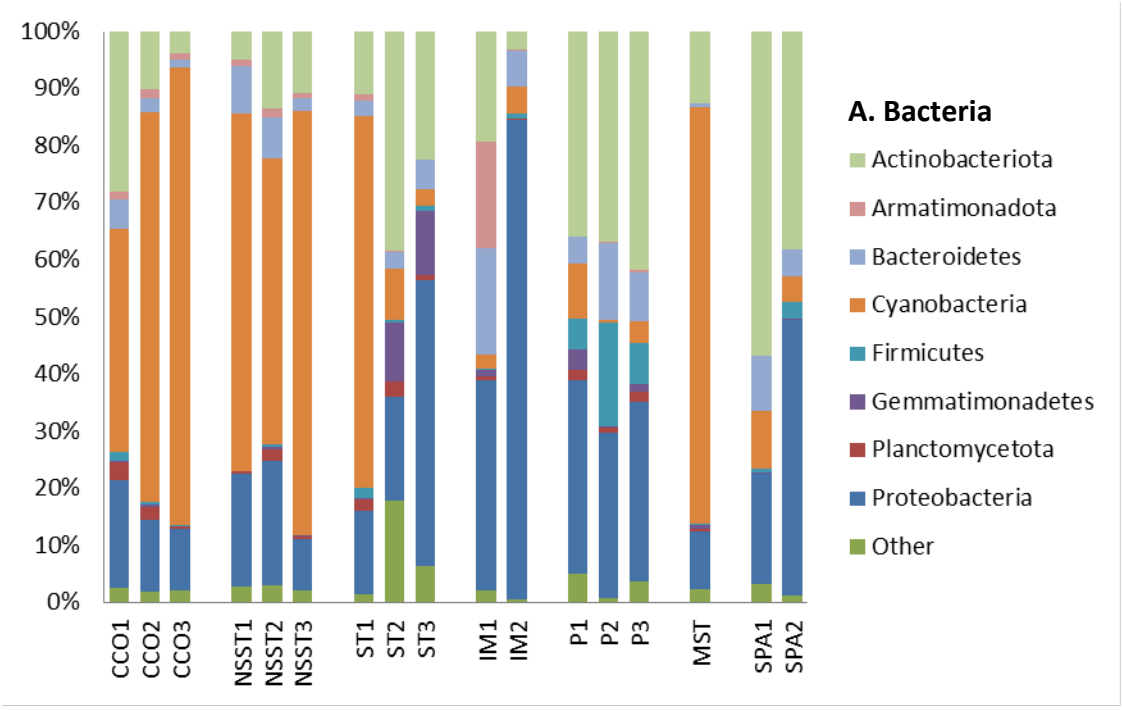

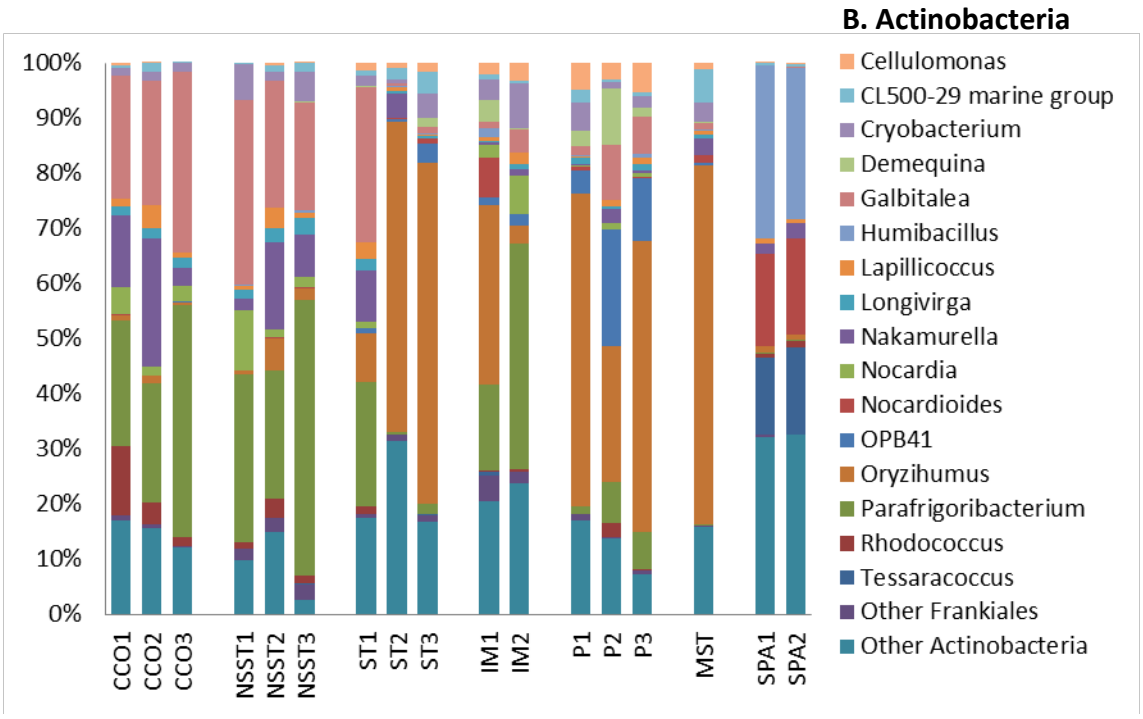

Figure 33 Relative abundance of bacteria (%) in Signy Island habitats. Samples are grouped by habitat type. **A** Bacterial phyla. Phyla contributing to <1% of the total abundance are grouped as "Other". **B-F** Relative abundance of genera within the top three most abundant phyla. Proteobacteria have been divided into Alpha-, Beta-, Delta- and Gammaproteobacteria. Genera contributing to <1% of the total abundance are grouped as "Other". Where a genus was unknown, lowest rank known is shown. Taxa were assigned according to the SILVA database.

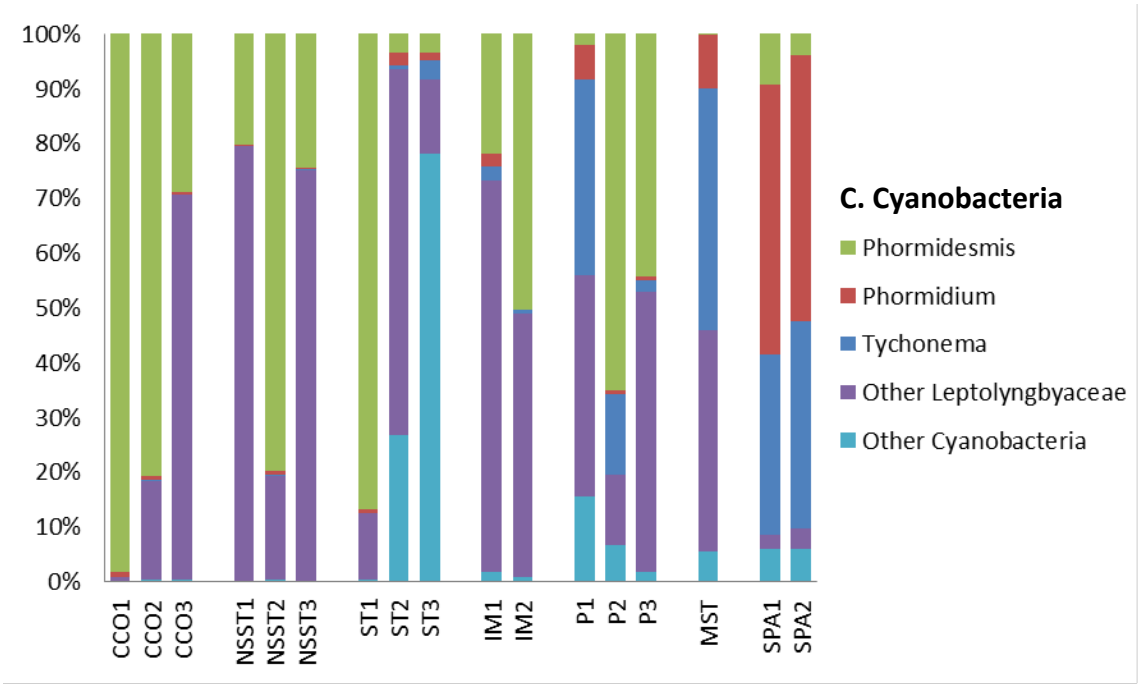

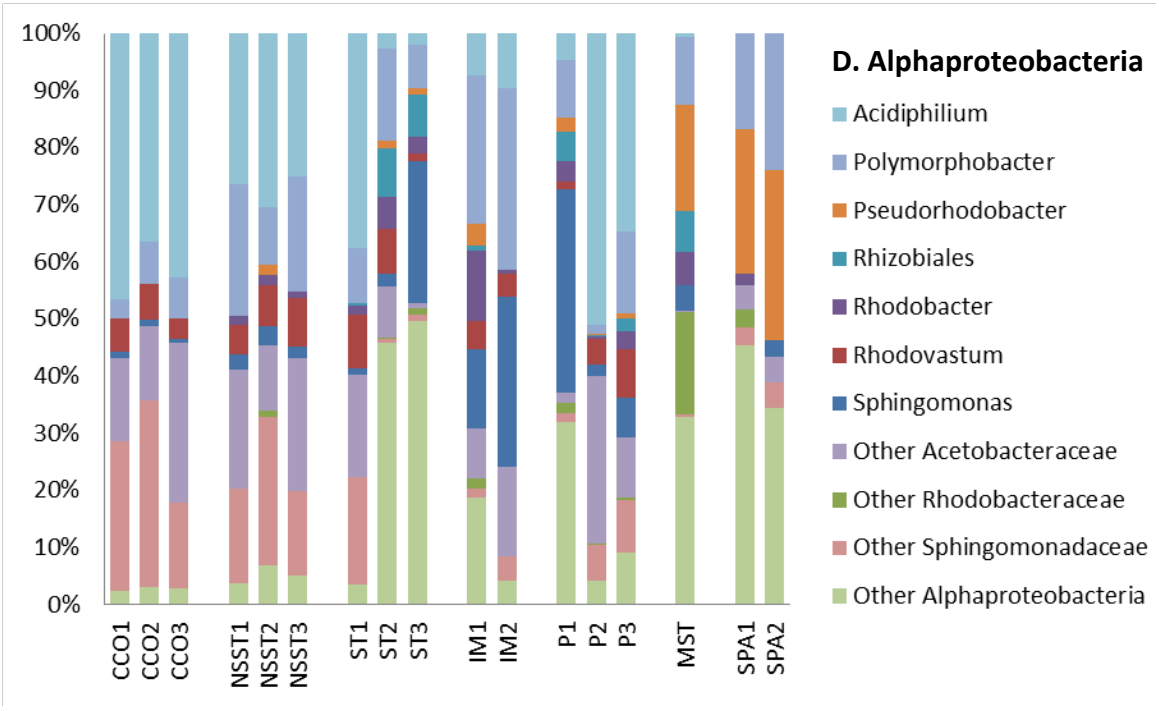

Figure 32 continued Relative abundance of bacteria (%) in Signy Island habitats. Samples are grouped by habitat type. **A** Bacterial phyla. Phyla contributing to <1% of the total abundance are grouped as "Other". **B-F** Relative abundance of genera within the top three most abundant phyla. Proteobacteria have been divided into Alpha-, Beta-, Delta- and Gammaproteobacteria. Genera contributing to <1% of the total abundance are grouped as "Other". Where a genus was unknown, lowest rank known is shown. Taxa were assigned according to the SILVA database.

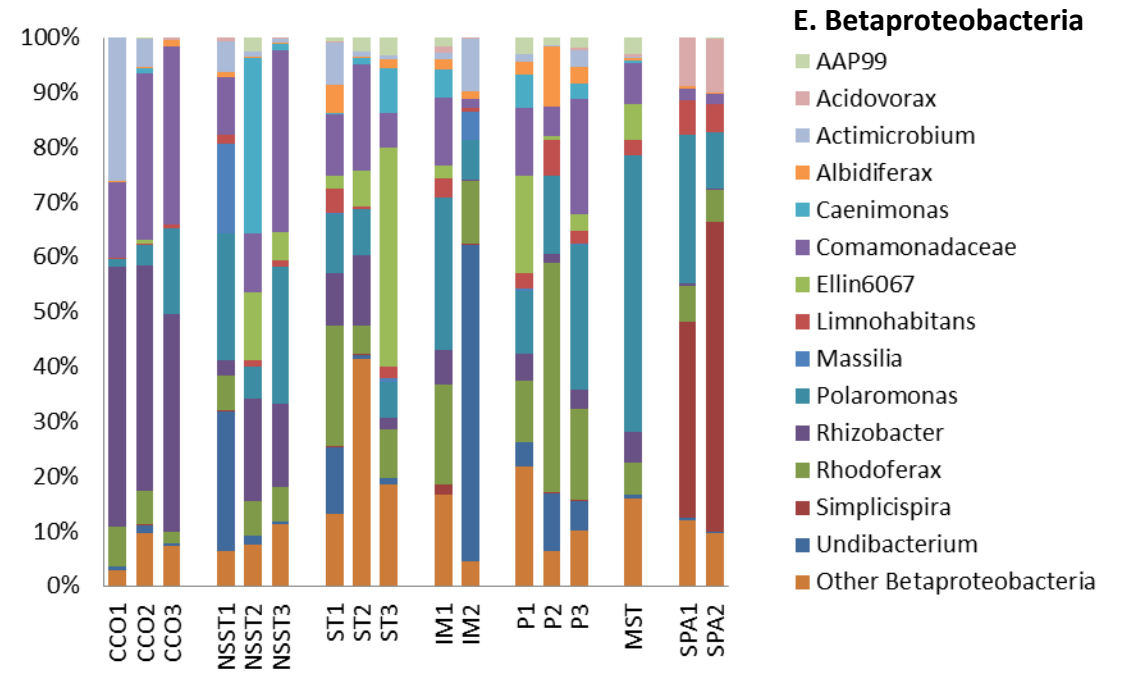

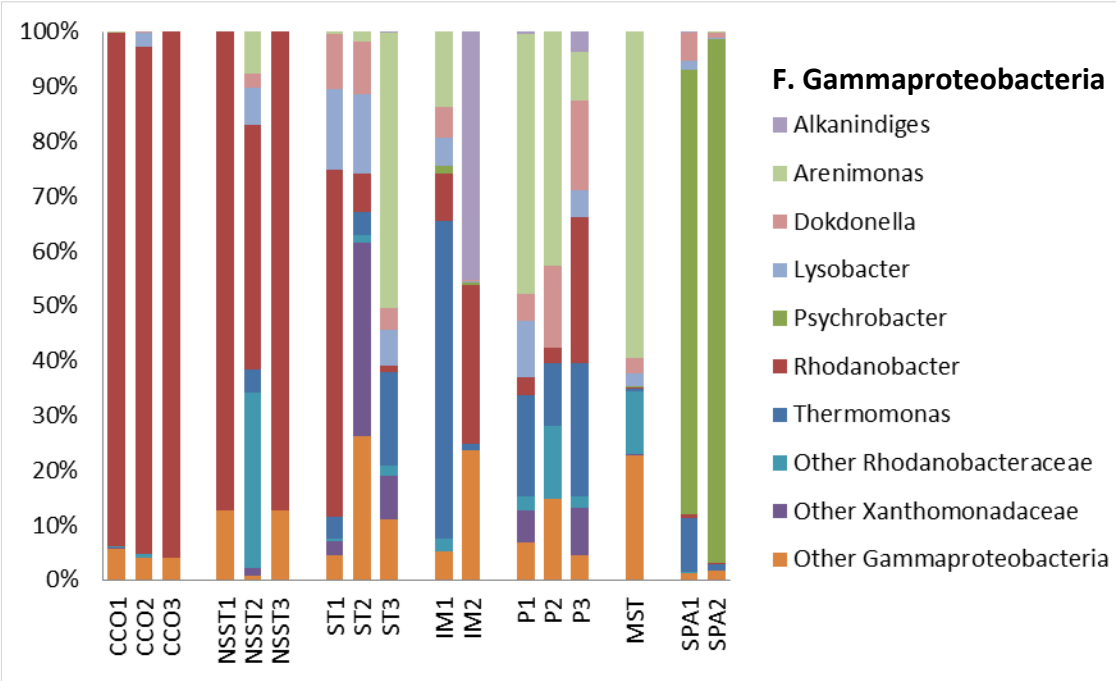

Figure 32 continued Relative abundance of bacteria (%) in Signy Island habitats. Samples are grouped by habitat type. **A** Bacterial phyla. Phyla contributing to <1% of the total abundance are grouped as "Other". **B-F** Relative abundance of genera within the top three most abundant phyla. Proteobacteria have been divided into Alpha-, Beta-, Delta- and Gammaproteobacteria. Genera contributing to <1% of the total abundance are grouped as "Other". Where a genus was unknown, lowest rank known is shown. Taxa were assigned according to the SILVA database.

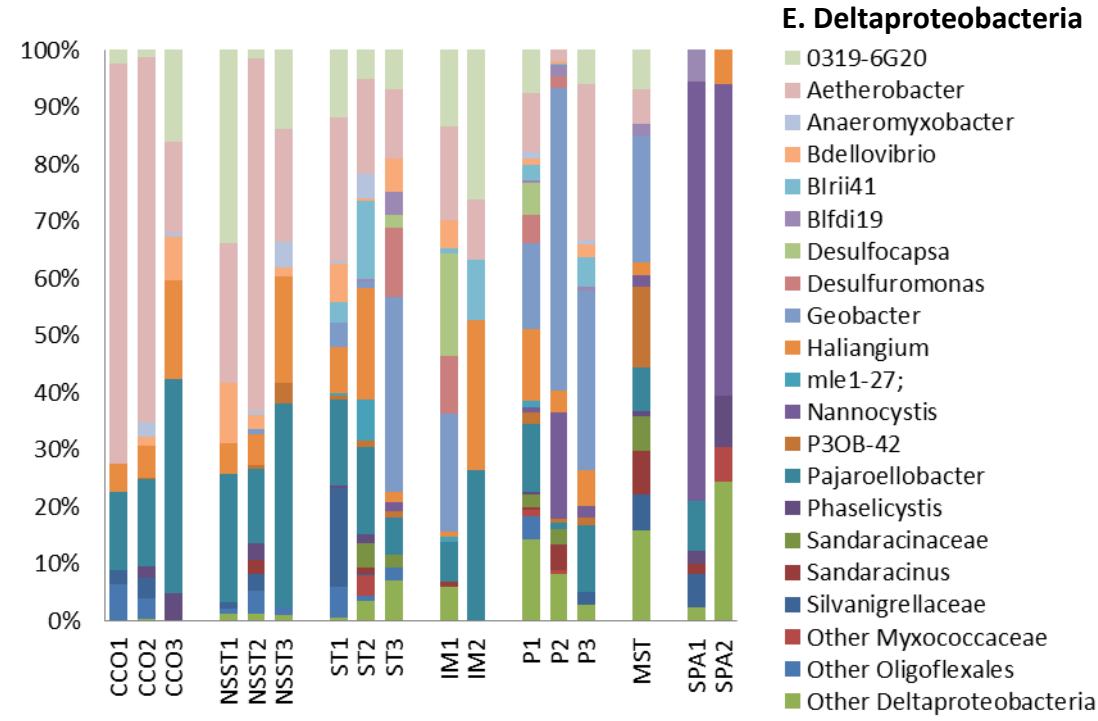

Figure 32 continued Relative abundance of bacteria (%) in Signy Island habitats. Samples are grouped by habitat type. **A** Bacterial phyla. Phyla contributing to <1% of the total abundance are grouped as "Other". **B-F** Relative abundance of genera within the top three most abundant phyla. Proteobacteria have been divided into Alpha-, Beta-, Delta- and Gammaproteobacteria. Genera contributing to <1% of the total abundance are grouped as "Other". Where a genus was unknown, lowest rank known is shown. Taxa were assigned according to the SILVA database.

when alpha diversity was measured according to Shannon and Simpson diversity indices (Figure 35).

The three most abundant bacterial phyla, Actinobacteria, Cyanobacteria and Proteobacteria were investigated further to elucidate the composition of their genera and contribution to similarity and dissimilarity between types (Figure 32). The most abundant Actinobacteria genera are *Oryzihumus* (21% of Actinobacterial ASVs), *Parafrigoribacterium* (10%), *Galbitalea* (9%) and *Humibacillus* (9%). However, 98% of the *Humibacillus* sequences were found in the seal populated area. The seal populated area was also unusual in its higher abundance of Nocardiodes and *Tessaracoccus* compared to other sample types (17% and 15% of seal populated area Actinobacteria ASVs respectively). The microbial mat, pond and stream samples contained high amounts of *Oryzihumus* (65% of microbial mat ASVs, 39% of pond Actinobacterial ASVs, 43% of stream Actinobacterial ASVs). The Erratics Stream however differed from the other stream sites in its comparatively

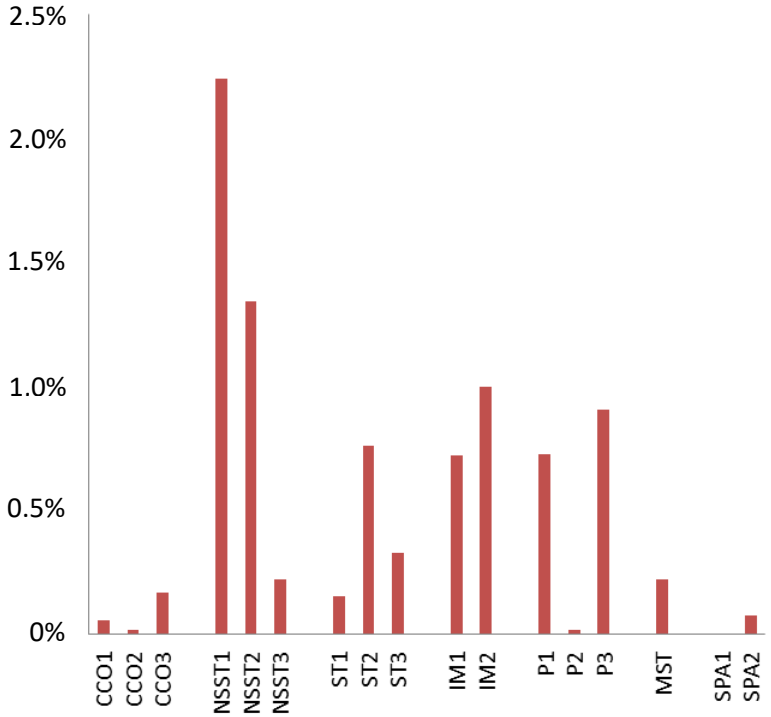

Figure 34 Relative abundance of 16S rRNA gene ASVs assigned to chloroplasts in Signy Island habitats. Bars are grouped by habitat type: CCO = cryoconite, NSST = narrow supraglacial stream, SST = supraglacial stream, IM = ice margin, P = pond, MST = moraine stream, SPA = seal wallow area.

high abundance of *Galbitalea* and *Parafrigoribacterium* and lower abundance of *Oryzihumus*. The pond samples also held a higher than average relative abundance of the Actinobacteria OPB41 group (15% of pond Actinobacterial sequences compared to an average of 3% among all sample types). Conversely, the cryoconite and narrow supraglacial streams had higher proportions of *Galbitale*a and *Parafrigoribacterium* (24% *Galbitalea* and 25% *Parafrigoribacterium* among the cryoconite Actinobacterial ASVs, 23% *Galbitalea* and 40% *Parafrigoribacterium* among the NSGS Actinobacterial ASVs). One ice margin site was also dominated by *Parafrigoribacterium* while the other contained a higher proportion of O*ryzihumus.*

Only four groups of Cyanobacteria contributed >1% to Cyanobacteria sequences. These were *Phormidesmis* (43%), *Phormidium* (3%), *Tychonema* (8%), and sequences assigned to Leptolyngbyaceae as their lowest rank (44%). All of these groups were present in some proportion in all samples. The seal populated area was unique in its high abundance of *Phormidium* (49% of SPA Cyanobacterial sequences). It also had higher than average proportion of *Tychonema* (34% of SPA Cyanobacterial sequences), as did the microbial mat (44% of microbial mat Cyanobacteria ASVs). There was considerable heterogeneity within samples of the remaining types. The Khyber pond and microbial mat shared a high proportion of *Tychonema* (36% and 44% of Cyanobacterial ASVs respectively) and the lowest proportions of *Phormidesmis* (2% and 0.3% of Cyanobacterial ASVs respectively). On average the Cryoconite had the highest proportion of *Phormidesmis* and lowest proportion of *Tychonema*.

The Alphaproteobacteria made up 34% of Proteobacteria ASVs, the Betaproteobacteria 45%, the Gammaproteobacteria 18% and Deltaproteobacteria 3%. In the cryoconite, which had a comparatively low relative abundance of Proteobacteria overall, the majority (78%) of Proteobacterial sequences belonged to the Alphaproteobacteria. The cryoconite Alphaproteobacteria was largely composed of *Acidiphilium*, Acetobacteraceae and Sphingomonadaceae. These three groups were the highest contributors to Alphaproteobactia on Signy Island overall (66% of Alphaproteobacteria ASVs across all types). However, *Acidiphilium* were absent in the seal populated area and the Acetobacteraceae and

Sphingomonadaceae were present in low abundance only (4% of each group in the seal populated area Alphaproteobacteria). The seal populated area had a higher relative abundance of *Pseudorhodobacter* than the other sample types. *Sphingomonas* was present at all sites but was particularly abundant in the ice margin sites, the Khyber pond and the Limestone Valley stream. Betaproteobacteria was the most abundant class of Proteobacteria accounting for 45% of Proteobacterial classes. The proportion of Betaproteobacteria was particularly high in the ice margin sites (71% of ice margin Proteobacterial sequences) and particularly low in the cryoconites (7% of cryoconite Proteobacterial sequences). The ice margin sites were different from one another. The Cummings ice margin contained a high proportion of *Undibacterium* (58%) while the Khyber ice margin contained <1% *Undibacterium* and the majority of Betaproteobacteria sequences belonged to Commandaceae, *Polaromonas* and *Rhodoferax*. The microbial mat was also high in *Polaromonas* (50% of Betaproteobacteria in the microbial mat). The cryoconite Betaproteobacteria was largely comprised of *Rhizobacter* and Commandaceae (43% and 23% of cryoconite Betaproteobacteria respectively). The seal populated area was unique in its high abundance of *Simplicispira* (49% of Betaproteobacteria identified in the seal populated area). There is considerable variation in Betaproteobacteria composition within pond, stream and narrow supraglacial stream types. 18% of Proteobacteria belonged to Gammaproteobacteria. The seal populated area had the highest proportion of Gammaproteobacteria in by a considerable margin, contributing 51% to its Proteobacterial abundance (compared to an average of 20% across all samples). 93% of Cryoconite Gammaproteobacteria belong to *Rhodanobacter*. All other genera contributed to <1% of cryoconite Gammaproteobacterial ASVs. *Rhodanobacter* were also the majority (66%) of narrow supraglacial stream Gammaproteobacterial ASVs. In contrast, the pond and microbial mat Gammaproteobacterial ASVs contained a relatively high proportion of *Arenimonas* (77% and 37% respectively) and the seal populated area samples a very high proportion of the psychrotolerant and osmotolerant *Psychrobacter* (92%). The stream and ice margin sites were each different from one another in Gammaproteobacteria composition. The remaining 3% of Proteobacteria belonged

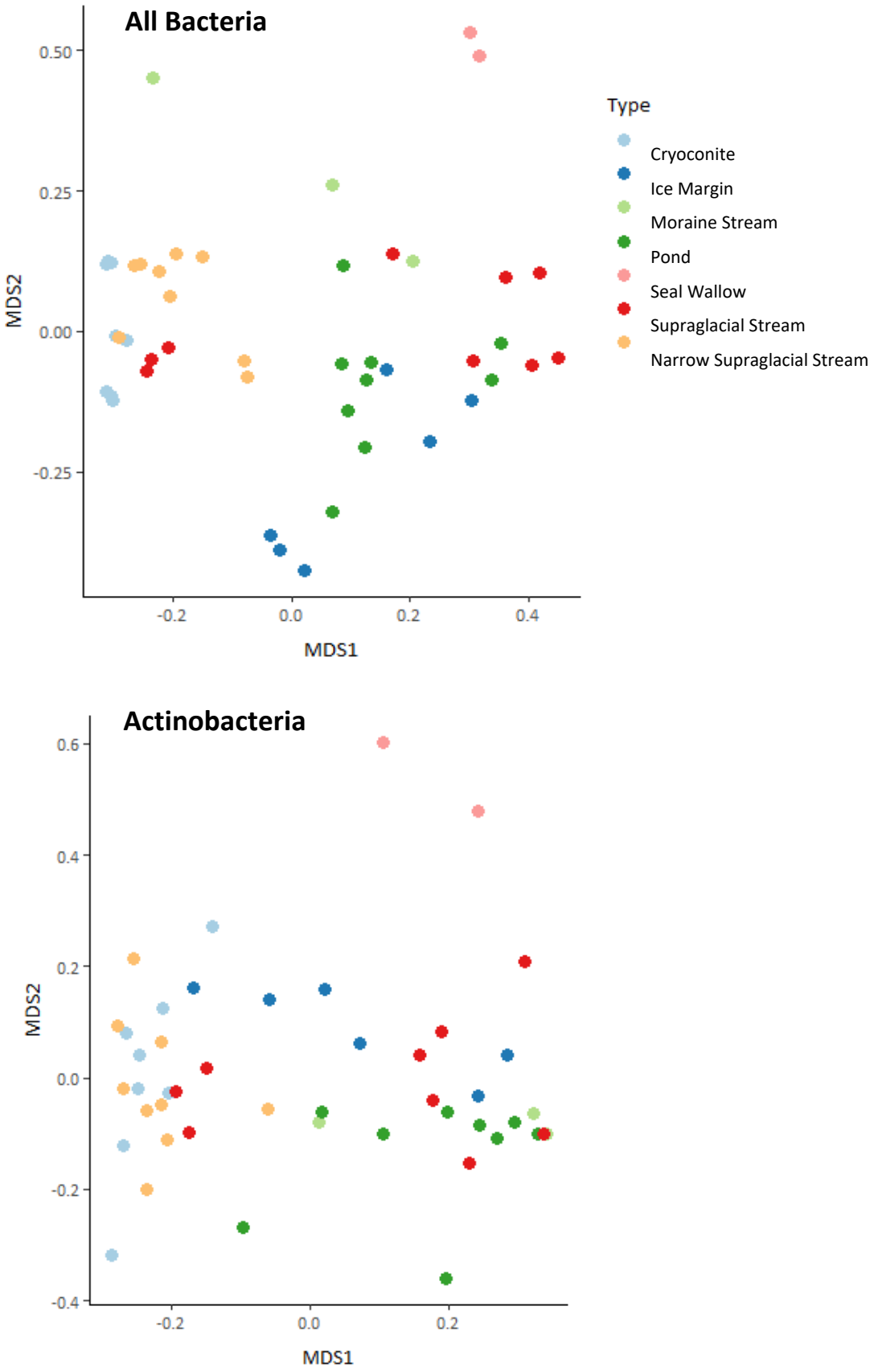

Figure 35 Bray-Curtis dissimilarity of 16S rRNA gene ASVs found in Signy Island habitats grouped by type and visualised by non-metric multidimensional scaling (NMDS) ordination. All sampling replicates are included.

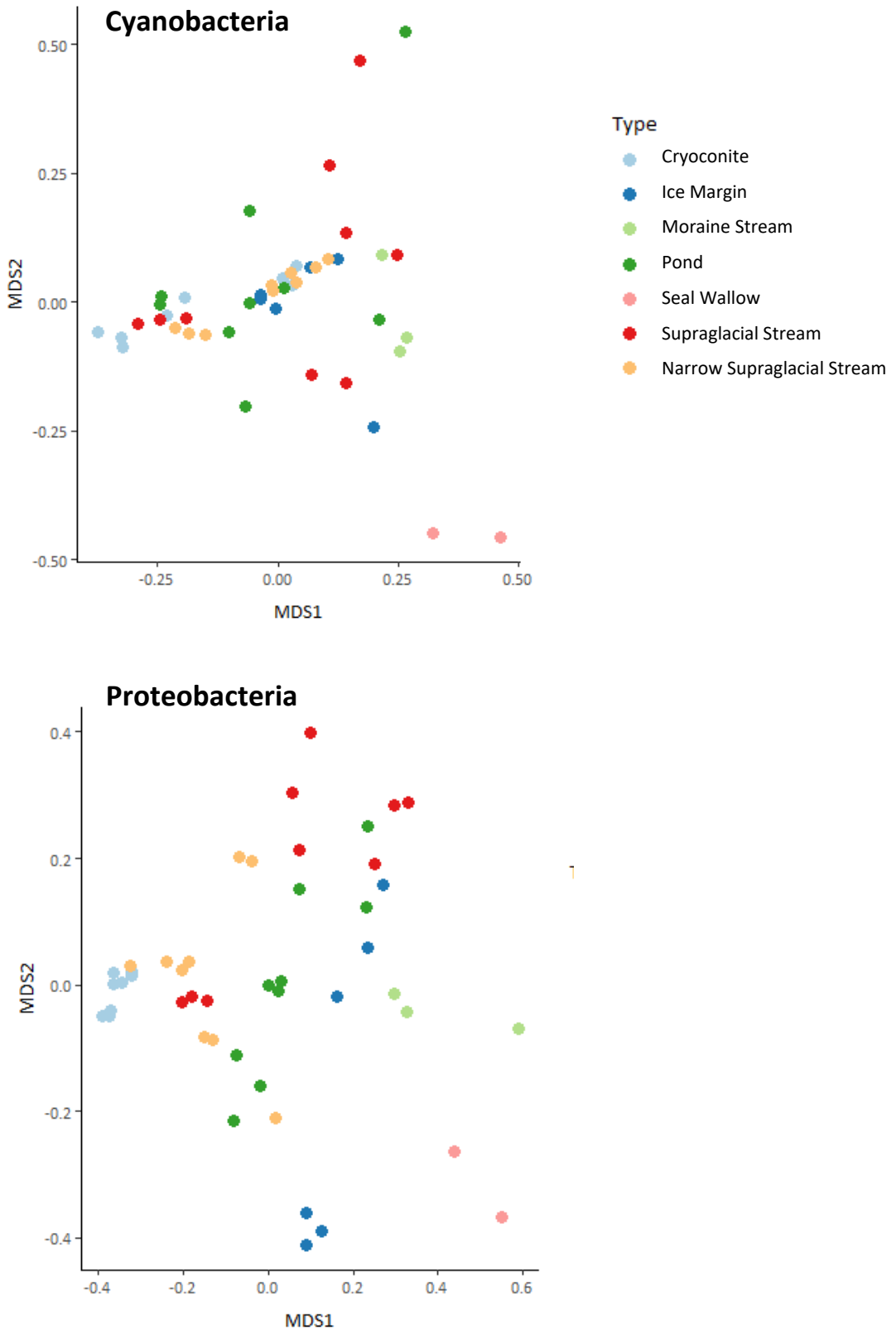

Figure 34 continued Bray-Curtis dissimilarity of 16S rRNA gene ASVs found in Signy Island habitats grouped by type and visualised by non-metric multidimensional scaling (NMDS) ordination. All sampling replicates are included.

to the Deltaproteobacteria. The most abundant genera of Deltaproteobacteria were *Aetherobacter, Pajaroellobacter* and *Geobacter*. The *Aetherobacter* were the major component of nunatak cryoconite Deltaproteobacteria (65% of cryoconite Deltaproteobacterial sequences). Meanwhile the cryoconite from further south on Gorlay Snowfield contained a lower proportion of *Aetherobacte*r and higher proportion of *Pajaroellobacter* (*Pajaroellobacter* accounted for 38% of Gorlay Snowfield cryoconite)*. Geobacter* was apparent in highest proportion in the pond samples and absent in the cryoconite and narrow supraglacial stream samples. Unlike the other sample types, in the seal populated area there was a high proportion of *Nannocystis* in the Deltaproteobacteria (71%).

Separate non-metric multidimensional scaling analysis of 16S rRNA gene ASVs belonging to the three most abundant phyla Cyanobacteria, Proteobacteria and Actinobacteria according to the Bray method showed these similarities and differences visually when ordinated (Figure 34). The consistent result was that the seal populated samples outlie from all other groups. ANOSIM results suggest low separation in the Cyanobacterial composition between sample types compared to differences within those types ($R=0.17$, $p = 0.0016$).

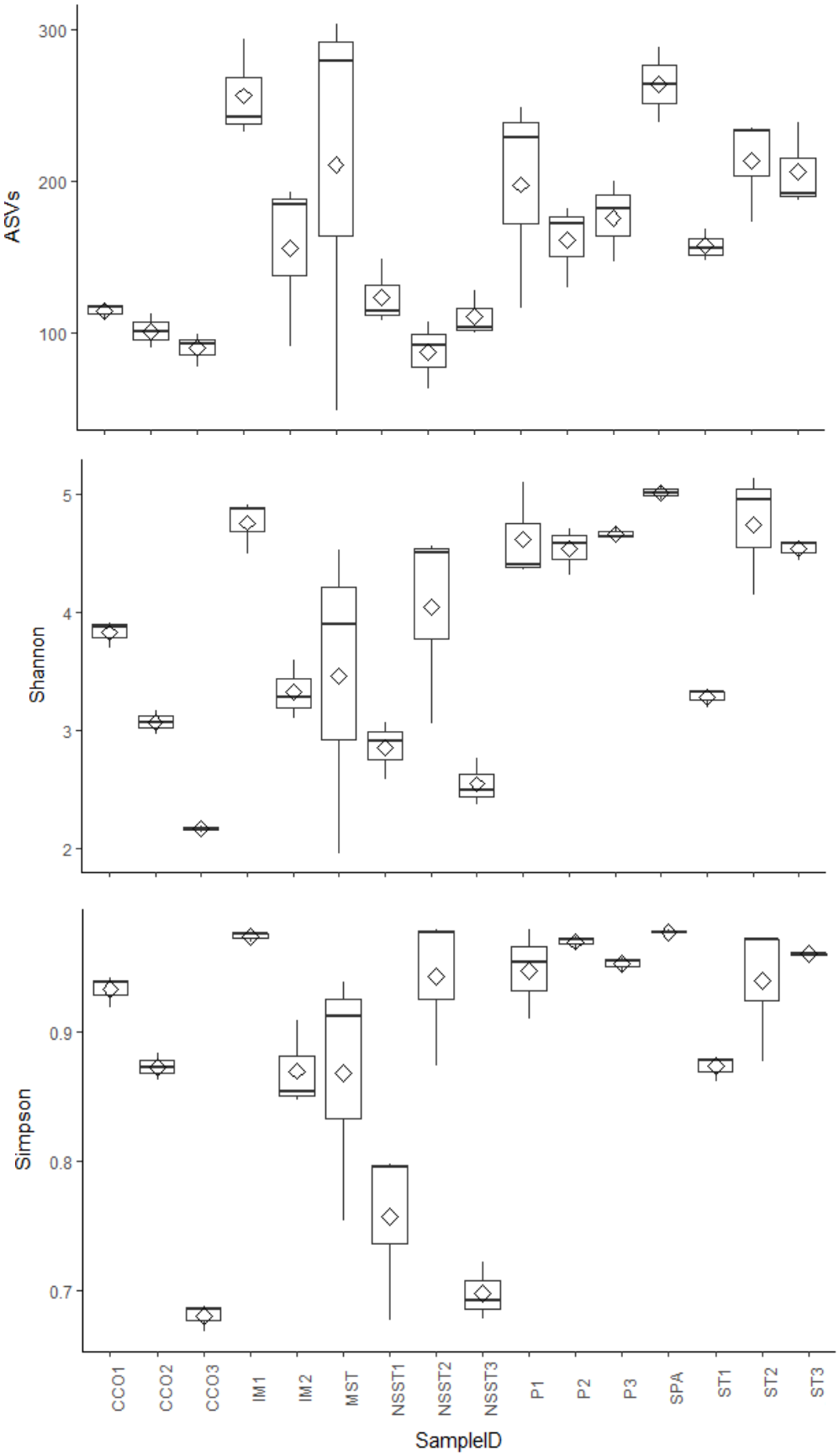

Figure 36 Alpha diversity microorganisms in Signy Islands samples as measured by average number of 16S and 18S ASVs, and the Shannon and Simpson indices. Diamonds indicate mean values.

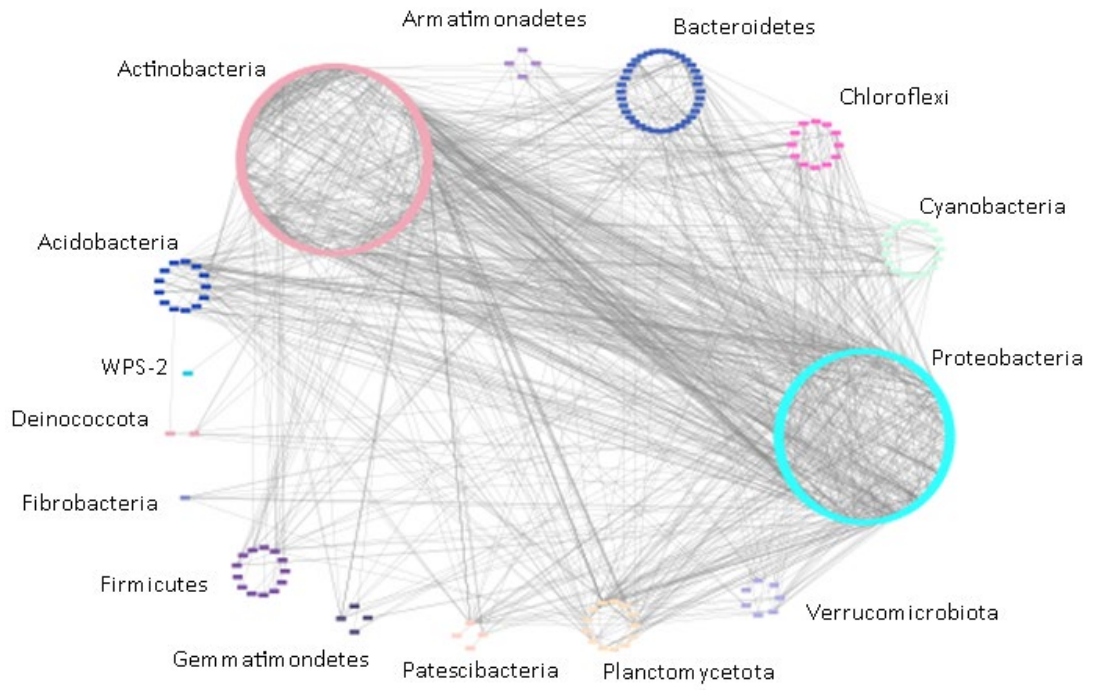

Figure 37 Probabilistic co-occurrence of lowest rank taxa. Coloured nodes are lowest-rank taxa found to co-occur at a significance of $p < 0.001$ with at least one other taxon. Nodes are grouped by phyla. Edges represent co-occurrences.

Co-occurrence of lowest-rank taxa was calculated using a probabilistic co-occurrence model (Veech, 2013) (Figure 36). 41987 pairs, 0.554% of the total potential pairs of lowest-rank taxa, were found to co-occur at a higher than expected rate at $p < 0.05$. 1411 pairs, 0.019% of all potential pairs, co-occurred at a lower rate than expected at $p < 0.05$. 37% of Proteobacteria, 41% of Actinobacteria and 30% of Cyanobacteria lowest rank taxa were found to co-occur significantly with at least one other taxon at $p < 0.05$ (Table 12). The average number of co-occurrences per taxon varied between phyla. The highest average and lowest range highlights a smaller subset of significant co-occurrences, at $p < 0.001$. At this significance level, 0.394% of the total potential pairs of lowest-rank taxa were found to co-occur at a higher than expected rate and 0.019% co-occurred at a lower rate than expected. 12% of Proteobacteria, 17% of Actinobacteria and 8% of Cyanobacteria lowest rank taxa were found to co-occur significantly with at least one other taxon at $p < 0.001$. Of the phyla contributing to >1% of the total ASV abundance (Actinobacteria, Armatimonadetes, Bacteroidetes, Cyanobacteria, Firmicutes, Gemmatimonadetes, Planctomycota and Proteobacteria) Planctomycota had the highest average

Table 12 Summary of significant co-occurrences between lowest rank taxa in Signy Island habitats by phyla. Phyla with no nodes resulting in significant co-occurrences were removed.

Phylum	Number of lowest-rank taxa	Proportion of each phyla with significant cooccurences		Average number of connections per node	
		$p < 0.05$ %	$p < 0.001$ %	$p < 0.05$	$p < 0.001$
Proteobacteria	1414	36.92%	11.60%	55.67	5.67
Actinobacteriota	1172	40.53%	16.72%	67.32	5.90
Bacteroidetes	423	35.93%	8.51%	38.15	4.19
Cyanobacteria	225	30.22%	7.56%	40.12	4.76
Firmicutes	143	36.36%	9.09%	45.27	3.85
Planctomycetota	99	31.31%	13.13%	84.81	9.85
Acidobacteriota	91	47.25%	14.29%	60.58	8.62
Chloroflexi	88	30.68%	13.64%	97.33	6.75
Verrucomicrobiota	75	33.33%	9.33%	50.00	6.00
Patescibacteria	60	38.33%	6.67%	47.57	9.25
Deinococcota	27	40.74%	7.41%	27.55	5.00
Gemmatimonadetes	20	50.00%	20.00%	81.50	4.75
Armatimonadota	15	53.33%	26.67%	58.38	4.75
Caldisericota	4	75.00%	0.00%	27.00	0.00
Abditibacteriota	4	50.00%	0.00%	12.50	0.00
Dependentiae	4	25.00%	0.00%	26.00	0.00
Fibrobacteria	4	25.00%	25.00%	162.00	8.00
Sumerlaeota	3	33.33%	0.00%	15.00	0.00
WPS-2	2	50.00%	50.00%	43.00	1.00

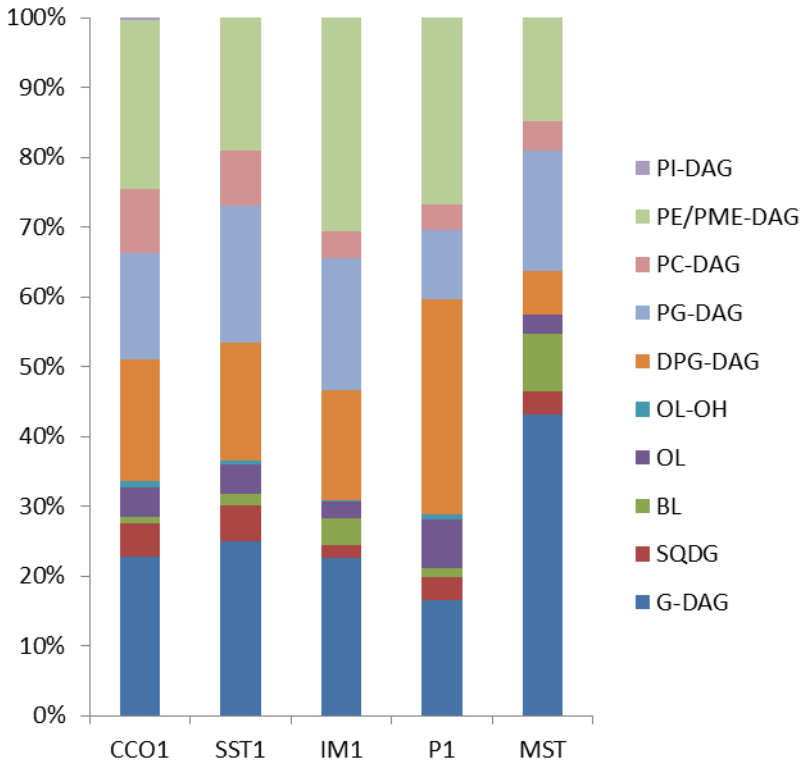

Figure 38 Relative abundance of intact polar lipids from Signy Island habitats.

connections per taxon (Table 12) (84.81 at $p < 0.05$, 9.85 at $p < 0.001$). At $p < 0.001$ the next five phyla with the highest average number of connections per taxon all belonged to less abundant groups (Patescibacteria, Acidobacteria, Fibrobacteria, Chloroflexi and Verrucomicrobiota). At $p < 0.05$ these groups rank differently in average connections per node, Fibrobacteria had the most connection by far at 162 and the succeeding phyla were Chloroflexi (97.33), Plantomycota (84.81), Gemmatimonadetes (81.50), Actinobacteria (67.32) and Acidobacteria (60.58). However, many of these groups, including Planctomycota, have a considerable range of connections per node.

Intact polar lipid distribution among supraglacial and periglacial habitats

One site of each type was selected for IPL analysis. Several IPLs were detected across all sample types (Figure 37). Bacterial and eukaryotic IPLs were detected, but none which belonged to the archaea. Glycolipids (G-DAGs), the dominant IPL group in Cyanobacteria (Siegenthaler, 2006; Wada & Murata, 2006) contributed an average relative abundance of 26% to the total IPLs. 63% of IPLs on average

belonged to the phospholipids (DPG-DAG, PG-DAG, PC-DAG, PE-DAG, PME-DAG and PI-DAG). The SQDGs contributed an average of 4% to the total relative IPL abundance and the aminolipids (BL, OL and OL-OH) an average of 8%. PC-DAGs which are primarily produced by eukaryotes were present in all samples, and ranged from 10%-20% of the relative IPL abundance at each site. The microbial mat from the moraine stream had the highest relative abundance of G-DAGs (43%) and the lowest relative abundance of PE/PME-DAGs (15%). The microbial mat also had a notably low relative abundance of DPG-DAGs (6%). The meltwater pond at the base McLeod glacier close to the Khyber pass (Figure 29) in contrast had a comparatively low relative abundance of G-DAGs (17%), and high relative abundance of PE/PME-DAGs (27%) and DPG-DAGs (31%). These differences place the microbial mat and pond as end members most distinct from one another. These differences between sample types were visualised using non-metric multi-dimensional scaling according to the Bray-Curtis method (Figure 38). This shows the segregation between the microbial mat IPL composition and the other samples, in particular those from the pond. It also shows that there was more difference

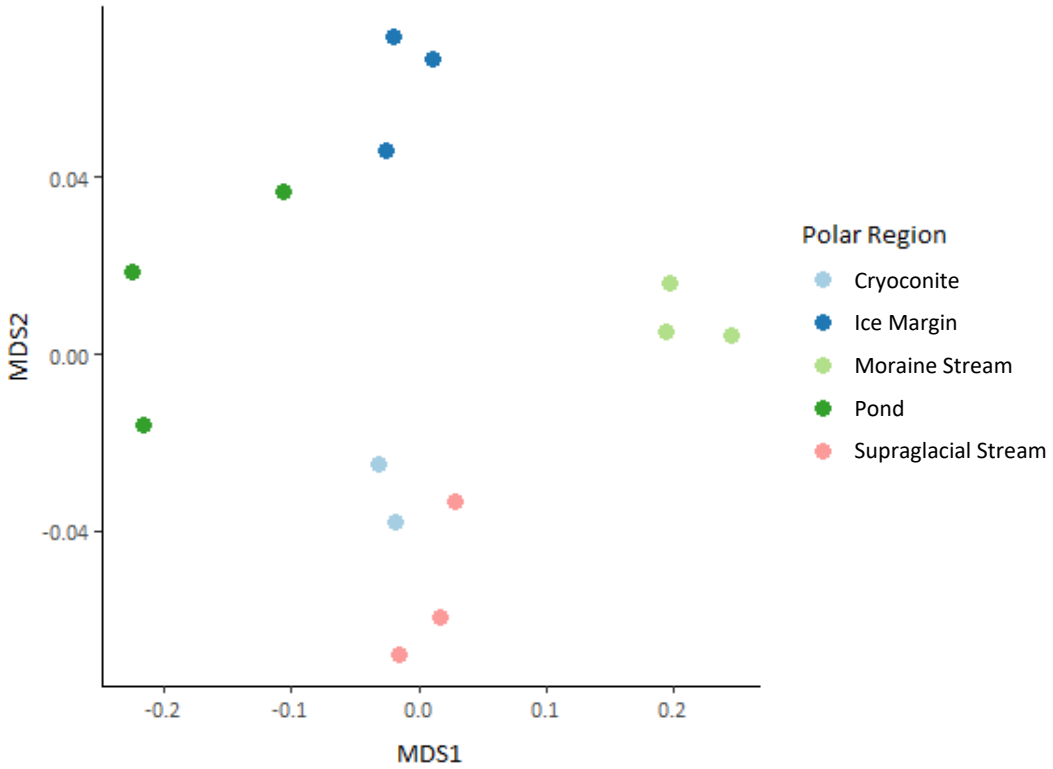

Figure 39 Bray-Curtis dissimilarity of intact polar lipids found in Signy Island habitats grouped by habitat type and visualised by non-metric multidimensional scaling (NMDS) ordination. All sampling replicates are included.

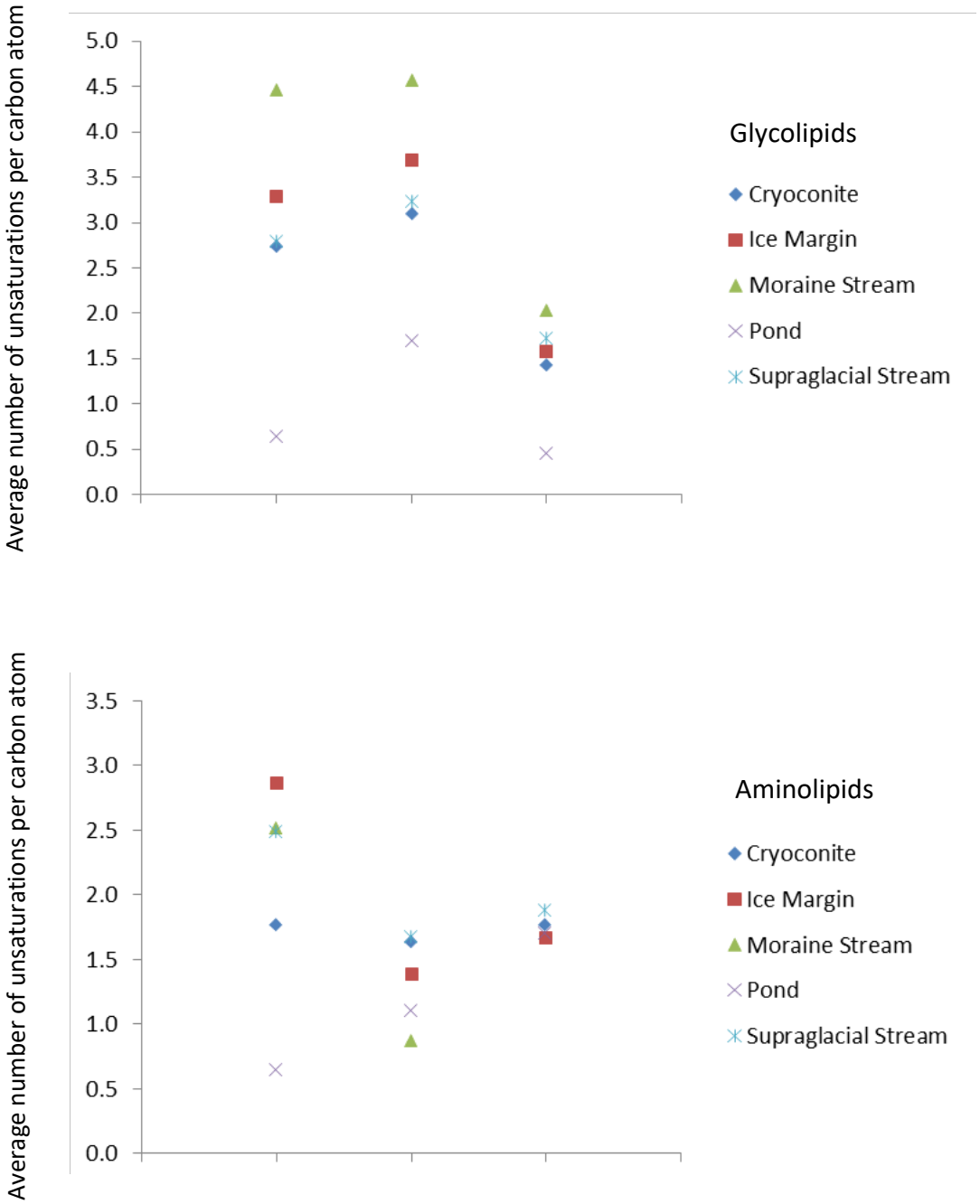

Figure 40 The average unsaturation per carbon atom in the intact polar lipids extracted from Signy Island habitats. Average standard deviation on mean unsaturations of each type was 0.1.

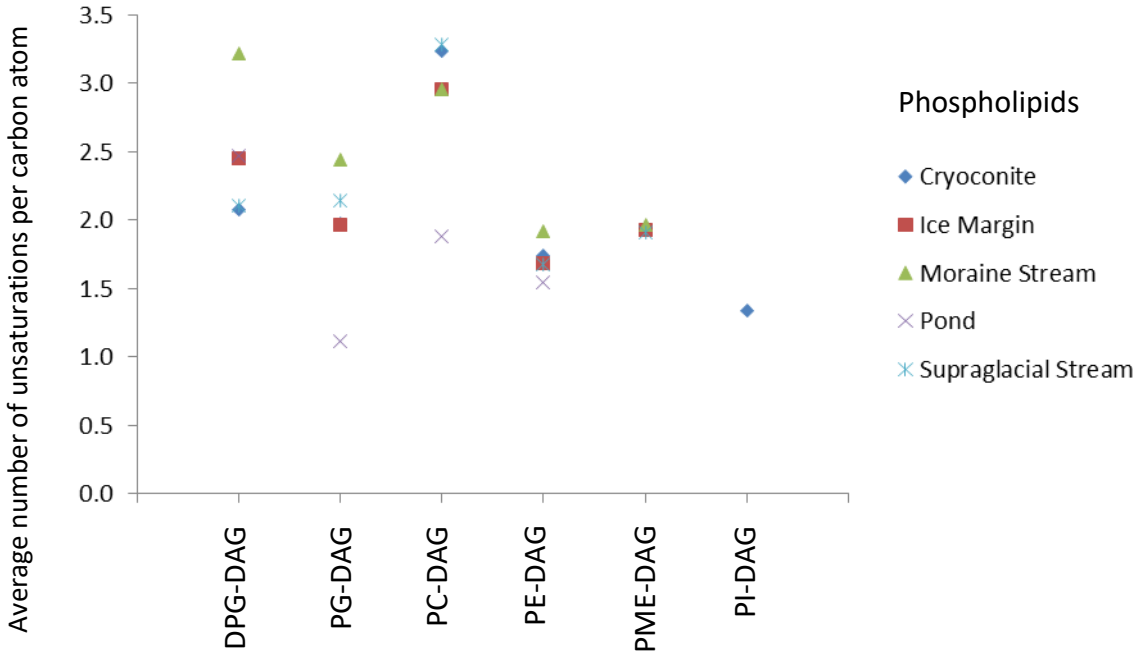

Figure 39 continued The average unsaturation per carbon atom in the intact polar lipids extracted from Signy Island habitats. Average standard deviation on mean unsaturations of each type was 0.1.

between sample types than within technical replicates. An ANOSIM test of the Bray-Curtis distances produces an R value of 0.85 at p = 0.0001. The proportion of unsaturated carbon bonds in the IPLs also set the pond and microbial mat samples apart from the other sample types (Figure 39). The pond samples had a low proportion of unsaturations in the glycolipids, and the microbial mat a high proportion. The pond samples also had low numbers o7g8inoml]fcf unsaturations in the PG-DAGs and PC-DAGs. The microbial mat had a comparatively high number of unsaturations in the DPG-DAGs.

Objective 3.2: Determine the community response of Signy Island sediments to isolated "oasis" incubation conditions

Signy island sediments were incubated under constant conditions, consistent with those used for the McMurdo Dry Valley control conditions (Results Chapter 2), for a period of 27 days (Figure 40). Two replicates of sample types cryoconite (CCO), narrow

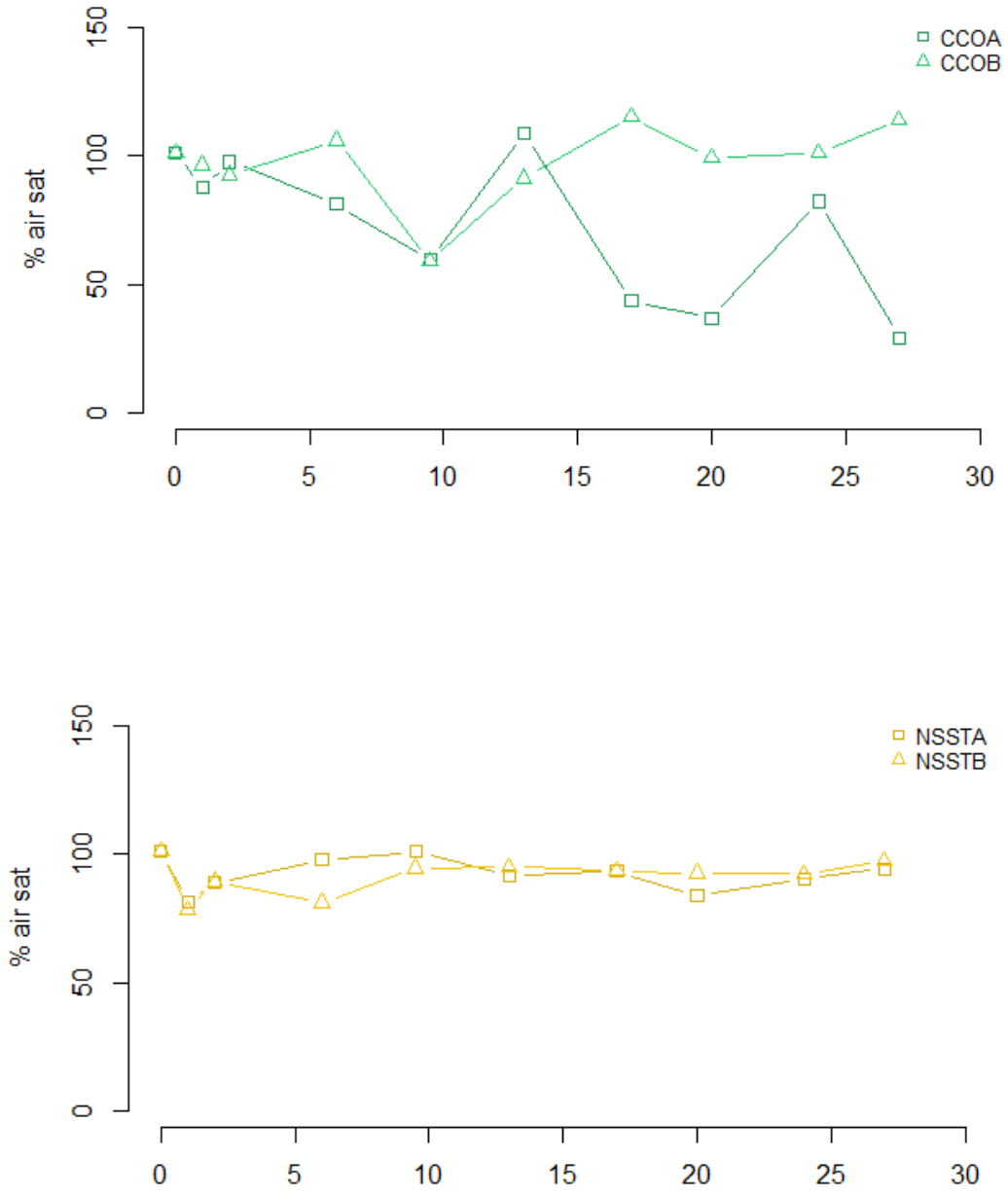

Figure 41 Microbial community response of sediments taken from various Signy Island habitats (cryoconite, narrow supraglacial channel, supraglacial stream, ice margin and pond) to 27 days of growth under "McMurdo Dry Valley control conditions" (used previously in objectives 2.1 and 2.2). Due to heterogeneity within samples, all replicates are shown as separate points.

)

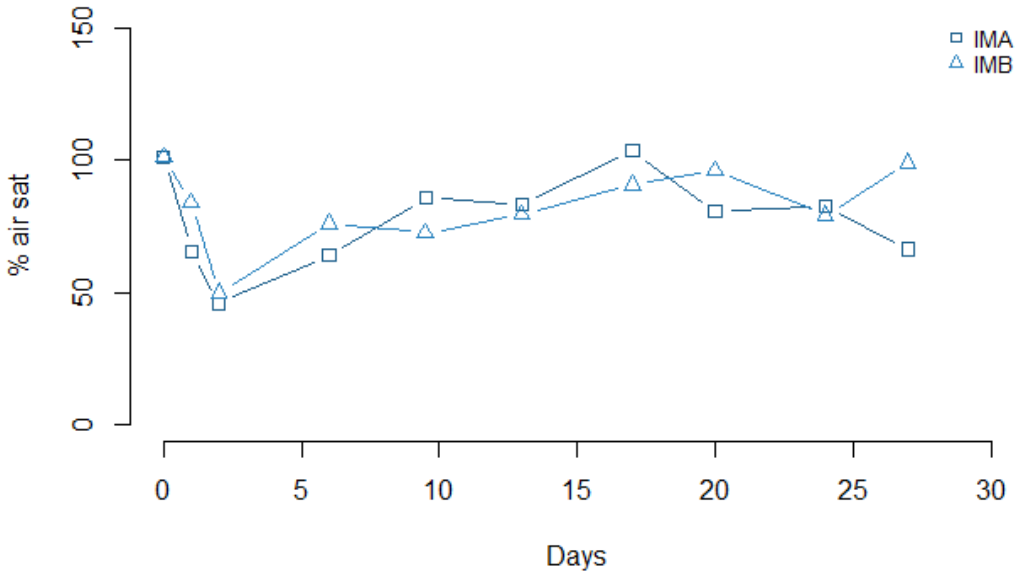

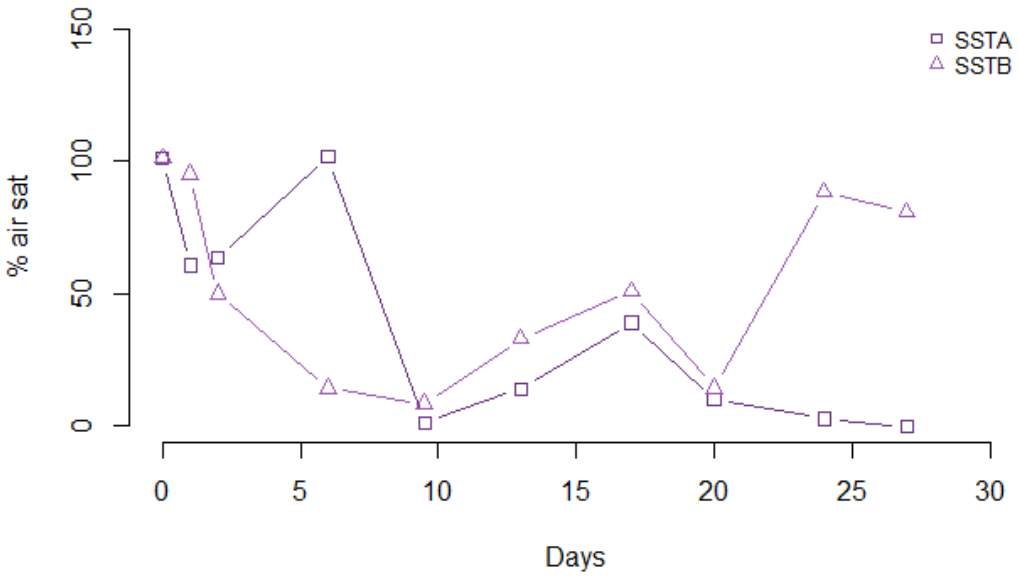

Figure 40 continued Microbial community response of sediments taken from various Signy Island habitats (cryoconite, narrow supraglacial channel, supraglacial stream, ice margin and pond) to 27 days of growth under "McMurdo Dry Valley control conditions" (used previously in objectives 2.1 and 2.2). Due to heterogeneity within samples, all replicates are shown as separate points.

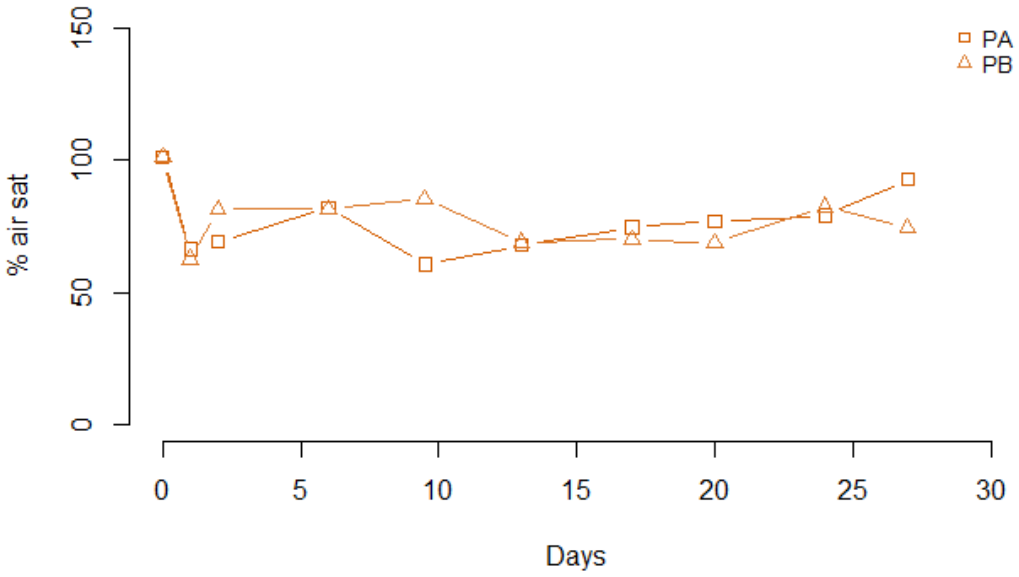

Figure 40 continued Microbial community response of sediments taken from various Signy Island habitats (cryoconite, narrow supraglacial channel, supraglacial stream, ice margin and pond) to 27 days of growth under "McMurdo Dry Valley control conditions" (used previously in objectives 2.1 and 2.2). Due to heterogeneity within samples, all replicates are shown as separate points.

supraglacial stream (NSST), larger downstream supraglacial stream (SST), ice margin (IM) and pond (P) were included (see Table 11). Oxygen saturation measurements were taken at regular intervals to monitor changes in ecosystem activity. Narrow supraglacial stream, ice margin, pond and CCO1B samples exhibited little change in oxygen saturation through the incubation period (range of values between 59% and 115%). The signature of exponential growth, detected in previous incubations as a sharp increase in oxygen saturation, was not present in any samples. CCO1A, sourced from cryoconite 1, exhibited fluctuations between 36% and 98% air saturation throughout the incubation, ending at 29.14% at day 27. By day 9 of incubation both stream sample replicates had depleted the oxygen in the water column (1.19% oxygen in SST1A and 8.37% oxygen in SST1B). From this point SST1A increased to 38.95% air saturation on day 17 and then a reduction again to -0.20% by day 27. SST1B also increased in air saturation on day 17 and reduced to day 20. However, in contrast to SST1A, SSTB then increased to 88.21% on day 24 and retained a comparatively high air saturation of 80.90% by day 27.

Discussion

Objective 3.1: Investigate geographical and ecological connections between interconnected glacial and near-glacial microbial ecosystems on Signy Island

Habitat structures, connections and geography

Several distinct but connected habitats were identified on Signy Island: cryoconite, streams, supraglacial ice margins, ponds, periglacial streams and seal wallow areas. The habitats were ephemeral and dynamic, with individual streams, ponds and cryoconite holes only appearing or becoming connected by meltwater after warm weather. Meltwater has been shown to carry dissolved organic matter between supraglacial, marginal and proglacial habitats (Dubnick *et al*., 2017). As Signy Island is only 20km^2, there is likely to be short range aeolian transport of microorganisms and sediment between some or all sites (Šabacká *et al*., 2012; Archer *et al*., 2019). Therefore the habitat contents and structure were connected to and dependent on one another. Such a network of habitats could have very plausibly existed during times of melt in the Cryogenian, when larger areas of land were exposed and sediment that had been trapped in cryolakes and cryoconite holes was released and connected to meltwater streams.

While thin biofilms and microbial mats were found on some ponds and the ice of some streams, the only large thick microbial mat was found on a moraine stream. During global deglaciation, microbial mats of Cyanobacteria and algae are likely to have spread across the land (similar processes to modern darkening ice sheets, and primary colonisation of moraine). This may have led to the first land plants from within the Streptophyta (Becker and Marin, 2009; Becker, 2013; de Vries *et al*., 2016).

During deglaciation the ice over the oceans would melt and glaciers would retreat as the rate of ablation exceeds accumulation. Many of these glaciers would terminate to terrestrial moraine. Streams from these land terminating glaciers would have distributed ions and subglacial microorganisms across the terrestrial surface and into the sea (Boyd *et al*., 2014; Lechte *et al*., 2019) and coastal and ice

marginal microorganisms and sediment would be regularly swept up onto glacier surfaces by winds and the reactivated hydrological cycle. This is likely a similar system to what we see on Signy Island in the present day.

Composition of supraglacial and periglacial communities across the Signy Island habitats

While third generation sequencing is still sometimes perceived as a developing area of molecular biology, the results here appear to be representative of glacial and near glacial environments as evidenced by the presence of cryophilic and cryotolerant organisms and its overall resemblance to previous studies of glacial communities (Liu *et al*., 2011; Cameron *et al*., 2012b; Edwards *et al*., 2013b; Gokul *et al*., 2019). This is unsurprising as nanopore metagenome sequencing has been shown to yield strong correlation to prior 16S rRNA gene profiles on a well characterised glacier microbiome and base calling algorithms in recent years have significantly approved accuracy (Edwards *et al*., 2019; Wick *et al*., 2019). Minor discrepancies such as the difference in Cyanobacteria relative abundance compared to Cameron *et al*., 2012 seem no more significant or frequent than discrepancies with previous studies that were found using Illumina sequencing in Results Chapter 1. As the supraglacial and periglacial habitats of Signy Island are relatively understudied, the reported data for comparison is limited, and there is no available sequence data for comparison to the genus level community composition.

Through 16S rRNA gene sequencing, 34 phyla and superphyla were recovered. The three most abundant groups (Actinobacteria, Cyanobacteria and Proteobacteria) were present in all locations although the relative abundance and genera present varied. Archaea were not detected, which may be in part due to the primers used. However, very low diversity of archaea is typical for many cryosphere habitats (Liu *et al*., 2011; Cameron *et al*., 2012b; Edwards *et al*., 2013b; Lutz *et al*., 2017). In addition there was a high proportion of IPLs associated with bacteria, some produced by eukaryotes (such as PC-DAGs) but no IPLs characteristic of archaea.

Genera with stress tolerant and/or extremophilic properties including *Cryobactierum, Polaromonas, Thermomonas* and *Psychrobacter* were found in all habitat types. Polyextremophiles Deinococcota were also found in all samples, but only contributed 0.3% to the total 16S rRNA gene ASVs. It is interesting that most of the sequences assigned to *Psychrobacter*, a psychrotolerant genus, were found in the seal wallow area which was the furthest from the cold ice cap. Overall this demonstrates that although Signy Island may not experience the same extreme cold as mid cryochron Snowball Earth or even the McMurdo Dry valleys, there is still a strong presence of organisms with cryotolerant capabilities. The community composition profile does not seem to reflect a warmer climate when compared to the results of amplicon sequencing from Results Chapter 1. Broadly tolerant microorganisms would be vital for the survival of life through the Neoproterozoic. Deglaciation is predicted to have happened rapidly in comparison to evolutionary timescales. A notable difference between the Signy Island results communities from Results Chapter 1 was the higher relative abundance of Firmicutes. Firmicutes are common anaerobes in glacial habitats, and have been a more significant contributor to cryoconite community composition results in other studies (Pearce, 2005; Liu *et al*., 2011; Cameron *et al*., 2012b; Zdanowski *et al*., 2017). Therefore it is difficult to confidently say whether the difference in relative abundance here is due to biogeography or sequencing methodology. Some Firmicutes also have endospore forming capabilities and these spores are highly tolerant of UV radiation, temperature stress and desiccation which can aid in their survival during aeolian transport and distribution to high environmental stress environments (Nicholson *et al*., 2002). These kinds of adaptations may have been key during the extreme cold and potentially high UV radiation of Snowball Earth. During deglaciation, where retreating glacier and ice caps became increasingly disconnected from one another and the climate was rapidly changing, tolerance to transport and dramatic change in local environment could have been highly beneficial (Hoffman, 2016).

Overall there was higher similarity within habitat types than between them. This result was found in both 16S rRNA gene composition and IPL composition. Groups did not cluster according to location on the island, even when they were connected

to each other by meltwater. This mirrors studies from other glaciated areas, which also found that microbial community composition varied between different habitat types, including cryoconite, streams, ice margins and proglacial ponds (Mindl *et al*., 2007; Liu *et al*., 2011; Stibal *et al*., 2012b, 2015; Edwards *et al*., 2013c).

The strongest similarity in 16S rRNA gene composition was found between the cryoconite and narrow supraglacial streams. For example, these habitats had a higher relative abundance of the Actinobacteria *Galbitalea and Parafrigoribacterium* and the Proteobacterium *Rhodanobacter*. They also both had a particularly high proportion of Cyanobacteria, which differs from the prior microbial community analysis of Signy Island cryoconite by Cameron *et al*. (2012). There are several reasons why the results presented here may differ those from Cameron *et al*. The sequencing methodology was different (T-RFLP vs Nanopore amplicon sequencing), as was the month of collection (January vs March). In the Cameron *et al*. study, cryoconite was collected from one west facing area of the ice cap whereas the cryoconite collected for this study originates from the southerly glacier and ice cap centre. While these areas are less than 2km apart, the winds and hydrology could be quite different on different sides on the island. The dynamic nature of the habitats on Signy island (streams and cryoconite holes sometimes forming or disappearing within a day) may also lead to highly variable ecosystems. It also sets apart the Signy Island cryoconite from the McMurdo Dry Valleys Antarctic cryoconite as described in Results Chapter 1 (Figure 13). In some ways the similarity between the narrow supraglacial stream and cryoconite habitats is unsurprising, as the cryoconite holes were enclosed and each under 15cm across whereas some narrow supraglacial meltwater streams had running water and stretched across the width of the ice cap. However, there were also similarities between the habitats that could explain this similarity in community composition. The sediment contained in these two habitats was similar in appearance and structure: dark, granular and less than 1cm in thickness. Little sediment was transported by the flowing water in the narrow supraglacial streams therefore, like the cryoconite holes, the habitat was a layer of dark static sediment on ice. The sediment remained in place until more substantial melt or rain occurred in that

area. It has been shown that even when cryoconite holes are connected by meltwater the mineral-microbe aggregates tend to remain in the original cryoconite hole (Gokul *et al*., 2016; Segawa *et al*., 2017). The same may be true for the narrow supraglacial stream. In contrast, the flow of the wider supraglacial streams was sufficient to carry sediment. They also contained thicker sediment at the bottom. The cryoconite and supraglacial meltwater channels also had low species richness. This may be a contributing factor to their similar community composition. These two habitats, cryoconite and narrow supraglacial stream, were also the furthest inland. It has been demonstrated previously that there are significant differences between cryoconite on ice sheet interiors and ice margin communities (Edwards *et al*., 2013c; Stibal *et al*., 2015). The shallow sediment combined with lack of input of nutrients and species associated with animal areas may have contributed to the low species richness and similar community composition between the cryoconite and narrow supraglacial streams. While a minor component of the lipid profile, PC-DAGs are highest in cryoconite which suggests a small but active eukaryote community, concurring with previous evidence of cryoconite as a refuge for fungi, microalgae and protists. Despite the similarities in bacterial composition between cryoconite and narrow supraglacial stream, there was a difference in the relative abundance of chloroplasts. The primers, methods and database used were not designed for the analysis of chloroplast but particularly low relative abundance of chloroplast DNA in cryoconite may possibly indicate a lower proportion of algae. Interestingly, SST1 which was more similar in 16S rRNA gene composition to the cryoconite and narrow supraglacial streams than the wider supraglacial streams, was not inland and uphill on the ice cap, rather it was at the bottom of Erratics valley, flowing into Erratics lake (P2) (Figure 29, Figure 31).

The seal wallow areas were a consistent outlier in 16S rRNA gene composition, consistent with prior research on Signy Island (Chong *et al*., 2009, 2010). They contained relatively high abundance of several groups that are absent or present in low abundance in all other samples, such as: *Tessaracoccus, Nocardiodes, Humibacillus, Phormidium, Nannocystis, Simplicispira*, and *Psychrobacte*r. The high species richness and distinct community composition is not surprising given that

these communities have input from animal disturbance and nutrient input via faeces. It is challenging to find modern analogues to Snowball Earth free from the influence of animals, which were not present during the Cryogenian, particularly in lower latitude glaciated areas. However, the strong division between microbial assemblages in the seal populated area and the supraglacial and periglacial habitats suggest the impact of megafauna on the inland microbial communities is minimal.

The moraine stream also had a noticeably different community composition to the other habitat types. Not only was the water temperature warmer in the moraine stream than the supraglacial habitats, it was the only habitat to contain a comparatively thick (20mm) microbial mat (Figure 30). This is reflected in the high proportion of Cyanobacteria relative to the neighbouring ponds and seal wallows. The moraine stream contained the highest proportion of PE and PME-DAGs and other glycolipids, indicating the presence of biologically active Cyanobacteria in the microbial mats. This shows that Cyanobacteria and other microbial communities are active and proliferate under these conditions, perhaps acting as colonisers of recently deglaciated moraine sediments (de Vries *et al*., 2016; de Vries and Archibald, 2018). During Cryogenian deglaciation Cyanobacteria and algae would have spread to these barren areas as the primary producers for a new ecosystem, the warmer temperature and stability allowing for complex microbial mats to form. The moraine stream microbial mat contained a high proportion of *Tychonema* and low proportion of *Phormidesmis* compared to other habitat types. While this could indicate that *Tychonema* is better suited to this habitat it may also reflect a different source and connectivity of microbial matter to the supraglacial and pond habitats. Cells may be transported inland towards the moraine from the moss banks in addition to any input from supraglacial habitats.

The proportion and structure of the IPLs may also reveal the impact of the habitat on the microorganisms present. The proportion of phospholipids was lowest in the moraine stream. Soil studies have previously found that in areas with low P availability, phospholipids can be substituted for betaine lipids (Warren, 2020). Indeed, the moraine stream also has the highest proportion of betaine lipids. It is possible that the high cell density of the moraine stream microbial mat has

depleted the bioavailable phosphorus in the local environment. The microbial mats from the moraine stream also had highly unsaturated glycolipids, in contrast to the more saturated glycolipids in the pond samples. Membrane desaturation has been shown to be an adaptation to cold environments (Marr and Ingraham, 1962; Suutari et al., 1990; Gombos et al., 1994) possibly due to the impact of saturation on membrane permeability and flexibility (Van de Vossenberg et al., 1995; Murata and Los, 1997). However, there was no significant difference between the temperature of the streams containing microbial mats and the meltwater ponds (all ranged between 0.4°C – 2.5°C). Unsaturations in the intact polar lipids can also protect against high intensity of light (Gombos *et al*., 1997) and it is the case that the moraine streams were not shaded by ice or snow for as much of the time as the other habitats.

Microbes in other Antarctic meltwater ponds have been found to have a high proportion of unsaturations (Evans *et al*., 2022). This is predicted to be an adaptation to the ice cover these ponds experience for most of the year, as experiments have found improved freeze tolerance among bacteria with membranes containing high proportions of unsaturated fatty acids (Evans *et al*. 2022, Goldberg and Eschar, 1977; Beal et al., 2001). They suppose that microbes in the meltwater ponds may desaturate their membranes to survive winter freezing. The meltwater ponds on Signy Island are also ice covered for much of the year. However, the moraine was also covered by snow so it's unclear whether this environmental difference is responsible for the difference in the proportion of saturated carbons in the IPLs. In contrast, the Cyanobacteria were a relatively low component of the 16S rRNA gene composition in pond sediment and the lack of Cyanobacteria-indicator IPLs also set the pond out as an end member in terms IPL distribution. Despite the fact that the moraine streams and ponds were connected by meltwater and are both bodies of meltwater on the moraine, their IPL profiles were the most dissimilar of all habitat types. While two ponds contained thin phototrophic biofilms, the overall active Cyanobacteria were low compared to the thick microbial mat of the moraine stream. The regular flushing and freezing of the meltwater ponds with daily and weekly changes in weather may mean it is

more difficult for a stable community of Cyanobacteria to establish. The warmer temperature of the moraine stream (2.5°C compared to a range of 0.4°C - 0.8°C and average of 0.5°C in the ponds) is likely to have provided more permissive conditions for Cyanobacteria growth. In Greenland, an ice sheet interior was found to have a considerably higher ratio of RNA to DNA than the ice sheet margin, and therefore a higher proportion of potentially active microorganisms (Stibal *et al*., 2015). Microbial activity and abundance was also found to be higher in aquatic environments further onto the ice sheet than near the ice margin (Stibal *et al*., 2012b). It is possible that equivalent studies on Signy Island glaciers may reveal differences in the quantity of active microorganisms between habitats, which may further explain the differences in 16S rRNA gene and IPL profiles between habitats.

Co-occurrence was studied with the aim to identify whether certain organisms tended to appear together, and therefore the possibility of certain habitats to be preferential for characteristic 'sets' of organisms. However, what was found was a large complex web of co-occurrences. Over 52% of the total lowest-rank taxa were found to co-occur more often than expected with at least one other taxon at $p<0.05$. Many of the strongest connections ($p<0.001$) were associated with less abundant phyla such as Armatimonadota, Acidobacteriota, Chloroflexi and Planctomycetota. These groups were also among those with the higher number of connections per species node. These co-occurrences may be due to commensal relationships between these organisms, or they may have shared favourable habitat conditions. This demonstrates that during times of melt and freeze when habitats change or microorganisms are transported to a new habitat, a large network of species are impacted. This mirrors the finding by Gokul *et al*. that taxon interactions are highly influential on bacterial community structure (Gokul *et al*., 2016). On modern glaciers, and presumably during the Cryogenian, alteration of a habitat will lead to alteration of whole ecosystem composition. For organisms to have survived on glacier surface oases they must also have been able to survive in transitional habitats. These results also suggest that the "surface ecosystem of the Cryogenian" cannot be defined as one type of community but rather varied greatly

geographically and temporally through the glaciations and deglaciations of the Cryogenian period.

Objective 3.2: Determine the community response of Signy Island sediments to isolated "oasis" incubation conditions

Just as Cryogenian cryoconite organisms must have been able to survive melt into streams ponds and distribution onto land and sea to persist at end-glaciations, suitable analogues to Cryogenian streams, ponds and other surface habitats must be resilient to icy conditions, including low temperatures and low nutrient input. Hoffman *et al*. (2016) proposed a theoretical habitat "cryoconite pans" formed by larger aggregates of sediment than typical cryoconite holes. The closest modern analogues are large cryoconite holes, cryolakes (which are formed at ice cliffs by strong winds (Laybourn-Parry and Wadham, 2014)), periglacial pond and lakes, or supraglacial lakes that contain sediment. The Signy Island pond, cryoconite and ice margin sediments when incubated under the cold (0.5°C) isolated conditions showed little activity. Unlike the McMurdo Dry Valleys cryoconite which under the same conditions entered a growth phase characterised by sharp increase in oxygen saturation in the water column at ~15 days, the oxygen levels produced by the Signy Island pond, cryoconite, and ice margin sediments stayed in a range between 65-110% air saturation. While these communities are active in their source habitats, they showed no signs of successful growth under the cold isolated conditions of the incubation. This, along with the finding that different habitats over a small area contain different community structures, suggests that in the transition between a wetter and more temperate cold earth similar to the conditions of Signy Island and a "hard" Snowball Earth the community compositions on the surface would have shifted. Microbes that had previously been successful may become minor components of communities, or be eliminated altogether. From this growth experiment it is not possible to tell what factors contributed to the minimal activity. It is also unclear whether a growth phase would have begun if the incubations were run for longer. The incubation temperature was not lower than the average pond temperature (0.5°C), however the communities may have responded poorly to the storage conditions at -20°C as temperatures rarely drop below -10°C and -20°C is

the lowest temperature the soil reaches (Bartlett *et al*., 2020). Another possibility is that the community activity is lower *in situ* than the McMurdo Dry Valley cryoconite sediments. The small size and changeable weather of Signy Island may result in limited activity in the sediments. The cryoconite and ponds were regularly covered in ice and thick snow providing low temperature and limited light. Consistently ice and snow free sources of microbe-mineral aggregates were also limited on the ice cap. However, visible biofilms were present in the ponds, and the IPL profile suggested an active community (including Cyanobacteria) in all habitat types. Additionally, the high ratio of phospholipids to aminolipids suggests availability of phosphates.

In contrast, the stream samples depleted the oxygen in the incubation vessels. These samples contained visible remnants of green biofilm. The sampling replicates behaved differently to one another, only one returning to expected levels of oxygen saturation by the end of the incubation period. This suggests heterogeneous sediment including active members that were thriving under the incubation conditions. It is unclear whether continued incubation in isolation would lead to anoxia or all replicates would return to 50%-100% oxygen saturation. The stream where these samples were recovered had the lowest temperature of all habitats investigated (0.1°C). Therefore, this habitat may have contained a higher proportion of particularly cold and stress tolerant organisms, explaining their higher activity than the other sediments. The strings of visible green biofilm suggests a stable community of eukaryotic microalgae.

The findings demonstrate that while the same microbial families and even genera are present in a range of habitats across the polar, sub polar and temperate regions, resilience to cryoconite-like cold and isolated conditions depends on specific attributes of microorganisms and community structure. The lack of an observable growth phase in many of the Signy Island sediments suggests that they are not resilient to cold and isolated conditions. However the incubations placed the sediments in different conditions immediately, whereas the cooling of the planet during the Cryogenian happened over a long period of time (Hoffman *et al*., 2017). While it may not be possible to find habitats that are immediately resilient to

the spectra of conditions of the Cryogenian, different areas of the modern cryosphere can be used as analogues for particular times and locations.

Conclusion

The supraglacial and periglacial habitats of Signy Island support distinct communities. The habitats furthest inland and on the ice cap were the most similar, variation increased down-glacier to the moraine. The activity of Cyanobacteria, as determined by intact polar lipid composition, set apart the warmer moraine stream from the neighbouring ponds which had the lowest proportion of active Cyanobacteria. Only the supraglacial streams were able to exhibit growth in *ex situ* incubation under 0.5°C. While certain microorganisms must have survived through a wide range of conditions and in a number of habitat formations to persist through the Cryogenian, resilience depends on particular highly local habitat conditions, community composition, and potentially community structure. Signy Island provides an analogous habitat for early melt during the Cryogenian, when local habitats began to merge, but still remained unconnected to colder distal ecosystems.

Conclusions

1. Hypothesis: Modern polar cryoconite hole communities are analogous to the biodiversity and eukaryotic key taxa of the Cryogenian

Cryoconite holes are known to be hotspots of biodiversity on glacier surfaces (Steinbock, 1936; Edwards *et al*., 2013c). They are host to bacteria, archaea, fungi, algae, protists, viruses and microanimals (Van Rompu, 1994; Cameron *et al*., 2012b; Bellas *et al*., 2013; Edwards *et al*., 2013b; Sommers *et al*., 2018; Lutz *et al*., 2019). This is one of the primary reasons they have been proposed as oases for life on Snowball Earth (Hoffman, 2016). Communities under the ocean would have been challenged by light limitation under ice. On the surface, the dry cold ice would have been a difficult environment for most microorganisms to establish. However, cryoconite holes could have provided a refuge of relative warmth, water, nutrient availability and community structure as they do on glaciers today.

1.1. Objective: Assess cryoconite hole microbial diversity and community composition

High-throughput 16S and 18S rRNA gene sequencing and intact polar lipid quantification was used to investigate the communities of a wide range of cryoconite holes from 15 locations across the Arctic and Antarctic. I recovered a total of 35 phyla and superphyla; a considerably higher taxonomic diversity compared to previous studies that did not use next generation sequencing (Mueller *et al*., 2001; Christner *et al*., 2003; Mueller and Pollard, 2004; Porazinska *et al*., 2004; Hodson *et al*., 2010; Cameron *et al*., 2012b). It was confirmed that the various biotic niches (grazer, predator, photoautotroph, chemotroph) are filled in every location and all locations sustained considerable biodiversity. Canada Glacier and Commonwealth Glacier cryoconite had particularly high species richness. I was able to determine the groups present to the family and genus level. Particularly abundant taxa included Microbacteriaceae, *Tychonema, Chamaesiphon, Solitalea,*

Acidiphilium, Vampyrellidae, *Pleurastrum, Chlamydomonas* and Ascomycota. I confirmed that there is a distinct difference between cryoconite communities found 60km onto the ice sheet and those within a few hundred metres of the ice margin in Greenland. There was significantly more variation between the types of Greenland samples (margin, ice core and ice sheet surface) than within groups. There is also a clear divide between the bacterial and microalgal communities of the Arctic and that of the Antarctic. While the Arctic cryoconite microalgae were dominated by *Chlamydomonas*, the Antarctic microalgae were dominated by *Pleurastrum*. The "core groups" (contributing to >1% of total relative abundance and present in the majority of cryoconite holes in each pole) of the Arctic and Antarctic shared only one common member, Microbacteriaceae. The compositional divide was also reflected in the intact polar lipid composition. One IPL group, the OL aminolipids, were absent in Antarctic samples but present in all Arctic samples. The highest contributor to the Antarctic IPLs was G-DAG, which is known to be the major constituent of Cyanobacterial lipids (Wada and Murata, 2006). In contrast, the highest contributor to Arctic IPLs was the PC-DAGs, which are commonly associated with eukaryotes, although they are also produced by a number of bacteria (Raetz, 1986; Geiger *et al*., 2013). Therefore cryoconite holes may be a global feature of glacier landscapes, but they are inhabited by regionally distinct microbial communities. This enabled identification of Cryogenian analogue communities according to similarities in taxonomic composition and local environment.

1.2. Objective: Compare cryoconite taxonomy to Cryogenian keystone taxa

All key Cryogenian taxa that were searched for were found in at least one location. Cercozoans and Alveolates were found at all locations. The presence of test-forming amoebozoa such as Rhogostoma show not only similar phylogenetically taxa present but also similar morphologies are present in modern cryoconite holes. Therefore, cryoconite holes are capable of supporting the key eukaryotic taxa which inhabited Snowball Earth. However, the Antarctic cryoconite holes in particular represent a strong analogue to Cryogenian communities due to the number of significant organisms present.

DNA and IPL results support the hypothesis that cryoconite sustains comparable taxa and biodiversity to the Cryogenian, as predicted by fossils, molecular clocks and known possible habitats. Due to the high species richness, close resemblance to the Cryogenian taxa, and parallels between source environment and Cryogenian environment, the Canada Glacier cryoconite was chosen for the remaining cryoconite experiments.

2. Hypothesis: Modern polar cryoconite is resilient to 'Snowball Earth' conditions

There are many differences between modern polar habitats and the equivalent Cryogenian environments. Temperatures during the cryochrons were considerably lower than modern day temperatures, only approaching 0°C at the tropical and equatorial regions (Abbot *et al.*, 2013). Therefore it was important to test whether cryoconite communities that are resilient to the low temperatures and freeze-adaptation of Antarctica could also grow in a low latitude environment.

2.1. Objective: Measure the response of cryoconite to 'low latitude Snowball Earth' light and temperature conditions

Cryoconite was incubated in serum vials under low-latitude type daily light dark cycles to simulate the warmest areas of the Cryogenian. The carbon production patterns were unchanged between cryoconite communities under the control and "Snowball Earth" conditions, as measured by oxygen saturation and ^{3}H-leucine incorporation. Results demonstrate that cryoconite communities are resilient to this change in light, since the relative organic carbon production trend remain unchanged between the light and day-night conditions. These results show that a cryoconite hole's community growth during a polar growth season is analogous to cryoconite communities growing under a day-night low latitude light cycle, despite the difference in light availability through the day. The presence and diversity of IPLs indicates an active community of both bacteria and eukaryotes under all light conditions.

Cryoconite was also incubated under daily freeze-thaw cycles, as might be expected to follow an equatorial day night cycle. Again, the carbon production pattern was

unchanged and the community was able to enter a growth phase comparable to the control community grown at a constant temperature. Despite the potential of regular freezing to damage microorganisms, the cryoconite community was able to tolerate these conditions.

2.2. Objective: Form cryoconite holes on ice in laboratory conditions, for closer replication of Snowball Earth conditions

I was able to create model cryoconite holes that develop in the same manner as cryoconite holes on glacier surfaces and compare productivity measurements against cryoconite incubated in serum vials. The cryoconite melted in an analogous topology to *in situ* cryoconite holes. Cryoconite was observed to melt the ice surface laterally to form a circular imprint in the underlying ice and then sink vertically into the ice surface. Melting then slowed and an ice lid formed at the water surface. Freezing of the cryoconite hole took place from the ice lid downwards and the sides of the cryoconite hole inwards. Several features of the ice cryoconite holes more closely represented a real cryoconite hole: dynamic water availability as the cryoconite hole thaws and freezes, an ice surface for adhesion, temperature buffering from ice below, reduction of light transmission as ice lid formed, dynamic sediment thickness and distribution. Although all of these factors have the potential to alter cryoconite hole biogeochemistry and therefore productivity (Fountain *et al*., 2004, 2008; Cook *et al*., 2010, 2015a; Zamora, 2018), there was a strong similarity between the oxygen concentrations measured from ice cryoconite hole and serum vial water columns. This firstly demonstrated the suitability of serum vials as analogues for cryoconite holes, and secondly the possibility studying cryoconite development in laboratories.

3. Hypothesis: Supraglacial and periglacial habitats contain distinct but interconnected ecosystems analogous to Snowball Earth meltwater habitats

While Cryoconite holes may have provided “biodiversity hotspots” on Snowball Earth, they cannot have been the sole habitat on the surface of the land and ice. Cryoconite is seeded from distal sources of microbe mineral aggregates. During times of melt, the cryoconite holes become more connected to streams and

meltwater channels, which in turn connect to ponds, lakes, moraine, sea and ice margins (Takeuchi *et al*., 2001a; Fountain *et al*., 2004). It has been proposed that for cryoconite to have provided a significant oasis for Snowball Earth life, many cryoconite holes and larger ponds known as 'cryoconite pans' must have formed, connected by streams. At the warmer beginnings and ends of the glaciations, these habitats may have been similar to those of the modern Arctic and maritime Antarctic. As time progressed to the mid-cryochrons, any supraglacial or periglacial habitats would have had to endure lower temperatures and reduced hydrological connections to neighbouring habitats. The ice cap of Signy Island was identified as a model system for the study of connections between supraglacial and periglacial habitats, and an analogue for 'islands of melt' at the start of Cryogenian deglaciations. However, Signy Island sediments showed little ability to grow under the cryoconite-type incubation conditions that simulated isolation and low temperature.

3.1. Objective: Investigate geographical and ecological connections between interconnected glacial and near-glacial microbial ecosystems on Signy Island

Several distinct habitat types were identified on and adjacent to the Signy Island ice cap, connected to one another by meltwater. These were cryoconite, supraglacial streams, ice margins, meltwater ponds and moraine streams. The habitats were highly dynamic and ephemeral. They were connected to one another by meltwater. Overall, the taxa contributing to the highest relative 16S rRNA gene abundance in the sediments included *Phormidesmis*, Leptolyngbyaceae, *Oryzihumus*, and *Acidiphilium*. However, as predicted, communities clustered by habitat type and were more similar between types than within types across several locations on the island. 16S rRNA gene composition varied with distance from the island's ice cap, with the supraglacial habitats showing the most similarity. The IPL profile, which indicates the active community in the sample, highlighted stark differences between the moraine habitats; the moraine stream contained an active mat of Cyanobacteria and the meltwater pond supported largely heterotrophs. Therefore during times of melt on Snowball Earth, as habitats become connected and merged, we can expect the community structure to change. Roughly one third of taxa

recovered co-occurred significantly with at least one other taxon, suggesting that some conditions were preferential for particular groups of organisms. However, since the majority of taxa were present at most or all locations, these did not form into clear clusters that could be tied to specific habitats or locations.

3.2. Objective: Determine whether Signy Island sediments are able to maintain isolated "oasis" communities through investigating community responses to isolated incubation

Under *ex situ* cryoconite hole-like incubation conditions the majority of sediments were unable to initiate a growth phase, with the exception of the supraglacial stream. We can therefore infer that highly local habitat differences impact community composition, and this community composition then determines resilience to habitat change. This supports the assertion that only particular supraglacial community types, such as McMurdo Dry Valleys cryoconite and Signy Island supraglacial streams, would have been successful through the Snowball Earth Cryochrons (Hoffman, 2016; Hoffman *et al.*, 2017). Therefore Signy Island is a suitable analogue for early deglaciation, where small areas began to form a variety of supraglacial and periglacial habitats as meltwater became more available under warmer temperatures (Abbot and Pierrehumbert, 2010; Le Hir *et al.*, 2010; Hoffman *et al.*, 2017).

Limitations and future directions

The identification of taxa throughout this study has relied on DNA metabarcoding. Firstly, genera are rarely all able to be assigned with 100% confidence, and assignments can vary depending which database is used. This is exemplified by the challenges in confidently assigning Cyanobacteria genera from Illumina sequencing. Secondly, the community surveyed does not necessarily reflect the active community of microorganisms. A comparison of the transcriptome of these habitats could provide a truer representation of the live microorganisms present (Bashiardes *et al*., 2016). During the growth experiments, it was also not possible to tell which organisms were active at the beginning and end of the incubations. It is possible that some organisms were killed or inactivated during storage of the communities

or through the experiment. Again, an assessment of active genes and microorganisms would allow us to confirm whether the ecosystem in its entirety was resilient to Snowball Earth conditions, or whether particular groups were responsible for the community productivity.

While IPLs provide some insight on the active community, IPLs often cannot yet be precisely tied to particular organisms or functions as they are produced by many microorganisms (Sturt *et al.*, 2004; Lipp *et al.*, 2008; Wörmer *et al.*, 2013; Evans *et al.*, 2017). As more comparisons of IPLs, taxonomy and transcriptome activity are published, it may be possible to resolve IPL "signature" compositions for improved utilisation of IPLs as an ecosystem diagnostic tool. Lipid biomarkers are becoming a key part of the Neoproterozoic fossil record (Brocks and Summons, 2003; Brocks and Pearson, 2005; Love *et al.*, 2009; Schubotz *et al.*, 2013; Zumberge *et al.*, 2018). By continuing to study the lipid signatures of modern day ecosystems, we can hopefully find further connections between organisms of the past and present.

DNA and IPL analyses here illustrated the differences between cryoconite between polar regions, and between habitats on Signy Island. However, the factors contributing to these differences are unclear. It would be beneficial to undertake a deeper study of biogeography and connections between ecosystem and local environment. This would allow for more accurate prediction of how the development of Snowball Earth habitats would have impacted the ecosystems within, and what the limits of transport and connection between ecosystems are.

In the incubation experiments, two proxies for carbon accumulation and therefore community growth were used. These methods produced different value ranges and used such different approaches that it was difficult to validate a true measure of community growth, particularly quantitatively. Additionally, creating a completely airtight system in which to use the dissolved oxygen method that is representative of a cryoconite hole is challenging and it appears in the experiments described here some oxygen leaked into the system through the experiment. In future cryoconite simulations purpose built vials and incubators would be beneficial. An incubation chamber where gas content could be controlled would aid in this kind of

experiment but also create an opportunity to incubate cryoconite under various Snowball Earth atmospheres.

Local relationships between environment and ecosystem could then be tested in climate chamber incubations. The creation of cryoconite holes in the laboratory presents a promising avenue for studying such connections. However, a larger climate controlled area would be beneficial for incubations carried out on ice. On glaciers, the thick ice acts as a temperature buffer to allow cryoconite holes to reach equilibrium of vertical melt into the glacier. A large quantity of ice must be used *ex situ* to create the same effect and allow meltwater environments on ice to be maintained for longer. As the dissolved oxygen method and ^{3}H-leucine methods produced significantly different values for carbon production, more effort would need to be made to produce reliable production quantification if studying specific impacts of local environment on growth.

The study of Signy Island as an analogue for a deglaciating Snowball Earth illustrates the advantages of using different areas of the cryosphere as analogues for different times and locations over the ~100 million years of the Cryogenian. It would be beneficial to examine the potential of modern low latitude supraglacial ecosystems such as those found in the Alps, Himalayas, and the glaciers of South America and Africa (Young and Hastenrath, 1991; Takeuchi *et al*., 2001a; Anesio *et al*., 2009; King *et al*., 2010; Edwards *et al*., 2014; Zawierucha *et al*., 2015, 2021). Although these areas are warmer than the polar regions and like the Signy Island sediments may not be resilient to the cold cryochron temperatures, they may be able to provide insight into the impact of a year of day-night cycles on supraglacial ecosystems.

This study has focused on the organisms and habitats that would have facilitated the survival of life on the Snowball Earth surface. However, identifying key genes for Snowball Earth tolerance was beyond the scope of this project. Combining transcriptomic data from environmental sediments and incubation experiments, metagenomic potential, and molecular clock records could identify what kinds of genes would have been required for survival in the Cryogenian (Sánchez-Baracaldo *et al.*, 2017; Zhang *et al.*, 2021). Some key genes of the Cryogenian may have since

been lost and new cold response genes could have been acquired during the many cycles of warming and cooling of the last 635 million years, in which case modern cold response genes could be used as potential analogues. However, molecular clocks may reveal some surviving genes haven been retained since the Proterozoic.

The climate conditions and geochronology of Snowball Earth are becoming increasingly tightly constrained (Abbot *et al.*, 2013; Hoffman, 2016; Prave *et al.*, 2016; Hoffman *et al.*, 2017). This has allowed researchers in this field to propose modern analogues for Snowball Earth habitats, and theoretical Cryogenian-specific Snowball Earth habitats (Hoffman, 2016; Hawes *et al.*, 2018). However, the biological evidence that microorganisms can survive in these 'Snowball Earth' type habitats is very limited. While supraglacial ecosystems may have provided hotspots of biodiversity, life in the oceans was undoubtedly a significant part of the global ecosystem. Yet the physiological response of microorganisms to Snowball Earth oceanic conditions has not been tested. In addition, it is not clear whether hypothetical habitats such as 'cryoconite pans' could sustain an ecosystem for any length of time, nor what these ecosystems would look like, as physical environment is highly influential on microbial community structure (Pearce, 2005; Cameron *et al*., 2012b; Edwards *et al*., 2013c; Langford *et al*., 2014; Millar *et al*., 2021). There is therefore considerable merit in developing the field of Snowball Earth microbiology.

Closing remarks

The primary aim of this study was to investigate the theory that supraglacial ecosystems could have provided refuge for life on Snowball Earth. This theory has so far centred on records of biodiversity and freeze tolerance in cryoconite and other supraglacial ecosystems. I have now been able to identify particularly suitable Cryogenian analogue cryoconite ecosystems through in-depth assessment of biodiversity across the polar regions and comparison to molecular clock and fossil records. This cryoconite was tested under 'Snowball Earth'-type environmental conditions, providing physiological evidence for the resilience of cryoconite to Snowball Earth conditions. Its success in these incubations set it apart from sub-Antarctic Signy Island sediments, illustrating that different areas of the modern

cryosphere can be used as analogues for different times and areas of Snowball Earth. The interconnected habitats on Signy Island show that habitat type has a strong impact on microbial community composition. From this we can infer what types of microorganisms may be have been successful as Snowball Earth ecosystems transformed from isolated meltwater pockets to a deglaciating 'Slushball' covered in meltwater streams, ponds and deposits of sediment at ice margins (Abbot and Pierrehumbert, 2010; Le Hir *et al.*, 2010). Together these results support the theory that supraglacial ecosystems could have created oases for biodiversity on the Cryogenian Snowball Earth, and modern polar ecosystems provide functional analogues for these communities.

Bibliography

Aalto, K. R. (1986). Depositional Sequence of Argillite, Diamictite, Hyaloclastite, and Lava Flows within the Franciscan Complex, Northern California. *J. Geol.* 94, 744–752.

Abbot, D. S. (2014). Resolved Snowball Earth Clouds. *J. Clim.* 27, 4391–4402.

Abbot, D. S., and Pierrehumbert, R. T. (2010). Mudball: Surface dust and Snowball Earth deglaciation. *J. Geophys. Res.* 115, D03104.

Abbot, D. S., Voigt, A., Li, D., Hir, G. L., Pierrehumbert, R. T., Branson, M., *et al*. (2013). Robust elements of Snowball Earth atmospheric circulation and oases for life. *J. Geophys. Res. D: Atmos.* 118, 6017–6027.

Allmon, W. D., Smrecak, T. A., and Ross, R. M. (2010). Climate Change Past, Present, and Future: A Very Short Guide. Available at: https://www.researchgate.net/publication/322641763_Climate_Change_Past_Present_and_Future_A_Very_Short_Guide [Accessed January 12, 2022].

Amaral-Zettler, L. A., McCliment, E. A., Ducklow, H. W., and Huse, S. M. (2009). A method for studying protistan diversity using massively parallel sequencing of V9 hypervariable regions of small-subunit ribosomal RNA genes. *PLoS One* 4, e6372.

Ammar, Y., Swailes, D., Bridgens, B., and Chen, J. (2015). Influence of surface roughness on the initial formation of biofilm. *Surf. Coat. Technol.* 284, 410–416.

Anesio, A. M., Hodson, A. J., Fritz, A., Psenner, R., and Sattler, B. (2009). High microbial activity on glaciers: importance to the global carbon cycle. *Glob. Chang. Biol.* 15, 955–960.

Anesio, A. M., and Laybourn-Parry, J. (2012). Glaciers and ice sheets as a biome. *Trends Ecol. Evol.* 27, 219–225.

Anesio, A. M., and Laybourn-Parry, J. (2021). 'Ecology of Arctic Glaciers', in *Arctic Ecology* (Wiley), 133–158.

Anesio, A. M., Lutz, S., Chrismas, N. A. M., and Benning, L. G. (2017). The microbiome of glaciers and ice sheets. *NPJ Biofilms Microbiomes* 3, 10.

Anesio, A. M., Sattler, B., Foreman, C., Telling, J., Hodson, A., Tranter, M., *et al*. (2010). Carbon fluxes through bacterial communities on glacier surfaces. *Ann. Glaciol.* 51, 32–40.

Archer, S. D. J., Lee, K. C., Caruso, T., Maki, T., Lee, C. K., Cary, S. C., *et al*. (2019). Airborne microbial transport limitation to isolated Antarctic soil habitats. *Nat Microbiol* 4, 925–932.

Aronson, R. B., Thatje, S., Clarke, A., Peck, L. S., Blake, D. B., Wilga, C. D., *et al*. (2007). Climate Change and Invasibility of the Antarctic Benthos. *Annu. Rev. Ecol. Evol. Syst.* 38, 129–154.

Arrigo, K. R., Perovich, D. K., Pickart, R. S., Brown, Z. W., van Dijken, G. L., Lowry, K. E., *et al*. (2012). Massive phytoplankton blooms under Arctic sea ice. *Science* 336, 1408.

Atkins, C. B., and Dunbar, G. B. (2009). Aeolian sediment flux from sea ice into Southern McMurdo Sound, Antarctica. *Glob. Planet. Change* 69, 133–141.

Bagshaw, E. A., Stibal, M., Anesio, A. M., Bellas, C., Tranter, M., Telling, J., *et al*. (2012). 'Glacier Surface Habitats', in *Life at Extremes: Environments, Organisms, and Strategies for Survival*, ed. E. Bell (CABI), 155–175.

Bagshaw, E. A., Tranter, M., Fountain, A. G., Welch, K. A., Basagic, H., and Lyons, W. B. (2007). Biogeochemical evolution of cryoconite holes on Canada Glacier, Taylor Valley, Antarctica. *J. Geophys. Res.* 112, G04S35.

Bagshaw, E. A., Tranter, M., Wadham, J. L., Fountain, A. G., and Basagic, H. (2010). Dynamic behaviour of supraglacial lakes on cold polar glaciers: Canada Glacier, McMurdo Dry Valleys, Antarctica. *J. Glaciol.* 56, 366–368.

Bagshaw, E. A., Tranter, M., Wadham, J. L., Fountain, A. G., Dubnick, A., and Fitzsimons, S. (2016a). Processes controlling carbon cycling in Antarctic glacier surface ecosystems. *Geochemical Perspectives Letters* 2, 44–54.

Bagshaw, E. A., Tranter, M., Wadham, J. L., Fountain, A. G., and Mowlem, M. (2011). High-resolution monitoring reveals dissolved oxygen dynamics in an Antarctic cryoconite hole. *Hydrol. Process.* 25, 2868–2877.

Bagshaw, E. A., Wadham, J. L., Tranter, M., Perkins, R., Morgan, A., Williamson, C. J., *et al*. (2016b). Response of Antarctic cryoconite microbial communities to light. *FEMS Microbiol. Ecol.* 92, fiw076.

Bagshaw, Elizabeth, A., Tranter, M., Fountain, Andrew, G., Welch, K., *et al*. (2013). Do Cryoconite Holes have the Potential to be Significant Sources of C, N, and P to Downstream Depauperate Ecosystems of Taylor Valley, Antarctica? *Arct. Antarct. Alp. Res.* 45, 440–454.

Bale, N. J., Hopmans, E. C., Dorhout, D., Stal, L. J., and Schouten, S. (2018). A novel heterocyst glycolipid detected in a pelagic N2 -fixing cyanobacterium of the genus Calothrix. *Org. Geochem.* 123.

Bao, H., Lyons, J. R., and Zhou, C. (2008). Triple oxygen isotope evidence for elevated CO2 levels after a Neoproterozoic glaciation. *Nature* 453, 504–506.

Barnes, D. K. A., and Conlan, K. E. (2007). Disturbance, colonization and development of Antarctic benthic communities. *Philos. Trans. R. Soc. Lond. B Biol. Sci.* 362, 11–38.

Bar-On, Y. M., and Milo, R. (2019). The Biomass Composition of the Oceans: A Blueprint of Our Blue Planet. *Cell* 179, 1451–1454.

Bartlett, J. C., Convey, P., and Hayward, S. A. L. (2020). Surviving the Antarctic winter-Life Stage Cold Tolerance and Ice Entrapment Survival in The Invasive Chironomid Midge Eretmoptera murphyi. *Insects* 11.

Bashiardes, S., Zilberman-Schapira, G., and Elinav, E. (2016). Use of Metatranscriptomics in Microbiome Research. *Bioinform. Biol. Insights* 10, 19–25.

Bauersachs, T., Hopmans, E. C., Compaoré, J., Stal, L. J., Schouten, S., and Damsté, J. S. S. (2009). Rapid analysis of long-chain glycolipids in heterocystous cyanobacteria using high-performance liquid chromatography coupled to electrospray ionization tandem mass spectrometry. *Rapid Commun. Mass Spectrom.* 23, 1387–1394.

Becker, B. (2013). Snow ball earth and the split of Streptophyta and Chlorophyta. *Trends Plant Sci.* 18, 180–183.

Becker, B., and Marin, B. (2009). Streptophyte algae and the origin of embryophytes. *Ann. Bot.* 103, 999–1004.

Bellas, C. M., Anesio, A. M., Telling, J., Stibal, M., Tranter, M., and Davis, S. (2013). Viral impacts on bacterial communities in Arctic cryoconite. *Environ. Res. Lett.* 8, 045021.

Bellas, C. M., Schroeder, D. C., Edwards, A., Barker, G., and Anesio, A. M. (2020). Flexible genes establish widespread bacteriophage pan-genomes in cryoconite hole ecosystems. *Nat. Commun.* 11, 4403.

Benítez-Páez, A., Portune, K. J., and Sanz, Y. (2016). Species-level resolution of 16S rRNA gene amplicons sequenced through the MinION^{TM} portable nanopore sequencer. *Gigascience* 5, 4.

Benn, D. I., Le Hir, G., Bao, H., Donnadieu, Y., Dumas, C., Fleming, E. J., *et al*. (2015). Orbitally forced ice sheet fluctuations during the Marinoan Snowball Earth glaciation. *Nat. Geosci.* 8, ngeo2502.

Berggren, S. (1871). *Alger från Grönlands inlandis*. PA Norstedt.

Bernhard, G., Booth, C. R., Ehramjian, J. C., and Nichol, S. E. (2006). UV climatology at McMurdo Station, Antarctica, based on version 2 data of the National Science Foundation's Ultraviolet Radiation Monitoring Network. *J. Geophys. Res.* 111.

Blazewicz, S. J., Barnard, R. L., Daly, R. A., and Firestone, M. K. (2013). Evaluating rRNA as an indicator of microbial activity in environmental communities: limitations and uses. *ISME J.* 7, 2061–2068.

Bligh, E. G., and Dyer, W. J. (1959). A rapid method of total lipid extraction and purification. *Can. J. Biochem. Physiol.* 37, 911–917.

Bobrovskiy, I., Hope, J. M., Nettersheim, B. J., Volkman, J. K., Hallmann, C., and Brocks, J. J. (2021). Algal origin of sponge sterane biomarkers negates the oldest evidence for animals in the rock record. *Nat Ecol Evol* 5, 165–168.

Boetius, A., Anesio, A. M., Deming, J. W., Mikucki, J. A., and Rapp, J. Z. (2015). Microbial ecology of the cryosphere: sea ice and glacial habitats. *Nat. Rev. Microbiol.* 13, 677–690.

Bolyen, E., Rideout, J. R., Dillon, M. R., Bokulich, N. A., Abnet, C. C., Al-Ghalith, G. A., *et al*. (2019). Reproducible, interactive, scalable and extensible microbiome data science using QIIME 2. *Nat. Biotechnol.* 37, 852–857.

Bottos, E. M., Woo, A. C., Zawar-Reza, P., Pointing, S. B., and Cary, S. C. (2014). Airborne bacterial populations above desert soils of the McMurdo Dry Valleys, Antarctica. *Microb. Ecol.* 67, 120–128.

Boyd, E. S., Hamilton, T. L., Havig, J. R., Skidmore, M. L., and Shock, E. L. (2014). Chemolithotrophic primary production in a subglacial ecosystem. *Appl. Environ. Microbiol.* 80, 6146–6153.

Boyd, E. S., Skidmore, M., Mitchell, A. C., Bakermans, C., and Peters, J. W. (2010). Methanogenesis in subglacial sediments. *Environ. Microbiol. Rep.* 2, 685–692.

Bradley, J. A., Arndt, S., Šabacká, M., Benning, L. G., Barker, G. L., Blacker, J. J., *et al*. (2016). Microbial dynamics in a High Arctic glacier forefield: a combined field, laboratory, and modelling approach. *Biogeosciences* 13, 5677–5696.

Braun, C., Hörner, J., Voigt, A., and Pinto, J. G. (2022). Ice-free tropical waterbelt for Snowball Earth events questioned by uncertain clouds. *Nat. Geosci.* 15, 489–493.

Bray, J. R., and Curtis, J. T. (1957). An ordination of the upland forest communities of southern Wisconsin. *Ecol. Monogr.* 27, 325–349.

Bristow, T. F., and Kennedy, M. J. (2008). Carbon isotope excursions and the oxidant budget of the Ediacaran atmosphere and ocean. *Geology* 36, 863–866.

Brocks, J. J. (2018). The transition from a cyanobacterial to algal world and the emergence of animals. *Emerg. Top. Life Sci.*, ETLS20180039.

Brocks, J. J., Jarrett, A. J. M., Sirantoine, E., Hallmann, C., Hoshino, Y., and Liyanage, T. (2017). The rise of algae in Cryogenian oceans and the emergence of animals. *Nature* 548, 578–581.

Brocks, J. J., and Pearson, A. (2005). Building the Biomarker Tree of Life. *Rev. Mineral. Geochem.* 59, 233–258.

Brocks, J. J., and Summons, R. E. (2003). Sedimentary Hydrocarbons, Biomarkers for Early Life. *Treatise on Geochemistry* 8, 682.

Butterfield, N. J. (2000). Bangiomorpha pubescens n. gen., n. sp.: implications for the evolution of sex, multicellularity, and the Mesoproterozoic/Neoproterozoic radiation of eukaryotes. *Paleobiology* 26, 386–404.

Butterfield, N. J., Knoll, A. H., and Swett, K. (1988). Exceptional preservation of fossils in an Upper Proterozoic shale. *Nature* 334, 424–427.

Callahan, B. J., McMurdie, P. J., Rosen, M. J., Han, A. W., Johnson, A. J. A., and Holmes, S. P. (2016). DADA2: High-resolution sample inference from Illumina amplicon data. *Nat. Methods* 13, 581–583.

Cameron, K. A., Hodson, A. J., and Osborn, A. M. (2012a). Carbon and nitrogen biogeochemical cycling potentials of supraglacial cryoconite communities. *Polar Biol.* 35, 1375–1393.

Cameron, K. A., Hodson, A. J., and Osborn, A. M. (2012b). Structure and diversity of bacterial, eukaryotic and archaeal communities in glacial cryoconite holes from the Arctic and the Antarctic. *FEMS Microbiol. Ecol.* 82, 254–267.

Cameron, K. A., Müller, O., Stibal, M., Edwards, A., and Jacobsen, C. S. (2020). Glacial microbiota are hydrologically connected and temporally variable. *Environ. Microbiol.* 22, 3172–3187.

Cameron, K. A., Stibal, M., Zarsky, J. D., Gözdereliler, E., Schostag, M., and Jacobsen, C. S. (2016). Supraglacial bacterial community structures vary across the Greenland ice sheet. *FEMS Microbiol. Ecol.* 92.

Caporaso, J. G., Lauber, C. L., Walters, W. A., Berg-Lyons, D., Huntley, J., Fierer, N., *et al*. (2012). Ultra-high-throughput microbial community analysis on the Illumina HiSeq and MiSeq platforms. *ISME J.* 6, 1621–1624.

Caporaso, J. G., Lauber, C. L., Walters, W. A., Berg-Lyons, D., Lozupone, C. A., Turnbaugh, P. J., *et al*. (2011). Global patterns of 16S rRNA diversity at a depth of millions of sequences per sample. *Proc. Natl. Acad. Sci. U. S. A.* 108 Suppl 1, 4516–4522.

Carns, R., Brandt, R. E., and Warren, S. (2015). Salt precipitation in sea ice and its effect on albedo, with application to Snowball Earth. 120.

Cavicchioli, R. (2006). Cold-adapted archaea. *Nat. Rev. Microbiol.* 4, 331–343.

Chang, Q., Luan, Y., and Sun, F. (2011). Variance adjusted weighted UniFrac: a powerful beta diversity measure for comparing communities based on phylogeny. *BMC Bioinformatics* 12, 118.

Charlesworth, J. K. (1966). *The Quaternary Era: with special reference to its glaciation*. St. Martin's Press.

Cheng, M., Li, C., Chen, X., Zhou, L., Algeo, T. J., Ling, H.-F., *et al*. (2018). Delayed Neoproterozoic oceanic oxygenation: Evidence from Mo isotopes of the Cryogenian Datangpo Formation. *Precambrian Res.* 319, 187–197.

Chintalapati, S., Kiran, M. D., and Shivaji, S. (2004). Role of membrane lipid fatty acids in cold adaptation. *Cell. Mol. Biol.* 50, 631–642.

Chong, C. W., Dunn, M. J., Convey, P., Tan, G. Y. A., Wong, R. C. S., and Tan, I. K. P. (2009). Environmental influences on bacterial diversity of soils on Signy Island, maritime Antarctic. *Polar Biol.* 32, 1571–1582.

Chong, C. W., Pearce, D. A., Convey, P., Tan, G. Y. A., Wong, R. C. S., and Tan, I. K. P. (2010). High levels of spatial heterogeneity in the biodiversity of soil prokaryotes on Signy Island, Antarctica. *Soil Biol. Biochem.* 42, 601–610.

Chrismas, N. A. M., Barker, G., Anesio, A. M., and Sánchez-Baracaldo, P. (2016). Genomic mechanisms for cold tolerance and production of exopolysaccharides in the Arctic cyanobacterium Phormidesmis priestleyi BC1401. *BMC Genomics* 17, 533.

Christie-Blick, N., Sohl, L. E., and Kennedy, M. J. (1999). Considering a Neoproterozoic snowball Earth.

Christner, B. C., Kvitko, B. H., 2nd, and Reeve, J. N. (2003). Molecular identification of bacteria and Eukarya inhabiting an Antarctic cryoconite hole. *Extremophiles* 7, 177–183.

Clark, P. U., Dyke, A. S., Shakun, J. D., Carlson, A. E., Clark, J., Wohlfarth, B., *et al*. (2009). The Last Glacial Maximum. *Science* 325, 710–714.

Clarke, K. R. (1993). Non-parametric multivariate analyses of changes in community structure. *Austral Ecol.* 18, 117–143.

Cohen, P. A., and Macdonald, F. A. (2015). The Proterozoic Record of Eukaryotes. *Paleobiology* 41, 610–632.

Colbath, G. K., and Grenfell, H. R. (1995). Review of biological affinities of Paleozoic acid-resistant, organic-walled eukaryotic algal microfossils (including "acritarchs"). *Rev. Palaeobot. Palynol.* 86, 287–314.

Conway-Morris, S. (2003). The Cambrian 'explosion' of metazoans and molecular biology: would Darwin be satisfied? *Int. J. Dev. Biol.* 47, 505–515.

Cook, J., Edwards, A., and Hubbard, A. (2015a). Biocryomorphology: Integrating Microbial Processes with Ice Surface Hydrology, Topography, and Roughness. *Front Earth Sci. Chin.* 3, 78.

Cook, J., Edwards, A., Takeuchi, N., and Irvine-Fynn, T. (2015b). Cryoconite: The dark biological secret of the cryosphere. *Prog. Phys. Geogr.* 40, 66–111.

Cook, J., Hodson, A., Telling, J., Anesio, A., Irvine-Fynn, T., and Bellas, C. (2010). The mass–area relationship within cryoconite holes and its implications for primary production. *Ann. Glaciol.* 51, 106–110.

Cook, J. M., Edwards, A., Bulling, M., Mur, L. A. J., Cook, S., Gokul, J. K., *et al*. (2016). Metabolome-mediated biocryomorphic evolution promotes carbon fixation in Greenlandic cryoconite holes. *Environ. Microbiol.* 18, 4674–4686.

Corsetti, F. A., Awramik, S. M., and Pierce, D. (2003). A complex microbiota from snowball Earth times: microfossils from the Neoproterozoic Kingston Peak Formation, Death Valley, USA. *Proc. Natl. Acad. Sci. U. S. A.* 100, 4399–4404.

Courtillot, V., and Gaudemer, Y. (1996). Effects of mass extinctions on biodiversity. *Nature* 381, 146.

Darcy, J. L., Gendron, E. M. S., Sommers, P., Porazinska, D. L., and Schmidt, S. K. (2018). Island Biogeography of Cryoconite Hole Bacteria in Antarctica's Taylor Valley and Around the World. *Frontiers in Ecology and Evolution* 6, 180.

Day, E. S., James, N. P., Narbonne, G. M., and Dalrymple, R. W. (2004). A sedimentary prelude to Marinoan glaciation, Cryogenian (Middle Neoproterozoic) Keele Formation, Mackenzie Mountains, northwestern Canada. *Precambrian Res.* 133, 223–247.

de Caire, G. Z., de Cano, M. S., Zaccaro de Mulé, M. C., Palma, R. M., and Colombo, K. (1997). Exopolysaccharide of Nostoc muscorum (Cyanobacteria) in the aggregation of soil particles. *J. Appl. Phycol.* 9, 249–253.

de Vries, J., and Archibald, J. M. (2018). Plant evolution: landmarks on the path to terrestrial life. *New Phytol.* 217, 1428–1434.

de Vries, J., Stanton, A., Archibald, J. M., and Gould, S. B. (2016). Streptophyte Terrestrialization in Light of Plastid Evolution. *Trends Plant Sci.* 21, 467–476.

Deamer, D., Akeson, M., and Branton, D. (2016). Three decades of nanopore sequencing. *Nat. Biotechnol.* 34, 518–524.

DeGeer, G. (1912). A geochronology of the last 12,000 years. in *Eleventh International Geological Congress, Stockholom* (ci.nii.ac.jp), 241–253.

Des Marais, D. J., Strauss, H., Summons, R. E., and Hayes, J. M. (1992). Carbon isotope evidence for the stepwise oxidation of the Proterozoic environment. *Nature* 359, 605–609.

Ding, S., Lange, M., Lipp, J., Schwab, V. F., Chowdhury, S., Pollierer, M. M., *et al*. (2020). Characteristics and origin of intact polar lipids in soil organic matter. *Soil Biol. Biochem.* 151, 108045.

Dong, Z., Kang, S., Qin, D., Li, Y., Wang, X., Ren, J., *et al*. (2016a). Provenance of cryoconite deposited on the glaciers of the Tibetan Plateau: New insights from Nd-Sr isotopic composition and size distribution. *J. Geophys. Res.* 121, 7371–7382.

Dong, Z., Qin, D., Kang, S., Liu, Y., Li, Y., Huang, J., *et al*. (2016b). Individual particles of cryoconite deposited on the mountain glaciers of the Tibetan Plateau: Insights into chemical composition and sources. *Atmos. Environ.* 138, 114–124.

Donlan, R. M. (2002). Biofilms: Microbial Life on Surfaces. *Emerging Infectious Disease journal* 8, 881.

Doran, P. T., Priscu, J. C., Lyons, W. B., Walsh, J. E., Fountain, A. G., McKnight, D. M., *et al*. (2002). Antarctic climate cooling and terrestrial ecosystem response. *Nature* 415, 517–520.

Douzery, E. J. P., Snell, E. A., Bapteste, E., Delsuc, F., and Philippe, H. (2004). The timing of eukaryotic evolution: does a relaxed molecular clock reconcile proteins and fossils? *Proc. Natl. Acad. Sci. U. S. A.* 101, 15386–15391.

Droser, M. L., and Gehling, J. G. (2015). The advent of animals: The view from the Ediacaran. *Proc. Natl. Acad. Sci. U. S. A.* 112, 4865–4870.

Dubnick, A., Wadham, J., Tranter, M., Sharp, M., Orwin, J., Barker, J., *et al*. (2017). Trickle or treat: The dynamics of nutrient export from polar glaciers. *Hydrol. Process.* 31, 1776–1789.

Edwards, A., Anesio, A. M., Rassner, S. M., Sattler, B., Hubbard, B., Perkins, W. T., *et al*. (2011). Possible interactions between bacterial diversity, microbial activity and supraglacial hydrology of cryoconite holes in Svalbard. *ISME J.* 5, 150–160.

Edwards, A., Cameron, K. A., Cook, J. M., Debbonaire, A. R., Furness, E., Hay, M. C., *et al*. (2020). Microbial genomics amidst the Arctic crisis. *Microb Genom* 6.

Edwards, A., Debbonaire, A. R., Nicholls, S. M., Rassner, S. M. E., Sattler, B., Cook, J. M., *et al*. (2019). In-field metagenome and 16S rRNA gene amplicon nanopore sequencing robustly characterize glacier microbiota. *bioRxiv*, 073965.

Edwards, A., Douglas, B., Anesio, A. M., Rassner, S. M., Irvine-Fynn, T. D. L., Sattler, B., *et al*. (2013a). A distinctive fungal community inhabiting cryoconite holes on glaciers in Svalbard. *Fungal Ecol.* 6, 168–176.

Edwards, A., Mur, L. A. J., Girdwood, S. E., Anesio, A. M., Stibal, M., Rassner, S. M. E., *et al*. (2014). Coupled cryoconite ecosystem structure-function relationships are revealed by comparing bacterial communities in alpine and Arctic glaciers. *FEMS Microbiol. Ecol.* 89, 222–237.

Edwards, A., Pachebat, J. A., Swain, M., Hegarty, M., Hodson, A. J., Irvine-Fynn, T. D. L., *et al*. (2013b). A metagenomic snapshot of taxonomic and functional diversity in an alpine glacier cryoconite ecosystem. *Environ. Res. Lett.* 8, 035003.

Edwards, A., Rassner, S. M. E., Anesio, A. M., Worgan, H. J., Irvine-Fynn, T. D. L., Wyn Williams, H., *et al*. (2013c). Contrasts between the cryoconite and ice-marginal bacterial communities of Svalbard glaciers. *Polar Res.* 32, 19468.

Ehlers, J., and Gibbard, P. (2008). Extent and chronology of Quaternary glaciation. *Episodes* 31, 211–218.

Ehrenberg, G. C. (1832). Uber die Entwicklung und Lebensdauer der Infusionsthieve, nebst ferneren Beitragen zu einer Vergleichung ihrer organischen System. *Koniglichen Akademie der Wissenschaften zu Berlin Abhandlungen, 1831, Physikalische Abhandlungen*, 1–154.

Eisbacher, G. H. (1981). Sedimentary tectonics and glacial record in the Windermere supergroup, Mackenzie mountains, northwestern Canada. Available at: https://pascal-francis.inist.fr/vibad/index.php?action=getRecordDetail&idt=PASCALGEODEBRGM8320466873 [Accessed December 7, 2021].

Eisenlord, S. D., Zak, D. R., and Upchurch, R. A. (2012). Dispersal limitation and the assembly of soil Actinobacteria communities in a long-term chronosequence. *Ecol. Evol.* 2, 538–549.

Epp, L. S., Gussarova, G., Boessenkool, S., Olsen, J., Haile, J., Schrøder-Nielsen, A., *et al*. (2015). Lake sediment multi-taxon DNA from North Greenland records early post-glacial appearance of vascular plants and accurately tracks environmental changes. *Quat. Sci. Rev.* 117, 152–163.

Erwin, D. H. (2015). Early metazoan life: divergence, environment and ecology. *Philos. Trans. R. Soc. Lond. B Biol. Sci.* 370.

Evans, D. A. D. (2000). Stratigraphic, geochronological, and paleomagnetic constraints upon the Neoproterozoic climatic paradox. *Am. J. Sci.* 300, 347–433.

Evans, T. W., Kalambokidis, M. J., Jungblut, A. D., Millar, J. L., Bauersachs, T., Grotheer, H., *et al*. (2022). Lipid Biomarkers From Microbial Mats on the McMurdo Ice Shelf, Antarctica: Signatures for Life in the Cryosphere. *Front. Microbiol.* 13, 903621.

Evans, T. W., Wörmer, L., Lever, M. A., Lipp, J. S., Lagostina, L., Lin, Y.-S., *et al*. (2017). Size and composition of subseafloor microbial community in the Benguela

upwelling area examined from intact membrane lipid and DNA analysis. *Org. Geochem.* 111, 86–100.

Evitt, W. R. (1963). A DISCUSSION AND PROPOSALS CONCERNING FOSSIL DINOFLAGELLATES, HYSTRICHOSPHERES, AND ACRITARCHS, I. *Proc. Natl. Acad. Sci. U. S. A.* 49, 158–164.

Eyles, N., and Januszczak, N. (2004). 'Zipper-rift': a tectonic model for Neoproterozoic glaciations during the breakup of Rodinia after 750 Ma. *Earth-Sci. Rev.* 65, 1–73.

Eyles, N., and Lazorek, M. (2014). 'Glacigenic Lithofacies Sediments in Glaciated Landscapes☆', in *Reference Module in Earth Systems and Environmental Sciences* (Elsevier).

Faizal, M., and Ahmed, M. R. (2011). On the ocean heat budget and ocean thermal energy conversion. *Int. J. Energy Res.* 35, 1119–1144.

Feng, L.-J., Chu, X.-L., Huang, J., Zhang, Q.-R., and Chang, H.-J. (2010). Reconstruction of paleo-redox conditions and early sulfur cycling during deposition of the Cryogenian Datangpo Formation in South China. *Gondwana Res.* 18, 632–637.

Fisher, C. R., Takai, K., and Le Bris, N. (2007). Hydrothermal Vent Ecosystems. *Oceanography* 20, 14–23.

Flint, R. F., Sanders, J. E., and Rodgers, J. (1960). DIAMICTITE, A SUBSTITUTE TERM FOR SYMMICTITE. *GSA Bulletin* 71, 1809–1810.

Foreman, C. M., Sattler, B., Mikucki, J. A., Porazinska, D. L., and Priscu, J. C. (2007). Metabolic activity and diversity of cryoconites in the Taylor Valley, Antarctica. *J. Geophys. Res.* 112.

Fountain, A. G., Nylen, T. H., Tranter, M., and Bagshaw, E. (2008). Temporal variations in physical and chemical features of cryoconite holes on Canada Glacier, McMurdo Dry Valleys, Antarctica. *J. Geophys. Res.* 113, G01S92.

Fountain, A. G., Tranter, M., Nylen, T. H., Lewis, K. J., and Mueller, D. R. (2004). Evolution of cryoconite holes and their contribution to meltwater runoff from glaciers in the McMurdo Dry Valleys, Antarctica. *J. Glaciol.* 50, 35–45.

Franzetti, A., Navarra, F., Tagliaferri, I., Gandolfi, I., Bestetti, G., Minora, U., *et al*. (2017). Potential sources of bacteria colonizing the cryoconite of an Alpine glacier. *PLoS One* 12, e0174786.

Fujii, M., Takano, Y., Kojima, H., Hoshino, T., Tanaka, R., and Fukui, M. (2010). Microbial community structure, pigment composition, and nitrogen source of red snow in Antarctica. *Microb. Ecol.* 59, 466–475.

Gaucher, C., and Sprechmann, P. (2009). 'Chapter 9.1 Neoproterozoic Acritarch Evolution', in *Developments in Precambrian Geology*, eds. C. Gaucher, A. N. Sial, H. E. Frimmel, and G. P. Halverson (Elsevier), 319–326.

Geiger, O., González-Silva, N., López-Lara, I. M., and Sohlenkamp, C. (2010). Amino acid-containing membrane lipids in bacteria. *Prog. Lipid Res.* 49, 46–60.

Gerdel, R. W., and Drouet, F. (1960). The Cryoconite of the Thule Area, Greenland. *Trans. Am. Microsc. Soc.* 79, 256–272.

Gibson, R. N., and Atkinson, R. J. A. (2003). *Oceanography and Marine Biology, An Annual Review, Volume 41: An Annual Review:*. CRC Press.

Gillies, J. E., Kuehn, K. A., Francoeur, S. N., and Neely, R. K. (2006). Application of the [3H]leucine incorporation technique for quantification of bacterial secondary production associated with decaying wetland plant litter. *Appl. Environ. Microbiol.* 72, 5948–5956.

Gokul, J. K., Cameron, K. A., Irvine-Fynn, T. D. L., Cook, J. M., Hubbard, A., Stibal, M., *et al*. (2019). Illuminating the dynamic rare biosphere of the Greenland Ice Sheet's Dark Zone. *FEMS Microbiol. Ecol.* 95.

Gokul, J. K., Hodson, A. J., Saetnan, E. R., Irvine-Fynn, T. D. L., Westall, P. J., Detheridge, A. P., *et al*. (2016). Taxon interactions control the distributions of cryoconite bacteria colonizing a High Arctic ice cap. *Mol. Ecol.* 25, 3752–3767.

Gold, D. A., Caron, A., Fournier, G. P., and Summons, R. E. (2017). Paleoproterozoic sterol biosynthesis and the rise of oxygen. *Nature* 543, 420–423.

Goldfine, H., and Hagen, P. (1968). N-methyl groups in bacterial lipids. 3. Phospholipids of hyphomicrobia. *J. Bacteriol.* 95, 367–375.

Gombos, Z., Kanervo, E., Tsvetkova, N., Sakamoto, T., Aro, E. M., and Murata, N. (1997). Genetic Enhancement of the Ability to Tolerate Photoinhibition by Introduction of Unsaturated Bonds into Membrane Glycerolipids. *Plant Physiol.* 115, 551–559.

Goodman, J. C., and Pierrehumbert, R. T. (2003). Glacial flow of floating marine ice in "Snowball Earth". *J. Geophys. Res.* 108, 3308.

Goodman, J. C., and Strom, D. C. (2013). Feedbacks in a coupled ice-atmosphere-dust model of the glacial Neoproterozoic "Mudball Earth". *J. Geophys. Res.* 118, 11,546-11,557.

Gorodetskaya, I. V., Van Lipzig, N. P. M., Van den Broeke, M. R., Mangold, A., Boot, W., and Reijmer, C. H. (2013). Meteorological regimes and accumulation patterns at Utsteinen, Dronning Maud Land, East Antarctica: Analysis of two contrasting years. *J. Geophys. Res.* 118, 1700–1715.

Graham, L. E., Cook, M. E., Wilcox, L. W., Graham, J., Taylor, W., Wellman, C. H., *et al*. (2013). Resistance of Filamentous Chlorophycean, Ulvophycean, and Xanthophycean Algae to Acetolysis: Testing Proterozoic and Paleozoic Microfossil Attributions. *Int. J. Plant Sci.* 174, 947–957.

Greco, C., Andersen, D. T., Hawes, I., Bowles, A. M. C., Yallop, M. L., Barker, G., *et al*. (2020). Microbial Diversity of Pinnacle and Conical Microbial Mats in the Perennially Ice-Covered Lake Untersee, East Antarctica. *Front. Microbiol.* 11, 607251.

Gribbon, P. W. F. (1979). Cryoconite Holes on Sermikavsak, West Greenland. *J. Glaciol.* 22, 177–181.

Grotzinger, J. P., and Knoll, A. H. (1995). Anomalous carbonate precipitates: is the Precambrian the key to the Permian? *Palaios* 10, 578–596.

Hambrey, M. J. (1987). *Late Precambrian Glaciation of Central East Greenland*. Museum Tusculanum Press.

Handelsman, J. (2004). Metagenomics: application of genomics to uncultured microorganisms. *Microbiol. Mol. Biol. Rev.* 68, 669–685.

Hanna, E., Mernild, S. H., Cappelen, J., and Steffen, K. (2012). Recent warming in Greenland in a long-term instrumental (1881–2012) climatic context: I. Evaluation of surface air temperature records. *Environ. Res. Lett.* 7, 045404.

Hanssen-Bauer, M. (1990). The climate of Spitsbergen. *Klima, Den Norske Meteorologiske Institutt Rapport* 39, 1–40.

Harrold, Z. R., Skidmore, M. L., Hamilton, T. L., Desch, L., Amada, K., van Gelder, W., *et al*. (2015). Aerobic and Anaerobic Thiosulfate Oxidation by a Cold-Adapted, Subglacial Chemoautotroph. *Appl. Environ. Microbiol.* 82, 1486–1495.

Harvey, H. R., Fallon, R. D., and Patton, J. S. (1986). The effect of organic matter and oxygen on the degradation of bacterial membrane lipids in marine sediments. *Geochim. Cosmochim. Acta* 50, 795–804.

Hawes, I., Jungblut, A. D., Matys, E. D., and Summons, R. E. (2018). The 'Dirty Ice' of the McMurdo Ice Shelf: Analogues for biological oases during the Cryogenian. *Geobiology* 16, 369–377.

Hawkings, J. R., Skidmore, M. L., Wadham, J. L., Priscu, J. C., Morton, P. L., Hatton, J. E., *et al*. (2020). Enhanced trace element mobilization by Earth's ice sheets. *Proceedings of the National Academy of Sciences* 117, 31648–31659.

Hayes, J. M., Strauss, H., and Kaufman, A. J. (1999). The abundance of 13C in marine organic matter and isotopic fractionation in the global biogeochemical cycle of carbon during the past 800 Ma. *Chem. Geol.* 161, 103–125.

Heckman, D. S., Geiser, D. M., Eidell, B. R., Stauffer, R. L., Kardos, N. L., and Hedges, S. B. (2001). Molecular evidence for the early colonization of land by fungi and plants. *Science* 293, 1129–1133.

Hell, K., Edwards, A., Zarsky, J., Podmirseg, S. M., Girdwood, S., Pachebat, J. A., *et al*. (2013). The dynamic bacterial communities of a melting High Arctic glacier snowpack. *ISME J.* 7, 1814–1826.

Hodson, A., Anesio, A. M., Tranter, M., Fountain, A., Osborn, M., Priscu, J., *et al*. (2008). GLACIAL ECOSYSTEMS. *Ecol. Monogr.* 78, 41–67.

Hodson, A., Bøggild, C., and Hanna, E. (2010). The cryoconite ecosystem on the Greenland ice sheet. *Annals of*. Available at: http://www.ingentaconnect.com/content/igsoc/agl/2010/00000051/00000056/art00015.

Hodson, A., Paterson, H., Westwood, K., Cameron, K., and Laybourn-Parry, J. (2013). A blue-ice ecosystem on the margins of the East Antarctic ice sheet. *J. Glaciol.* 59, 255–268.

Hoffman, P. F. (2011). Strange bedfellows: glacial diamictite and cap carbonate from the Marinoan (635 Ma) glaciation in Namibia. *Sedimentology* 58, 57–119.

Hoffman, P. F. (2016). Cryoconite pans on Snowball Earth: supraglacial oases for Cryogenian eukaryotes? *Geobiology* 14, 531–542.

Hoffman, P. F., Abbot, D. S., Ashkenazy, Y., Benn, D. I., Brocks, J. J., Cohen, P. A., *et al*. (2017). Snowball Earth climate dynamics and Cryogenian geology-geobiology. *Sci Adv* 3, e1600983.

Hoffman, P. F., Halverson, G. P., Domack, E. W., Husson, J. M., Higgins, J. A., and Schrag, D. P. (2007). Are basal Ediacaran (635 Ma) post-glacial “cap dolostones” diachronous? *Earth Planet. Sci. Lett.* 258, 114–131.

Hoffman, P. F., Kaufman, A. J., Halverson, G. P., and Schrag, D. P. (1998). A neoproterozoic snowball earth. *Science* 281, 1342–1346.

Hoffman, P. F., Macdonald, F. A., and Halverson, G. P. (2011). Chapter 5 Chemical sediments associated with Neoproterozoic glaciation: iron formation, cap carbonate, barite and phosphorite. *Geological Society, London, Memoirs* 36, 67–80.

Hoffman, P. F., and Schrag, D. P. (2002). The snowball Earth hypothesis: testing the limits of global change. *Terra Nova* 14, 129–155.

Hoffman, P. F., Schrag, D. P., and Schrag, D. P. (1999). Response: Considering a Neoproterozoic snowball Earth. *Science*.

Hoffman, P., and Halverson, G. (2008). Otvi Group of the Western Northern Platform, the Eastern Kaoko Zone and the Western Northern Margin Zone. Available at: https://agris.fao.org/agris-search/search.do?recordID=AU2019115313.

Hoffmann, K.-H., Condon, D. J., Bowring, S. A., and Crowley, J. L. (2004). U-Pb zircon date from the Neoproterozoic Ghaub Formation, Namibia: Constraints on Marinoan glaciation. *Geology* 32, 817–820.

Holdgate, M. W., and Smith, J. E. (1967). Signy Island. *Philos. Trans. R. Soc. Lond. B Biol. Sci.* 252, 173–177.

Hongoh, Y., Yuzawa, H., Ohkuma, M., and Kudo, T. (2003). Evaluation of primers and PCR conditions for the analysis of 16S rRNA genes from a natural environment. *FEMS Microbiol. Lett.* 221, 299–304.

Horvat, C., Seabrook, S., Cristi, A., Matthes, L., and Bisson, K. M. (2021). The case for phytoplankton blooms under antarctic sea ice. *Earth and Space Science Open Archive*.

Hugerth, L. W., Wefer, H. A., Lundin, S., Jakobsson, H. E., Lindberg, M., Rodin, S., *et al*. (2014). DegePrime, a program for degenerate primer design for broad-taxonomic-range PCR in microbial ecology studies. *Appl. Environ. Microbiol.* 80, 5116–5123.

Huner, N. P. A., Öquist, G., and Sarhan, F. (1998). Energy balance and acclimation to light and cold. *Trends Plant Sci.* 3, 224–230.

Hyde, W. T., Crowley, T. J., Baum, S. K., and Peltier, W. R. (2000). Neoproterozoic 'snowball Earth' simulations with a coupled climate/ice-sheet model. *Nature* 405, 425–429.

Ingall, E., and Jahnke, R. (1997). Influence of water-column anoxia on the elemental fractionation of carbon and phosphorus during sediment diagenesis. *Mar. Geol.* 139, 219–229.

Irvine-Fynn, T. D. L., Bridge, J. W., and Hodson, A. J. (2010). Rapid quantification of cryoconite: granule geometry and in situ supraglacial extents, using examples from Svalbard and Greenland. *J. Glaciol.* 56, 297–308.

Irvine-Fynn, T. D. L., Edwards, A., Stevens, I. T., Mitchell, A. C., Bunting, P., Box, J. E., *et al*. (2021). Storage and export of microbial biomass across the western Greenland Ice Sheet. *Nat. Commun.* 12, 3960.

Irvine-Fynn, T. D. L., Hodson, A. J., Moorman, B. J., Vatne, G., and Hubbard, A. L. (2011). POLYTHERMAL GLACIER HYDROLOGY: A REVIEW. *Rev. Geophys.* 49, 95.

Javaux, E. J., and Knoll, A. H. (2017). Micropaleontology of the lower Mesoproterozoic Roper Group, Australia, and implications for early eukaryotic evolution. *J. Paleontol.* 91, 199–229.

Jiang, G., Kennedy, M. J., and Christie-Blick, N. (2003). Stable isotopic evidence for methane seeps in Neoproterozoic postglacial cap carbonates. *Nature* 426, 822–826.

Jiang, G., Wang, X., Shi, X., Zhang, S., Xiao, S., and Dong, J. (2010). Organic carbon isotope constraints on the dissolved organic carbon (DOC) reservoir at the Cryogenian–Ediacaran transition. *Earth Planet. Sci. Lett.* 299, 159–168.

Jørgensen, B. B., and Boetius, A. (2007). Feast and famine--microbial life in the deep-sea bed. *Nat. Rev. Microbiol.* 5, 770–781.

Jungblut, A. D., Allen, M. A., Burns, B. P., and Neilan, B. A. (2009). Lipid biomarker analysis of cyanobacteria-dominated microbial mats in meltwater ponds on the McMurdo Ice Shelf, Antarctica. *Org. Geochem.* 40, 258–269.

Junge, K., Imhoff, F., Staley, T., and Deming, J. W. (2002). Phylogenetic diversity of numerically important Arctic sea-ice bacteria cultured at subzero temperature. *Microb. Ecol.* 43, 315–328.

Junge Karen, Eicken Hajo, and Deming Jody W. (2004). Bacterial Activity at −2 to −20°C in Arctic Wintertime Sea Ice. *Appl. Environ. Microbiol.* 70, 550–557.

Kaczmarek, Ł., Jakubowska, N., Celewicz-Gołdyn, S., and Zawierucha, K. (2016). The microorganisms of cryoconite holes (algae, Archaea, bacteria, cyanobacteria, fungi, and Protista): a review. *Polar Rec.* 52, 176–203.

Kato, M., Sakai, M., Adachi, K., Ikemoto, H., and Sano, H. (1996). Distribution of betaine lipids in marine algae. *Phytochemistry* 42, 1341–1345.

Katoh, K., and Standley, D. M. (2013). MAFFT multiple sequence alignment software version 7: improvements in performance and usability. *Mol. Biol. Evol.* 30, 772–780.

Kawecka, B., and Drake, B. G. (1978). Biology and ecology of snow algae. *Acta Hidrobiológica* 20, 111–116.

Kellerhals, P., and Matter, A. (2003). Facies analysis of a glaciomarine sequence, the Neoproterozoic Mirbat Sandstone Formation, Sultanate of Oman. *Eclogae Geol. Helv.* 96, 22.

Kendall, B., Creaser, R. A., and Selby, D. (2006). Re-Os geochronology of postglacial black shales in Australia: Constraints on the timing of “Sturtian” glaciation. *Geology* 34, 729–732.

Kennedy, M. J. (1996). Stratigraphy, sedimentology, and isotopic geochemistry of Australian Neoproterozoic postglacial cap dolostones; deglaciation, delta 13 C excursions, and carbonate precipitation. *J. Sediment. Res.* 66, 1050–1064.

Kerepesi, C., and Grolmusz, V. (2017). The ‘Giant Virus Finder’ discovers an abundance of giant viruses in the Antarctic dry valleys. *Arch. Virol.* 162, 1671–1676.

Kerkhof, L. J. (2021). Is Oxford Nanopore sequencing ready for analyzing complex microbiomes? *FEMS Microbiol. Ecol.* 97.

King, A. J., Freeman, K. R., McCormick, K. F., Lynch, R. C., Lozupone, C., Knight, R., *et al*. (2010). Biogeography and habitat modelling of high-alpine bacteria. *Nat. Commun.* 1, 53.

Kirchman, D. (2001). 'Measuring bacterial biomass production and growth rates from leucine incorporation in natural aquatic environments', in *Methods in Microbiology* (Academic Press), 227–237.

Kirschvink, J. L. (1992). 'Late Proterozoic Low-Latitude Global Glaciation: the Snowball Earth', in *The Proterozoic biosphere: a multidisciplinary study*, eds. J. W. Schopf and C. Klein (New York: Cambridge University Press), 51–52.

Klein, C., and Beukes, N. J. (1993). Sedimentology and geochemistry of the glaciogenic late Proterozoic Rapitan Iron-Formation in Canada. *Econ. Geol.* 88, 542–565.

Knight, P. G., Waller, R. I., Patterson, C. J., Jones, A. P., and Robinson, Z. P. (2002). Discharge of debris from ice at the margin of the Greenland ice sheet. *J. Glaciol.* 48, 192–198.

Knoll, A. H., Javaux, E. J., Hewitt, D., and Cohen, P. (2006a). Eukaryotic organisms in Proterozoic oceans. *Philos. Trans. R. Soc. Lond. B Biol. Sci.* 361, 1023–1038.

Knoll, A., Walter, M., Narbonne, G., and Christie-Blick, N. (2006b). The Ediacaran Period: a new addition to the geologic time scale. *Lethaia* 39, 13–30.

Komárek, J., and Johansen, J. R. (2015). 'Chapter 4 - Filamentous Cyanobacteria', in *Freshwater Algae of North America (Second Edition)*, eds. J. D. Wehr, R. G. Sheath, and J. P. Kociolek (Boston: Academic Press), 135–235.

Lahr, D. J. G., Kosakyan, A., Lara, E., Mitchell, E. A. D., Morais, L., Porfirio-Sousa, A. L., *et al*. (2019). Phylogenomics and Morphological Reconstruction of Arcellinida Testate Amoebae Highlight Diversity of Microbial Eukaryotes in the Neoproterozoic. *Curr. Biol.* 29, 991-1001.e3.

Lakkala, K., Aun, M., Sanchez, R., Bernhard, G., Asmi, E., Meinander, O., *et al*. (2020). New continuous total ozone, UV, VIS and PAR measurements at Marambio, 64° S, Antarctica. *Earth Syst. Sci. Data* 12, 947–960.

Lalibertè, G., and de la Noüie, J. (1993). Auto-, hetero-, and mixotrophic growth ofchlamydomonas Humicola(cmloroimiyckak) on acetate1. *J. Phycol.* 29, 612–620.

Lan, Z., Li, X.-H., Zhang, Q., and Li, Q.-L. (2015). Global synchronous initiation of the 2nd episode of Sturtian glaciation: SIMS zircon U–Pb and O isotope evidence from the Jiangkou Group, South China. *Precambrian Res.* 267, 28–38.

Langford, H., Hodson, A., and Banwart, S. (2010). The microstructure and biogeochemistry of Arctic cryoconite granules. *Annals of*. Available at: http://www.ingentaconnect.com/content/igsoc/agl/2010/00000051/00000056/art00011.

Langford, H. J., Irvine-Fynn, T. D. L., Edwards, A., Banwart, S. A., and Hodson, A. J. (2014). A spatial investigation of the environmental controls over cryoconite aggregation on Longyearbreen glacier, Svalbard. *Biogeosciences* 11, 5365–5380.

Laybourn-Parry, J., Ellis-Evans, J. C., and Butler, H. (1996). Microbial dynamics during the summer ice-loss phase in maritime Antarctic lakes. *J. Plankton Res.* 18, 495–511.

Laybourn-Parry, J., and Wadham, J. L. (2014). 'Lakes and ponds on glaciers and ice shelves', in *Antarctic Lakes* (Oxford University Press).

Le Brocq, A. M., Ross, N., Griggs, J. A., Bingham, R. G., Corr, H. F. J., Ferraccioli, F., *et al*. (2013). Evidence from ice shelves for channelized meltwater flow beneath the Antarctic Ice Sheet. *Nat. Geosci.* 6, 945–948.

Le Heron, D. P. (2015). The significance of ice-rafted debris in Sturtian glacial successions. *Sediment. Geol.* 322, 19–33.

Le Heron, D. P., and Busfield, M. E. (2014). Neoproterozoic ice sheets and olistoliths: Multiple glacial cycles in the Kingston Peak Formation, California. *J. Geol. Soc. London*. Available at: https://jgs.lyellcollection.org/content/171/4/525.short?casa_token=0T8TLOMXGU4AAAAA:MKmAbxBEJ0iKKix-BOu9-kYG2G6QmwNJ-icJYpQHY5k3t7mlo1kXWhbxH-ydImTQTS4eKPECH-Gh.

Le Heron, D. P., Busfield, M. E., and Kamona, F. (2013). An interglacial on snowball Earth? Dynamic ice behaviour revealed in the Chuos Formation, Namibia. *Sedimentology* 60, 411–427.

Le Hir, G., Donnadieu, Y., Krinner, G., and Ramstein, G. (2010). Toward the snowball earth deglaciation…. *Clim. Dyn.* 35, 285–297.

Le Hir, G., Goddéris, Y., Donnadieu, Y., and Ramstein, G. (2008a). A geochemical modelling study of the evolution of the chemical composition of seawater linked to a 'snowball' glaciation. *Biogeosciences* 5, 253–267.

Le Hir, G., Ramstein, G., Donnadieu, Y., and Goddéris, Y. (2008b). Scenario for the evolution of atmospheric pCO2 during a snowball Earth. *Geology* 36, 47–50.

Lechte, M. A., Wallace, M. W., Hood, A. van S., Li, W., Jiang, G., Halverson, G. P., *et al*. (2019). Subglacial meltwater supported aerobic marine habitats during Snowball Earth. *Proc. Natl. Acad. Sci. U. S. A.* 116, 25478–25483.

Leppäranta, M., Järvinen, O., and Mattila, O.-P. (2013). Structure and life cycle of supraglacial lakes in Dronning Maud Land. *Antarct. Sci.* 25, 457–467.

Letsch, D., and Kiefer, L. (2017). A marine pebbly mudstone from the Swiss Alps: palaeotectonic implications and some consequences for the interpretation of Precambrian diamictites. *Swiss J. Geosci.* 110, 753–776.

Leventer, A. (1998). 'The fate of Antarctic "sea ice diatoms" and their use as paleoenvironmental indicators', in *Antarctic Sea Ice: Biological Processes, Interactions and Variability* Antarctic research series. (Washington, D. C.: American Geophysical Union), 121–137.

Lewis, J. P., Weaver, A. J., and Eby, M. (2007). Snowball versus slushball Earth: Dynamic versus nondynamic sea ice? *J. Geophys. Res.* 112.

Lewis, J. P., Weaver, A. J., Johnston, S. T., and Eby, M. (2003). Neoproterozoic "snowball Earth": Dynamic sea ice over a quiescent ocean. *Paleoceanography* 18.

Li, H. (2018). Minimap2: pairwise alignment for nucleotide sequences. *Bioinformatics* 34, 3094–3100.

Li, Z.-X., Evans, D. A. D., and Halverson, G. P. (2013). Neoproterozoic glaciations in a revised global palaeogeography from the breakup of Rodinia to the assembly of Gondwanaland. *Sediment. Geol.* 294, 219–232.

Lipp, J. S., and Hinrichs, K.-U. (2009). Structural diversity and fate of intact polar lipids in marine sediments. *Geochim. Cosmochim. Acta* 73, 6816–6833.

Lipp, J. S., Morono, Y., Inagaki, F., and Hinrichs, K.-U. (2008). Significant contribution of Archaea to extant biomass in marine subsurface sediments. *Nature* 454, 991–994.

Liston, G. E., Winther, J.-G., Bruland, O., Elvehøy, H., and Sand, K. (1999). Below-surface ice melt on the coastal Antarctic ice sheet. *J. Glaciol.* 45, 273–285.

Little, C. T. S., and Vrijenhoek, R. C. (2003). Are hydrothermal vent animals living fossils? *Trends Ecol. Evol.* 18, 582–588.

Liu, Y., Vick-Majors, T. J., Priscu, J. C., Yao, T., Kang, S., Liu, K., *et al*. (2017). Biogeography of cryoconite bacterial communities on glaciers of the Tibetan Plateau. *FEMS Microbiol. Ecol.* 93.

Liu, Y., Yao, T., Jiao, N., Tian, L., Hu, A., Yu, W., *et al*. (2011). Microbial diversity in the snow, a moraine lake and a stream in Himalayan glacier. *Extremophiles* 15, 411–421.

Lliboutry, L. (1968). General Theory of Subglacial Cavitation and Sliding of Temperate Glaciers. *J. Glaciol.* 7, 21–58.

Loron, C. C., François, C., Rainbird, R. H., Turner, E. C., Borensztajn, S., and Javaux, E. J. (2019). Early fungi from the Proterozoic era in Arctic Canada. *Nature* 570, 232–235.

Love, G. D., Grosjean, E., Stalvies, C., Fike, D. A., Grotzinger, J. P., Bradley, A. S., *et al*. (2009). Fossil steroids record the appearance of Demospongiae during the Cryogenian period. *Nature* 457, 718–721.

Lutz, S., Anesio, A. M., Edwards, A., and Benning, L. G. (2015). Microbial diversity on Icelandic glaciers and ice caps. *Front. Microbiol.* 6, 307.

Lutz, S., Anesio, A. M., Edwards, A., and Benning, L. G. (2017). Linking microbial diversity and functionality of arctic glacial surface habitats. *Environ. Microbiol.* 19, 551–565.

Lutz, S., Anesio, A. M., Jorge Villar, S. E., and Benning, L. G. (2014). Variations of algal communities cause darkening of a Greenland glacier. *FEMS Microbiol. Ecol.* 89, 402–414.

Lutz, S., McCutcheon, J., McQuaid, J. B., and Benning, L. G. (2018). The diversity of ice algal communities on the Greenland Ice Sheet as revealed by oligotyping. *Microb Genom*.

Lutz, S., Ziolkowski, L. A., and Benning, L. G. (2019). The Biodiversity and Geochemistry of Cryoconite Holes in Queen Maud Land, East Antarctica. *Microorganisms* 7.

Lyons, T. W., Reinhard, C. T., Love, G. D., and Xiao, S. (2012). 'Geobiology of the Proterozoic Eon', in *Fundamentals of Geobiology* (John Wiley & Sons, Ltd), 371–402.

Macdonald, F. A., Schmitz, M. D., Crowley, J. L., Roots, C. F., Jones, D. S., Maloof, A. C., *et al*. (2010). Calibrating the Cryogenian. *Science* 327, 1241–1243.

MacDonell, S., and Fitzsimons, S. (2008). The formation and hydrological significance of cryoconite holes. *Prog. Phys. Geogr.* 32, 595–610.

Macdonell, S., Sharp, M., and Fitzsimons, S. (2016). Cryoconite hole connectivity on the Wright Lower Glacier, McMurdo Dry Valleys, Antarctica. *J. Glaciol.* 62, 714–724.

Maggiori, C., Raymond-Bouchard, I., Brennan, L., Touchette, D., and Whyte, L. (2021). MinION sequencing from sea ice cryoconites leads to de novo genome reconstruction from metagenomes. *Sci. Rep.* 11, 21041.

Maikova, A., Zalutskaya, Z., Lapina, T., and Ermilova, E. (2016). The HSP70 chaperone machines of Chlamydomonas are induced by cold stress. *J. Plant Physiol.* 204, 85–91.

Maltsev, Y., Maltseva, K., Kulikovskiy, M., and Maltseva, S. (2021). Influence of Light Conditions on Microalgae Growth and Content of Lipids, Carotenoids, and Fatty Acid Composition. *Biology* 10.

Marizcurrena, J. J., Cerdá, M. F., Alem, D., and Castro-Sowinski, S. (2019). 'Living with Pigments: The Colour Palette of Antarctic Life', in *The Ecological Role of Micro-organisms in the Antarctic Environment* (unknown), 65–82.

Marmur, J. (1963). '[100] A procedure for the isolation of deoxyribonucleic acid from microorganisms', in *Methods in Enzymology* (Academic Press), 726–738.

Mattinson, J. M. (2011). Extending the Krogh legacy: development of the CA–TIMS method for zircon U–Pb geochronologyThis article is one of a series of papers published in this Special Issue on the theme of Geochronology in honour of Tom Krogh. *Can. J. Earth Sci.* 48, 95–105.

McIntyre, N. F. (1984). Cryoconite hole thermodynamics. *Can. J. Earth Sci.* 21, 152–156.

McKay, C. P. (2000). Thickness of tropical ice and photosynthesis on a snowball Earth. *Geophys. Res. Lett.* 27, 2153–2156.

McMurdie, P. J., and Holmes, S. (2013). phyloseq: an R package for reproducible interactive analysis and graphics of microbiome census data. *PLoS One* 8, e61217.

Michaud, A. B., Šabacká, M., and Priscu, J. C. (2012). Cyanobacterial diversity across landscape units in a polar desert: Taylor Valley, Antarctica. *FEMS Microbiol. Ecol.* 82, 268–278.

Michel, C., Legendre, L., Ingram, R. G., Gosselin, M., and Levasseur, M. (1996). Carbon budget of sea-ice algae in spring: Evidence of a significant transfer to zooplankton grazers. *J. Geophys. Res.* 101, 18345–18360.

Millar, J. L., Bagshaw, E. A., Edwards, A., Poniecka, E. A., and Jungblut, A. D. (2021). Polar Cryoconite Associated Microbiota Is Dominated by Hemispheric Specialist Genera. *Front. Microbiol.* 12, 3318.

Mindl, B., Anesio, A. M., Meirer, K., Hodson, A. J., Laybourn-Parry, J., Sommaruga, R., *et al*. (2007). Factors influencing bacterial dynamics along a transect from supraglacial runoff to proglacial lakes of a high Arctic glacier [corrected]. *FEMS Microbiol. Ecol.* 59, 307–317.

Moczydłowska, M. (2008). The Ediacaran microbiota and the survival of Snowball Earth conditions. *Precambrian Res.* 167, 1–15.

Moczydłowska, M., Kear, B. P., Snitting, D., Liu, L., Lazor, P., and Majka, J. (2021). Ediacaran metazoan fossils with siliceous skeletons from the Digermulen Peninsula of Arctic Norway – CORRIGENDUM. *J. Paleontol.* 95, 1112–1112.

Montross, S. N., Skidmore, M., Tranter, M., Kivimäki, A.-L., and John Parkes, R. (2013). A microbial driver of chemical weathering in glaciated systems. *Geology* 41, 215–218.

Moore, K. R., Bosak, T., Macdonald, F. A., Lahr, D. J. G., Newman, S., Settens, C., *et al*. (2017). Biologically agglutinated eukaryotic microfossil from Cryogenian cap carbonates. *Geobiology* 15, 499–515.

Mueller, D. R., and Pollard, W. H. (2004). Gradient analysis of cryoconite ecosystems from two polar glaciers. *Polar Biol.* 27, 66–74.

Mueller, D. R., Vincent, W. F., Pollard, W. H., and Fritsen, C. H. (2001). Glacial cryoconite ecosystems: A bipolar comparison of algal communities and habitats. *Nova Hedwigia* 123, 173–197.

Murakami, H., Nobusawa, T., Hori, K., Shimojima, M., and Ohta, H. (2018). Betaine Lipid Is Crucial for Adapting to Low Temperature and Phosphate Deficiency in Nannochloropsis. *Plant Physiol.* 177, 181–193.

Murakami, T., Takeuchi, N., Mori, H., Hirose, Y., Edwards, A., Irvine-Fynn, T., *et al*. (2022). Metagenomics reveals global-scale contrasts in nitrogen cycling and cyanobacterial light-harvesting mechanisms in glacier cryoconite. *Microbiome* 10, 50.

Musilova, M., Tranter, M., Bamber, J. L., Takeuchi, N., and Anesio, A. (2016). Experimental evidence that microbial activity lowers the albedo of glaciers. *Geochem. Persp. Let.*, 106–116.

Newman, W. A. (1985). The abyssal hydrothermal vent invertebrate fauna: A glimpse of antiquity? *Bulletin of the Biological Society of Washington* 6, 231–242.

Nicholes, M. J., Williamson, C. J., Tranter, M., Holland, A., Poniecka, E., Yallop, M. L., *et al*. (2019). Bacterial Dynamics in Supraglacial Habitats of the Greenland Ice Sheet. *Front. Microbiol.* 10, 1366.

Nicholson, W. L., Fajardo-Cavazos, P., Rebeil, R., Slieman, T. A., Riesenman, P. J., Law, J. F., *et al*. (2002). Bacterial endospores and their significance in stress resistance. *Antonie Van Leeuwenhoek* 81, 27–32.

Nordenskiöld (1872). I.—Account of an Expedition to Greenland in the year 1870. *Geol. Mag.* Available at: https://www.cambridge.org/core/journals/geological-magazine/article/iaccount-of-an-expedition-to-greenland-in-the-year-1870/6A4AAA87384056DBCD22813785F04A3C.

Nordenskjold, E. A. (1875). Cryoconite found 1870, July 19th-25th, on the inland ice, east of Auleitsivik Fjord, Disco Bay, Greenland. *Geol. Mag., Decade 2* 2, 157–162.

Obryk, M. K., Doran, P. T., Fountain, A. G., Myers, M., and McKay, C. P. (2020). Climate from the McMurdo dry valleys, Antarctica, 1986–2017: Surface air temperature trends and redefined summer season. *J. Geophys. Res.* 125.

Oehlert, A. M., and Swart, P. K. (2014). Interpreting carbonate and organic carbon isotope covariance in the sedimentary record. *Nat. Commun.* 5, 4672.

Ogg, J. (2004). Status of Divisions of the International Geologic Time Scale. *Lethaia* 37, 183–199.

Oksanen, J., Blanchet, F. G., Friendly, M., Kindt, R., Legendre, P., McGlinn, D., *et al*. (2019). vegan: Community Ecology Package. Available at: https://CRAN.R-project.org/package=vegan.

Olcott, A. N., Sessions, A. L., Corsetti, F. A., Kaufman, A. J., and de Oliviera, T. F. (2005). Biomarker evidence for photosynthesis during neoproterozoic glaciation. *Science* 310, 471–474.

Osborn, A. M., Moore, E. R., and Timmis, K. N. (2000). An evaluation of terminal-restriction fragment length polymorphism (T-RFLP) analysis for the study of microbial community structure and dynamics. *Environ. Microbiol.* 2, 39–50.

Palmer, S. J., Dowdeswell, J. A., Christoffersen, P., Young, D. A., Blankenship, D. D., Greenbaum, J. S., *et al*. (2013). Greenland subglacial lakes detected by radar. *Geophys. Res. Lett.* 40, 6154–6159.

Parada, A. E., Needham, D. M., and Fuhrman, J. A. (2016). Every base matters: assessing small subunit rRNA primers for marine microbiomes with mock communities, time series and global field samples. *Environ. Microbiol.* 18, 1403–1414.

Parfrey, L. W., Lahr, D. J. G., Knoll, A. H., and Katz, L. A. (2011). Estimating the timing of early eukaryotic diversification with multigene molecular clocks. *Proc. Natl. Acad. Sci. U. S. A.* 108, 13624–13629.

Parish, T. R., and Cassano, J. J. (2003). The Role of Katabatic Winds on the Antarctic Surface Wind Regime. *Mon. Weather Rev.* 131, 317–333.

Peach, P. A., and Perrie, L. A. (1975). GRAIN-SIZE DISTRIBUTION WITHIN GLACIAL VARVES. *Geology* 3, 43–46.

Pearce, D. A. (2005). The structure and stability of the bacterioplankton community in Antarctic freshwater lakes, subject to extremely rapid environmental change. *FEMS Microbiol. Ecol.* 53, 61–72.

Pearce, D. A., Bridge, P. D., Hughes, K. A., Sattler, B., Psenner, R., and Russell, N. J. (2009). Microorganisms in the atmosphere over Antarctica. *FEMS Microbiol. Ecol.* 69, 143–157.

Pearce, D. A., van der Gast, C. J., Woodward, K., and Newsham, K. K. (2005). Significant changes in the bacterioplankton community structure of a maritime Antarctic freshwater lake following nutrient enrichment. *Microbiology* 151, 3237–3248.

Pearson, E. S. (1931). The Test of Significance for the Correlation Coefficient. *J. Am. Stat. Assoc.* 26, 128–134.

Perkins, R. G., Bagshaw, E., Mol, L., Williamson, C. J., Fagan, D., Gamble, M., *et al*. (2017). Photoacclimation by Arctic cryoconite phototrophs. *FEMS Microbiol. Ecol.* 93.

Petersen, J. M., Zielinski, F. U., Pape, T., Seifert, R., Moraru, C., Amann, R., *et al*. (2011). Hydrogen is an energy source for hydrothermal vent symbioses. *Nature* 476, 176–180.

Peterson, K. J., and Butterfield, N. J. (2005). Origin of the Eumetazoa: testing ecological predictions of molecular clocks against the Proterozoic fossil record. *Proc. Natl. Acad. Sci. U. S. A.* 102, 9547–9552.

Pierrehumbert, R. T., Abbot, D. S., Voigt, A., and Koll, D. (2011). Climate of the Neoproterozoic. *Annu. Rev. Earth Planet. Sci.* 39, 417–460.

Pollard, D., and Kasting, J. F. (2005). Snowball Earth: A thin-ice solution with flowing sea glaciers. *J. Geophys. Res.* 110, C07010.

Poniecka, E. (2020). The role of heterotrophs in glacier surface ecosystem productivity.

Poniecka, E. A., Bagshaw, E. A., Sass, H., Segar, A., Webster, G., Williamson, C., *et al*. (2020). Physiological Capabilities of Cryoconite Hole Microorganisms. *Front. Microbiol.* 11, 1783.

Poniecka, E. A., Bagshaw, E. A., Tranter, M., Sass, H., Williamson, C. J., Anesio, A. M., *et al*. (2018). Rapid development of anoxic niches in supraglacial ecosystems. *Arct. Antarct. Alp. Res.* 50, S100015.

Poniecka, E., Bagshaw, E., Sass, H., Williamson, C., Anesio, A., and Tranter, M. (2019). The Secrets of Black Holes on Ice: Eco-physiology of Microorganisms in Cryoconite Holes. in *Geophysical Research Abstracts*.

Porazinska, D. L., Fountain, A. G., Nylen, T. H., Tranter, M., Virginia, R. A., and Wall, D. H. (2004). The Biodiversity and Biogeochemistry of Cryoconite Holes from McMurdo Dry Valley Glaciers, Antarctica. *Arct. Antarct. Alp. Res.* 36, 84–91.

Porter, S. M., and Knoll, A. H. (2000). Testate Amoebae in the Neoproterozoic Era: Evidence from Vase-Shaped Microfossils in the Chuar Group, Grand Canyon. *Paleobiology* 26, 360–385.

Porter, S. M., Meisterfeld, R., and Knoll, A. H. (2003). VASE-SHAPED MICROFOSSILS FROM THE NEOPROTEROZOIC CHUAR GROUP, GRAND CANYON: A CLASSIFICATION GUIDED BY MODERN TESTATE AMOEBAE. *J. Paleontol.* 77, 409–429.

Post, A., and Larkum, A. W. D. (1993). UV-absorbing pigments, photosynthesis and UV exposure in Antarctica: comparison of terrestrial and marine algae. *Aquat. Bot.* 45, 231–243.

Prave, A. R., Condon, D., Hoffmann, K. H., Tapster, S., and Fallick, A. E. (2016). Duration and nature of the end-Cryogenian (Marinoan) glaciation. *Geology* 44, 631–634.

Preiss, W. V. (1987). *The Adelaide Geosyncline: Late Proterozoic stratigraphy, sedimentation, palaeontology and tectonics*. , ed. J. F. Drexel Department of Mines and Energy.

Price, M. N., Dehal, P. S., and Arkin, A. P. (2009). FastTree: computing large minimum evolution trees with profiles instead of a distance matrix. *Mol. Biol. Evol.* 26, 1641–1650.

Quast, C., Pruesse, E., Yilmaz, P., Gerken, J., Schweer, T., Yarza, P., *et al*. (2013). The SILVA ribosomal RNA gene database project: improved data processing and web-based tools. *Nucleic Acids Res.* 41, D590-6.

Quesada, A., and Vincent, W. F. (2012). 'Cyanobacteria in the Cryosphere: Snow, Ice and Extreme Cold', in *Ecology of Cyanobacteria II: Their Diversity in Space and Time* Scientific reports of the British Antarctic Survey 98., ed. B. A. Whitton (Dordrecht: Springer Netherlands), 387–399.

R Core Team (2021). *R: A Language and Environment for Statistical Computing*. Vienna, Austria: R Foundation for Statistical Computing Available at: https://www.R-project.org/.

Raetz, C. R. (1986). Molecular genetics of membrane phospholipid synthesis. *Annu. Rev. Genet.* 20, 253–295.

Rassner, S. M. E., Anesio, A. M., Girdwood, S. E., Hell, K., Gokul, J. K., Whitworth, D. E., *et al*. (2016). Can the Bacterial Community of a High Arctic Glacier Surface Escape Viral Control? *Front. Microbiol.* 7, 956.

Remias, D. (2012). 'Cell Structure and Physiology of Alpine Snow and Ice Algae', in *Plants in Alpine Regions* (Springer, Vienna), 175–185.

Renkonen, O. (1967). 'The Analysis of Individual Molecular Species of Polar Lipids', in *Advances in Lipid Research*, eds. R. Paoletti and D. Kritchevsky (Elsevier), 329–351.

Rew, D. A. (2003). Deinococcus radiodurans. *Eur. J. Surg. Oncol.* 29, 557–558.

Řezanka, T., Kolouchová, I., and Sigler, K. (2016). Lipidomic analysis of psychrophilic yeasts cultivated at different temperatures. *Biochim. Biophys. Acta* 1861, 1634–1642.

Riebesell, U., Schloss, I., and Smetacek, V. (1991). Aggregation of algae released from melting sea ice: implications for seeding and sedimentation. *Polar Biol.* 11.

Rieu, R., and Allen, P. A. (2008). Siliciclastic sedimentation in the interlude between two Neoproterozoic glaciations, Mirbat area, southern Oman: A missing link in the Huqf Supergroup? *GeoArabia* 13, 45–72.

Rooney, A. D., Strauss, J. V., Brandon, A. D., and Macdonald, F. A. (2015). A Cryogenian chronology: Two long-lasting synchronous Neoproterozoic glaciations. *Geology* 43.

Rose, B. E. J. (2015). Stable "Waterbelt" climates controlled by tropical ocean heat transport: A nonlinear coupled climate mechanism of relevance to Snowball Earth. *J. Geophys. Res. D: Atmos.* 120, 1404–1423.

Röthlisberger, H. (1972). Water Pressure in Intra- and Subglacial Channels. *J. Glaciol.* 11, 177–203.

Ruby, E. G., Wirsen, C. O., and Jannasch, H. W. (1981). Chemolithotrophic sulfur-oxidizing bacteria from the galapagos rift hydrothermal vents. *Appl. Environ. Microbiol.* 42, 317–324.

Runcie, J. W., and Riddle, M. J. (2006). Photosynthesis of marine macroalgae in ice-covered and ice-free environments in East Antarctica. *Eur. J. Phycol.* 41, 223–233.

Runnegar, B. (2000). Loophole for snowball Earth. *Nature* 405, 403–404.

Rütters, H., Sass, H., Cypionka, H., and Rullkötter, J. (2002). Phospholipid analysis as a tool to study complex microbial communities in marine sediments. *J. Microbiol. Methods* 48, 149–160.

Šabacká, M., Priscu, J. C., Basagic, H. J., Fountain, A. G., Wall, D. H., Virginia, R. A., *et al*. (2012). Aeolian flux of biotic and abiotic material in Taylor Valley, Antarctica. *Geomorphology* 155–156, 102–111.

Samui, G., Antony, R., and Thamban, M. (2018). Chemical characteristics of hydrologically distinct cryoconite holes in coastal Antarctica.

Sánchez-Baracaldo, P., Raven, J. A., Pisani, D., and Knoll, A. H. (2017). Early photosynthetic eukaryotes inhabited low-salinity habitats. *Proc. Natl. Acad. Sci. U. S. A.* 114, E7737–E7745.

SanClements, M. D., Smith, H. J., Foreman, C. M., Tedesco, M., Chin, Y.-P., Jaros, C., *et al*. (2017). Biogeophysical properties of an expansive Antarctic supraglacial stream. *Antarct. Sci.* 29, 33–44.

Sansjofre, P., Ader, M., Trindade, R. I. F., Elie, M., Lyons, J., Cartigny, P., *et al*. (2011). A carbon isotope challenge to the snowball Earth. *Nature* 478, 93–96.

Sanyal, A., Antony, R., Samui, G., and Thamban, M. (2018). Microbial communities and their potential for degradation of dissolved organic carbon in cryoconite hole environments of Himalaya and Antarctica. *Microbiol. Res.* 208, 32–42.

Schinteie, R., and Brocks, J. J. (2017). Paleoecology of Neoproterozoic hypersaline environments: Biomarker evidence for haloarchaea, methanogens, and cyanobacteria. *Geobiology* 15, 641–663.

Schmidt, J. E. E., and Ahring, B. K. (1994). Extracellular polymers in granular sludge from different upflow anaerobic sludge blanket (UASB) reactors. *Appl. Microbiol. Biotechnol.* 42, 457–462.

Schrag, D. P., Berner, R. A., Hoffman, P. F., and Halverson, G. P. (2002). On the initiation of a snowball Earth. *Geochemistry, Geophysics, Geosystems* 3, 1–21.

Schubotz, F., Meyer-Dombard, D. R., Bradley, A. S., Fredricks, H. F., Hinrichs, K.-U., Shock, E. L., *et al*. (2013). Spatial and temporal variability of biomarkers and microbial diversity reveal metabolic and community flexibility in Streamer Biofilm Communities in the Lower Geyser Basin, Yellowstone National Park. *Geobiology* 11, 549–569.

Schubotz, F., Xie, S., Lipp, J. S., Hinrichs, K.-U., and Wakeham, S. G. (2018). Intact polar lipids in the water column of the eastern tropical North Pacific: abundance and structural variety of non-phosphorus lipids. *Biogeosciences* 15, 6481–6501.

Segawa, T., Yonezawa, T., Edwards, A., Akiyoshi, A., Tanaka, S., Uetake, J., *et al*. (2017). Biogeography of cryoconite forming cyanobacteria on polar and Asian glaciers. *J. Biogeogr.* 44, 2849–2861.

Selby, D., and Creaser, R. A. (2003). Re–Os geochronology of organic rich sediments: an evaluation of organic matter analysis methods. *Chem. Geol.* 200, 225–240.

Sergeev, V. N., Vorob'eva, N. G., and Yu. Petrov, P. (2017). The biostratigraphic conundrum of Siberia: Do true Tonian–Cryogenian microfossils occur in Mesoproterozoic rocks? *Precambrian Res.* 299, 282–302.

Sevim, V., Lee, J., Egan, R., Clum, A., Hundley, H., Lee, J., *et al*. (2019). Shotgun metagenome data of a defined mock community using Oxford Nanopore, PacBio and Illumina technologies. *Sci Data* 6, 285.

Shakya, M., Lo, C.-C., and Chain, P. S. G. (2019). Advances and Challenges in Metatranscriptomic Analysis. *Front. Genet.* 10, 904.

Shannon, C. E. (1948). A mathematical theory of communication. *Bell Syst. tech. j.* 27, 379–423.

Shannon, P., Markiel, A., Ozier, O., Baliga, N. S., Wang, J. T., Ramage, D., *et al*. (2003). Cytoscape: a software environment for integrated models of biomolecular interaction networks. *Genome Res.* 13, 2498–2504.

Sharp, M., Parkes, J., Cragg, B., Fairchild, I. J., Lamb, H., and Tranter, M. (1999). Widespread bacterial populations at glacier beds and their relationship to rock weathering and carbon cycling. *Geology* 27, 107–110.

Sharp, R. P. (1949). Studies of superglacial debris on valley glaciers. *Am. J. Sci.* 247, 289–315.

Shields, G. A. (2005). Neoproterozoic cap carbonates: a critical appraisal of existing models and the plumeworld hypothesis. *Terra Nova* 17, 299–310.

Shivaji, S., Kiran, M. D., and Chintalapati, S. (2007). Perception and Transduction of Low Temperature in Bacteria. *Physiology and Biochemistry of Extremophiles*, 194–207.

Siliakus, M. F., van der Oost, J., and Kengen, S. W. M. (2017). Adaptations of archaeal and bacterial membranes to variations in temperature, pH and pressure. *Extremophiles* 21, 651–670.

Simon, M., and Azam, F. (1989). Protein content and protein synthesis rates of planktonic marine bacteria. *Mar. Ecol. Prog. Ser.* 51, 201–213.

Simpson, E. H. (1949). Measurement of Diversity. *Nature* 163, 688–688.

Singh, P., Hanada, Y., Singh, S. M., and Tsuda, S. (2014a). Antifreeze protein activity in Arctic cryoconite bacteria. *FEMS Microbiol. Lett.* 351, 14–22.

Singh, P., Kapse, N., Arora, P., Singh, S. M., and Dhakephalkar, P. K. (2015). Draft genome of Cryobacterium sp. MLB-32, an obligate psychrophile from glacier cryoconite holes of high Arctic. *Mar. Genomics* 21, 25–26.

Singh, P., and Singh, S. M. (2012). Characterization of yeast and filamentous fungi isolated from cryoconite holes of Svalbard, Arctic. *Polar Biol.* 35, 575–583.

Singh, P., Singh, S. M., and Dhakephalkar, P. (2014b). Diversity, cold active enzymes and adaptation strategies of bacteria inhabiting glacier cryoconite holes of High Arctic. *Extremophiles* 18, 229–242.

Singh, P., Tsuji, M., Singh, S. M., and Takeuchi, N. (2020). Contrasting Patterns of Microbial Communities in Glacier Cryoconite of Nepali Himalaya and Greenland, Arctic. *Sustain. Sci. Pract. Policy* 12, 6477.

Singh, S. M., Avinash, K., Sharma, P., Mulik, R. U., Upadhyay, A. K., and Ravindra, R. (2017). Elemental variations in glacier cryoconites of Indian Himalaya and Spitsbergen, Arctic. *Geoscience Frontiers* 8, 1339–1347.

Skidmore, M. L., Foght, J. M., and Sharp, M. J. (2000). Microbial life beneath a high arctic glacier. *Appl. Environ. Microbiol.* 66, 3214–3220.

Smith, and Azam (1992). A simple, economical method for measuring bacterial protein synthesis rates in seawater using 3H-leucine. *Mar. Microb. Food Webs*.

Smith, R. I. L. (1990). Signy Island as a Paradigm of Biological and Environmental Change in Antarctic Terrestrial Ecosystems. in *Antarctic Ecosystems* (Springer Berlin Heidelberg), 32–50.

Sohm, J. A., Niederberger, T. D., Parker, A. E., Tirindelli, J., Gunderson, T., Cary, S. C., *et al*. (2020). Microbial Mats of the McMurdo Dry Valleys, Antarctica: Oases of Biological Activity in a Very Cold Desert. *Front. Microbiol.* 11, 537960.

Sommers, P., Darcy, J. L., Gendron, E. M. S., Stanish, L. F., Bagshaw, E. A., Porazinska, D. L., *et al*. (2018). Diversity patterns of microbial eukaryotes mirror those of bacteria in Antarctic cryoconite holes. *FEMS Microbiol. Ecol.* 94.

Sommers, P., Porazinska, D. L., Darcy, J. L., Zamora, F., Fountain, A. G., and Schmidt, S. K. (2019). Experimental cryoconite holes as mesocosms for studying community ecology. *Polar Biol.* 42, 1973–1984.

Sperling, E. A., Robinson, J. M., Pisani, D., and Peterson, K. J. (2010). Where's the glass? Biomarkers, molecular clocks, and microRNAs suggest a 200-Myr missing Precambrian fossil record of siliceous sponge spicules. *Geobiology* 8, 24–36.

Stanish, L. F., Bagshaw, E. A., McKnight, D. M., Fountain, A. G., and Tranter, M. (2013). Environmental factors influencing diatom communities in Antarctic cryoconite holes. *Environ. Res. Lett.* 8, 045006.

Statham, P. J., Skidmore, M., and Tranter, M. (2008). Inputs of glacially derived dissolved and colloidal iron to the coastal ocean and implications for primary productivity. *Global Biogeochem. Cycles* 22.

Steinbock, O. (1936). Cryoconite holes and their biological significance. *Z. Gletscherkd. Glazialgeol.* 24, 1–21.

Stibal, M., Lawson, E. C., Lis, G. P., Mak, K. M., Wadham, J. L., and Anesio, A. M. (2010). Organic matter content and quality in supraglacial debris across the ablation zone of the Greenland ice sheet. *Ann. Glaciol.* 51, 1–8.

Stibal, M., Šabacká, M., and Žárský, J. (2012a). Biological processes on glacier and ice sheet surfaces. *Nat. Geosci.* 5, 771.

Stibal, M., Schostag, M., Cameron, K. A., Hansen, L. H., Chandler, D. M., Wadham, J. L., *et al*. (2015). Different bulk and active bacterial communities in cryoconite from the margin and interior of the Greenland ice sheet. *Environ. Microbiol. Rep.* 7, 293–300.

Stibal, M., Telling, J., Cook, J., Mak, K. M., Hodson, A., and Anesio, A. M. (2012b). Environmental controls on microbial abundance and activity on the greenland ice sheet: a multivariate analysis approach. *Microb. Ecol.* 63, 74–84.

Stibal, M., and Tranter, M. (2007). Laboratory investigation of inorganic carbon uptake by cryoconite debris from Werenskioldbreen, Svalbard. *J. Geophys. Res.* 112, G04S33.

Stibal, M., Tranter, M., Telling, J., and Benning, L. G. (2008). Speciation, phase association and potential bioavailability of phosphorus on a Svalbard glacier. *Biogeochemistry* 90, 1–13.

Stibal, M., Wadham, J. L., Lis, G. P., Telling, J., Pancost, R. D., Dubnick, A., *et al*. (2012c). Methanogenic potential of Arctic and Antarctic subglacial environments with contrasting organic carbon sources. *Glob. Chang. Biol.* 18, 3332–3345.

Strauss, J. V., Rooney, A. D., Macdonald, F. A., Brandon, A. D., and Knoll, A. H. (2014). 740 Ma vase-shaped microfossils from Yukon, Canada: Implications for Neoproterozoic chronology and biostratigraphy. *Geology* 42, 659–662.

Sturt, H. F., Summons, R. E., Smith, K., Elvert, M., and Hinrichs, K.-U. (2004). Intact polar membrane lipids in prokaryotes and sediments deciphered by high-performance liquid chromatography/electrospray ionization multistage mass spectrometry--new biomarkers for biogeochemistry and microbial ecology. *Rapid Commun. Mass Spectrom.* 18, 617–628.

Sumner, D. Y., Kirschvink, J. L., and Runnegar, B. N. (1987). Soft-sediment paleomagnetic fold tests of late Precambrian glaciogenic sediments. *Eos*.

Sutcliffe, O. E., Dowdeswell, J. A., Whittington, R. J., Theron, J. N., and Craig, J. (2000). Calibrating the Late Ordovician glaciation and mass extinction by the eccentricity cycles of Earth's orbit. *Geology* 28, 967–970.

Takeuchi, N., Kohshima, S., and Seko, K. (2001a). Structure, Formation, and Darkening Process of Albedo-reducing Material (Cryoconite) on a Himalayan Glacier: A Granular Algal Mat Growing on the Glacier. *Arct. Antarct. Alp. Res.* 33, 115–122.

Takeuchi, N., Kohshima, S., and Seko, K. (2001b). Structure, Formation, and Darkening Process of Albedo-Reducing Material (Cryoconite) on a Himalayan Glacier: A Granular Algal Mat Growing on the Glacier. *Arctic, Antarctic, and Alpine Research* 33, 115–122.

Takeuchi, N., Kohshima, S., Yoshimura, Y., Seko, K., and Fujita, K. (2000). Characteristics of cryoconite holes on a Himalayan glacier, Yala Glacier Central Nepal. *Bull. Glaciol. Res.* 17, 51–59.

Takeuchi, N., Nishiyama, H., and Li, Z. (2010). Structure and formation process of cryoconite granules on Ürümqi glacier No. 1, Tien Shan, China. *Ann. Glaciol.* 51, 9–14.

Tang, H., and Chen, Y. (2013). Global glaciations and atmospheric change at ca. 2.3 Ga. *Geoscience Frontiers* 4, 583–596.

Tappan, H. N. (1980). *The paleobiology of plant protists*. San Francisco: W.H. Freeman.

Telford, R. J., Vandvik, V., and Birks, H. J. B. (2006). Dispersal limitations matter for microbial morphospecies. *Science* 312, 1015.

Telling, J., Anesio, A. M., Hawkings, J., Tranter, M., Wadham, J. L., Hodson, A. J., *et al*. (2010). Measuring rates of gross photosynthesis and net community production in cryoconite holes: a comparison of field methods. *Ann. Glaciol.* 51, 153–162.

Telling, J., Anesio, A. M., Tranter, M., Fountain, A. G., Nylen, T., Hawkings, J., *et al*. (2014). Spring thaw ionic pulses boost nutrient availability and microbial growth in entombed Antarctic Dry Valley cryoconite holes. *Front. Microbiol.* 5, 694.

Telling, J., Anesio, A. M., Tranter, M., Irvine-Fynn, T., Hodson, A., Butler, C., *et al*. (2011). Nitrogen fixation on Arctic glaciers, Svalbard. *J. Geophys. Res.* 116.

Telling, J., Anesio, A. M., Tranter, M., Stibal, M., Hawkings, J., Irvine-Fynn, T., *et al*. (2012). Controls on the autochthonous production and respiration of organic matter in cryoconite holes on high Arctic glaciers. *J. Geophys. Res.* 117.

Thatje, S., Hillenbrand, C.-D., and Larter, R. (2005). On the origin of Antarctic marine benthic community structure. *Trends Ecol. Evol.* 20, 534–540.

Thomas, R. H., and MacAyeal, D. R. (1982). Derived Characteristics of the Ross Ice Shelf, Antarctica. *J. Glaciol.* 28, 397–412.

Tranter, M., Fountain, A. G., Fritsen, C. H., Berry Lyons, W., Priscu, J. C., Statham, P. J., *et al*. (2004). Extreme hydrochemical conditions in natural microcosms entombed within Antarctic ice. *Hydrol. Process.* 18, 379–387.

Tranter, M., Sharp, M. J., Lamb, H. R., Brown, G. H., Hubbard, B. P., and Willis, I. C. (2002). Geochemical weathering at the bed of Haut Glacier d'Arolla, Switzerland?a new model. *Hydrol. Process.* 16, 959–993.

Treonis, A. M., Wall, D. H., and Virginia, R. A. (1999). Invertebrate Biodiversity in Antarctic Dry Valley Soils and Sediments. *Ecosystems* 2, 482–492.

Turbet, M., Forget, F., Leconte, J., Charnay, B., and Tobie, G. (2017). CO2 condensation is a serious limit to the deglaciation of Earth-like planets. *Earth Planet. Sci. Lett.* 476, 11–21.

Uetake, J., Tanaka, S., Segawa, T., Takeuchi, N., Nagatsuka, N., Motoyama, H., *et al*. (2016). Microbial community variation in cryoconite granules on Qaanaaq Glacier, NW Greenland. *FEMS Microbiol. Ecol.* 92.

Valledor, L., Furuhashi, T., Hanak, A.-M., and Weckwerth, W. (2013). Systemic cold stress adaptation of Chlamydomonas reinhardtii. *Mol. Cell. Proteomics* 12, 2032–2047.

van As, D., Hubbard, A. L., Hasholt, B., Mikkelsen, A. B., van den Broeke, M. R., and Fausto, R. S. (2012). Large surface meltwater discharge from the Kangerlussuaq sector of the Greenland ice sheet during the record-warm year 2010 explained by detailed energy balance observations. *cryosphere* 6, 199–209.

Van Cappellen, P., and Ingall, E. D. (1996). Redox stabilization of the atmosphere and oceans by phosphorus-limited marine productivity. *Science* 271, 493–496.

van Maldegem, L. M., Nettersheim, B. J., Leider, A., Brocks, J. J., Adam, P., Schaeffer, P., *et al*. (2021). Geological alteration of Precambrian steroids mimics early animal signatures. *Nat Ecol Evol* 5, 169–173.

Van Rompu, W. I. L. H. D. E. S. a. nd E. A. (1994). ROTIFERA AND TARDIGRADA FROM SOME CRYOCONITE HOLES ON A SPITSBERGEN (SVALBARD) GLACIER. *Belg. J . Zoo* 12.

Vaneechoutte, M. (1996). DNA fingerprinting techniques for microorganisms. A proposal for classification and nomenclature. *Mol. Biotechnol.* 6, 115–142.

Vass, I., Cser, K., and Cheregi, O. (2007). Molecular mechanisms of light stress of photosynthesis. *Ann. N. Y. Acad. Sci.* 1113, 114–122.

Veech, J. A. (2013). A probabilistic model for analysing species co-occurrence. *Glob. Ecol. Biogeogr.* 22, 252–260.

Venkatesan, B. M., and Bashir, R. (2011). Nanopore sensors for nucleic acid analysis. *Nat. Nanotechnol.* 6, 615–624.

Vidal, G., and Ford, T. D. (1985). Microbiotas from the late proterozoic chuar group (northern Arizona) and uinta mountain group (Utah) and their chronostratigraphic implications. *Precambrian Res.* 28, 349–389.

Vidal, G., and Knoll, A. H. (1982). Radiations and extinctions of plankton in the late Proterozoic and early Cambrian. *Nature* 297, 57–60.

Vidal, G., and Moczydłowska-Vidal, M. (1997). Biodiversity, speciation, and extinction trends of Proterozoic and Cambrian phytoplankton. *Paleobiology* 23, 230–246.

Vincent, W. F., Gibson, J. A., Pienitz, R., Villeneuve, V., Broady, P. A., Hamilton, P. B., *et al*. (2000). Ice shelf microbial ecosystems in the high arctic and implications for life on snowball earth. *Naturwissenschaften* 87, 137–141.

Vinšová, P., Pinseel, E., Kohler, T. J., Van de Vijver, B., Žársk\`y, J. D., Kavan, J., *et al*. (2015). Diatoms in cryoconite holes and adjacent proglacial freshwater sediments, Nordenskiöld glacier (Spitsbergen, High Arctic). *Czech Polar Reports* 5, 112–133.

Virginia, R. A., and Wall, D. H. (1999). How Soils Structure Communities in the Antarctic Dry Valleys. *Bioscience* 49, 973–983.

von Drygalski, E., and Kühl, W. H. (1897). Die Kryoconitlöcher. *Erde*, 93–103.

Vonnahme, T. R., Devetter, M., Žárský, J. D., Šabacká, M., and Elster, J. (2016). Controls on microalgal community structures in cryoconite holes upon high-Arctic glaciers, Svalbard. *Biogeosciences* 13, 659–674.

Wada, H., and Murata, N. (2006). 'Membrane Lipids in Cyanobacteria', in *Lipids in Photosynthesis: Structure, Function and Genetics* (unknown), 65–81.

Wadham, J. L., and Nuttall, A.-M. (2002). Multiphase formation of superimposed ice during a mass-balance year at a maritime high-Arctic glacier. *J. Glaciol.* 48, 545–551.

Wadham, J. L., Tranter, M., Skidmore, M., Hodson, A. J., Priscu, J., Lyons, W. B., *et al*. (2010). Biogeochemical weathering under ice: Size matters. *Global Biogeochem. Cycles* 24.

Wagnon, P., Linda, A., Arnaud, Y., Kumar, R., Sharma, P., Vincent, C., *et al*. (2007). Four years of mass balance on Chhota Shigri Glacier, Himachal Pradesh, India, a new benchmark glacier in the western Himalaya. *J. Glaciol.* 53, 603–611.

Walker, J. C. G., Hays, P. B., and Kasting, J. F. (1981). A negative feedback mechanism for the long-term stabilization of Earth's surface temperature. *J. Geophys. Res.* 86, 9776.

Warren, C. R. (2020). Soil microbial populations substitute phospholipids with betaine lipids in response to low P availability. *Soil Biol. Biochem.* 140.

Warren, S. G., and Brandt, R. E. (2006). Comment on "Snowball Earth: A thin-ice solution with flowing sea glaciers" by David Pollard and James F. Kasting. *J. Geophys. Res.* 111, C09016.

Warren, S. G., Brandt, R. E., Grenfell, T. C., and McKay, C. P. (2002). Snowball Earth: Ice thickness on the tropical ocean. *J. Geophys. Res.* 107, 3167.

Webster-Brown, J. G., Hawes, I., Jungblut, A. D., Wood, S. A., and Christenson, H. K. (2015). The effects of entombment on water chemistry and bacterial assemblages in closed cryoconite holes on Antarctic glaciers. *FEMS Microbiol. Ecol.* 91.

Webster-Brown, J., Gall, M., Gibson, J., Wood, S., and Hawes, I. (2010). The biogeochemistry of meltwater habitats in the Darwin Glacier region (80°S), Victoria Land, Antarctica. *Antarct. Sci.* 22, 646–661.

Weisleitner, K., Perras, A. K., Unterberger, S. H., Moissl-Eichinger, C., Andersen, D. T., and Sattler, B. (2020). Cryoconite Hole Location in East-Antarctic Untersee Oasis Shapes Physical and Biological Diversity. *Front. Microbiol.* 11, 1165.

Werner, I. (1997). Grazing of Arctic under-ice amphipods on sea-ice algae. *Mar. Ecol. Prog. Ser.* 160, 93–99.

Wharton, R. A., Jr, McKay, C. P., Simmons, G. M., Jr, and Parker, B. C. (1985). Cryoconite holes on glaciers. *Bioscience* 35, 499–503.

Wheeler, B. M., Heimberg, A. M., Moy, V. N., Sperling, E. A., Holstein, T. W., Heber, S., *et al*. (2009). The deep evolution of metazoan microRNAs. *Evol. Dev.* 11, 50–68.

White, D. C., Davis, W. M., Nickels, J. S., King, J. D., and Bobbie, R. J. (1979). Determination of the sedimentary microbial biomass by extractible lipid phosphate. *Oecologia* 40, 51–62.

Wick, R. R., Judd, L. M., and Holt, K. E. (2019). Performance of neural network basecalling tools for Oxford Nanopore sequencing. *Genome Biol.* 20, 129.

Wickham, H. (2016). ggplot2: Elegant Graphics for Data Analysis. Available at: https://ggplot2.tidyverse.org.

Widzgowski, J., Vogel, A., Altrogge, L., Pfaff, J., Schoof, H., Usadel, B., *et al*. (2020). High light induces species specific changes in the membrane lipid composition of Chlorella. *Biochem. J* 477, 2543–2559.

William Schopf, J., and Klein, C. (1992). *The Proterozoic Biosphere: A Multidisciplinary Study*. Cambridge University Press.

Williams, D. L., Von Herzen, R. P., Sclater, J. G., and Anderson, R. N. (1974). The Galapagos spreading centre: Lithospheric cooling and hydrothermal circulation. *Geophys. J. Int.* 38, 587–608.

Williams, G. E., Schmidt, P. W., and Young, G. M. (2016). Strongly seasonal Proterozoic glacial climate in low palaeolatitudes: Radically different climate system on the pre-Ediacaran Earth. *Geoscience Frontiers* 7, 555–571.

Williamson, C. J., Cameron, K. A., Cook, J. M., Zarsky, J. D., Stibal, M., and Edwards, A. (2019). Glacier Algae: A Dark Past and a Darker Future. *Front. Microbiol.* 10, 524.

Williamson, C. J., Cook, J., Tedstone, A., Yallop, M., McCutcheon, J., Poniecka, E., *et al*. (2020). Algal photophysiology drives darkening and melt of the Greenland Ice Sheet. *Proc. Natl. Acad. Sci. U. S. A.* 117, 5694–5705.

Wolynski, J. J. (2012). The Cause for the Huronian Glaciation. Available at: http://citeseerx.ist.psu.edu/viewdoc/download?doi=10.1.1.671.8901&rep=rep1&type=pdf

Wörmer, L., CirÉs, S., VelÁzquez, D., Quesada, A., and Hinrichs, K.-U. (2012). Cyanobacterial heterocyst glycolipids in cultures and environmental samples: Diversity and biomarker potential. *Limnol. Oceanogr.* 57, 1775–1788.

Wörmer, L., Lipp, J. S., Schröder, J. M., and Hinrichs, K.-U. (2013). Application of two new LC–ESI–MS methods for improved detection of intact polar lipids (IPLs) in environmental samples. *Org. Geochem.* 59, 10–21.

Wyrtki, K. (1961). The thermohaline circulation in relation to the general circulation in the oceans. *Deep Sea Research (1953)* 8, 39–64.

Xin, M.-X., and Zhou, P.-J. (2007). Mrakia psychrophila sp. nov., a new species isolated from Antarctic soil. *J. Zhejiang Univ. Sci. B* 8, 260–265.

Yallop, M. L., Anesio, A. M., Perkins, R. G., Cook, J., Telling, J., Fagan, D., *et al*. (2012). Photophysiology and albedo-changing potential of the ice algal community on the surface of the Greenland ice sheet. *ISME J.* 6, 2302–2313.

Yang, J., Jansen, M. F., Macdonald, F. A., and Abbot, D. S. (2017). Persistence of a freshwater surface ocean after a snowball Earth. *Geology* 45, 615–618.

Yang, J., Richard Peltier, W., and Hu, Y. (2012). The Initiation of Modern “Soft Snowball” and “Hard Snowball” Climates in CCSM3. Part I: The Influences of Solar Luminosity, CO2 Concentration, and the Sea Ice/Snow Albedo Parameterization. *J. Clim.* 25, 2711–2736.

Ye, Y., Wang, H., Zhai, L., Wang, X., Wu, C., and Zhang, S. (2018). Contrasting Mo–U enrichments of the basal Datangpo Formation in South China: Implications for the Cryogenian interglacial ocean redox. *Precambrian Res.* 315, 66–74.

Yonkee, W. A., Dehler, C. D., Link, P. K., Balgord, E. A., Keeley, J. A., Hayes, D. S., *et al*. (2014). Tectono-stratigraphic framework of Neoproterozoic to Cambrian strata, west-central U.S.: Protracted rifting, glaciation, and evolution of the North American Cordilleran margin. *Earth-Sci. Rev.* 136, 59–95.

Yoshimura, Y., Kohshima, S., and Ohtani, S. (1997). A Community of Snow Algae on a Himalayan Glacier: Change of Algal Biomass and Community Structure with Altitude. *Arct. Alp. Res.* 29, 126–137.

Young, G. M. (2002). Stratigraphic and tectonic settings of Proterozoic glaciogenic rocks and banded iron-formations: relevance to the snowball Earth debate. *J. Afr. Earth. Sci.* 35, 451–466.

Young, J. A. T., and Hastenrath, S. (1991). Glaciers of Africa. *Glaciers of the Middle East and Africa* Satellite Image Atlas of Glaciers of the World. US Geological Survey Professional Paper*, G49.

Zamora, F. J. (2018). Measuring and Modeling Evolution of Cryoconite Holes in the McMurdo Dry Valleys, Antarctica.

Zarsky, J. D., Stibal, M., Hodson, A., Sattler, B., Schostag, M., Hansen, L. H., *et al*. (2013). Large cryoconite aggregates on a Svalbard glacier support a diverse microbial community including ammonia-oxidizing archaea. *Environ. Res. Lett.* 8, 035044.

Zawierucha, K., Kolicka, M., Takeuchi, N., and Kaczmarek, Ł. (2015). What animals can live in cryoconite holes? A faunal review. *J. Zool.* 295, 159–169.

Zawierucha, K., Porazinska, D. L., Ficetola, G. F., Ambrosini, R., Baccolo, G., Buda, J., *et al*. (2021). A hole in the nematosphere: tardigrades and rotifers dominate the cryoconite hole environment, whereas nematodes are missing. *J. Zool.* 313, 18–36.

Zdanowski, M. K., Bogdanowicz, A., Gawor, J., Gromadka, R., Wolicka, D., and Grzesiak, J. (2017). Enrichment of Cryoconite Hole Anaerobes: Implications for the Subglacial Microbiome. *Microb. Ecol.* 73, 532–538.

Zhang, H., Sun, Y., Zeng, Q., Crowe, S. A., and Luo, H. (2021). Snowball Earths, population bottlenecks, and the evolution of marine photosynthetic bacteria. *Cold Spring Harbor Laboratory*, 2020.11.24.395392.

Zheng, S., Bawazir, M., Dhall, A., Kim, H.-E., He, L., Heo, J., *et al*. (2021). Implication of Surface Properties, Bacterial Motility, and Hydrodynamic Conditions on Bacterial Surface Sensing and Their Initial Adhesion. *Front Bioeng Biotechnol* 9, 643722.

Zhu, H., Li, X., Zhai, W., Liu, Y., Gao, Q., Liu, J., *et al*. (2017). Effects of low light on photosynthetic properties, antioxidant enzyme activity, and anthocyanin accumulation in purple pak-choi (Brassica campestris ssp. Chinensis Makino). *PLoS One* 12, e0179305.

Zolitschka, B. (2014). 'The Use of Varved Lake Sediments in Dating☆', in *Reference Module in Earth Systems and Environmental Sciences* (Elsevier).

Zumberge, J. A., Love, G. D., Cárdenas, P., Sperling, E. A., Gunasekera, S., Rohrssen, M., *et al*. (2018). Demosponge steroid biomarker 26-methylstigmastane provides evidence for Neoproterozoic animals. *Nat Ecol Evol* 2, 1709–1714.

Zumberge, J. A., Rocher, D., and Love, G. D. (2020). Free and kerogen-bound biomarkers from late Tonian sedimentary rocks record abundant eukaryotes in mid-Neoproterozoic marine communities. *Geobiology* 18, 326–347.